REPORT DOCUMENTATION PAGE

Public reporting burden for this collection of information is estimated to average 1 hour per response, including the time for reviewing instructions, searching existing data sources, gathering and maintaining the data needed, and completing and reviewing the collection of information. Send comments regarding this burden estimate or any other aspect of this collection of information, including suggestions for reducing this burden, to Washington Headquarters Services, Directorate for Information Operations and Reports, 1215 Jefferson Davis Highway, Suite 1204, Arlington, VA 22202-4302, and to the Office of Management and Budget, Paperwork Reduction Project (0704-0188), Washington, DC 20503.

1. AGENCY USE ONLY (Leave blank)	2. REPORT DATE 25.Jun.03	3. REPORT TYPE AND DATES COVERED DISSERTATION

4. TITLE AND SUBTITLE
"MODELING AND OPERATION OF SINGLE AND MULTIPLE TUBE MEMBRANE BJOREACTOR

5. FUNDING NUMBERS

6. AUTHOR(S)
MAJ ENGLAND ELLEN C

7. PERFORMING ORGANIZATION NAME(S) AND ADDRESS(ES)
UNIVERSITY OF MISSOURI ROLLA

8. PERFORMING ORGANIZATION REPORT NUMBER

CI02-989

9. SPONSORING/MONITORING AGENCY NAME(S) AND ADDRESS(ES)
THE DEPARTMENT OF THE AIR FORCE
AFIT/CIA, BLDG 125
2950 P STREET
WPAFB OH 45433

10. SPONSORING/MONITORING AGENCY REPORT NUMBER

11. SUPPLEMENTARY NOTES

12a. DISTRIBUTION AVAILABILITY STATEMENT
Unlimited distribution
In Accordance With AFI 35-205/AFIT Sup

DISTRIBUTION STATEMENT A
Approved for Public Release
Distribution Unlimited

12b. DISTRIBUTION CODE

13. ABSTRACT (Maximum 200 words)

20030710 003

14. SUBJECT TERMS			15. NUMBER OF PAGES 273
			16. PRICE CODE

17. SECURITY CLASSIFICATION OF REPORT	18. SECURITY CLASSIFICATION OF THIS PAGE	19. SECURITY CLASSIFICATION OF ABSTRACT	20. LIMITATION OF ABSTRACT

MODELING AND OPERATION OF SINGLE AND MULTIPLE TUBE

MEMBRANE BIOREACTORS

by

ELLEN CLAIRE ENGLAND

A DISSERTATION

Presented to the Faculty of the Graduate School of the

UNIVERSITY OF MISSOURI-ROLLA

In Partial Fulfillment of the Requirements for the Degree

DOCTOR OF PHILOSOPHY

in

CIVIL ENGINEERING

2003

Mark W. Fitch, Advisor	Craig D. Adams
Cesar Mendoza	David J. Wronkiewicz

Joel G. Burken

ABSTRACT

A mathematical model was developed and experimental work completed to examine the removal of volatile organic compounds from air using single and multiple tube membrane bioreactors. Both bench-sale and a small pilot-scale reactor's performance were reasonably predicted by the mathematical model. Both model predictions and experimental work indicated the liquid suspension does not significantly contribute to the removal of contaminants from air. Experimental results indicate that membrane bioreactor performance is not detrimentally affected by phosphorous or nitrogen limitation after an initial period with adequate nutrient supply. Stopping the liquid flow in the reactor module also did not lead to a declination in performance. VOC removal in a polyporous membrane reactor remained constant under diurnal loading conditions when compared with continuously operated bioreactors. A heated bioreactor also was found to remove contaminant at the same rate as a reactor operated at ambient temperature while measured heat transfer coefficients for several module configurations ranged from 2.9-17.4 W m^{-2} K^{-1}. Bioreactors operated in series provided additional removal of contaminant from the air.

ABSTRACT

A mathematical model was developed and experimental work completed to examine the removal of volatile organic compounds from air using single and multiple tube membrane bioreactors. Both bench-sale and a small pilot-scale reactor's performance were reasonably predicted by the mathematical model. Both model predictions and experimental work indicated the liquid suspension does not significantly contribute to the removal of contaminants from air. Experimental results indicate that membrane bioreactor performance is not detrimentally affected by phosphorous or nitrogen limitation after an initial period with adequate nutrient supply. Stopping the liquid flow in the reactor module also did not lead to a declination in performance. VOC removal in a polyporous membrane reactor remained constant under diurnal loading conditions when compared with continuously operated bioreactors. A heated bioreactor also was found to remove contaminant at the same rate as a reactor operated at ambient temperature while measured heat transfer coefficients for several module configurations ranged from 2.9-17.4 W m^{-2} K^{-1}. Bioreactors operated in series provided additional removal of contaminant from the air.

ACKNOWLEDGEMENTS

TABLE OF CONTENTS

List of Tables

List of Figures

CHAPTER 1
INTRODUCTION AND PURPOSE

1.1 PROBLEM IDENTIFICATION:

Contamination of air with volatile organic compounds (VOCs) is a prevalent, pressing problem in the United States as well as in developing and industrializing nations. Concern about VOCs in the atmosphere stems from their ability to increase ground level ozone as well as some VOC's inherent toxicity or irritant effects. Low-cost, effective treatment strategies for air pollution are needed to remove these troublesome contaminants from the air. Those treatment methods ideally should not simply transfer the air contamination to another phase but should degrade the compounds into harmless components. Treatment strategies that employ microorganisms may meet these desires and requirements.

A novel approach for separating and biodegrading VOCs is the hollow fiber membrane reactor. Hollow fiber membrane reactors consist of tubular membranes that separate contaminated air from microorganisms that grow on the exterior of the tube (and within a liquid suspension surrounding those tubes). Of particular interest are membrane modules that are of low cost (such as silicone rubber) and are very permeable both to volatile organic compounds commonly found as air contaminants (such as toluene) and to oxygen. The research conducted and reported in this dissertation was directed toward development of larger silicone tube membrane bioreactors than are currently in existence and to determine the performance of these reactor systems under operating conditions anticipated in the field.

1.2 RESEARCH APPROACH:

The biological treatment systems used in this work were composed of glass or polyvinyl chloride (PVC) modules containing silicone tubes through which contaminated air is passed. Several systems were constructed including single, dual, and multiple tube systems. Abiotic studies were performed to measure the mass transfer of toluene across reactor membranes without the presence of microorganisms. Biotic studies were performed under a variety of operating conditions to determine the performance of the membrane bioreactor systems.

A computer model of the processes occurring within a single silicone tube membrane bioreactor was developed. The model was calibrated for the single tubing system and validated using further experimental data from the single silicone tube system, a dual tube bioreactor, and a semi-pilot-scale multiple tube configuration. The model was then used in a predictive manner.

1.3 GOALS AND OBJECTIVES:

The proposed research combines information from the literature and on-going bench-scale work in contaminant removal from air using membrane bioreactors at the University of Missouri-Rolla, Rolla, MO (Ergas et al, 1999; Fitch et al, 2000). The overall goal of the work is to demonstrate and evaluate the use of single and multiple silicone tube membrane bioreactors for the removal of a common VOC (toluene) from waste gas streams under a variety of operating conditions and to further the understanding of the system operation. Multiple tube silicone membrane bioreactors are a low cost venture with a potential high rate of return for many types of industry that

produce waste air streams. Determination of ways to optimize the mechanisms of removal through modeling will allow for better design and operation of full-scale membrane bioreactors.

The objectives of the research included the following:

(1) Investigate the scale-up of silicone membrane bioreactors from single, through dual and to multiple tubes by monitoring air contaminant removal and developing loading curves for each type of reactor system.

(2) Manufacture a semi-pilot-scale multiple tube reactor system for air treatment.

(3) Construct, calibrate, and validate a computer model to predict removal in single and multiple tube silicone membrane bioreactors.

(4) Use the model to optimize design of silicone tubing membrane bioreactors and apply the model to other similar systems, i.e. benzene removal using latex tubing bioreactors.

(5) Examine the operation of single and multiple tube bioreactors under a variety of operating conditions that reflect potential operating or desired operating conditions including:

(a) Stagnant liquid conditions in the module.

(b) Nutrient limitation in the liquid suspension.

(c) Heated liquid conditions.

(d) In-series operation of membrane bioreactors.

(e) Diurnal operation.

(6) Measure overall heat transfer coefficients for three membrane module configurations.

1.4 SIGNIFICANCE:

Membrane and conventional biofiltration strategies are unique among air contaminant remediation technologies. Biofiltration allows the complete decomposition of VOCs to CO_2 and H_2O with virtually no additional energy expenditure and without simply transferring the chemical to another waste form. While membrane biofiltration has shown much potential in the laboratory there is no single accepted method to predict the removal of contaminants. This information and the modeling procedures developed could lead to a better understanding of the fate, within the biofilm and the reactor volume, of numerous contaminants and contaminant classes in membrane biofiltration. This understanding may lead to improved design of membrane biofiltration systems and to a greater acceptance from regulatory bodies and the general public. The goals and objectives of this research are directly tied to further developing and enhancing the performance of a low-cost, low-impact, remediation technology for organic contaminants contained within industrial waste gas streams.

CHAPTER 2
LITERATURE REVIEW

2.1 BACKGROUND:

2.1.1 Environmental Regulation: Adequate methods for the treatment of VOC-contaminated gas streams are needed, as more than 20,000 tons of VOCs were discharged to the atmosphere in 1997 (EPA, 1998). Legislation affecting the control of this VOC release includes the Clean Air Act and its amendments of 1970 (USC, 1970) and 1990 and the Emergency Planning and Community Right-to-Know Act (EPCRA) of 1986 as promulgated in 40 CFR. Under the 1990 Clean Air Act Amendments, a 90% reduction in the production of 189 listed air toxics was required by the year 2000 and a 15% reduction in ground level ozone in the country's most polluted areas (Zahodiakin, 1995). EPCRA requires data compilation and reporting of chemical releases to the environment via the Toxic Release Inventory (EPA, 2002).

2.1.2 Air Pollution Control Technology: When source reduction measures such as substitution, reduction, and recycling have been unsuccessful in removing contaminants from the air stream, industry has typically employed chemico-physico techniques to control emissions (Devinny et al, 1999). The more commonly cited conventional treatment techniques are condensation, incineration, absorption/stripping, and adsorption (Devinny et al, 1999; van Groenestijn and Hesselink, 1994; Daubert et al, 1999) or combinations of these techniques (Hounsell, 1995; Patkar and Reinhold, 1993). Each of these techniques has some drawbacks - condensation requires concentrated waste streams (Devinny et al, 1999), thermal incineration has proven to be costly because of the fuel requirements to treat dilute air streams (Yeom and Daugulis, 2000), while adsorption and

absorption processes may only convert the air pollutant to another form or phase, i.e. air contaminant to water contaminant. Some selection criteria for air pollution control schemes include recycle potential, stream composition, stream flow, flammability, temperature, cost, corrosion, contaminants, halogenated composition, contaminants such as particulates, energy expenditure, location and complexity (Hounsell, 1995).

In contrast, biological treatment typically results in total destruction of the compounds rather than physical transfer of the contaminant to another medium and has the potential for low cost implementation (Parvatiyar et al, 1996). Biological methods for treating contaminated air are usually divided into four categories: biofilters, biotrickling filters, bioscrubbers, and membrane bioreactors (Waweru et al, 2000). Two of the main differences between the bioreactor types include the state of the microorganisms and the state of the water phase. Table 2-1 shows the classifications of bioreactors for waste gas purification (Devinny et al, 1999). A comparison of air pollution control treatment technologies is shown in Figure 2-1; the niche that has been identified for biofilters is for low concentration air flows which will not sustain combustion without supplemental fuel.

Table 2-1. Classifications of bioreactors.

Reactor Type	Microorganisms	Water Phase
Biofilter	Fixed	Stationary
Biotrickling filter	Fixed	Flowing
Bioscrubber	Suspended	Flowing
Membrane Bioreactor[1]	Fixed/Suspended[1]	Stationary/Flowing[1]

[1]Added by author of current document

Gas Flow (m³ h⁻¹)
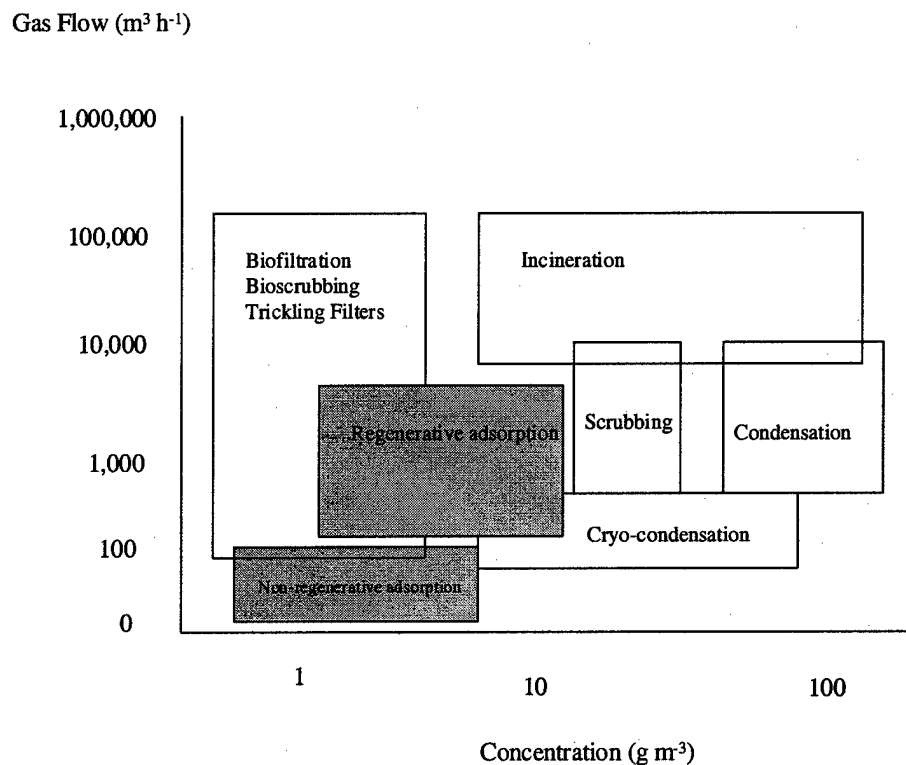
Figure 2-1. Comparison of various air pollution control technologies (reproduced from Devinny et al, 1999). Biological methods of treatment typically are employed at low influent concentrations.

2.1.3 Biofiltration History: Biofiltration has a relatively short history world wide and has yet to be fully exploited in the United States. Anit and Artuz (2000) provide a brief timeline of biofiltration events:

1923 - biological methods proposed to treat odorous emissions;

1955 - biological methods applied to treat odorous emissions at low concentrations in

Germany;

1960s - biofiltration used for treatment of gaseous pollutants both in Germany and US;

1970s - biofiltration used with high success in Germany;

1980s - biofiltration used for the treatment of toxic emissions and volatile organic

compounds from industry;

1990s - more than 500 biofilters operating both in Germany and the Netherlands and biofiltration spreading widely in the U.S.

Biofilter technology has proliferated primarily in Europe because of high energy costs and sophisticated odor regulations making biofiltration a viable economic alternative for waste air treatment (Reynolds and Grafton, 1999). Conversely, biofiltration has not gained acceptance in the United States because of low energy prices and a lack of regulatory acceptance (particularly regulations requiring minimum percent removal levels at all times), leaving thermal and catalytic oxidation as more attractive air treatment alternatives. Biofilters originated were first used in Orange County, CA in the 1960s with failures of biofilters due to poor design and construction significantly impacting the biofilters' ability to penetrate the United States market (Reynolds and Grafton, 1999).

In general, biofiltration has been found most suitable for low concentrations of contaminants in large air volumes ($1000 - 50,000$ m^3 h^{-1}) (Devinny et al, 1999). The most successful remediation has been with low molecular weight contaminants and highly water-soluble organics with simple bond structures. Elimination capacities have been shown to range from $10 - 300$ g m^{-3} h^{-1} (elimination capacity is defined as the mass rate of removal divided by the volume of the reactor). The most promising industries for application of biofiltration include the surface coating, site remediation, municipal composting, and pulp, paper, and wood products industries (Devinny et al, 1999). Other industries with potential for the use of biofilters include publicly owned treatment works, printing facilities, bakeries, and metal manufacturing facilities where high flow rates and low concentrations of alcohols and ketones exist. (Reynolds and Grafton, 1999).

2.1.4 Advantages of Biofiltration over Conventional Treatment: Advantages of biofiltration processes over conventional treatment strategies include low investment and operating costs, minimal maintenance, reliable operational stability, and high removal efficiency for VOC concentrations less than 1000 ppm. Furthermore, biofiltration offers the added advantage of being a benign treatment technology characterized by low overall energy requirements, no secondary pollutant discharge, absence of chemical reagents and no cross media contamination (Eszenyiova et al, 2001)

2.1.5 Biofiltration Costs: Biofiltration is frequently touted as a more cost effective option for treating high quantities of low contaminant level air streams. In an exergy analysis [a type of energy cost analysis] that formed the basis of a life cycle comparison and employed thermodynamic principles, a comparison of carbon adsorption, biofiltration, catalytic and thermal oxidation showed that biofiltration was found to be the lowest cost option (Dewulf et al, 2001)

Costs of biofiltration vary between units and manufacturers. Purchase costs of the portable Dessau-Sorpin process range from $1000 for a unit treating 2 m^3 gas min^{-1}, to $15,000 for a capacity of 20 m^3 min^{-1} with operating costs varying from $0.5 to $5 per 1000 m^3 of air treated (Enviro-Access, 2001). The purchase cost for a biofiltration unit, with life span of 6 months to seven years depending upon the filter media, is between $300 - 600 m^3 min^{-1}. The main operating cost is for an energy input of the order of 4 kW for every 10,000 m^3 hr^{-1} of air treatment, equivalent to about $0.03 per 1000 m^3 of treated gas (Air Science Technologies, 2001). Devinny et al (1999) indicates costs range from $1000 - $3500 m^3 of filter bed for small units and $300 - $1000 m^3 of filter bed for large units.

2.2 CONVENTIONAL BIOFILTRATION:

As background reading for general information about biofiltration, numerous journal articles were reviewed. The following is by no means an exhaustive recitation of conventional biofiltration studies, as hundreds were found during a standard computer based literature search using OVID®. However, this information provides a general "feel" for what biofilter information is present in the current literature.

2.2.1 Peat Packing: Two of the most common packing materials for conventional biofilters are peat and compost or natural materials of the same consistency. These natural materials have shown their ability to host microorganisms capable of efficient VOC degradation. Xylene was removed using a peat-containing biofilter operated at 0.4 $m^3 h^{-1}$ with inlet loads up to 60 g $m^{-3} h^{-1}$ (Elmrini et al, 2000). Removal efficiencies decreased at higher gas flow rates and higher pollutant inlet loads. In two bench-scale peat biofilters, xylene was found to be more efficiently degraded than toluene at high loading rates (Marek et al, 2001). The best removal was found when the biofilters were first fed toluene only, and thereafter xylene was added. Higher pH values of the peat led to better removal of both pollutants. In another reactor, 120 g VOC m^{-3} peat h^{-1} were removed from a mixture of chlorinated and aromatic compounds (Malhautier et al, 2001). Removals of dichlorobenzene after air stripping from water followed by biofiltration varied from 0-79% with the lower portions of the efficiency range at low inlet concentrations (Roberge et al, 2001). A maximum elimination capacity of 242 g $m^{-3} h^{-1}$ for toluene and 63 g $m^{-3} h^{-1}$ for styrene were found in two separate bench-scale biofilters packed with peat and glass beads (Zilli et al, 2001).

Removal rates of 120 g VOC m^{-3} h^{-1} were found at an organic load of 220 g m^{-3} peat h^{-1} (Aizpuru et al, 2000). Competition between substrates in the complex mixture of aromatics and chlorinated compounds was suggested. Compost biofilters have been shown to be capable of eliminating either n-butane or benzene vapor from air streams with high efficiency (>90%) at concentrations up to 200 ppm (Allen, 1996). In the case of n-butane elimination, a long acclimation period was required to sufficiently populate the biofilter with n-butane degrading microorganisms. The maximum elimination capacity obtained for n-butane on conditioned compost was found to be 25 g m^{-3} h^{-1}. Under pseudo-steady state conditions, a maximum elimination capacity of 70 g m^{-3} h^{-1} was obtained for an inlet load of 190 g m^{-3} h^{-1} (Bibeau, 1997).

Conventional biofilters have been used extensively for the treatment of odors. Biofilters have been shown to be effective at treating essentially all of the odors associated with composting, including ammonia and a wide range of volatile organic compounds, including sulfur compounds and amines (Richard, 2001). Five separate biofilters (biochips, coconut fibers, chopped bark and wood, bioContact filter pellets, and biocompost) were used to treat odors and microbial bioaersol emissions from a piggery (Martens et al, 2001). Significant differences were found between the filter materials with the biochip test material providing the best odor removal. Biofilters were found to reduce the concentration and offensiveness of odors produced by a rendering plant (Luo and Lindsey, 2000). Even gas distribution was found to be the most important factor affecting odor removal efficiency by the biofilters. A biofilter made up of wood chips, bark mulch leaf compost, and oyster shells provided 99% removal of hydrogen sulfide (Cooper et al, 2001).

2.2.2 Other Packing: Other natural packing materials have also been employed in conventional biofilters with good success. Porous ceramics, calcinated cristobalite, calcinated and formed obsidian, and granulated and calcinated soil were compared for their ammonia and H_2S removal capabilities. The amount of NH_3 removed per unit volume of packing material was greatest for porous ceramics and poorest for calcinated cristobalite (Hirai et al, 2001a) while ceramic and obsidian were best for H_2S removal (Hirai et al, 2001b). Nitrogen dioxide was removed from a contaminated air stream using *Thiobacillus* denitrifiers immobilized on an activated alumina bed (Krishna et al, 2000). 99% removal efficiency was achieved with an influent gas concentration of 2735 ppm. Rockwool mats were successfully used to treat restaurant air emissions (Andersson, 2000). Rockwool mats showed decreased pressure drops and improved gas flow compared to loose rock wool.

Perlite (a natural volcanic glass), biofoam, and compost were compared for their ability to remove nitric oxide from gas streams (Lee et al, 2000). The perlite and biofoam offer longer term thermal stability while the compost performed better under short residence times. In a study where alkylbenzene vapors were removed using a conventional biofilter containing perlite, the maximum elimination capacity was higher during long term operation than short term operation, suggesting biofilter studies should be run for longer periods (Veiga and Kennes, 2001). Elimination capacity was found to decrease when water content dropped below 35-40% but original performance was recovered in less than 24 h when water content was restored.

Perlite and granular activated carbon were used in a lab-scale four-stage bioreactor (Paca and Koutsky, 2000). Short vapor contact times caused slight decreases

in removal efficiencies at the same overall loading rates. Activated carbon was shown to result in higher elimination capacities, lower pressure drops, pH more favorable for the inoculum, and could successfully treat higher styrene concentrations than the perlite. A low pH system, using lava rock, gravel, and a commercially prepared support material was found to be effective for simultaneous treatment of H_2S and VOCs (Chang et al, 2000).

2.2.3 Novel Arrangements: Fungi, as well as bacteria, are being used successfully to treat contaminated air streams. A fungus was able to degrade several VOCs, with the exception of benzene and xylene (Woertz and Kinney, 2000). VOC degradation was inhibited when the pH was less than 3 and when nitrogen was not supplemented to the culture. In contrast, five fungal strains able to grow with toluene as their sole carbon and energy source showed the propensity to grow at low water activities, in acidic conditions, and with the ability to grow on aromatic hydrocarbons; making fungi a promising biofilter inoculant when harsh environmental conditions and near zero net growth is preferred (Prenafeta-Boldu et al, 2001). A combination of both fungi and bacteria may also be advantageous for contaminant removal. Biofilters based on bacteria were found to have improved toluene removal efficiencies after fungal invasion (van Groenestijn et al, 2001). High volumetric toluene elimination capacities of 80 - 125 $g\ m^{-3}\ h^{-1}$ were found; at low pH, fungi appeared to be preferentially selected over bacteria. In addition to VOCs, other compounds have been removed from contaminated air using a fungus. Fungal bioreactors removed NO from contaminated airstreams when an external carbon and energy source was provided (Woertz et al, 2001). The fungal bioreactor achieved a

maximum NO removal efficiency of 93%, however, the fungi may have been inhibited by the presence of high NH_4^+ concentrations.

In addition to the use of novel organisms, novel arrangements and combinations of biofiltration and other techniques have been demonstrated and validated. In a study by Webster et al (2000) organic vapors from a spray booth were concentrated on granular activated carbon (GAC) and later regenerated using microwave heating to supply an organic-loaded biofilter a constant supply of contaminated air. In this system, 87% of contaminant removal occurred in the first 0.5 ft of bed and a 6 g m^{-3} h^{-1} elimination capacity was measured. Perlite biofilters arranged in series were used to remove styrene and their start-up characteristics were studied (Weigner et al, 2001). 18 days after start-up, nearly 85% of styrene was removed at an organic loading of 170 g m^{-3} h^{-1}. A modified conventional biofilter (horizontal flow with baffles) was found to have a higher elimination capacity for ammonia (0.16 - 0.66 g NH_3 kg^{-1} dry matter) than a vertical flow biofilter (Lee et al, 2001). Bacteria have even been isolated that degrade the very compounds that are used to destroy them. A highly solvent tolerant bacterial consortium was successfully used for the biofiltration of high concentration isopropanol vapor within a packed bed reactor (Bustard et al, 2001).

2.2.4 Biotrickling Filters: The trickle bed air biofilter or biotrickling filter usually employs synthetic, inorganic media and receives liquid nutrient and buffer through a nozzle system positioned on top of it. Due to better control of pressure drop across the bed, pH and nutrient feed, trickle bed biofilters have more consistent operation than natural media biofilters and do not suffer the aging effects of natural media (Chang et al, 2001).

Numerous studies have shown the effective operation of biotrickling filters. The total maximum loads of a two-stage system using cylindrical ceramic particles were 1150 g m^{-2} d^{-1} for H$_2$S-S, 879 g m^{-3} d^{-1} in a gas mixture (Ruokojarvi et al, 2001). In this biofilter, a decrease in retention time from 2 to 1 min had very little effect on removal efficiency. A porous ceramic biofilter was used to remove odor generated by composting facilities (predominantly ammonia and hydrogen sulfide) (Park et al, 2001). Despite changes in weather and moisture levels of composting materials, more than 95% of odor was removed with an acclimation period of 30 days.

Various polyurethane foam materials were used in a biotrickling filter to remove paint spray emissions (Martinez et al, 2000). Increased sorption capacities of a combination activated carbon/polyurethane foam material was demonstrated. Polyurethane foam media was used to remove toluene with removals over 99% (Moe and Irvine, 2001b). Stable operation was observed with nutrient addition with favorable head loss when compared to other media. A trickle-bed air filter with a coal column for leveling of influent concentrations effectively treated VOCs emitted during the production of polyurethane and epoxy (Chang et al, 2001).

A biotrickling filter removed both o-dichlorobenzene and ethanol from a contaminated air stream (Bhattacharya and Baltzis, 2000). Biomass removal every four months improved operation with VOC removal occurring in both the biofilm and the liquid. More than 90% and 80% removal efficiencies in a trickle-bed air filter were achieved for n,n-dimethylacetamide loadings below 20.2 and 34.5 g m^{-3} h^{-1} (Lu et al, 2001a) while 85 and 90% removal efficiencies were achieved for ethylacetate loadings below 490 and 810 g m^{-3} h^{-1}, respectively, in a trickle bed air filter (Lu et al, 2001c).

2.2.5 Bioscrubbers: In a unique arrangement, large amounts of a xenobiotic substrate were transferred from a gas phase to a hydrophobic organic phase, and then allowed to partition to cells (Yeom and Daugulis, 2000). In this scheme, the mass transfer rate was much higher than the biodegradation rate. In another bioscrubber, complete degradation of phenol at a feed concentration of 8 g L^{-1} was obtained (Leonard et al, 1998).

2.2.6 Disadvantages: Although conventional biofiltration offers advantages over other pollution control technologies, such as low capital and operating costs and minimal secondary pollution problems, there are some disadvantages. They include the requirement of large cross sectional areas because of required low gas velocities (2 ft s^{-1}), long acclimatization periods (10-15 days), sensitivity of the microorganisms to change in load (type and concentration of VOC) and lack of full scale data on industrial applications (Patkar and Reinhold, 1993).

One common problem with biofilters treating certain contaminants is acid formation (TRG Biofilter, 2001). For example, common species of microorganisms can readily oxidize H_2S to sulfuric acid effectively removing the highly odorous and toxic compound from the air. However, the acid accumulates, lowering the pH of the biofilter, ultimately inhibiting microbial activity, causing channeling and compacting as the packing material is degraded, causing the biofilter to fail. Technology development by TRG Biofilter (2001) suggests that a two-stage biofilter will solve the problem of acidification. The first stage will hold an inert, readily drained, acid resistant support medium and will operate at low pH to remove H_2S while the second stage will use compost at pH 7 to remove any remaining volatile organics.

Release of bioaerosols has also been a concern, especially for those systems treating indoor air. However, several studies have indicated that the environmental risk of bioaerosol release from immobilized technology is minimal and the systems can be considered safe when placed close to populated areas (Chung et al, 2001; Mallany et al, 2000)

2.2.7 Pressure Drop: Another problem encountered with conventional biofilter units has been pressure drop across the reactor (Devinny et al, 1999). A large area of research concerning biofilters is devoted to controlling the pressure drop across the biofilter bed, associated with excess biomass accumulation. Biomass accumulation, which is usually greater at the inlet sections of biofilters, leads to a change in bed characteristics, such as the reduction of the interparticle void space and the compaction of natural packing materials, which subsequently causes channeling and increased pressure drops. This translates into higher operating and maintenance costs that become significant for long-term biofilter operations. The highest pressure drops in beds were caused by layers of biomass with high exopolysacchride or exopolymeric substance (EPS) concentration that retained a very high amount of moisture, which increased the biomass specific volume and significantly decreased the bed porosity at the top levels of the first sections of a biofilter (Morgan-Sagastume et al, 2001). Weber and Hartmans (1996) found that by applying regular NaOH washes, clogging of trickle-bed reactors could be prevented while still maintaining high removal rates of toluene (Weber and Hartmans, 1996).

A pressure transducer was used to monitor pressure drops in a reactor employing foam packing material; pressure drop within the reactor was chosen as a control parameter for clogging of the reactor with biomass (Thalasso et al, 2001). During the

course of a study comparing operation of a biofilter and bioscrubber, the use of pressure drop monitoring was proposed as a tool to control and optimize the running conditions of biological systems of air treatment (Le Cloirec et al, 2001). An expression correlating biofilm density and biofilm thickness, as determined from on-line pressure drop measurements, was proposed for an upflow fixed-bed bioreactor (Deront et al, 1998).

Fungi immobilized on an inert carrier with mites had lower pressure drops than a similar system without mites while the carrier material was found to be an important factor that impacted removal efficiency (van Heiningen et al, 2000). A model of biomass accumulation and plugging suggests selection of material with relatively uniform, large pores may be more effective for biofiltration (Schwarz et al, 2000). Reduction of surplus biomass by stirring and trickling water caused a prolonged service life and prevented clogging of the trickle bed and associated pressure drop increase. The reduction in biomass and intermittent percolation of mineral medium resulted in high volumetric degradation rates of about 100 g of toluene m^{-3} h^{-1} at a load of 150 g of toluene m^{-3} h^{-1} (Laurenzis et al, 1998). Such a high removal rate with a trickle-bed reactor was not reported before.

2.2.8 Summary of Issues with Conventional Biofilters: Numerous issues regarding conventional biofilters and their operation have been discussed while other issues have not been acknowledged in this document. In summary, general considerations include (Devinny et al, 1999):

- the waste gas stream to be treated

- the biofilter media

- waste gas stream air flow

- contaminant and concentration

- interfering contaminants such as dust and grease

- and influent gas temperature must be considered.

- media inorganic nutrient content and organic content, additives,

- media water content, pH, porosity,

- media mechanical properties, service time, cost and odor

- pressure drop across the filter

2.3 MEMBRANE BIOREACTORS:

2.3.1 Background: In membrane bioreactors, the gaseous pollutants are transferred

from the gas to the liquid phase (where they are degraded) via a membrane. A conceptual

diagram of the membrane bioreactor is shown in Figure 2-2. Two categories of

membrane materials are available for treating contaminants, hydrophobic microporous

and dense phase membranes while two types of biomass may be used: fixed film cultures

(biofilms) and suspended growth cultures (Burgess et al, 2001).

Hydrophobic microporous membranes consist of a polymer matrix, e.g.

polypropylene, polysulfone, or Teflon®, and contain pores with a diameter in the range of

0.01 - 1 micrometer. Since the membrane material is hydrophobic, the pores are filled

with gas. Water does not enter the pores unless a critical pressure at the liquid side is

exceeded (Reij et al, 1998). Microporous material is generally made into hollow fibers,

although spiral wound and plate and frame modules have also been used (Reij et al,

1998).

Dense material is available as tubes with a wall thickness of at least several

hundred micrometers (Reij et al, 1998). Composite membranes are a combination of the

two types (dense and microporous) and consist of a thin, selective top layer (1-30

microns) of dense material, supported by a highly porous support layer (e.g. non-woven

polyester or a microfiltration membrane (Reij et al, 1998)).
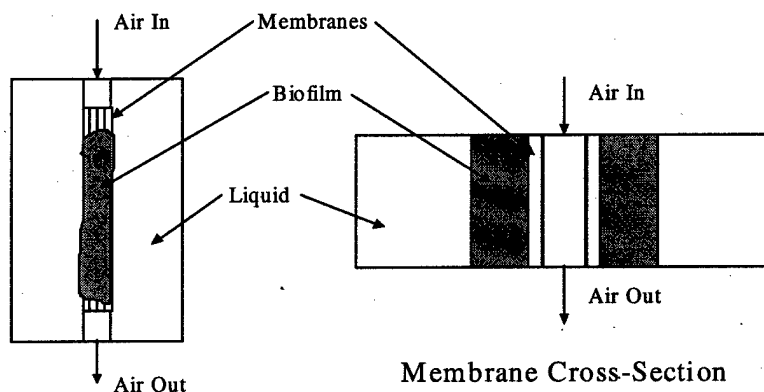
Figure 2-2. Conceptual diagram of a tubular membrane bioreactor (Neemann, 1998).
Contaminated air enters the interior of the tube, diffuses across the membrane into the
biofilm where it is degraded by microorganisms.

Mass transfer and kinetics of a contaminant within the membrane bioreactor

module can be described as a sequence of events. Those events are:

- bulk mixing of the contaminant in the air entering the bioreactor,

- boundary layer transport,

- sorption and diffusion into the membrane,

- exit from the membrane and dissolution and diffusion into the biofilm,

- diffusion through and degradation within the biofilm,

- boundary layer transport into the liquid phase, and

- subsequent mixing and degradation within the suspension.

The resistance to mass transfer through the membrane is a major issue in membrane bioreactors, especially dense phase membranes. To affect mass transfer, a compound must transfer across a gas phase resistance then sorb into the polymer and diffuse through to the other side. The concentration difference between the gas phase and the liquid phase provides the driving force for diffusive transport across the membrane. The driving force depends strongly on the air-water partition coefficient (H) of the diffusing volatile (Reij et al, 1998). Low values of the partition coefficient implicate a high water solubility, and consequently more efficient gas/liquid mass-transfer (Hartmans, 1992b). This mass transfer compares poorly with conventional biofilters, in which there is no membrane resistance.

The intrinsic permeability of a material in a dense phase membrane is a function of its solubility and diffusivity in that material (Brookes and Livingston, 1995). As a consequence, components can be selectively extracted from or retained in the gas phase by a proper choice of the membrane material (Reij et al, 1998). The high permeability of silicone rubber (polydimethylsiloxane) to certain VOCs and oxygen and its hydrophobicity (Favre et al, 1993) makes the material attractive for use in membrane bioreactors.

At the interface of the membrane and the liquid phase/biofilm, two phenomena affect mass transfer - solubility of the compound in the liquid phase as compared to the solubility in the membrane, and diffusion of the contaminant through the stagnant liquid layer. Maximizing mass transfer per unit membrane surface area will, therefore, be a prime design consideration (Pressman et al, 1999).

For a biofilm-free surface, the resistance to mass transfer is determined by fluid velocity, and models for this mass transfer exist (Yang and Cussler, 1986). However, the presence of a biofilm presents an even larger stagnant layer and the diffusion coefficient in a biofilm may be substantially lower than in water (Beyenal et al, 1997; Characklis and Marshall, 1990; Holden et al, 1997). Thus in the absence of biological activity (a dead biofilm), a decreased rate of mass transfer might be expected due to the presence of the biofilm. Countering this greater resistance to mass transfer is degradation in the biofilm, potentially increasing the concentration gradient as compared to a biofilm-free surface.

2.3.2 Advantages and Disadvantages of Membrane Bioreactors: Because of the separation of the biofilm from the air stream, many limitations associated with conventional biofilters can be overcome in a membrane biofilter. The main advantage of membrane bioreactors is that separation between the air and liquid phase. The separation allows for ease of nutrient amendment, constant humidification, and pH adjustment if required (Fitch et al, 2000). Another potential advantage of membrane biofiltration is the ability to pass very concentrated or dilute pollutant gas streams through the bioreactor without damage to or death of the bacterial consortia. With proper membrane material selection mass transfer to the liquid phase could potentially be controlled or manipulated.

Other advantages of membrane biofiltration over conventional biofiltration include no clogging, no channeling, and a minimal required level of operator expertise (Fitch, 2000). Membrane bioreactors also offer some advantages over biotrickling filters and bioscrubbers. The gas-liquid interface that can be created in hollow fiber reactors is larger than in other types of gas-liquid contactors (Reij et al, 1998). In hollow fiber membrane reactors the specific area can be as high as 10,000 $m^2 m^{-3}$ (Yang and Cussler,

1987). Under fixed operating conditions with a given gas flow rate, and under the same conditions, results illustrate that the membrane bioreactor is able to achieve volumetric mass transfer fluxes almost 3 times higher than those of a direct bioscrubbing system (Freitas do Santos et al, 1995d). Moreover, membrane reactors do not contain moving parts, are easy to scale up, and the flows of gas and liquid can be varied independently, without the problems of flooding, loading, or foaming commonly encountered in bubble columns (Reij et al, 1998).

A disadvantage to the use of membrane biofiltration has been the cost of the membranes, such as those used in the oxygenation of blood (e.g. Spectrum Microgon) or purification of pharmaceuticals (e.g. Koch Membrane Systems) and the associated cost of construction (Reij et al, 1998). However, dense phase membranes, such as silicone or latex, are relatively inexpensive (Cole Parmer Instrument Company) and might be configured in a similar manner to their higher cost relatives. Further potential disadvantages of membrane bioreactors include possible clogging of the liquid channels due to excessive biomass growth (Reij and Hartmans, 1996) and their long-term operational stability has yet to be demonstrated (Reij et al, 1998).

2.3.3 Membrane Bioreactors Treating Gas Contaminants: Relatively few studies and few researchers have focused on membrane bioreactors for waste gas treatment. Although membrane technology has been studied fairly extensively and used in water treatment (Clapp et al, 1994; Aziz et al, 1995), it still remains a novel gas treatment alternative (Ergas, 2002). Membrane reactors have been used for laboratory-scale treatment of several VOCs and gases, however, no reports of pilot- or full-scale operation

were found. Additionally, membrane bioreactors apparently have not been exploited for odor reduction.

2.3.3.1 Dense Membranes: As stated by De Bo (2000), Bauerle et al (1986) developed a membrane bioreactor with tubular nonporous silicone rubber (polydimethylsiloxane) membranes for waste gas treatment. The performance of the bioreactor increased at higher gas residence times (up to 10 s) and organic loadings (up to 250 g substrate m^{-3} d^{-1}). The removal of p-xylene and n-butanol was excellent while the elimination of the chlorinated compound was less successful as there was a pH-decrease and a lack of dense biomass growth. By controlling the pH of the liquid phase and by increasing the gas residence time to 14 s, elimination efficiencies up to 70% could be obtained.

A dense phase latex membrane bioreactor was found to remove 70-80% of an influent benzene in a contaminated air stream (150 ppm) (Neemann, 1998). In a continuation of the work with aromatics, an abiotic removal of 13% for toluene was measured, while a 100% removal was achieved with a biofilm for an influent gas concentration of 72 ppm (Cole, 2001). In the most recent study located, Attaway et al (2001) examined the removal of BTEX from air using a dual tube silicone reactor. The reactor tubing was wrapped in a spiral fashion and provided benzene, toluene, ethyl benzene and xylene (BTEX) removal rates of 30 μg h^{-1} cm^{-2} with removal efficiencies of 75% - 99%.

One dense material, silicone rubber, or polydimethylsiloxane (PDMS) is of particular interest for use in membrane reactors. Silicone rubber is known to be very permeable to oxygen (Coté et al, 1989) and also very permeable to volatile organic compounds. The structure of silicone is shown in Figure 2-3. PDMS tends to coil up and

exhibit molecular conformation as a helix with the methyl groups facing outwards. Distortion of the helix causes exposure of the oxygen groups which impart the lubricating properties and gives the silky feel (Elkay Silicones, 2002). Silicone tubing is manufactured by a four-step extrusion process that includes mill blending, extrusion feed, profile forming and vulcanization (Heide, 1999). Silicone exhibits good performance properties including biocampatibility, temperature resistance, chemical resistance, and high tear and tensile strength (Heide, 1999).

$$\left[-O-\underset{\underset{CH_3}{|}}{\overset{\overset{CH_3}{|}}{Si}}- \right]_n$$
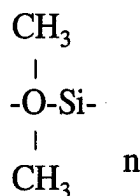
Figure 2-3. Repeating structural unit of silicone also known as poly(dimethyl)siloxane, the primary membrane material used throughout this work (Allcock and Lampe, 1981).

Silicone rubber shows very high diffusivity for gases, apparently connected with high internal mobility due to the presence of the -Si-O-Si- configuration in the chains of its molecules. The diffusion coefficient of the lower hydrocarbons in this rubber are about 10-20 times as high as in natural rubber and this makes it the rubber providing the highest known diffusivity (Van Amerongen, 1967). Solid rubber does not behave at all like a porous material as regards diffusion. Only molecules or particles of molecular dimensions can penetrate the rubber after forming a true solution. In forming such a solution, rubber behaves exactly like any organic amorphous, freely-deformable compound, in other words, like an ordinary organic liquid (Van Amerongen, 1967).

Diffusion through rubber involves not only Brownian motion of the penetrant molecules but also a micro-Brownian motion of segments of rubber molecules. It must be assumed that in rubber, as a result of thermal energy fluctuations, holes covering a whole spectrum of volumes and involving segments of several rubber molecules are continuously formed and destroyed. These holes are, therefore, not fixed in space, but on the average with time and at constant temperature there is a definite size distribution. The rate of diffusion will depend on the concentration of the holes that are of sufficient size to receive the diffusing molecules. If a Boltzmann distribution (the skewed probability curve associated with the kinetic energy distribution of particles (University of Idaho, 2002)) is assumed, the concentration of holes at any given moment will decrease exponentially with their size and this would cause a decrease in rate of diffusion when the diffusing molecules become larger (Van Amerongen, 1967).

The larger the diffusing molecules, the larger the difference between the rates of diffusion in various rubbers, and cyclization and branching of the diffusing molecules cause a considerable decrease in diffusion coefficients (Van Amerongen, 1967). The easier a gas is condensed, the higher the solubility. The process of solution of a gas involves condensation of the gas and mixing of the condensed gas with the rubber. The degree of solubility of a given gas in a rubber depends on their compatibility, i.e. on a specific interaction between the gas and the rubber molecules (Van Amerongen, 1967). Permeability of a rubber membrane typically is measured by placing the membrane between a reservoir containing gas at given constant pressure, for instance one atmosphere, and an initially evacuated reservoir, and measuring the relatively small pressure increase of the latter manometrically (Van Amerongen, 1967). .

2.3.3.2 Microporous Membranes: Several researchers have examined removal of gas-phase contaminants in microporous membranes including propene (Reij, 1996), toluene and dichloromethane (Hartmans, 1992a, 1992b), trichloroethylene (Pressman, 2000), trichloroethylene (Parvatiyar, 1996a, 1996b), benzene (Neemann, 1998) , and toluene (Ergas, 1999) . Mass transfer in hollow fibers has been previously studied and is well summarized in Pressman (1995) with specific explanations of mass transfer formulae found in Wickramasinghe and Semmens (1992) and Yang and Cussler (1986), while oxygen transfer in such membranes is described in Beeton et al (1994), Beeton (1991), and Coté et al (1989).

Others have examined VOC removal using these modules. During abiotic testing of a polysulfone module, less than 1% of the toluene was transferred to the liquid phase, showing that in the absence of bioactivity, negligible amounts of toluene would be removed from the air due to its dissolution in the membrane and aqueous phases (Parvatiyar et al, 1996b). In a membrane bioreactor designed to treat trichloroethylene, higher air flow rates (or lower gas residence times) led to lower removal efficiencies (Parvatiyar et al, 1996a).

Trichloroethylene (TCE) was degraded in a hollow fiber membrane module (HFMM) with a maximum trichloroethylene removal of 30% while toluene was continuously supplied (Dolasa and Ergas, 2000). Removal of TCE from contaminated air was accomplished with air on the shell side and water flow in the lumen (Pressman et al, 2000). 92 - 96% of TCE was cometabolized in the HFMM reactor loop. Short shell residence times, 1.6 to 5.0 minutes, gave adequate removal and demonstrated the quick throughput of TCE contaminated air (Pressman et al, 2000).

In other research, the effectiveness of a hollow fiber membrane bioreactor was investigated for biological nitrification; ammonia-containing gas was sent through the lumen and a nutrient/biomass solution was circulated in the shell (Keskiner and Ergas, 2000). After three weeks of operation, a gas phase ammonia removal efficiency of 83% was achieved. Toluene was degraded in a HFMM with removals ranging from 28-72% with a maximum removal of 42 g m^{-3} min^{-1} (Ergas et al, 1999).

Propene transfer from air to a suspension of propene-utilizing *Xanthobacter* Py2 cells in the membrane bioreactor was controlled by mass transfer in the liquid phase (Reij et al, 1995). The propene flux into the biofilm was 1x10^{-6} mol m^{-2} s^{-1} at a propene concentration of 9.3x10^{-2} mol m^{-3}. However, the activities observed in the reactor were less than 10% of the theoretical maximum consumption capacities of the biomass present in the reactor, demonstrating that mass transfer was limited by diffusion. In a reactor operated with liquid flow through the interior of the membrane clogging of the fibers by excess biomass was observed (Reij and Hartmans, 1994b). Maximum removal rates were 70-110 g propene m^{-3} h^{-1} in another HFMM (Reij and Hartmans, 1996). A gas residence time of 80 s was required to remove 95% of an initial propene concentration of 0.84 g m^{-3}. Clogging of individual fibers occurred as the biofilter aged when slow liquid flow rates were used. In the fast liquid flow reactor, none of the fibers were clogged with biomass and most fibers appeared to contain an evenly distributed biofilm. Higher conversion rates were found if the residence time of the gas in the membrane module was increased.

In an 8 cm^3 bioreactor with a flat PTFE membrane, 52-97% elimination of toluene was achieved with an influent of 75 mg toluene m^{-3} with a residence time of 4 - 24 seconds (Hartmans et al, 1990). The mass transfer coefficient calculated, (10^{-3} m s^{-1}),

was more than 4 times that of a trickle bed reactor. In another study, dichloromethane elimination was found to be 99% at a residence time of 9.6 s (Hartmans et al, 1992b). Several commercially available hydrophobic membrane materials (Teflon, Goretex, polyvinylidene fluoride, and polypropylene) were evaluated in a membrane bioreactor. The Accurel polypropylene membrane was determined to be the best choice for toluene and dichloromethane removal from air in a laboratory scale membrane bioreactor (Hartmans et al, 1992a).

2.4 LOAD CHANGES DURING BIOREACTOR OPERATIONS:

2.4.1 Introduction: Of the limited publications that exist, the majority of membrane biofilter research studies reported in the current literature have focused on VOC removal by bioreactors operating at a steady-state, or constant influent concentration (Ergas and McGrath, 1997; Neemann, 1999; Reij et al, 1997). Only one study (Parvatiyar et al, 1996b) was found that specifically examined the effect of load changes within membrane bioreactors. A limited number of studies with conventional biofiltration units have specifically examined the effects of step changes, transient and/or spike loading. Generally, after a spike loading or step loading has been applied, an efficiency decline occurs. Recovery time of the biofilters after increased loading has been mixed, with most researchers reporting rapid improvement and others reporting more lengthy recovery times. Some studies subjecting conventional biofilters to decreased loads or starvation periods have also been completed. Generally, researchers have found that biofilter recovery time is proportional to the length of the starvation period. The following very briefly recounts the information found within the literature concerning increased and decreased loads applied to biofilters.

2.4.2 Increased Loading: Mohseni and Allen (1997) examined the removal of alpha-pinene under continuous and unsteady state conditions using bench-scale biofiltration units operating with loading rates of 5-35 g α-pinene m^{-3} h^{-1}. An immediate decrease in removal efficiency was observed after step loads of α-pinene were applied, with recovery taking place after 24 hours. Biofilters removing hydrogen sulfide, methyl mercaptan, dimethyl sulphide, and dimethyl disulfide required approximately 30-40 hours to respond to step changes in loading (Wani et al, 2001). After step changes in concentration, about 2-5 hours were needed to reach new stationary conditions, while pollutant pulses gave reduced MEK and MIBK biodegradation rates in the upper part of a biofilter (Deshusses et al, 1996). For step changes, two biofilters in another study, one of hog fuel (a waste product of the forest industry) and one of compost, did not show any breakthrough for the five step changes applied, however, a contaminant spike of hydrogen sulfide caused an immediate increase in the outlet concentration (Wani et al, 1998). Three full-scale operational biofilters removing hydrogen sulfide maintained their ability to remove 99% of hydrogen sulfide during diurnal peak fluctuations in hydrogen sulfide concentration (Schowengerdt et al, 1999).

A biofilter with an inorganic filter bed designed for odor control at a wastewater treatment plant removed 99% of monitored gases and was found to react rapidly to sudden increases in loading (Patria et al, 2001) while a biofilter removing acetone showed recovery within 8 h after step changes in load (Tawil and Hamer, 2000). In a polysulfone membrane bioreactor removing toluene, step changes in load resulted in immediate efficiency declines with full recovery taking place after several weeks (Parvatiyar et al, 1996b).

2.4.3 Decreased Loading: In a study by Mohseni and Allen (1997), a 70 h period of starvation led to little removal of α-pinene, however, the biofilters regained their efficiency after 24 h of operation. In other biofilters, the re-acclimation times to reach full removal capacity after short periods of starvation were also short, ranging between 15 and 120 h. Extended periods of starvation resulted in longer re-acclimation periods in a study by Wani et al (1998). After a five-day stoppage, prompt and efficient treatment was readily reestablished for MIBK and MEK elimination (Deshusses et al, 1996). Broadly speaking, the longer the period of starvation, the longer it takes the filter to get back to steady-state (Gerrard et al 1997).

In an attempt to limit detrimental excess biomass growth at the inlet of a biofilter the results on performance of changing the direction of the feed flow to a silicate pellet-containing biofilter was investigated (Song and Kinney, 2001). The bioreactor operated with a three day switching frequency had the highest removal capacity with a maximum elimination capacity of greater than 120 g toluene m^{-3} h^{-1}, recovered from switching after approximately 24 h, and provided the most stable performance. A seven-day switching frequency was found, however, to deprive the heterotrophic organisms of carbon for too long to maintain their viability. Biofilter communities removing methanol and α-pinene at increased temperatures were also able to quickly recover from a shut-down period of up to two weeks (Allen et al, 2000). Three lab-scale biofilters with mixtures of chaff/compost, diatomaceous earth/compost, and granular activated carbon/compost used for removing toluene responded effectively to shut down and granulated activated carbon added to the filter bed was found to improve the biofilter performance (Tang et al, 1995)

2.5 SUMMARY OF PILOT- AND FULL-SCALE OPERATIONS:

Although numerous studies have examined the performance of pilot- and full-scale conventional biofilters and biotrickling filters, no study has reported the operational results of pilot- or full-scale membrane bioreactors. Many pilot- and full-scale biofilters and biotrickling filters are reported to provide both good removal on a mass basis and good efficiency of removal on a percentage basis. The results of some representative studies are summarized in the following paragraphs and an extensive table of results of pilot studies is shown in Devinny et al (1999).

A mobile pilot-scale biofilter operated for 119 days gave 96-98% removal efficiency for BTEX, ethanol, and styrene compounds at loading rates of 15.4 - 74.9 g m^{-3} h^{-1} (Eszenyiova et al, 2001). A pilot scale unit at a Ford assembly plant captured and degraded all hydrophyllic solvents, such as butanol, while for toluene a 74 - 91% removal without powdered activated carbon (PAC) and 86 - 93% removal with the addition of PAC was accomplished (Kim et al, 2000). A compost composite biofilter pilot plant, designed to treat 470 m^3 air hr^{-1}, was constructed to treat the effluent from bakery ovens (Hodges, 2001b). During the first loading period, ethanol elimination rates ranged from 171 - 236 g m^{-3} h^{-1} with ethanol loads ranging from 418 to 498 g m^{-3} h^{-1}. Average ethanol removal efficiency was 41%. For the second loading period, elimination rates ranged from 92 to 166 g m^{-3} h^{-1} with loads ranging from 106-266 g m^{-3} h^{-1}. Average removal efficiency for the second sampling was 78%. A compost/bark biofilter removed more than 70% of VOCs and approximately 85% of ethanol from an off-gas containing up to 3.5 g m^{-3} of organic compounds from a casting operation (Hodges, 2001a). Typical elimination rates of 145 g m^{-3} h^{-1} were found under these conditions while the chlorofluorocarbons present in the off-gas were not removed.

Eighteen pilot-scale biofilters were used to compare the effects of varying the ratio of compost and wood chips and moisture content on odor, ammonia, and hydrogen sulfide emissions from a swine facility (Nicolai and Janni, 2001). Moisture content was the critical factor for odor, ammonia and hydrogen sulfide removal with the ratio of compost to wood chips important for controlling pressure drop; a 20-30% compost percentage recommended for the best treatment of air contaminants from the swine facility. Bark/soil biofilters with new media and lower air loading rates generally performed better with low air loading rates giving the best removal rates (Luo, 2001). A biotrickling filter was examined for its ability to remove odors from a wastewater treatment plant during high H_2S loading conditions (Wu et al, 2001). Reducing the gas residence time from 30 s to 5 s had little impact on removal efficiency when influent concentrations were less than 20 ppm. Shock loadings decreased performance, however, recovery was relatively fast.

A pilot-scale biofilter utilizing peat attained an elimination capacity of 165 g m^{-3} h^{-1} for toluene, 66 g m^{-3} h^{-1} for xylene and 115 g m^{-3} h^{-1} for a mixture of toluene and xylene (Jorio et al, 1998). The performance was found to be dependent on the temperature of the filter media and the pressure drop across the bed. In a pilot-scale peat biofilter, toluene removal efficiencies approached 99% at an influent load of 0.71 kg COD m^{-3} d^{-1} with adequate moisture contributing to the consistent long-term performance of the biofilter (Sorial et al, 1997). In a pilot-scale reactor containing peat, >99% of influent H_2S and methanethiol were removed from exhaust gas of a waste treatment facility (Cho et al, 1992).

An open bed biofilter was used to treat discharge air from a total phase extraction system at a former petroleum bulk storage terminal (Matrix Environmental Technologies, 2001). The biofilter operated between 90% and 100% efficiency through most of the data collection period. A pilot and full-scale compost, peat, and wood chip biofilter was used to treat acrylic resin precursors (Hsu et al, 2000). Odor was reduced up to 99% with flow rates of 120 m^3 min^{-1} in the full-scale plant. A deep bed dairy biofilter and a naturally ventilated swine finishing barn manure pit biofilter case studies were described by Janni and Nicolai (2000). Long term performance of the biofilter at the dairy barn ranged from 57 - 95% odor reduction, 75-100% hydrogen sulfide and 60 -100% ammonia reduction with performance apparently related to moisture content of the bed; reductions at the swine finishing biofilter were found to be similar.

"Package" plants or proprietary designs have also apparently exhibited good removals of organic compounds. A pilot study involving four biofilters, loaded with proprietary mixes of BIOMIX and BIOSORBENS were used to treat waste gas from a PCB and vinyl resins industry. The inorganic media, BIOSORBENS, was reported to require much less volume to treat the same contaminant load (Shareefdon and Cantwell, 2000). Long term performance of BIOREACTOR plants currently in full-scale operation have been described (Popov, 2000).

2.6 CONVENTIONAL BIOFILTER DESIGN INFORMATION:

Because of extensive study and operation of pilot- and full-scale units, some design generalizations can be made concerning conventional biofiltration units. The design parameters include (Anit and Artuz, 2000): (1) space constraints - a small biofiltration unit can handle gas flows of approximately 0.85 m^3 min^{-1} in as little space as

2.3 m^2; (2) chemical constituents and concentrations - biofilters perform best when treating hydrophyllic compounds with concentrations (mixing ratios) <1000 ppm; (3) residence time - most biofilters are designed with residence times of 30 s to 1 min; (4) humidity - humidification is required and >95% is usually desired; (5) pH control - buffering may be required as the result of biological activity that can yield organic acids; (6) media selection - natural and/or man-made; (7) pressure drop; and (8) maintenance frequency - weekly in the beginning reducing to bi-weekly or monthly.

Devinny et al (1999) echoes some of the same considerations in the design of a full-scale conventional biofilter including whether to choose a closed or open bed system, series or parallel operation, the filter bed medium, the air distribution systems, pre-processing of the waste gas, temperature of operation, moisture content, compaction/nutrient loading, computer control and analytical systems, and electrical requirements (Devinny et al, 1999).

2.7 DESIGN OF THE MEMBRANE BIOREACTOR:

No journal articles or texts were located that specifically discussed design parameters for membrane bioreactors with the exception of Ergas et al (1999) who presented a model that may be used to design polyporous hydrophobic membrane bioreactors. However, many parameters are alluded to and discussed individually in research articles that would affect design of a pilot-scale or full-scale membrane bioreactor unit. The design parameters for a membrane bioreactor unit are discussed in the modeling chapter, however, are mentioned here in summary. The design of a pilot- or full-scale dense phase membrane biofilter would have to consider at least the influent VOC concentration and the VOC itself, air flow rate, temperature of the influent air,

number of tubes and their resulting membrane surface area, the total reactor volume,

organisms used for inoculation, type and dimensions (O.D., I.D. thickness) of the dense

phase material, its composition (latex or silicone), and the membrane's resulting

permeability for the VOC of interest, and the liquid recirculation rate desired if any.

As a comparison of reactor systems, the "footprint" or floor space requirement of

the current semi-pilot scale reactor was compared to the hypothetical design of a packed

bed tower and a conventional biofilter. For the design of the conventional biofilter

empirical information is required from lab-scale or similar tests (Devinny et al, 1999).

Scale-up is then based primarily on the empty bed residence time encountered in that

initial reactor system. A biofilter removing BTEX compounds was found to give a 70%

removal of BTEX compounds at an empty bed residence time of 1.8 minutes (0.03 h)

(Devinny et al, 1999, p. 227). Using this empty bed residence time value and the known

airflow ($19.8 \text{ m}^3 \text{ h}^{-1}$) into the semi-pilot-scale reactor used during the present study, the

bed volume was calculated using Equation 2-1.

$$Vf = EBRT*Q = (0.03 \text{ h})(19.8 \text{ m}^3 \text{ h}^{-1}) = 0.6 \text{ m}^3 \qquad (2\text{-}1)$$

EBRT = empty bed residence time (h)
Q = volumetric airflow ($\text{m}^3 \text{ h}^{-1}$)
Vf = volume of bed (m^3)

Countercurrent packed bed tower design equations may be found in appropriate

references (Hesketh, 1996; Davis, 2000). Countercurrent packed tower capacities may be

found by fixing the desired pressure drop, using the physical properties and flow rates of

the liquid and gas streams involved and using generalized pressure drop correlations

(Hesketh, 1996). Equation 2-2 is one such pressure drop correlation (Hesketh, 1996)

$$X = \frac{LM_l}{GM_g}\left(\frac{\rho_l}{\rho_l}\right)^{0.5}$$

(2-2)

where

L = liquid flow rate (g mole cm^{-2} h^{-1})
G = gas flow rate (g mole cm^{-2} h^{-1})
M_l = molecular weight of liquid
M_g = molecular weight of gas

Equation 2-3 calculates the corrected gas flow rate (Hesketh, 1996):

$$G = \left[\frac{Y\rho_g\rho_l}{M_g^2 F\psi\mu_l^a}\right]^{0.5}$$

(2-3)

where

G = gas flow rate (g mole cm^{-2} h^{-1})
Y = ordinate of pressure drop graph
F = packing factor
Ψ = ρ_{H2O}/ρ_l
μ_l = viscosity of liquid (g cm^{-1} sec^{-1})
a = 0.2 when F>90 and 0.1 when F<90

Equation 2-4 calculates the tower diameter (Hesketh, 1996):

$$D_T = 1.25\left[\frac{QP_T}{G(273+t)}\right]^{0.5}$$

(2-4)

D_T = tower diameter (m)
Q = gas volumetric flow rate (m^{-3} h^{-1})
P_T = tower pressure (atm)
T = temperature (^{o}C)

For the conditions in the laboratory, 20 °C, 1 atm pressure, Table 2-1 compares the "footprint" or diameter of various cylindrical reactor systems.

Table 2-1 Comparison of reactor systems.

	Media	Diameter (cm)
Membrane Bioreactor	Silicone Tubing	25
Conventional Biofilter	Wood Compost	87
Countercurrent Packed Tower	Plastic Pall Rings	7
Countercurrent Packed Tower	Ceramic Raschig rings	11

The footprint of the conventional biofilter is the largest while the countercurrent packed towers are the smallest. The membrane bioreactor falls between the two extremes. Therefore, if space was a predominant concern, the packed towers and membrane bioreactors might offer the best solutions for contaminant removal. The results shown in Table 2-1 also suggest mass transfer (and thus removal from the gas stream) occurs most efficiently within the packed tower reactors. However, the packed towers do not offer the benefit of immediate destruction or biodegradation of the contaminant. In the packed tower design, the contaminant is transferred to the liquid phase but then must be sent to a wastewater treatment plant or similar facility. The membrane bioreactor and the conventional biofilter offer the advantage of destruction immediately after mass transfer into a liquid phase.

2.8 BACTERIAL DEGRADATION PATHWAYS:

It is expected that toluene was used by the organisms within the bioreactors as both a carbon source for cell building and maintenance and as an electron donor.

Through the catabolic process of toluene degradation, ATP is formed to be used in cell

maintenance and cell building. The basic process of cell metabolism and ATP formation

is covered in Brock and Madigan (1991). An overall oxidation-reduction equation is

shown in Equation 2-5 (Gottschalk, 1986).

$$X_{red} + A_{ox} \longrightarrow X_{ox} + A_{red} \qquad (2\text{-}2)$$
$$ADP + P_i \qquad\qquad ATP + H_2O$$
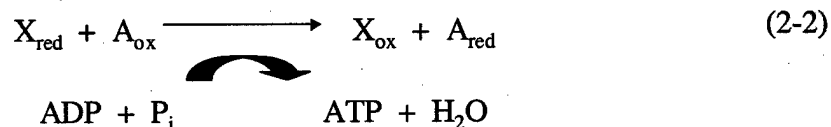
where

X_{red} = electron donor (toluene)
A_{ox} = electron acceptor
X_{ox} = oxidized compound
A_{red} = reduced compound
P_i = inorganic phosphate
ADP = adenosine diphospate
ATP = adenosine triphosphate

There are several pathways by which toluene is aerobically degraded. One

bacterial degradation pathway for toluene is the benzoate pathway that leads to the

formation of catechol. Catechol may then be degraded by two alternate pathways, the

ortho-cleavage (3-oxoadipate) and the meta-cleavage pathway. The degradation of

toluene through both of these pathways is shown in Figures 2-4 and 2-5 (Gottschalk,

1986). Each figure shows the names of the compounds formed and their carbon (C) atom

numbers. The chemical structures of the end products, acetaldehyde, pyruvate, succinate,

and acetyl coenzyme A are shown in Figures (2-6). Another source (UMN, 2002)

indicates alternate degradation pathways for toluene, depending upon the bacteria

present. Those pathways are shown in Figures (2-7) - (2-9). Each step in the process of degradation is catalyzed by a specific enzyme.

Toluene (7C)

↓

Benzyl alcohol (7C)

↓

Benzaldehyde (7C)

↓

Benzoate (7C)

↓

Catechol (6C)

↓   ← O_2

Cis,cis-muconate (6C)

↓

Muconolactone (6C)

↓

4-oxoadipate enol lactone (6C)

↓

3-oxoadipate (6C)

Acetyl (2C) - SCoA   Succinate (4C)
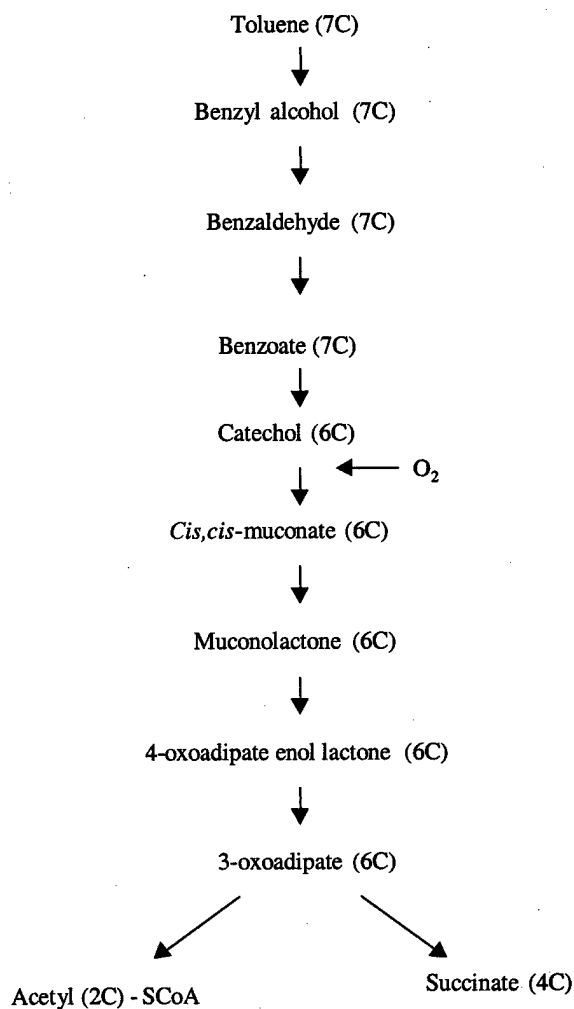
Figure 2-4. Ortho-cleavage or 3-oxoadipate (catechol) pathway, an aerobic toluene degradation pathway.

Toluene (7C)

↓

Benzyl alcohol (7C)

↓

Benzaldehyde (7C)

↓

Benzoate (7C)

↓

Catechol (6C)

↓ ◀— O_2

2-hydroxymuconic semialdehyde (6C)

H_2O ——▶ ↓ ——▶ HCOOH

2-oxopent-4-enoate (5C)

↓◀— H_2O

4-hydroxy-2-oxovalerate (5C)

↙   ↘

Pyruvate (3C)   Acetaldehyde (2C)
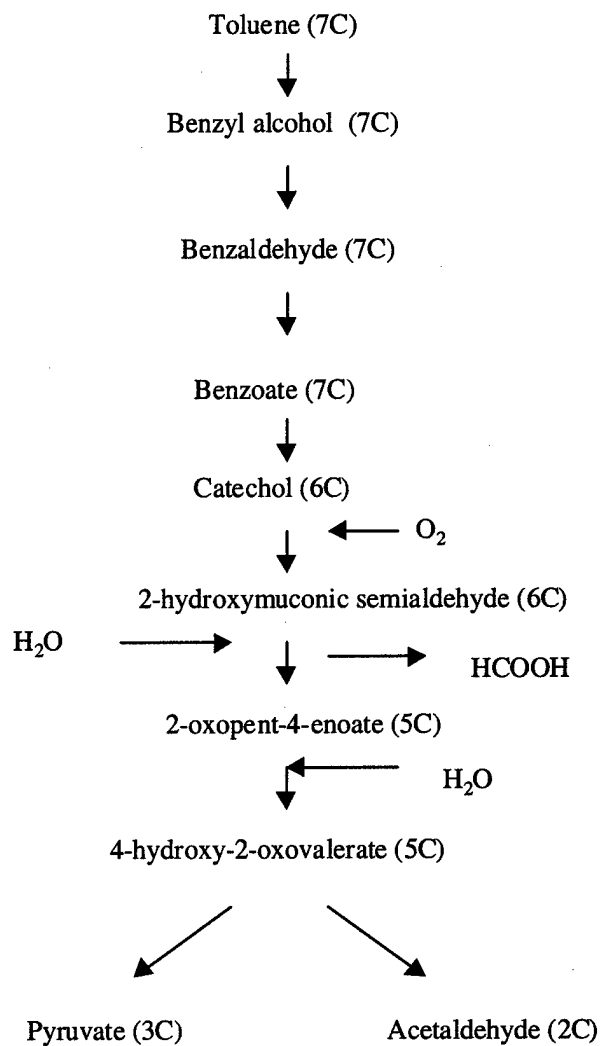
Figure 2-5. Meta-cleavage (catechol) pathway for toluene, an aerobic toluene degradation pathway.

$$
\begin{array}{cccc}
\text{O} & \text{COOH} & \text{CH}_2\text{-COOH} & \text{O} \\
\| & \text{C=O} & \text{CH}_2\text{-COOH} & \| \\
\text{CH}_3\text{CH} & \text{CH}_3 & & \text{CoA-SCCH}_3
\end{array}
$$
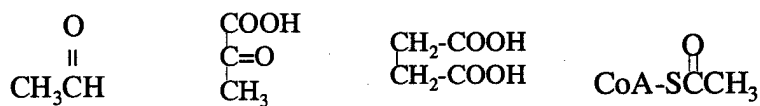
Figure 2-6. Structure of acetaldehyde (Whitten and Gailey, 1981), pyruvate, succinate, and acetyl coenzyme A (Gottschalk, 1986), products of bacterial degradation.

Toluene

↓

Benzyl alcohol

↓

Benzaldehyde

↓

Benzoate

↓

cis-1,6-dihydroxy-2,4-cyclohexadiene-1-carboxylic acid

↓

Catechol

↓

2-hydroxymuconic semialdehyde

↓

cis-2-hydroxy-penta-2,4-dienoate

↓

4-hydroxy-2-oxovalerate

Pyruvate   Acetaldehyde
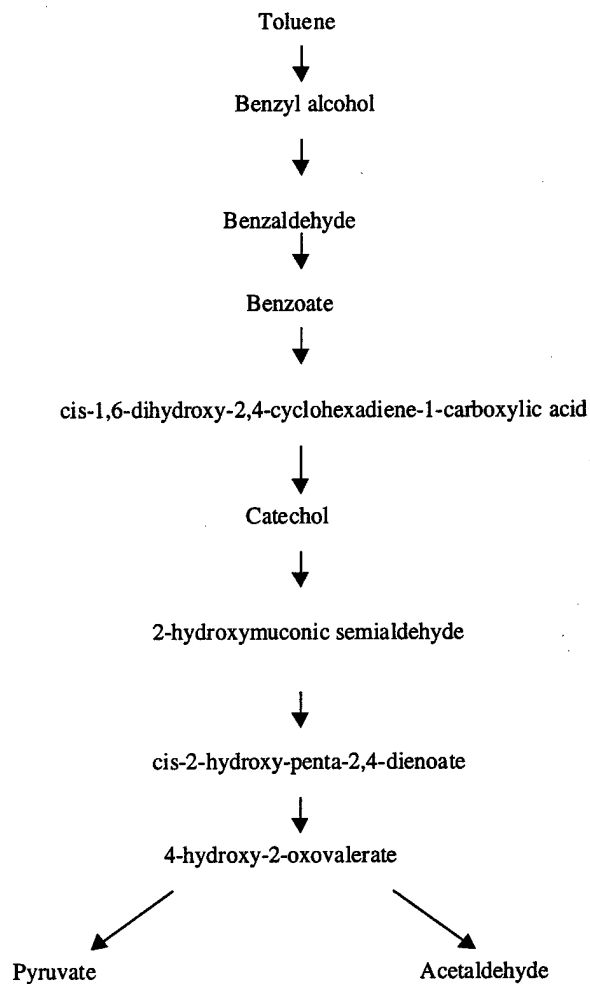
Figure 2-7. The aerobic toluene degradation pathway initiated by *Pseudomonas putida*.

Toluene
Burkholderia cepacia

Toluene
Pseudomonas picketti

Toluene
Pseudomonas putida

2-hydroxy-toluene

3-hydroxy-toluene

Toluene cis-dihydrodiol

3-methyl catechol

cis, cis-2-hydroxy -6-oxohepta-2,4-dienoate

cis-2-hydroxypenta - 2,4 -dienoate

4-hydroxy-2-oxo-valerate

Pyruvate

Acetaldehyde
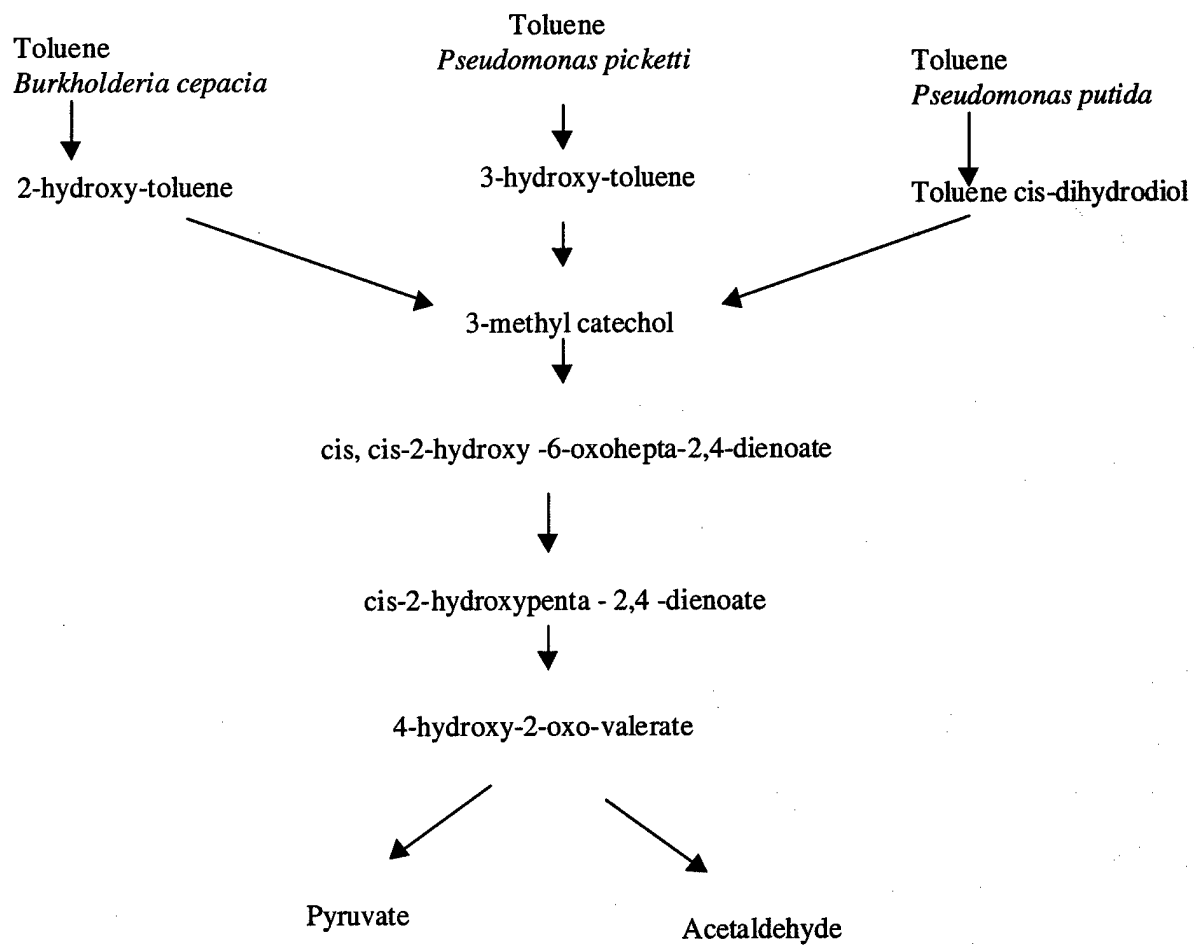
Figure 2-8. The aerobic toluene degradation pathway initiated by *Burkholderia cepacia*, *Pseudomonas picketti*, and *Pseudomonas putida*.

Toluene

↓

4-hydroxy-toluene

↓

4-hydroxy-benzaldehyde

↓

4-hydroxy-benzoate

↓

3,4-dihydroxybenzoate

3-carboxy-cis,cis-muconate   2-hydroxy-4-carboxymuconate semialdehyde
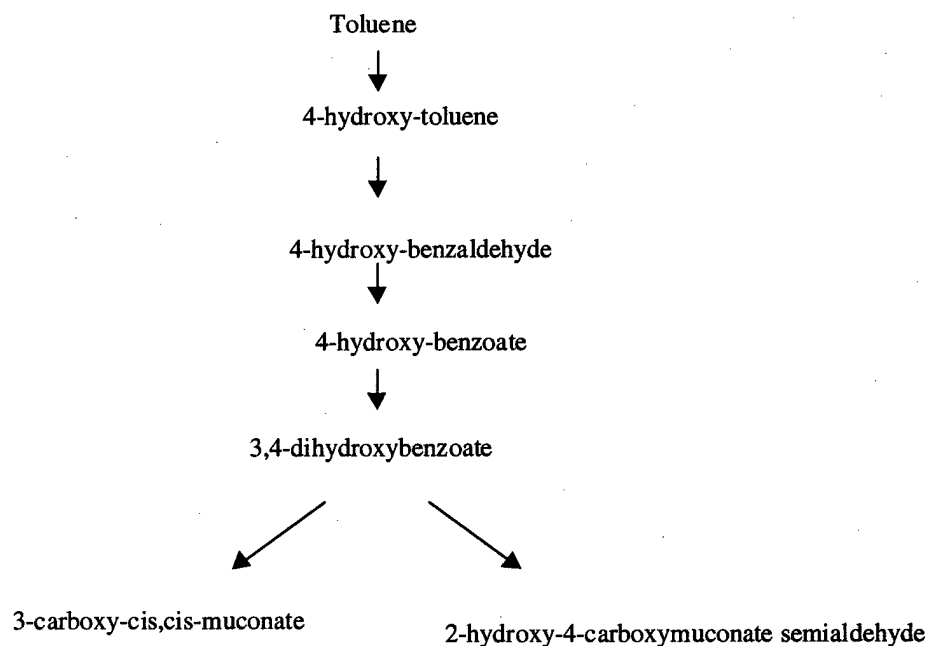
Figure 2-9. The aerobic toluene degradation pathway initiated by *Pseudomonas mendocina.*

The anaerobic metabolism of toluene is shown in Figure 2-10. The metabolic sequence proceeds through benzyl succinate to the benzoate anaerobic pathway, which is detailed elsewhere (University of Minnesota, 2002). Anaerobes may use either nitrate, sulfate, or organic substrates as electron acceptors.

Toluene Anaerobic Pathway
Thauera aromatica
Azoarcus sp. strain T.

Toluene

↓

Benzyl succinate

↓

Benzylsuccinyl-CoA

↓

E-phenylitaconyl-CoA

↓

Benzoyl-CoA

↓

Benzoate Anaerobic Pathway
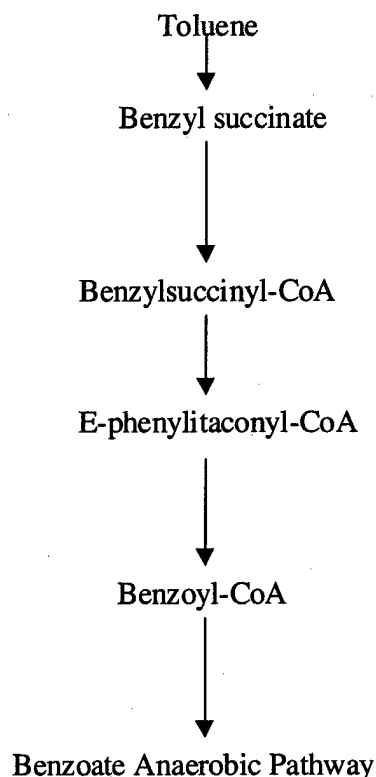
Figure 2-10. The anaerobic metabolism of toluene, (University of Minnesota, 2002)

Because biomass growth is apparently controlled by limiting nutrients, nutrient

limitation within a membrane bioreactor might be expected to cause either a limitation in

biomass growth or cause a decline in removal efficiency. To explore the hypothesis that

nutrient limitation might hinder biofilter performance, several studies were examined.

Kinney et al (1998) (in Moe and Irvine, 2001a) operated a laboratory biofilter packed

with ceramic pellets using NH_4Cl as a nitrogen source that experienced efficiency

declines after depletion of the ammonia nitrogen. Efficiency decline could be either

related to a change in organism degradation kinetics or related to the organisms that actually develop under the nutrient limited conditions. The proliferation of organisms in a particular environment will depend on the specific nutrients available and the nutrient concentration. Depending on the limiting nutrient, different enzymes within the cell may limit growth, and the microorganisms may exhibit different saturation coefficients (Characklis and Marshall, 1990, p 240). In one specific instance, nutrient limitation resulted in a gradual decrease in elimination capacity of a dimethyl sulfide-removing biofilter (Smet et al, 1999). In another instance, a compost that released nitrogen slowly was found to be desirable to keep removal of contaminants elevated (Hwang et al, 2000)

2.10 CURRENT STUDY CONTAMINANTS:

Toluene was selected for study because it is a common air pollutant generated from the refining of crude oil; up to a billion pounds a year are never isolated from the crude oil and are added directly to gasoline (EPA, 1994b). Toluene is also used in the manufacture of benzene, coatings, strippers, adhesives, cosmetics, perfumes, anti-freeze (EPA, 1994b). Toluene at concentrations found in indoor workplaces can be associated with irritation to the eyes, nose, and skin and may affect the liver, kidneys and central nervous system (NIOSH, 1997). Toluene is listed as an "A4 category - not classifiable as a human carcinogen", and has an OSHA Permissible Exposure Limit of 200 ppm (ACGIH, 2000; OSHA, 2002). Toluene is an aromatic hydrocarbon, has the chemical formula C_7H_8, and is shown in Figure 2-11 (Whitten and Gailey, 1981).
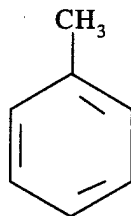
Figure 2-11. Chemical structure of toluene, the primary contaminant examined during this work.

1-butanol was selected for part of this study because benzene, the contaminant originally chosen for study in a polysulfone module by Zhang (2000), was found to be absorbed into the polysulfone. 1-butanol was not anticipated to be absorbed, as predicted by chemical structure of the polysulfone polymer (Allcock and Lampe, 1981). Additionally, 1-butanol is an industrial contaminant of interest with 1.3 billion pounds produced in 1992 (USEPA, 1994a) with some health effects possible at levels found within work environments (NIOSH, 1997). As an indoor air contaminant, 1-butanol has a Threshold Limit Value (TLV-Ceiling) of 50 ppm and an Occupational Safety and Health Administration Permissible Exposure Limit of 100 ppm. 1-butanol is produced from the anaerobic batch fermentation of corn starch to glucose then butanol, followed by distillation for recovery of the butanol (Illinois Corn Growers Association, 2001). 1-butanol has the chemical structure $CH_3CH_2CH_2CH_2$-OH (Whitten and Gailey, 1981).

A very limited number of studies have addressed the use of conventional biofilters for treating elevated temperature gas streams. In a conventional biofilter, heated gas streams would come into direct contact with the biofilm while in a membrane bioreactor, the tube material might offer some resistance to heat transfer, potentially protecting the biofilm. A biotrickling filter removed 220 g ethanol m^{-3} h^{-1} at both 22 °C and 53 °C (Cox et al, 2001), a compost biofilter removed 110 g toluene m^{-3} h^{-1} at 45 - 55 °C (Matteau and

Ramsay, 1997), and another compost biofilter removed 90 - 95% of nitric oxide with an influent concentration 500 ppm at 55 °C (Lee et al, 2001). Greater than 95% removal was seen for alpha-pinene (15 ppm) and methanol (110 ppm) at 55 °C by Dhamwichukorn et al, (2001).

In other elevated temperature studies, removal rates for alpha-pinene and methanol were found to be 60 g m^{-3} h^{-1} and 100 g m^{-3} h^{-1}, respectively (Allen et al, 2000). Kong et al (2001) showed that high removal levels of alpha-pinene (540 ppm) in a trickling filter are possible at thermophilic temperatures as high as 55 °C. The removal rate and acclimation time were found to be dependent upon the temperature (higher rates of alpha pinene removal were seen with higher temperatures). The effects of operating temperature were examined for a jacketed trickle-bed biofilter packed with porous foam for treatment of NO (Klasson and Davison, 2001). Removal of NO was 100% with an empty bed residence time of 2 minutes and there was no apparent temperature effects over the interval studied. Some researchers have mathematically modeled these contaminant removal processes (Karamanev et al, 1999; Ahmed, 1997) in conventional biofilter units while others have demonstrated the use of extremophiles in novel, multi-phase bioreactor technologies (Wright et al, 2000). Another study examined membrane biofiltration at elevated temperatures; NO_x removal efficiency was maintained at 70% regardless of gas composition or temperature changes (20-55 °C) (Min et al, 2002).

Heat transfer information for dense phase membranes is also limited. The majority of heat transfer coefficients commonly cited are associated with heat transfer from the suspension in fluidized beds (Golriz, 1996; Tia et al, 1996), however, a few

coefficients were found for membrane distillation processes (Martinez-Diez and

Vazquez-Gonzalez, 2000; Garcia-Payo et al, 2000; Gryta et al, 1997).

CHAPTER 3
METHODS AND MATERIALS

3.1 OVERVIEW:

Several bioreactor designs, measurement techniques, and analytical methods were used to meet the goals and objectives of this project. The bioreactor designs used included a small microporous membrane (polypropylene) module bioreactor, single silicone tube bench-scale membrane bioreactors, a larger dual silicone tube bench-scale bioreactor, and a multiple silicone tube semi-pilot-scale bioreactor. Measurement techniques included:

- growth of microbial batch cultures with subsequent headspace analysis using gas chromatography to determine microbial kinetic rates;

- gas and liquid inlet and outlet sampling of abiotically and biotically operated bioreactors; and

- microorganism identification using microbial plating, gram staining, and 16S rDNA analysis.

Pressure drop, pH, dissolved oxygen, optical density, temperature, and water loss were also periodically monitored for the reactors. Other techniques used included ion chromatography for analysis of liquids and temperature measurements to determine heat transfer coefficients.

3.2 BIOREACTORS:

3.2.1 Butanol Reactors: The butanol removal study focused on three separate phases: continuous, steady-state operation of the bioreactor (Phase I) performed by a masters student, Bo Zhang (2000); start-up with immediate placement onto an 8-h "on" and 16-h

"off" condition with a weekend "off" condition, added later (Phase II); and start-up into a continuous operation followed by an 8-h "on" and 16-h "off" condition (Phase III).

The bioreactor operated during Phases I and II incorporated a Koch Membrane Systems microporous polysulfone membrane module (part # 0.3-75-PM500-PB). The module contained 42 fibers with internal diameter of 75 μm and a pore size diameter of 0.05 μm. The module was 17.78 cm in length, 2.54 cm in diameter, and had a lumen volume of 39.5 mL. The bioreactor operated during Phase III was also a Koch Membrane Systems microporous polysulfone membrane module (part # 0.2-106-PM500-PB), but contained 17 fibers with internal diameter of 106 μm and a pore size diameter of 0.05 μm. The module was 17.78 cm in length and 2.54 cm in diameter.

The gas phase schematic of the bioreactor is shown in Figure 3-1. Air supplied by an aquarium air pump (Renaissance 300; 115 V, 4 W, 60 Hz) was split with both flows passing through rotameters; a small amount of the air flowed through the headspace of a flask containing 1-butanol. The split of air was controlled to deliver the desired concentration of 1-butanol. After rejoining, the air stream passed into the bioreactor, through a moisture trap and was vented. The air flow was downward, allowing any liquid which passed into the gas phase to easily flow out of the system. Sampling ports for gas extraction were placed in-line. Sampling ports were brass tees with one side sealed with a Teflon®/silicone rubber septum. Stainless steel tubing, brass Swagelok® fittings, neoprene rubber stoppers and Teflon®-lined silicone rubber septa were used for all VOC-containing gases to minimize any losses. A Toastmaster 24-h timer and manually operated valve were used to control entry of 1-butanol-contaminated air during Phase II; a solenoid valve replaced the manual valve during Phase III.
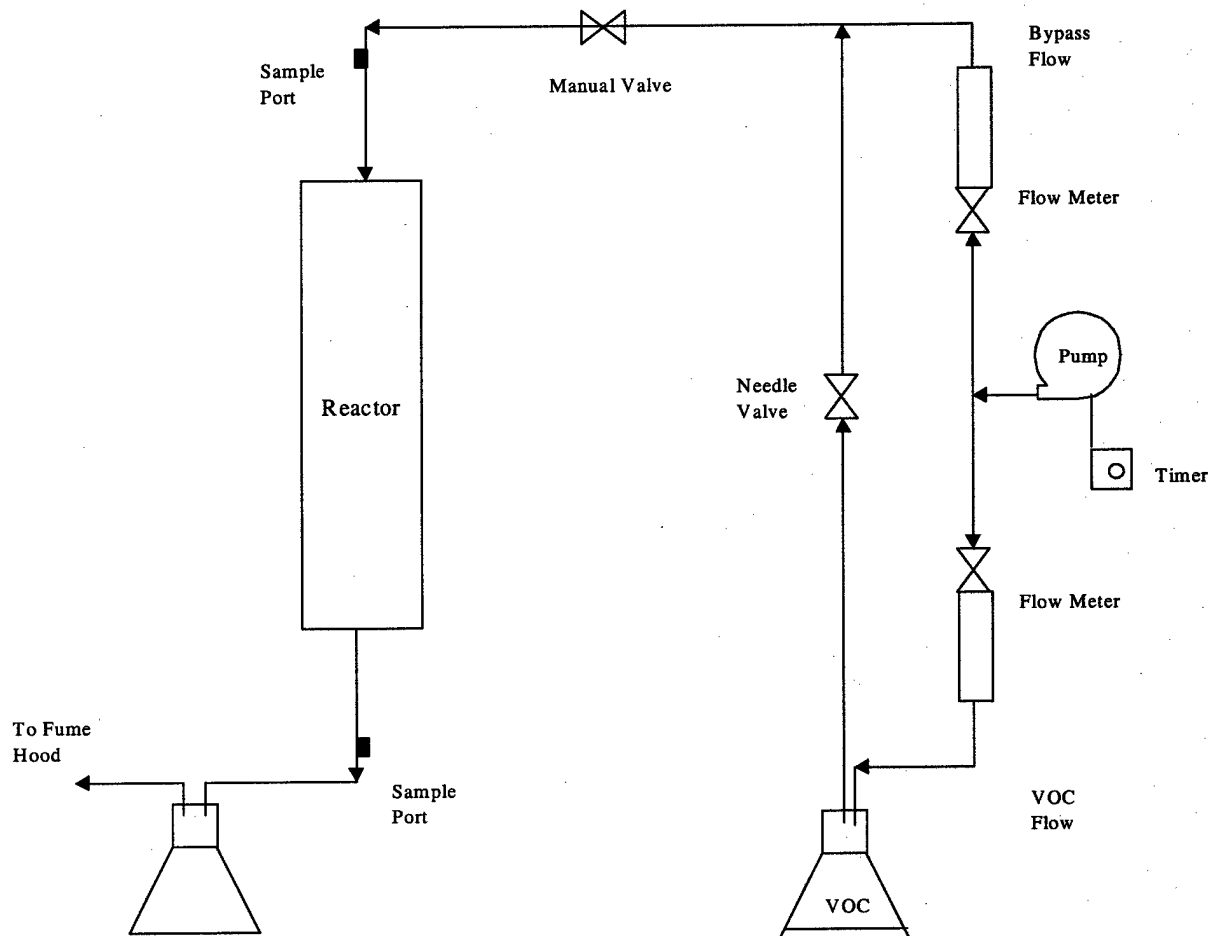
Figure 3-1. Gas phase schematic of the butanol membrane bioreactor.

The bioreactor liquid phase schematic is shown in Figure 3-2. Liquid flow

through the reactor was from bottom to top, countercurrent to the gas flow. The choice of

flow direction allowed any gas bubbles in the liquid to be purged up and out of the

reactor. A peristaltic pump (Cole Parmer Instrument Company, Model 7553-85) with

Masterflex speed controller (Cole Parmer Instrument Company, Model 7553-71, 50/60

Hz, 115 V, 3 Amp) circulated the nutrient solution and a bubble-catching system was

added to minimize disturbance of the biofilm. This bubble catcher was a glass

Erlenmeyer flask with a liquid drip inlet, submerged outlet, and an opening vented to the

atmosphere to allow any excess liquid or any gas bubbles to be removed from the system.
The liquid side had a total liquid volume of approximately 600 mL of nutrient solution
determined by adding the liquid volume of the reactor module, the bubble catcher and
tubing. Flexible Tygon® tubing and Teflon®-lined silicone rubber septa were used
throughout the liquid phase configuration.
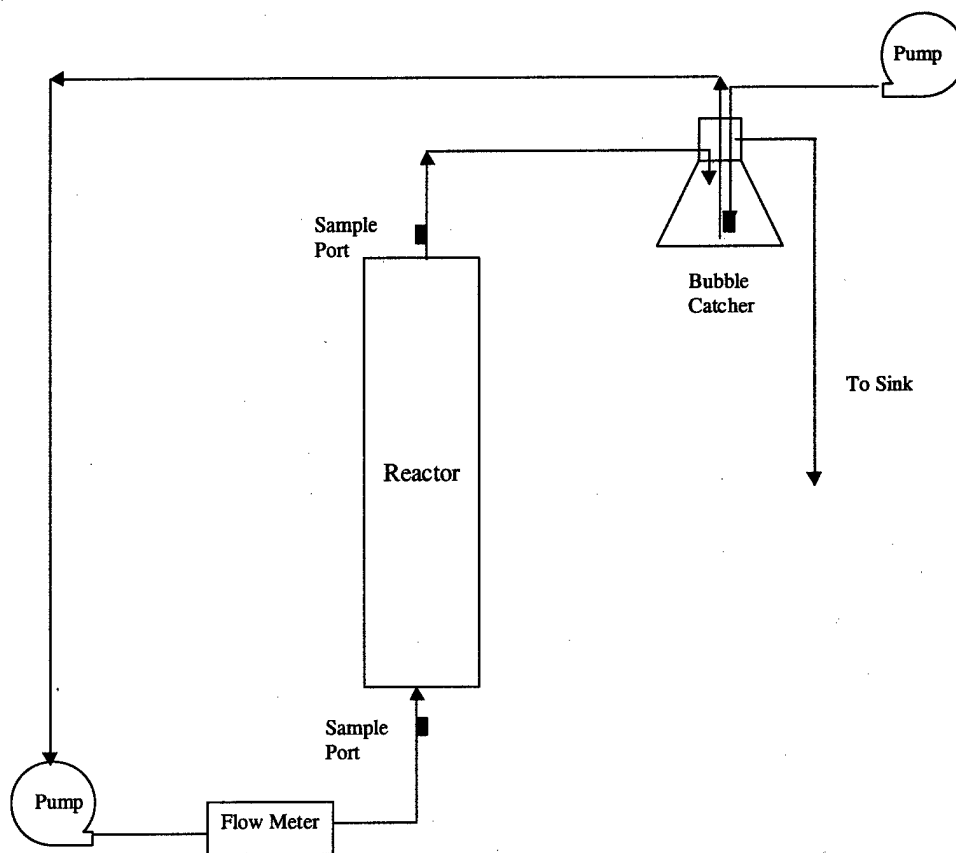
Figure 3-2. Liquid phase schematic of the butanol membrane bioreactor.

3.2.2 Toluene Reactors: Three cylindrical bench-scale bioreactors were used to remove toluene from contaminated air. The first was a short, single silicone rubber tube membrane bioreactor, the second, a long, single silicone rubber tube membrane bioreactor, while the third was a larger, dual silicone rubber tube membrane bioreactor. A semi-pilot-scale bioreactor with 25 silicone rubber tubes was also constructed and operated. All toluene-removing bioreactors employed 3/8" I.D., 1/2" O.D., 1/16" wall thickness silicone tubing membrane(s) (Cole-Parmer Incorporated, catalog number 06411-12). The bioreactor general information is summarized in Table 3-1.

Table 3-1. Summary of reactor configurations.

	Reactor #1	Reactor #2	Reactor #3	Reactor #4
Name	Short, single tube	Long, single tube	Dual tube	Semi-pilot-scale
Tube number	1	1	2	25
Module (outer shell) material	Glass	Glass	Clear PVC	PVC
Module volume (cm^3)	965	1390	1990	78,500
Module length (cm)	30.5	60.9	77.5	155
Module I.D. (cm)	5.08	4.13	5.08	--
Module O.D. (cm)	6.35	5.39	5.72	25.4
Tube O.D. (cm)	1.27	1.27	1.27	1.27
Tube I.D. (cm)	0.953	0.953	0.953	0.953
Tube length (cm)	18.6	53.3	66.0	130
Total lumen volume (cm^3)	13.3	39.9	94.1	2310
Total tube outer surface (cm^2)	74.2	213	527	12,900
Airflow (mL min^{-1})	760	760	1370	Variable
Gas residence time (s)	1	3.1	4.1	Variable
Liquid flow rate (mL min^{-1})	10	10	15	2000

The short, single tube module consisted of a glass Kimax process beaded pipe, 30.5 cm in length, 5.08 cm internal diameter, 6.35 cm external diameter with two neoprene rubber stoppers cored to accommodate 0.3 cm (1/8") stainless steel tubing carrying the gas phase and 0.6 cm (1/4") Tygon® tubing containing the liquid phase with a reactor volume of 965 cm^3. The silicone tube was 18.6 cm in length with a lumen volume of 13.3 cm^3 and an external silicone tube surface area of 74.2 cm^2. The air flow

in the reactor was 760 mL min^{-1} yielding a gas residence time of 1.0 s. The liquid flow rate was 10 mL min^{-1}.

The long single tube module was a glass pipe, 4.13 cm internal diameter, 5.39 cm external diameter, length of 60.9 cm, lumen volume of 39.9 mL and reactor volume of 1390 cm^3. The silicone tube was 53.3 cm in length and had an external tube surface area of 213 cm^2. The reactor had an air flow of 760 mL min^{-1} with a gas residence time of 3.1 s and a water flow rate of 10 mL min^{-1}.

The large, dual tube module was a 77.5 cm in length, 5.72 cm outer diameter clear polyvinyl chloride (PVC) pipe, with two plastic end caps, and a reactor volume of 1990 cm^3. Each silicone tube had an external tube surface area of 263.5 cm^2, for a total surface area of 527 cm^2, with a total lumen volume of 94.11 mL. The reactor had an air flow of 1370 mL min^{-1} and a gas residence time of 4.1 s.

The semi-pilot-scale reactor consisted of a PVC cylindrical reactor module 155 cm in length, 25.4 cm in diameter, and a module volume of 78,500 cm^3. The module contained 25 silicone tubes, each of length 130 cm with a total lumen volume of 2310 cm^3, and external tube area of 12,900 cm^2. When air flow through the reactor was 313 L min^{-1} the gas residence time was 0.4 s.

The gas and liquid side configurations of the toluene bioreactors were essentially the same as the configurations of the butanol bioreactor, as shown in Figures 3-1 and 3-2. A modification was made during experiments involving bioreactor operation at elevated temperatures and is shown in Figure 3-3. The modification involved placement of a hot plate on the liquid side.
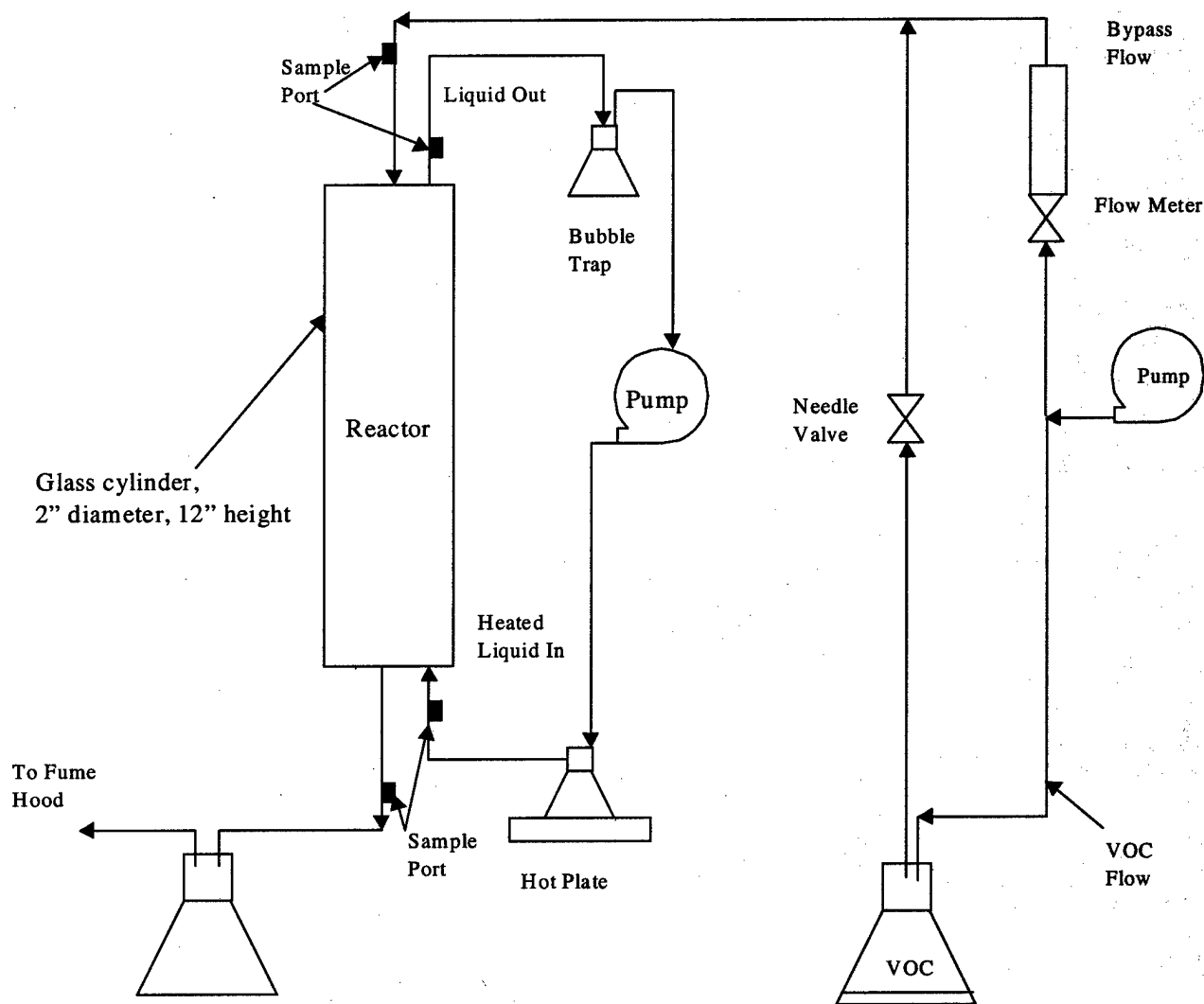
Figure 3-3. Bioreactor schematic during elevated temperature operation.

The liquid side of the short single tube, long single tube, and dual tube bioreactors, had total liquid volumes of approximately 794, 948, 1108 cm^3, respectively, of nutrient solution. The pilot scale bioreactor had a liquid side volume of 63,536 cm^3. Digital photos of the short, single tube reactor and the large, dual tube bioreactor are shown in Figure 3-4.
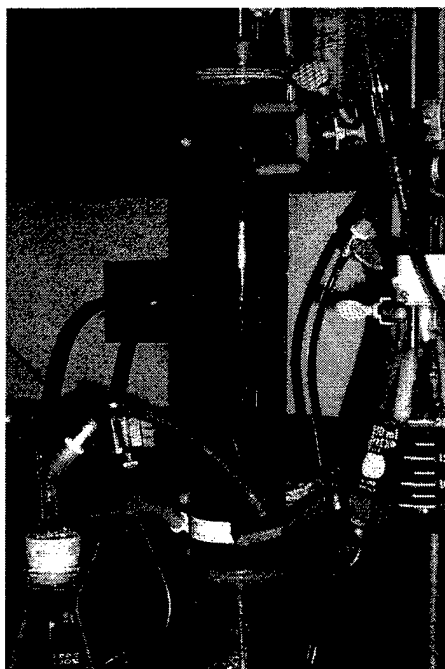
(a)   (b)
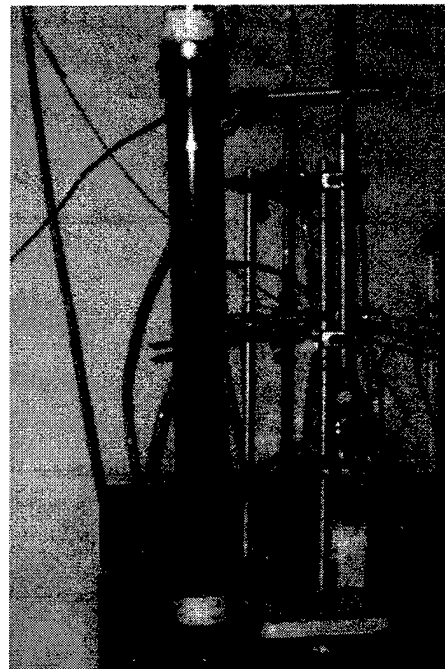
Figure 3-3. Short, single tube bioreactor (a), and large, dual tube bioreactor (b), both bench scale units.

3.3 BACTERIAL INOCULUM:

Bacterial cultures were initially started by Jeff Neemann (1998) and subsequently maintained by Bo Zhang, Steve Sauer, and Scott Cole. According to Neemann (1998), bacterial cultures were initially grown within an aerated, continuously-stirred tank reactor (CSTR) equipped with a constant liquid feed containing the contaminant of interest. The CSTR was seeded with return activated sludge obtained from the Rolla, MO Southeast wastewater treatment plant, operated with a six-day hydraulic retention time, and supplied with a nutrient solution adapted from American Type Culture Collection[®] (ATCC) Culture Medium 1981 M-R2A (Neemann, 1998), which is shown in Table 3-2. The carbon sources initially supplied to the CSTR included 500 mg L^{-1} glucose, 15 mg L^{-1} benzene, and 15 mg L^{-1} toluene. During the academic years 2000 - 2001, the cultures

were maintained as semi-batch, with nutrient solution added as necessary and toluene and

butanol supplied at a concentration of 10 mg L^{-1} as the carbon source.

Table 3-2. Nutrient solution composition, ATCC Culture Medium 1981 M-R2A (from Neemann, 1998).

Nutrient	Concentration (mg L^{-1})
NH_4Cl	800
KH_2PO_4	250
Na_2HPO_4	326
KNO_3	505
$CaCl_2 \cdot 2H_2O$	15
$MgSO_4$	16.1
$FeSO_4 \cdot 7H_2O$	7
$Na_2MoO_4 \cdot 2H_2O$	10
$MnCl_2$	5
H_3BO_3	0.5
$ZnSO_4$	1.05
$CoCl_2 \cdot 6H_2O$	0.5
$NiCl_2 \cdot 6H_2O$	0.45
$CuCl_2 \cdot 2H_2O$	0.3

3.4 BIOKINETIC PARAMETERS:

Kinetic parameters for biodegradation were determined from batch degradation

assays. 50-mL batch cultures were grown with inoculant from either the biofilm or

suspension of the bioreactor of interest and grown with varying concentrations (5 - ~ 50

mg L^{-1}) of toluene or butanol. Biokinetic parameters, the maximum specific utilization

rate (k) and half-saturation constant (K_S), were determined from these subcultures by

fitting values to multiple batch degradation assays. Toluene degradation rates were

determined as a function of substrate concentration using an averaging of time course

data. A pulse of toluene was added to a subculture and the headspace concentration was

monitored over time. Toluene and biomass concentrations were determined using gas

chromatography and volatile suspended solids (VSS) analyses (APHA 1995),

respectively. The resulting concentration vs. time data were fit using numeric

differentiation to find the substrate utilization rate, which was divided by the VSS to give

a specific utilization rate for each time datum. VSS was assumed constant over the

course of these short batch assays (Neemann, 1999; Zhang, 2000). The resulting specific

utilization rate against substrate concentration plot was fit to Monod-like kinetics using

nonlinear least squares regression using Excel's "solver". Example spreadsheet headings,

to show the method of calculation are shown in Figure 3-5.

Parameter Explanation	Time	Time(hr) Given Units	Lconc Given (mg/L)	VSS Given (mg)	dt T1-T0 (hr)	Gas Conc Gc H x Lconc (mg/L)	dsliquid S1-S0 (mg/L)	Vliquiddsliquid 0.05 L * (S1-S0) (mg)	dsgas S1-S0 (mg/L)	Vgasdsgas 0.210 L * (S1-S0) (mg)	ds total Vdsliquid + Vdsgas (mg)	ds/Vliquid ds total/0.05 L (mg/L)
ds/dt (mg/L hr)	X VSS/0.05 L (mg/L)	ds/Xdt (1/hr)	(-)ds/Xdt (1/hr)	Savg (S1+S0)liquid/2 + (S1+S0)gas/2 (mg/L)	kS/(ks+S) (1/hr)	[kS/ks+S]-ds/Xdt (1/hr)	Difference Squared					

Figure 3-5. Example spreadsheet headings used for determination of Monod-like kinetic constants.

3.5 ABIOTIC MASS TRANSFER:

Mass transfer and mass closure were determined abiotically under recirculating

conditions. Gas inlet, gas outlet, and liquid outlet concentrations were monitored

periodically to determine progress to an apparent steady-state; parameters were measured

after steady state conditions were attained. Overall mass transfer coefficients were

calculated using equations for the mass balance over the gas loop (Reij et al, 1995) and

are analogous to heat transfer coefficient calculations found in Kakac and Liu (1998).

The formulae are shown in Equations (3-1) - (3-3):

$$0 = \text{Mass In - Mass Out - Flux Through Membrane} \qquad (3\text{-}1)$$

$$0 = (Q_{air} C_{in}) - (Q_{air} C_{out}) - K_{ov} A (C_{air}/H - C_{liquid})_{lm} \qquad (3\text{-}2)$$

where:

Q_{air} = Airflow rate

C_{in} = Concentration of airflow in

C_{out} = Concentration of airflow out

C_{liquid} = Concentration in the liquid

H = Dimensionless Henry's Law Constant for toluene (0.275, Sawyer et al, 1994)

A = Area

K_{ov} = Overall mass transfer coefficient

and the log mean concentration difference,

$$(C_{air}/H - C_{liquid})_{lm} = \frac{(C_{gas}/H - C_{liquid,inlet}) - (C_g/H - C_{liquid,outlet})}{\ln(C_{gas}/H - C_{liquid,inlet}) - \ln(C_{gas}/H - C_{liquid,outlet})} \qquad (3\text{-}3)$$

Mass closures were calculated using Equation (3-4) where mass flow (mg min^{-1}) is equal to the flow rate (L min^{-1}) multiplied by the concentration (mg L^{-1}):

$$\% \ Mass \ Closure = \frac{Mass \ Flow \ Out}{Mass \ Flow \ In} x100\% \qquad (3\text{-}4)$$

3.6 BIOFILTRATION:

After characterizing abiotic mass transfer in the reactor, the reactors were operated as biofilters. Toluene-degrading bacteria from batch cultures were used to seed the reactors by injection through the liquid inlet sampling port. Gas and liquid inlet and outlet toluene or 1-butanol concentrations were monitored to determine removal efficiencies. As a minimum, triplicate gas and liquid samples were taken from each respective sampling port or headspace vial and the results averaged.

3.7 GASEOUS AND LIQUID STANDARD PREPARATION:

All gaseous toluene standards for use during gas chromatography were prepared with distilled deionized water and certified HPLC grade toluene. Toluene analyses by gas chromatography (G.C.) used external calibration standards. Gaseous standards were made by adding 11.1 μL of toluene to 1 L of deionized water, contained within a 1 L capped volumetric flask to make a concentration of 10 mg L^{-1} after equilibrium with the head space at 20°C; the H constant for toluene being 0.0066 atm m^3 mol^{-1}, dimensionless H of 0.275 (Sawyer et al, 1994). Measured amounts of the 10 mg L^{-1} standard, determined using Equation 3-5 (Whitten and Gailey, 1981), were then added to 260-mL bottles containing appropriate amounts of deionized water to give the desired equilibrium air concentrations in the headspace.

$$M_1V_1 = M_2V_2 \qquad (3\text{-}5)$$

Where

M_1 = Molarity of first solution (moles L^{-1})
M_2 = Molarity of second solution (moles L^{-1})
V_1 = Volume of first solution (L)
V_2 = Volume of second solution (L)

1-butanol standards were prepared in a similar manner with ACS grade butanol. 1-butanol analyses by gas chromatography (G.C.) also used external calibration standards. Gaseous standards were made by adding measured amounts of 1-butanol to 50 mL of deionized water contained within 260-mL bottles capped with a Mini-nert® valve to give the desired concentrations at equilibrium at 20°C. The 1-butanol Henry's Constant was found to be 9.16 atm cm^3 mol^{-1}, a dimensionless H of 0.0004 at 20 °C(Kim,

2000). Standards were allowed to equilibrate for at least one hour on a Lab-Line orbital shaker at 80 -100 rpm.

External calibration standards were used for each sampling event. Therefore external calibration standards were prepared daily and used for the GC that same day. Frequent standard preparation was required because of the toluene's volatility and the propensity for the toluene to escape the bottles overnight. An example GC calibration curve is shown in Figure 3-6. The regression line equation for this curve was y = 0.000174x + 1.765.
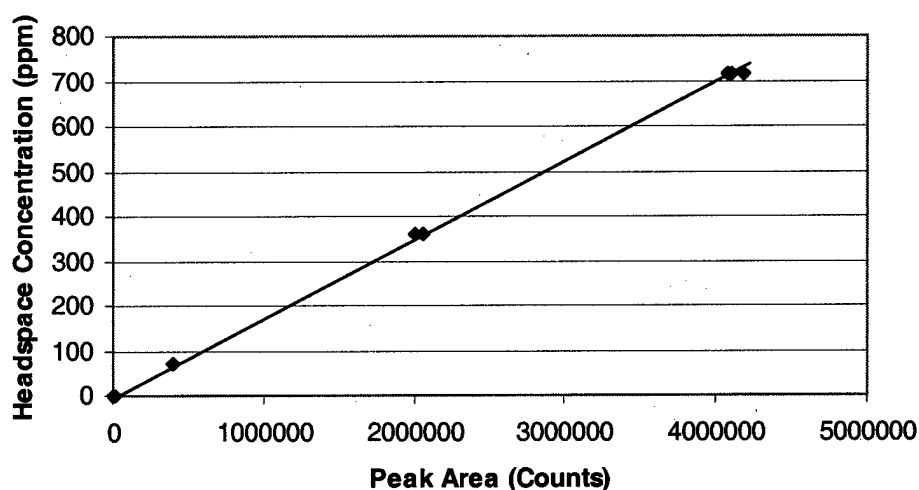
Figure 3-6. An example calibration curve used to determination headspace concentration of toluene based upon gas chromatograph peak area.

3.8 SAMPLE COLLECTION AND ANALYSIS:

3.8.1 Liquid and Gaseous Sample Collection and Analysis: Gaseous samples were collected through sampling ports using a 1-mL gas-tight sampling syringe while liquid samples were collected using a 10-mL sampling syringe. After collection, 10 mL liquid samples were expelled into a 22-mL vial containing 20 µL of 5N H_2SO_4 to acidify the

sample, capped, and then placed on an orbital shaker for a minimum of ten minutes at 80 rpm and allowed to reach equilibrium.

Headspace (gas above the liquid) samples were analyzed using a Hewlett Packard 5890 Series II Gas Chromatagraph with Flame Ionization Detector. A J&W Scientific 15 m, 0.53 mm ID, and a 3.0 μm film thickness DB-1 capillary column was used during analysis. Nitrogen flow was 40 mL min^{-1} at an isothermal 90 °C. Toluene standards were observed to elute at 0.368 minutes using this method. Butanol standards and samples were analyzed in the same manner, with elution at 0.3 min.

3.8.2 Calculations: Gas concentrations were determined from liquid concentrations using the dimensionless Henry's Law coefficient. The formula is shown in Equation (3-6), where C is the concentration, usually expressed as mg L^{-1}. The dimensionless H for toluene was found to be 0.275 at 20 °C(Sawyer et al, 1994).

$$C_{air\ phase} = HC_{liquid\ phase} \qquad (3\text{-}6)$$

Gas or vapor concentrations in the headspace and the influent and effluent gas streams of the bioreactors were generally expressed in parts per million (ppm), a volume to volume ratio. Equation (3-7) was used to convert to a mass per volume unit where $C_{mg/L}$ is the head space concentration in mg L^{-1}, C_{ppm} is the head space concentration in ppm, 1000 a conversion factor, and 24.45 the molar volume of gas at 77 °F, 760 mm Hg (Caravanos, 1991).

$$C_{mg/L} = \frac{C_{ppm} * MW}{24.45 * 1000} \qquad (3\text{-}7)$$

Comparison of gas inlet and gas outlet samples were completed by calculating 95%

confidence limits around the average of the three measurements for the gas inlet

concentration and for the gas out let concentration of toluene. The confidence limit

calculation was based upon the student's "t" distribution and is shown subsequently.

Calculation of removal per area of membrane surface was completed using

Equation (3-8) where air flow rate is in L min^{-1}, amount of contaminant removed in mg

L^{-1} of air, and membrane area in m^2.

$$Flux = \frac{Air\,Flow\,Rate * Amount\,Removed}{Membrane\,Area} \tag{3-8}$$

Calculation of removal per unit module volume (elimination capacity) used

Equation (3-9), where air flow rate is in L min^{-1}, amount of contaminant removed in mg

L^{-1} of air, module volume in m^3. Appropriate conversions of 60 min h^{-1} and 1000 mg g^{-1}

are then applied to obtain the more standard measurement unit of g m^{-3} h^{-1}.

$$E.C. = \frac{Air\,Flow\,Rate * Amount\,Removed}{Module\,Volume} \tag{3-9}$$

3.8.3 Method Detection Limit: The GC headspace analysis method detection limit for

toluene was determined to be <0.05 mg L^{-1} as measured in the liquid. The method

detection limit was determined by preparing liquid standards of varying concentrations,

sampling the headspace 10 times for each respective concentration, and calculating a

95% confidence limit. The lowest value where confidence intervals overlap would be the

method limit of detection. Figure 3-7 shows the information graphically; confidence

intervals were too small to warrant showing. The confidence limit information is also

shown in Table (3-3).
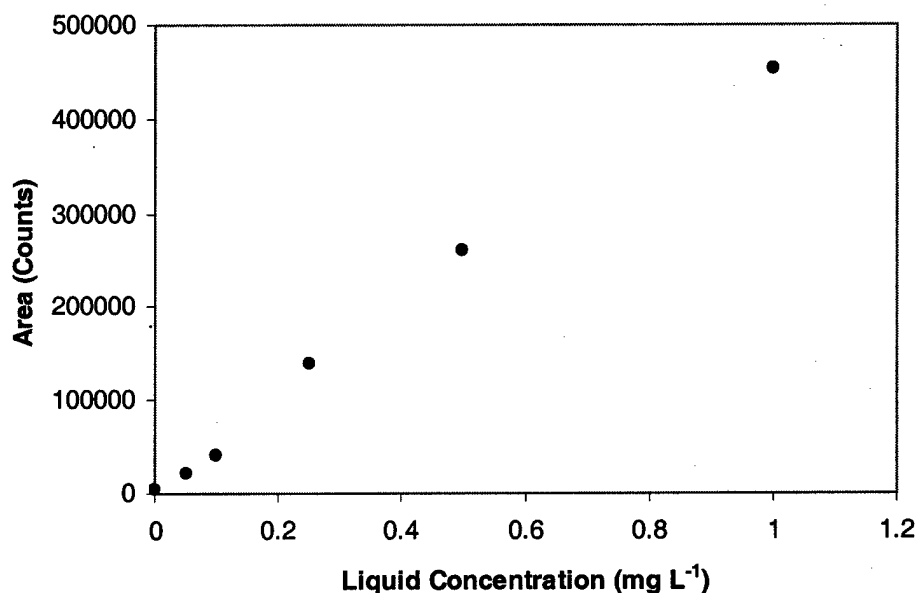
Figure 3-7. Graphical representation of the headspace limit method of detection test for the chemical toluene.

Table 3-3. Tabular representation of method limit of detection data.

Liquid Toluene Concentration (mg L^{-1})	Average (Counts)	LCL$_{95}$ (Counts)	UCL$_{95}$ (Counts)
0.00	4818	2,773	6,864
0.05	21497	20,309	22,486
0.10	41451	39,587	43,315
0.25	139744	136,425	143,063
0.50	261277	257,043	265,510
1.00	453224	450,529	455,919

3.9 HEAT TRANSFER COEFFICIENT MEASUREMENT:

A diagram of the bench-scale heat transfer apparatus used during temperature

measurements is shown in Figure 3-8. The membrane reactor units used during heat

transfer experiments were constructed similarly to bench-scale bioreactors used during previous research (Fitch et al, 2000). Temperature differentials and the effect of varying gas and liquid flow rates through the system were determined abiotically at steady state. Trials were completed using both dense phase (silicone and latex rubber) and polyporous polysulfone membrane units, both insulated and uninsulated. Insulated units were jacketed around the membrane module only with several layers (3/4" thickness) of polyester insulating material. All membrane module configurations resembled shell and tube heat exchangers.
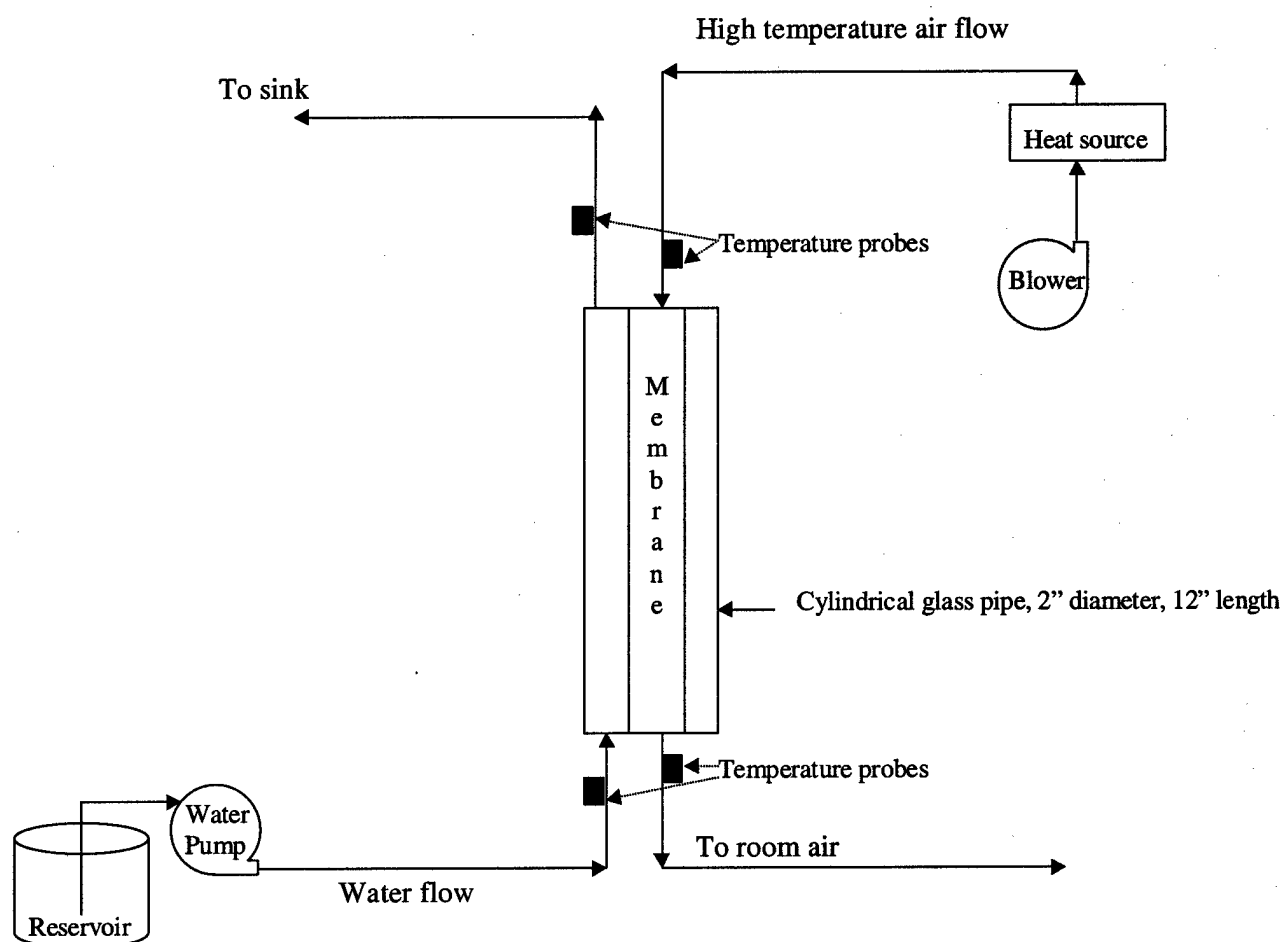
Figure 3-8. Schematic of the heat transfer measurement experimental configuration.

Gas inlet, gas outlet, liquid inlet and liquid outlet temperatures were monitored periodically to determine progress to an apparent steady-state; parameters were measured in duplicate after steady state conditions were attained. Additionally, one temperature reading for each module was recorded by placing the thermocouple at the outer membrane surface. Temperatures were measured using dual wire thermocouples attached to an Omega DP460; the difference in resistance between the two wires was recorded as a digital temperature readout on the Omega DP460. As a control, before measurements were taken, the output of all four thermocouples was monitored at room temperature; measurements were within one-tenth °C of one another. Air was supplied by an aquarium air pump for low flow conditions while bench air, with a pressure relief hose to limit pressure to near ambient, was used to supply higher air flows.

Heat flux and heat transfer coefficients were calculated using the model relationships shown in Equations (3-10) - (3-12) (Kakac and Liu, 1998)

$$Q = mc_p(T_{h1} - T_{h2}) \qquad (3\text{-}10)$$

$$Q = UA\Delta T_{lm} \qquad (3\text{-}11)$$

$$\Delta T_{lm} = \frac{(T_{h1} - T_{c2}) - (T_{h2} - T_{c1})}{\ln\left(\dfrac{T_{h1} - T_{c2}}{T_{h2} - T_{c1}}\right)} \qquad (3\text{-}12)$$

Q = the total heat transfer rate (J s^{-1}, W)

A = outside (liquid side) surface area of the tube (m^2)

U = overall heat transfer coefficient (W m^{-2} K^{-1})

ΔT_{lm} = log-mean temperature differential (K),

T_{h1} = influent air temperature (K)

T_{h2} = effluent air temperature (K)

T_{c1} = influent liquid temperature (K)

T_{c2} = effluent liquid temperature (K)

m = mass flow rate (kg s^{-1})

c_p = heat capacity of the respective fluid (J kg^{-1} K^{-1}).

3.10 OTHER ANALYTICAL METHODS:

3.10.1 pH: pH readings were taken using an IQ Scientific Instruments pH meter and probe. A two point calibration was performed using pH buffers of 4.00 and 7.00 (Fisher Scientific, Fair Lawn, NJ). pH meters use a glass electrode to measure the hydrogen ion potential of solutions. The principles of operation of the pH meter are detailed in Sawyer et al (1994).

3.10.2 Water Loss: Water loss was measured periodically by replacing missing fluids within the reactors or the bubble catchers. Water was measured in a graduated cylinder before addition to the reactors' liquid phase.

3.10.3 Dissolved Oxygen: Dissolved oxygen measurements were taken by either inserting the Corning Incorporated Dissolved Oxygen Meter Probe into the reactor or extracting a small volume of liquid into a beaker and then reading the oxygen concentration. A two point calibration was performed using 100% (saturated air above water) and 0% oxygen (Corning Incorporated, Corning, NY). The principles of operation of the dissolved oxygen meter are detailed in Sawyer et al (1994).

3.10.4 Pressure Drop: Pressure drop across the membrane module was periodically monitored using a U-tube manometer filled with water (Neemann, 1998). When measurements were taken, the manometer was attached to the influent and effluent sampling ports and the difference in water heights manually read with a ruler at the time of measurement.

3.10.5 Optical Density: Optical density was measured using a Hach DR/2010 Spectrophotometer with the results used to determine cell density. 25-mL samples were placed in glass cuvettes and the absorbance read at 600 nm (Rogers and Reardon, 2000). A typical calibration curve for VSS as a function of A_{600} is shown in Figure 3-9. The principle of operation of the spectrophotometer is detailed in Sawyer et al (1994).
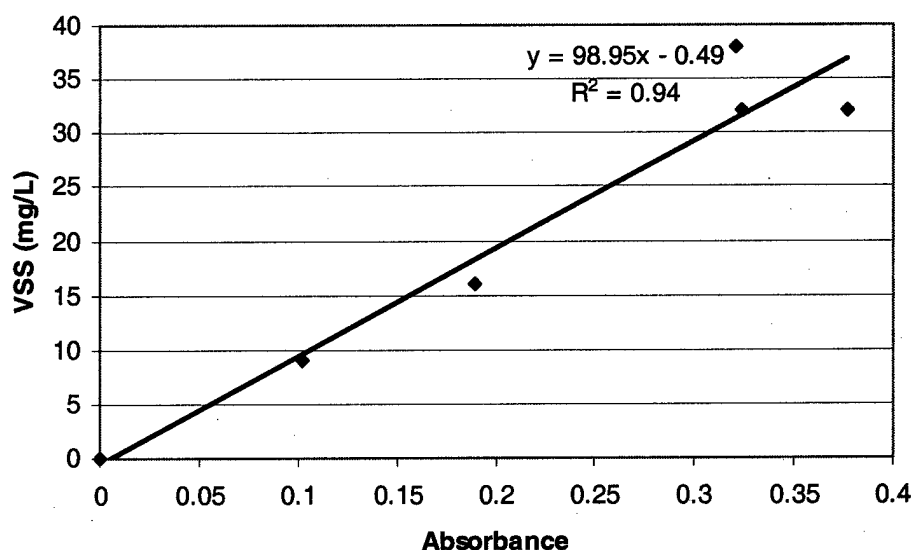
Figure 3-9. A_{600} absorbance calibration curve for determination of microorganism concentration in solution, measured using volatile suspended solids analysis.

3.10.6 Colony Plating/Isolation/Gram Staining: Morphological characteristics such as size, color and form of bacterial colonies isolated on nutrient agar were examined visually, while gram staining was accomplished according to methods found in Gerhardt

et al (1994). Additionally, two anaerobic growth tests were completed. For the anaerobic tests, mineral salts agar plates were prepared, streaked with biofilm, and allowed to grow at room temperature anaerobically (sealed in a Gas-Pak bag) (Westenberg, 2002; Mihalcik, 2002).

3.10.7 Biofilm Density and Thickness: Biofilm thickness of the silicone tube bioreactors was measured using a Vernier caliper (Scienceware, Part # 134150000). After operational shut-down, the tubes were removed and the diameter of the biofilm/tube structure measured and recorded. Biofilm was then scraped from the tubes and the diameter of the tube measured and recorded. The differences in diamter provided the thickness of the biofilm. Biofilm density was calculated by measuring the volatile suspended solids content of biofilm samples scraped from the tubing of a disassembled reactor (APHA, 1995) and dividing by the biofilm volume.

3.10.8 Ion Chromatography: Ion chromatography was accomplished using a Dionex Ion Chromatograph and Dionex Ion Pac AS9-HC-4mm column with assistance from Keith Loftin. Liquid standards ($\sim$1, 10, 100 mg L^{-1}) were prepared for NaCl, NaBr, NaNO$_3$, Na$_2$HPO$_4$, Na$_2$SO4, NaNO$_2$ by measuring known amounts of dry chemical and diluting to 1 L. Samples of the bioreactor suspension were filtered using a 0.2 μm nitrocellulose filter, and diluted 1:25 before analysis. Principles of ion chromatography are detailed in Sawyer et al (1994).

3.10.9 16S rDNA: In addition to classical isolation and characterization of bacterial species, biofilm 16S rDNA was extracted and amplified by polymerase chain reaction (PCR) and the sequence of this gene determined for each isolate using methods described by Mormile (2002). DNA was extracted from biofilm samples using a MoBio

Laboratories UltraClean Soil DNA isolation kit. The extracted rDNA was then amplified using PCR with universal primers. The DNA was visualized on an agarose gel, cut from the gel, and purified using a GeneClean procedure. Cloning was accomplished using the Invitrogen TA Cloning kit and competent cells. Plasmids were then extracted and purified using the Qiagen Mini Plasmid Kit. The resulting samples were sent for DNA sequencing at MWG Biotech.

3.10.10: Water Flow Rate: Water flow rates were measured using a graduated cylinder and a stop watch. The volume of water (mL) collected during a measured time period (s) was recorded and results converted to mL min^{-1}.

3.10.11: Air Flow Rate: Air flow rates were measured using a bubble tube and a stop watch. The volume of air (mL) traversed by a soap bubble during a measured time period (s) was recorded and results converted to mL min^{-1}. Larger air flow rates were measured using a wet test meter. The principle of operation for the wet test meter is the displacement of water by air.

3.10.12: Metabolite Determination: Detection of metabolites from bacterial action was accomplished using headspace and liquid sample analysis on the GC. 10-mL samples of liquid from the semi-pilot scale reactor were placed in 22-mL vials, capped, allowed to equilibrate and headspace analysis completed. DI water was amended with toluene to form a 1 mg L^{-1} solution, 10 mL placed in 22-mL vials, capped, allowed to equlibrate, and headspace analysis completed. Liquid from the semi-pilot-scale reactor was filtered using a 0.2 μm nitrocellulose filter to remove biomass. 1 μL of liquid was then injected onto the column. 1 μL of nutrient solution amended with 1 mg L^{-1} toluene was also injected onto the GC column as a control. Headspace and liquid analysis was

accomplished using the DB-1 column, inlet 250 °C, detector 300 °C, oven at 100 °C for two minutes, ramp of 10 °C min^{-1}, followed by two minutes at 200 °C. Both headspace and liquid samples were run in triplicate. Amended solution results for headspace and liquid samples were then compared to determine the presence of metabolites.

3.10.13: Toluene Degradation, Presence/Absence of Oxygen: Three headspace vials, sequentially evacuated and filled with nitrogen (Mormile, 2002) were prepared to provide an anaerobic environment. 10 mL aliquots of liquid suspension from the dual tube reactor were carefully extracted with a syringe to avoid introduction of oxygen, and then dispensed into the capped/sealed headspace vials. 10 mL aliquots of liquid suspension were also placed into three air-filled headspace vials. GC headspace analysis was accomplished for both sets of vials over time, recording the concentraion of toluene. To validate the results of the first experiment, a duplicate experiment was accomplished six days later.

3.11 STATISTICS:

3.11.1 95% Confidence Interval Calculation: 95% confidence intervals were calculated using Equation 3-13 (Moore and McCabe, 1993).

$$\bar{X} \pm t * \left(\frac{s}{\sqrt{n}} \right) \tag{3-13}$$

where:

$\bar{X}$ = sample mean

s = standard deviation

t* = t statistic for 95% confidence for df

df = n-1, degrees of freedom

n = sample size

95% - confidence intervals were used to determine differences between experimental

outcomes and to determine differences between inlet and outlet sample values. For each

set of injections, a 95% - confidence interval was calculated for the gas inlet readings and

another for the gas outlet readings. An example of inlet and outlet readings and their

confidence limits is shown in Figure 3-10; confidence intervals were calculated for each

set of injections but are not shown in the text.
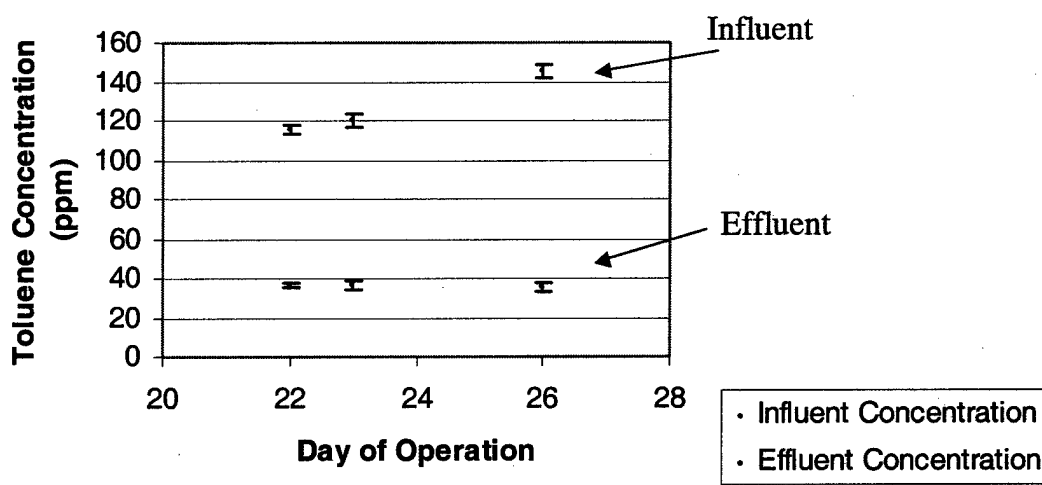
Figure 3-10. Illustration of confidence intervals for gas influent and effluent sampling
points. Higher values for each location on the x axis are the gas inlet concentrations
while the lower values are the gas outlet concentrations.

3.11.2 Measurement Error for Calculated Values: The measurement error of a

calculated value may be determined as shown in Equations (3-14) - (3-18). Figure (3-11)

shows the plotting of example points from experimentation.

For the example numbers, where e represents the experimental error and X,Y, and

Z are real numbers,

$$X \pm e_1 \qquad (3\text{-}14)$$

$$Y \pm e_2 \qquad\qquad (3\text{-}15)$$

$$Z \pm e_3 \qquad\qquad (3\text{-}16)$$

the following is used to determine the resultant error when addition or subtraction

is required for X, Y, and Z (Harris, 1999):

$$e_4 = \sqrt{e_1^2 + e_2^2 + e_3^2} \qquad\qquad (3\text{-}17)$$

and the following is used to determine the resultant error when multiplication

and/or division is required for X, Y, and Z (Harris, 1999):

$$\%e_4 = \sqrt{\left(\%e_1\right)^2 + \left(\%e_2\right)^2 + \left(\%e_3\right)^2} \qquad\qquad (3\text{-}18)$$

As an example, the measurement of the influent toluene concentration into a
reactor is:

$$727 \pm 82 \ \text{mg}\,\text{L}^{-1}$$

The measured effluent toluene concentration was

$$275 \pm 89 \ \text{mg}\,\text{L}^{-1}$$

The actual removal would be determined as follows:

$$727 - 275 = 452 \ \text{mg L}^{-1}$$

$$e_3 = \sqrt{e_1^2 + e_2^2} = \sqrt{82^2 + 89^2} = 121 \ \text{mgL}^{-1}$$

and reported as

$$452 \pm 121 \ \text{mg}\,\text{L}^{-1}$$
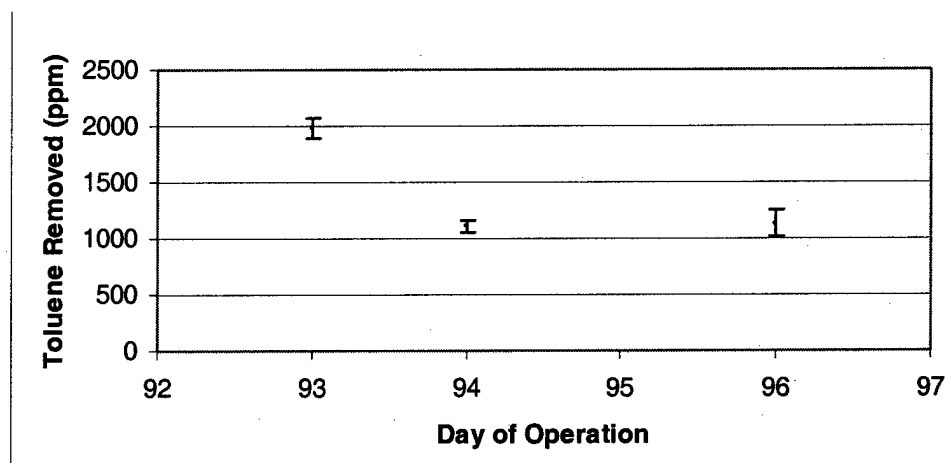
Figure 3-11. Error associated with calculated results of contaminated removal.

3.12 OTHER DEFINITIONS:

Several definitions are frequently used in the biofilter literature and are listed

below based on Devinny et al (1999).

$$\text{Gas residence time} = \frac{V_{lumen}}{Q} \tag{3-19}$$

$$\text{Surface loading} = \frac{Q_{air} C_{in}}{A} \tag{3-20}$$

$$\text{Removal efficiency} = 100\% \frac{C_{in} - C_{out}}{C_{in}} \tag{3-21}$$

$$EC = \frac{(C_{in} - C_{out})Q}{V_{reactor}} \tag{3-22}$$

where:

V_{lumen} = Total lumen volume (m^3)

$V_{reactor}$ = Reactor total volume (m^3)

Q = Air flow rate $(L\ min^{-1})$

C = Concentration of contaminant in air stream (mg L^{-1})

A = Surface area of the membrane (m^2)

EC = Elimination capacity

CHAPTER 4
MODEL DEVELOPMENT

4.1 BACKGROUND:

Numerous models have been presented to describe biofilms in conventional biofilters (Metris et al, 2001; Mysliwiec et al, 2001; Karamanev et al, 1999; Malhautier et al, 2000) and biotrickling filters (Baltzis et al, 1997; Mpanias and Baltzis, 1998), in hollow fiber membrane reactors (Aziz et al, 1995; Ergas et al, 1999), and within biofilms (Bae and Rittmann, 1995; Bekins et al, 1998). However, no models have been proposed that specifically modeled interactions or predicted removal in dense phase materials (such as silicone) contained within bioreactors used to treat VOC-contaminated air. Therefore, the model presented subsequently was developed. The value of modeling a process such as combined mass transfer and biodegradation in the silicone tubing membrane module is two-fold. First, a well-developed model presents insight into the limiting factors in reactor operation. Second, the model, if verified, may be used as a predictive tool [for design] which can save significant experimental time (Fitch, 1996).

The model presented here builds upon modeling efforts previously completed within the University of Missouri-Rolla Environmental Engineering Laboratory (Neemann, 1998). A dual substrate model, with toluene and oxygen as the limiting substrates, is proposed for analysis of single and multiple silicone tube membrane bioreactor systems. The model incorporates information and ideas from Ergas et al (1999), Neemann (1998), and Harris and Hansford (1976). During experiments to validate the dual substrate model, it was determined that toluene was degraded both aerobically and anaerobically. Therefore, the dual substrate model was simplified to apply to the specific experimental conditions used here.

79

The model development chapter, Chapter 4, is organized as follows to show how the model works. How the model predicts in a variety of circumstances is described in Chapter 5.

4.2 Geometry of the system.

4.3 Mass transfer and resistance to mass transfer.

4.4 Parameter values.

4.5 Chemical stoichiometry.

4.6 Model assumptions.

4.7 Modeling of each section.

4.8 Numeric approximation.

4.9 Second derivative determination.

4.10 Single substrate limitation and the biofilm concentration profile equation.

4.11 Main premise of the model.

4.12 Applicability of a numeric solving technique using Excel®.

4.13 Solving the single tube model.

4.14 Multiple tube model considerations.

4.15 Input parameters for sensitivity analysis.

4.16 Sensitivity analysis.

4.17 Actual removal versus predicted removal in the single tube system.

4.18 Limitations of the model.

4.2 GEOMETRY:

For clarity, a picture of the single tube bioreactor being modeled is shown in Figure 4-1. Contained within the glass module is a single silicone tube. Contaminated

air flows downward through the interior (lumen) of the silicone tube. A biofilm grows on the exterior of the silicone tube (membrane). Oxygen and toluene diffuse through the silicone membrane and into the biofilm where the toluene is broken down (metabolized), primarily to carbon dioxide and water, or is used for cell growth. Gaseous by-products of cellular metabolism, such as carbon dioxide, diffuse back through the membrane into the air stream. A nutrient solution, containing suspended biomass that also degrades toluene, flows between the silicone tube and the glass module, countercurrent to the air stream. The single silicone tube membrane module can be envisioned as a tube within a tube while the multiple tube modules may be compared to a shell and tube heat exchanger.
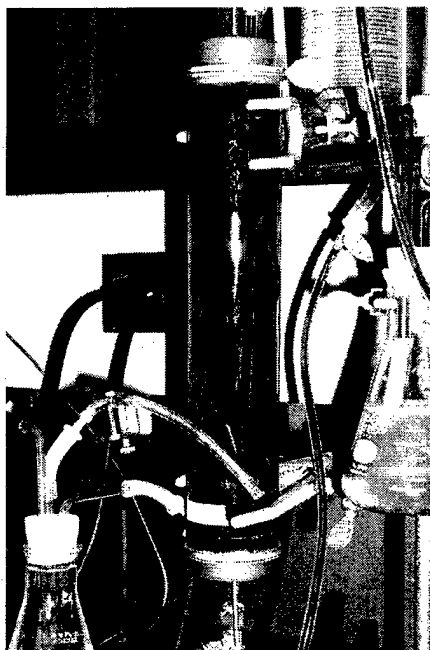
Figure 4-1. Picture of the single dilicone tube bioreactor. Inner tube seen as dark cylinder in middle of module.

A top view schematic of the single tube model system is shown in Figure 4-2. The toluene and oxygen are transferred from the air in the interior of the silicone tube, through the tube, into the biofilm, and then into the liquid.
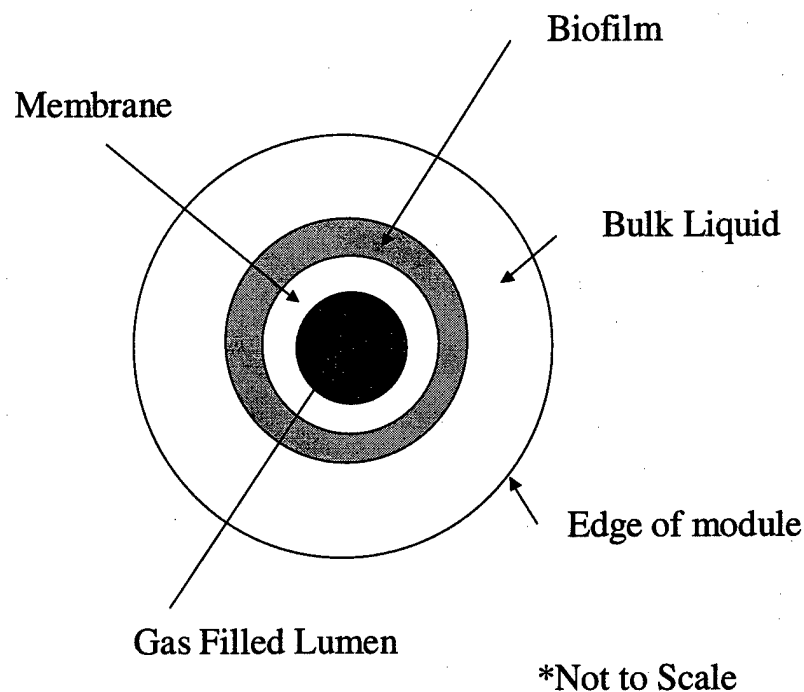
Figure 4-2. Top view schematic of single tube biofiltration module.

The module is analyzed using the cylindrical coordinate system as shown in Figure 4-3. In the cylindrical coordinate system, z represents the vertical axis (referred to as the axial direction), r the radial axis (referred to as the radial direction) and θ the angular or third direction. To analyze the complex geometry, the cylindrical tube-within-a-tube is sliced horizontally into "n" slices, numbered from i = 1 to n where the position "0" is located at the contaminated air influent and the end of the "nth" section is located at the air effluent. The cylinder is also sliced radially into "m" slices, numbered from j = 1 to m, with the position j = 0 at very interior of the silicone tube and j = m at the edge of reactor module. Therefore within the cylindrical coordinates, a toluene concentration of interest exists at a point P(i,j).
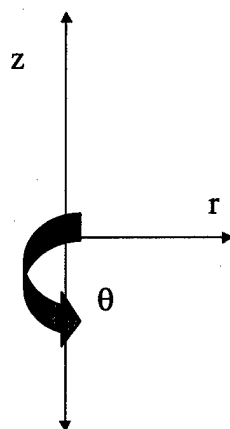
Figure 4- 3. Cylindrical coordinate system.

Several radii are important for understanding and analyzing the geometry of the

system and are shown in Figure 4-4 where:

r_i = Inner radius of the silicone tube
r_o = Outer radius of the silicone tube
r_b = Outer radius of the biofilm
r_m = Outer radius of the module
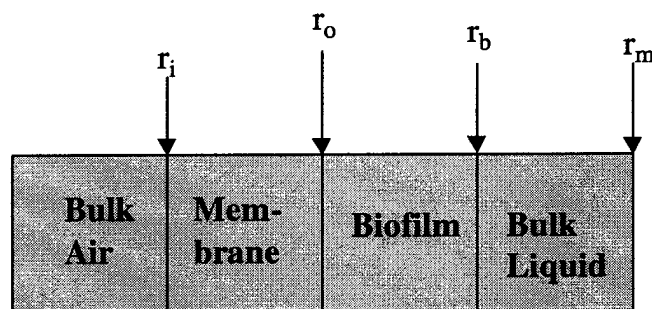
Figure 4-4. Important radii within the reactor system.

4.3 MASS TRANSFER AND RESISTANCE TO MASS TRANSFER:

4.3.1 Mass Transfer Coefficient Definitions: The radial cut-away illustration (Figure

4-5) shows the locations where mass transfer of substrate (toluene) occurs. The mass

transfer coefficients associated with the thin films and the membrane are defined below.

The same names of mass transfer coefficients must be considered for both toluene and oxygen but will be of different values.

k_g = Mass transfer coefficient of the gas phase (cm s^{-1})
k_m = Mass transfer coefficient of the membrane (cm s^{-1})
k_l = Mass transfer coefficient of the liquid phase (cm s^{-1})
K_{OV} = Overall mass transfer coefficient of the module (cm s^{-1})
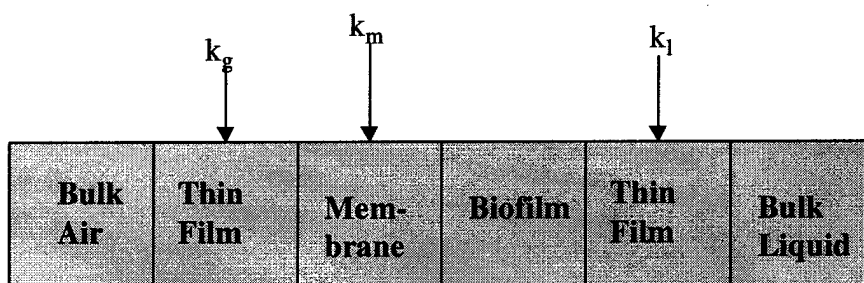
Figure 4-5 . Cut-away schematic showing locations of mass transfer.

4.3.2 Overall Resistance to Mass Transfer: The overall resistance to mass transfer of toluene, shown in Equation 4-1, may be modeled as the sum of three mass transfer resistances (Zhang and Cussler, 1985) and is modified for toluene, using Equation 4-2a, and for oxygen using Equation 4-2b, to fit a silicone membrane system with air flowing through the lumen and liquid in the shell (Freitos dos Santos et al,1995; Coté et al, 1989):

$$\frac{1}{K_{OV}} = \frac{1}{k_l} + \frac{1}{k_m} + \frac{1}{k_g} \tag{4-1}$$

$$\frac{1}{K_{OV}} = \frac{1}{k_l} + \frac{r_i(\ln(r_o/r_i))}{D_m S} + \frac{r_o/r_i}{k_g H} \tag{4-2a}$$

$$\frac{1}{K_{OV}} = \frac{1}{k_l} + \frac{r_o(\ln(r_o/r_i))}{PH} + \frac{r_o/r_i}{Hk_g} \tag{4-2b}$$

where:

k_g = Mass transfer coefficient in the gas phase (cm s^{-1})
k_m = Mass transfer coefficient in the membrane (cm s^{-1})
k_l = Mass transfer coefficient in the liquid phase (cm s^{-1})
K_{OV} = Overall mass transfer coefficient in the module (cm s^{-1})
D_m = Diffusion coefficient of substrate in silicone membrane (cm^2 s^{-1})
S = Solubility of substrate in silicone membrane (dimensionless)
H = Henry's Law coefficient (dimensionless)
r_i = Inner radius of the silicone tube (cm)
r_o = Outer radius of the silicone tube (cm)
P = Permeability within the membrane (cm^2 s^{-1})

The permeability of the membrane is the product of the diffusion coefficient and the solubility within the membrane; $P = D_m * S$. Because the permeability will be adjusted later during model fitting, it will be subsequently referred to as the "effective permeability".

The same type of mass transfer resistance equation must be developed for oxygen, as well as toluene. As shown as part of Equation 4-2b, for the oxygen transfer across a silicone membrane the membrane mass transfer coefficient can be represented by Equation 4-3 (Coté et al, 1989)

$$k_m = \frac{PH}{r_o \ln(\frac{r_o}{r_i})} \qquad (4\text{-}3)$$

where P is the permeability of oxygen (mol m^{-1} s^{-1} Pa^{-1}) through the membrane and H is the Henry's Law coefficient (Pa m^3 mol^{-1}). A unit conversion (100 cm:1 m) must also be made to account for the radii being defined in cm and the other parameters being listed in meters.

Throughout the literature, the mass transfer boundary layer resistance on the gas

or vapor side of the membrane is considered small with respect to the diffusional

resistance in the membrane, and only the liquid side boundary layer is considered.

However, for membranes with high selectivity and flux, ignoring the possibility of a gas

(vapor) side boundary layer can be an erroneous assumption. (Pellegrino and Sikdar,

1998). Although Coté et al (1989) ignored the gas phase resistance, it is taken into

account in Equations 4-2a and 4-2b.

4.3.3 Individual Mass Transfer Coefficients: Each of the other individual mass

transfer coefficients may be modeled. The gas phase mass transfer coefficient of was

modeled as Equation 4-4 (Yang and Cussler, 1986):

$$\text{Sherwood Number} = \frac{k_g d_i}{D_a} = 1.64 \left(\frac{d_i^2 v}{D_a l} \right)^{0.33} \tag{4-4}$$

where:

k_g = Mass transfer coefficient in the gas phase (cm s^{-1})
d_i = Fiber inner diameter (cm)
l = Fiber length (cm)
v = Air velocity (cm s^{-1})
D_a = Diffusion coefficient of substrate in air (cm^2 s^{-1})

The liquid phase resistance of Equation 4-5 was presented by Zhang and Cussler,

(1985) and Knudsen and Katz (1956).

$$\text{Sherwood Number} = \frac{k_l d_o}{D_w} = 0.22 Re^{0.6} Sc^{0.33} = 0.22 \left(\frac{\rho d v_w}{\mu} \right)^{0.6} \left(\frac{\mu}{\rho D_w} \right)^{0.33} \tag{4-5}$$

where:

k_l = Mass transfer coefficient in the liquid phase (cm s^{-1})
d_o = Fiber outer diameter (cm)

Re = Reynolds number (dimensionless)
Sc = Schmidt number (dimensionless)
μ = Shear viscosity (g cm^{-1} s^{-1})
ρ = Density of water (g cm^{-3})
v_w = Water velocity (cm s^{-1})
D_w = Diffusion coefficient of substrate in water (cm^2 s^{-1})

Other liquid resistance relationships were detailed extensively in Pressman (1995).

The membrane mass transfer coefficient of Equation 4-6 (as described previously when discussing the membrane resistance) is shown again in Equation 4-6,

$$k_m = \frac{D_m S}{r_i (\ln(r_o/r_i))}$$ (4-6)

where:

k_m = Mass transfer coefficient in the membrane (cm s^{-1})
D_m = Diffusion coefficient of substrate in silicone membrane (cm^2 s^{-1})
S = Solubility of substrate in silicone membrane (dimensionless)
r_i = Inner radius of the silicone tube (cm)
r_o = Outer radius of the silicone tube (cm)
P = Permeability = $D_m S$

4.3.4 Variable Naming in the Reactor System:
A cut-away view, formed by slicing the tube vertically shows the different portions of the reactor system. Such a cut-away view is shown in Figure 4-6, where the following variables represent the toluene concentrations:
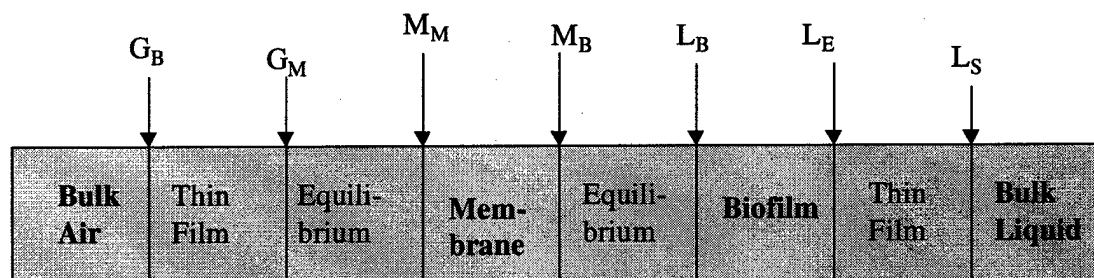

Figure 4-6. Variable naming along a radial cut-away view of the reactor.

G_B = Bulk gas concentration (mg L^{-1})
G_M = Gas concentration at the membrane inner surface (mg L^{-1})
M_M = Concentration in membrane at the gas/membrane interface (mg L^{-1})
M_B = Concentration in membrane at the membrane/biofilm interface (mg L^{-1})
L_B = Concentration in liquid at biofilm/membrane interface (mg L^{-1})
L_E = Concentration in liquid at biofilm edge (mg L^{-1})
L_S = Concentration in bulk suspension (mg L^{-1})

The same variables would be defined for the concentration of oxygen at the various

locations within the reactor module.

4.4 PARAMETER VALUES:

Parameters needed to determine concentration profiles across the bioreactor are

shown in Table 4-1. Parameters were either found within the literature or were measured

experimentally in the single silicone tube system.

Table 4-1. Parameter values used for initial single tube model solution.

Parameter	Value	Source
$K_{S(Biofilm - Toluene)}$	1.0 mg L^{-1}	Measured/Modeled
$K_{S(Suspension - Toluene)}$	1.0 mg L^{-1}	Measured
$k_{(Biofilm - Toluene)}$	0.198 h^{-1}	Measured/Modeled
$k_{(Suspension - Toluene)}$	0.1 h^{-1}	Measured
$K_{O(Biofilm - Oxygen)}$	0.000025 mg cm^{-3}	Harris and Hansford (1976)
$K_{O(Suspension - Oxygen)}$	0.000025 mg cm^{-3}	Harris and Hansford (1976)
$P_{(Oxygen in Silicone)}$	$1.63*10^{-13}$ mol m^{-1} s^{-1} Pa^{-1}	Cote' et al (1989)
$P_{(Toluene in Silicone)}$ = D_mS	$8.2*10^{-5}$ cm^2 s^{-1} 0.001 - 0.003 cm^2 s^{-1}	Nijhuis et al (1991) Adjusted
$H_{(Oxygen)}$	73,800 Pa m^3 mol^{-1}	Coté et al (1989)
$D_{(Toluene in Biofilm)}$	$0.8*D_{Toluene in Water}$ cm^2 s^{-1}	Characklis (1990, p 117)
$D_{(Oxygen in Biofilm)}$	$1.2*10^{-5}$ cm^2 s^{-1}	Khlebnikov et al (1998) also Beyenal et al (1997)
$D_{(Oxygen in Water)}$	$2.26*10^{-5}$ cm^2 s^{-1}	Casey et al (2000)
$D_{(Oxygen in Air)}$	0.219 cm^2 s^{-1}	Richard (2002)
$D_{(Toluene in Water)}$	$9*10^{-6}$ cm^2 s^{-1}	Schwarsenbach (1993) in Holden et al (1997)
$D_{(Toluene in Air)}$	0.0849 cm^2 s^{-1}	Lugg (1968)
Q_{Air}	0.769 L min^{-1}	Measured
Q_{Liquid}	0.01 L min^{-1}	Measured

$X_{Biofilm}$	10 - 130 mg cm^{-3} 23,800 mg L^{-1}	Frietos dos Santos and Livingston (1995) Measured
$X_{Suspension}$	29 mg L^{-1}	Measured
$H_{(Toluene\ 20^oC)}$	0.275	Sawyer et al (1994)
$H_{(Oxygen\ 20^oC)}$	73,800 Pa m^3 mol^{-1}	Cote et al (1989)
$\mu_{(water\ 20^oC)}$	0.01002 g cm^{-1} s^{-1}	Metcalf and Eddy (1991)
μ_{air20^oC}	0.000182 g cm^{-1} s^{-1}	Kakac and Liu (1998)
ρ_{air20^oC}	0.001205 g cm^{-3}	Weast (1977)
$\rho_{(water\ 20^oC)}$	998.2 kg m^{-3}	Metcalf and Eddy (1991)
Δz	0.5 cm	Chosen
Δr	0.01 cm	Chosen
Length	18.5 cm	Measured
r_i	0.47625 cm	Cole Parmer
r_o	0.635 cm	Cole Parmer
r_b	0.875 cm	Measured
Cross sectional A_{liquid}	17.86 cm^2	Measured/calculated
Cross sectional A_{air}	0.71 cm^2	Measured/calculated

Determination of the air velocity and water velocity is also required for modeling and is

shown in Equation 4-7,

$$V = \frac{Q}{A} \hspace{4cm} (4\text{-}7)$$

where:

V = Velocity (cm s^{-1})
A = Cross sectional lumen total area (cm^2)
Q = Flow rate (cm^3 s^{-1})

4.5 CHEMICAL STOICHIOMETRY:

Although the stoichiometric ratio of oxygen used for toluene consumption does

not appear to apply in this study it may be important in the dual substrate model applied

to other bioreactors where a carbon substrate is aerobically degraded. A ratio of 0.3

oxygen to glucose is applied in the degradation model described by Harris and Hansford

(1976). If the cells are using toluene strictly for maintenance and its required generation

of ATP, Equation (4-8) likely represents the ratio of oxygen to toluene consumed (Metris

et al, 2001). In this equation, 288 g of oxygen (MW 16) are consumed during consumption of one mole of toluene (MW 92.14), for a ratio of 3.125 g oxygen:1 g C_7H_8.

$$C_7H_8 + 9\ O_2 \longrightarrow 7\ CO_2 + 4\ H_2O \qquad (4\text{-}8)$$
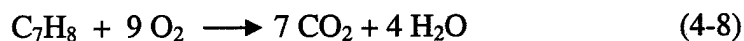
If, however, the cells are strictly storing materials, the other oxygen ratio may be approached. Bacterial cells may store energy as glycogen, polyphosphate, or poly-β-hydroxybutyrate (PHB) in granules within the cell. PHB is a typical prokaryotic storage material and is widespread in bacilli, chemolithotrophic and phototrophic bacteria and psuedomonads (Gottschalk, 1986). The synthesis of poly-β-hydroxybutyrate (in *Azotobacter beijerinckii* and *Rhodospirillum rubrum*) begins with acetyl coenzyme A and is shown in Figure 4-7 (Gottschalk, 1986). The structure of poly-β-hydroxybutyric acid is shown in Figure 4-8. At some future time, the poly-β-hydroxybutyrate formed may be used to generate ATP.
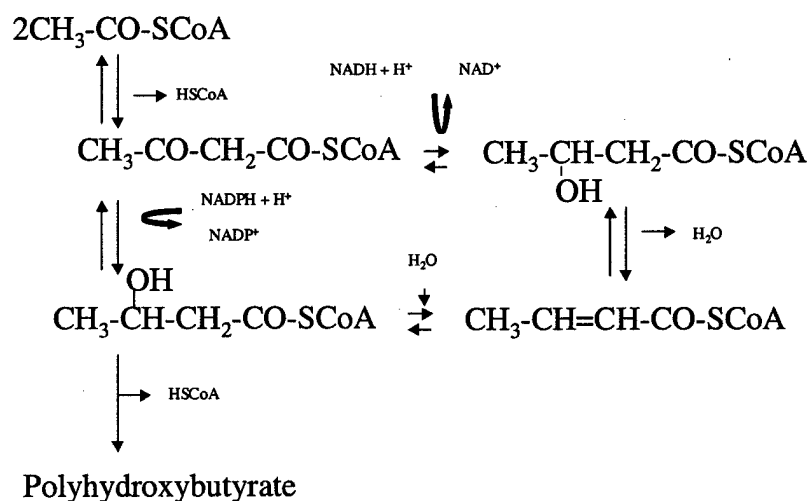
Figure 4-7. Formation of polyhydroxybutyrate, a bacterial food storage compound, from acetylcoenzymeA.

$$HO\text{-}CH\text{-}H_2C\text{-}C\text{-}[\text{-}O\text{-}CH\text{-}CH_2\text{-}C\text{-}]_n\text{-}O\text{-}CH\text{-}CH_2\text{-}COOH$$
$$\quad CH_3 \quad\quad O \quad\quad CH_3 \quad\quad O \quad\quad CH_3$$
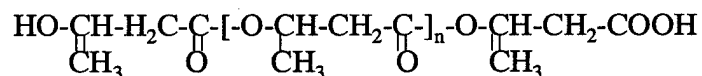
Figure 4-8. Structure of poly-β-hydroxybutyric acid.

If storage only is the case, Equation (4-9) may likely represent the oxygen to toluene ratio (as diagramed in Figure 2-4). This equation gives a ratio of 104 g oxygen consumed for each mole toluene consumed, or 1.13 g oxygen:1 g toluene, creating an acetyl group and succinate.

$$C_7H_8 + (1/2)H_2O + (13/4)O_2 \longrightarrow C_2H_3O + C_4H_6O_4 + CO_2 \quad (4\text{-}9)$$

The true ratio of oxygen per toluene consumed most likely lies somewhere between the two extremes, 1.13 and 3.125 g oxygen/g toluene. It may also differ between biofilms and bioreactors, as the fraction of contaminant converted to biomass depends upon conditions within the biofilter including starving, stress, and the presence of predators (Devinny et al, 1999). If a carbon dioxide balance was completed, by taking carbon dioxide measurements at the inlet and the outlet, perhaps a better estimate of the actual ratio of oxygen consumed to toluene consumed could be acquired.

4.6 MODEL ASSUMPTIONS:

To allow a first run of the model to be solved, numerous assumptions must be made. They include the following:

1. Steady-state operation ($\delta S/\delta t = 0$), no changes in substrate input with time.

2. No accumulation of toluene or oxygen within the silicone membrane. Effective permeability of both oxygen and toluene remains constant throughout the silicone tube and additionally, the effective permeability of the silicone is independent of concentration.

3. No advection in the biofilm (V_r, V_θ, V_z, = 0); transport in the biofilm is due only to diffusion.

4. No net diffusion of the substrate in the z and θ directions, radial gradients expected to be greater than axial gradients (Characklis, 1990 p.514; Kuelin et al, 1997).

5. Dual substrate Monod-like kinetics describe both toluene degradation and oxygen use (Harris and Hansford, 1976; Casey et al (2000)); rate limiting substrates are organic carbon and/or oxygen.

6. Steady-state biofilm growth and decay (Metris et al, 2001; Diks et al, 1994).

7. Axial gradients are small between liquid sections (measured in this study and in Neemann (1999) and Casey et al (2000)).

8. When flow is present on the liquid side, the liquid suspension is completely mixed, essentially reducing the liquid resistance to zero. Recirculation velocity has been found to have no effect on compound removal efficiency once a biofilm was established (Min et al, 2002).

9. Oxygen consumption in the biofilm is stoicheometrically related to toluene consumption (Harris and Hansford, 1975).

10. Kinetic parameters such as the half saturation constant, maximum specific utilization rate, substrate and oxygen saturation coefficients and mass transfer coefficients remain constant (Harris and Hansford, 1975).

11. The toluene-contaminated air is completely mixed inside the silicone tube.

12. The biofilm density is constant throughout the biofilm and the suspension density is constant throughout the completely mixed volume. The biomass has a constant density within the biofilm, which can be assumed at a macroscale, even if at a microscale there is strong evidence of high biofilm heterogeneity (Morgan-Sagastume et al, 2001).

13. The dimensions of the silicone tube remain constant, i.e. there is no swelling of the membrane.

14. A constant, immediately developed velocity profile is present within the lumen of each bioreactor tube(s). Thus, the air-side mass transfer boundary layer is the same thickness throughout the lumen.

15. As is customary, the mass transfer rate expressions in the model ignore biodegradation in the liquid film (Pressman et al, 1999).

16. All, or a large portion of the biofilm, is responsible for the degradation of toluene.

17. Biofilm sloughing and endogenous respiration do not affect the operation of the bioreactor.

4.7 MODELING EACH SECTION:

4.7.1 Air Phase:

Each disc-shaped section of height (Δz) and radius (r) is modeled by performing a mass balance over each area within the disc including the air side, membrane, biofilm,

liquid resistance and the suspension. A pictorial representation of the mass flow from the gas towards the membrane in shown in Figure 4-9(a) while the axial segments are shown in Figure 4-9 (b). Recalling that the numbering of individual discs, illustrated in Figure 4-9, runs from i =1 to n. The gas is assumed to be completely mixed within each axial element.

(a)   (b)
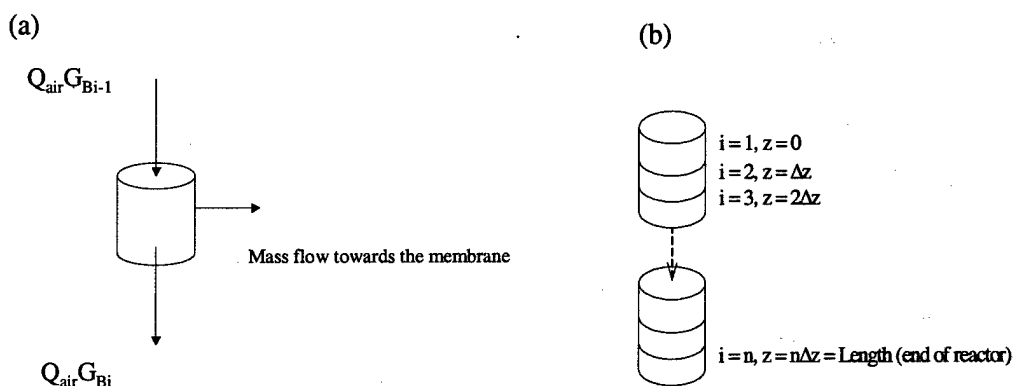
Figure 4-9. Pictorial representation of the bulk gas mixing and flux of contaminant towards the membrane (Fitch, 2002).

Equations (4-10) - (4-13) describe mathematically what is occurring on the air side. A separate, yet identical set of equations would be needed for both oxygen and toluene.

$$\text{In - Out} = 0 \qquad \text{(No accumulation within the air phase cell)} \qquad (4\text{-}10)$$

$$Q_{air}(G_{(Bi-1)}) - Q_{air}(G_{Bi}) - A_i k_g(G_{(Bi-1)} - G_{(Mi-1)}) = 0 \qquad (4\text{-}11a)$$

$$A_i = 2\Pi r_i \Delta z \qquad (4\text{-}11b)$$

$$-\left(\frac{Q_{air}\left(G_{Bi-1} - G_{Bi}\right)}{\left(2\Pi r_i \Delta z\right)k_g} - G_{Bi-1}\right) = G_{mi-1} \qquad (4\text{-}12)$$

To simplify all further calculations, the gas phase concentration was described in terms of a liquid phase concentration.

$$C_{gas} = HC_{liquid} \qquad (4\text{-}13)$$

4.7.2 Membrane Section: A pictorial representation of mass flow across the membrane is shown in Figure 4-10.
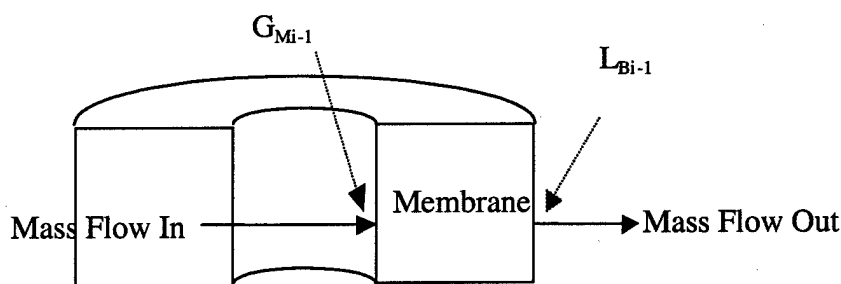

Figure 4-10. Mass flow into, across, and out of the membrane (Fitch, 2002).

The sorption into, transport across and desorption from the membrane is taken into account with the membrane mass transfer coefficient modeled previously, Equation 4-6. Therefore, the flux into and the flux out of the membrane will be equal as there is no accumulation within the membrane at steady state. This statement is represented mathematically in Equations (4-14) - (4-17). A separate, yet identical set of equations would be needed for both oxygen and toluene.

$$\text{In - Out} = 0 \quad \text{(No accumulation within the membrane)} \qquad (4\text{-}14)$$

$$A_i k_g (G_{(Bi\text{-}1)} - G_{(Mi\text{-}1)}) - A_o k_m (G_{(Mi\text{-}1)} - L_{B(i\text{-}1)}) = 0 \qquad (4\text{-}15)$$

$$A_o = 2\Pi r_o \Delta z \qquad (4\text{-}16)$$
$$A_i = 2\Pi r_i \Delta z \qquad (4\text{-}17)$$

4.7.3 Combined Gas and Membrane Resistances: Because of the number of unknowns, the gas and membrane resistances were combined to yield a combined gas/membrane resistance, subsequently yielding a combined mass transfer coefficient ($K_{gas\ and\ membrane}$). By combining the resistances, Equation (4-18) results:

$$Q_{air}(G_{(Bi-1)}) - Q_{air}(G_{Bi}) - A_O K_{gas\ and\ membrane}(G_{(Bi-1)} - L_{(Bi-1)}) = 0 \qquad (4\text{-}18)$$

4.7.4 Biofilm Section: The biofilm sections or discs are modeled using the continuity equation of mass in cylindrical coordinates (Equation 4-19, Bird et al, 1960). The objective is to plot the substrate and oxygen profile within the biofilm at each successive ring radius. The same set of equations is used to determine both the toluene and oxygen profiles, with S replaced by O when determining the oxygen profile.

$$\frac{\partial S}{\partial t} + \left[V_r \frac{\partial S}{\partial r} + V_\theta \frac{1}{r}\frac{\partial S}{\partial \theta} + V_z \frac{\partial S}{\partial z} \right] = D_S \left(\frac{1}{r}\frac{\partial}{\partial r}\left(r\frac{\partial S}{\partial r} \right) + \frac{1}{r^2}\frac{\partial^2 S}{\partial \theta^2} + \frac{\partial^2 S}{\partial z^2} \right) + R_S \qquad (4\text{-}19)$$

where in this case,

S = substrate (toluene) concentration

r = radial position

t = time

z = axial location

V = velocity in each respective direction

θ = angular direction as discussed previously

D_S = diffusion coefficient within the biofilm for toluene

R_S = reaction rate

With V_r, V_θ, V_z, $\delta^2S/\delta\theta^2$, $\delta^2S/\delta z^2$, and $\delta S/\delta t = 0$, the continuity equation reduces to Equation (4-20)

$$D_s\left(\frac{1}{r}\frac{\partial}{\partial r}\left(r\frac{\partial S}{\partial r}\right)\right)+R_s=0 \qquad (4\text{-}20)$$

Taking the derivative ($\delta/\delta r$) using the product rule (Stewart, 1995, p. 115) the expression becomes Equation (4-21). With R_s actually being used here as a removal term instead of a generation rate, that is, positive values = removal, Equation (4-22) results.

$$\frac{D_s}{r}\left[r\frac{\partial^2 S}{\partial r^2}+\frac{\partial S}{\partial r}\right]+R_s=0 \qquad (4\text{-}21)$$

$$\frac{D_s}{r}\left[r\frac{\partial^2 S}{\partial r^2}+\frac{\partial S}{\partial r}\right]-R_s=0 \qquad (4\text{-}22)$$

The only known reaction occurring in the biofilm is that of substrate (toluene) consumption by microorganisms contained within the biofilm. That reaction is expressed in Equations (4-23) - (4-25) and the reaction equations take into account both the toluene concentration and oxygen concentration (Sinclair and Ryder, 1975). The term dual limitation refers to a type of multiple-substrate limitation in which the electron-donor and electron-acceptor substrates together limit the overall cell-growth rate. A theoretical basis for the multiplicative model may be found from a special case of enzyme-substrate reactions in which two substrates react together at the active site of one enzyme to produce a single product. Since both substrates bind the single enzyme to form an intermediate, the rate of product formation is affected by both concentrations in a multiplicative manner (Bae and Rittmann, 1996).

$$R = \frac{\mu' X}{Y} \left(\frac{S}{K_s + S} \right) \left(\frac{O}{K_o + O} \right) \hspace{2cm} \text{(4-23)}$$

In Equation 4-23, μ' is the maximum specific growth rate of the organisms, X is the

biofilm density, Y is the yield coefficient of the organisms on toluene, S the

concentration of toluene and O the concentration of oxygen. Using the substitution,

where k is the maximum specific substrate utilization rate, shown in Equation (4-24)

(Metcalf and Eddy, 1991, p 699),

$$k = \frac{\mu'}{Y} \hspace{2cm} \text{(4-24)}$$

Equation (4-25) is then developed.

$$\frac{D_s}{r} \left[r \frac{\partial^2 S}{\partial r^2} + \frac{\partial S}{\partial r} \right] - kX \left(\frac{S}{K_s + S} \right) \left(\frac{O}{K_o + O} \right) = 0 \hspace{2cm} \text{(4-25)}$$

4.7.5 Liquid Phase: The liquid phase diagram is shown in Figure 4-11. Mathematical

expressions for the transfer of substrate from the biofilm to the bulk liquid are shown in

Equations 4-26 and 4-27. Because the thin film is stationary, Q = 0. The mass flow from

the last cell of the biofilm is then set equal to the concentration gradient multiplied by the

area.

Mass flow from biofilm   Mass flow towards suspension
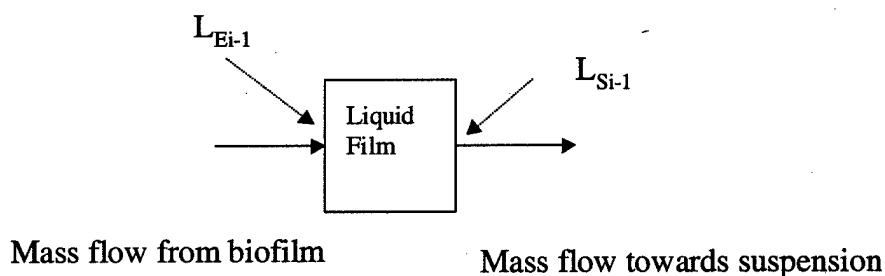
Figure 4-11. Diagram of liquid resistance and mass flow into the suspension.

$$\frac{V_{lastcell}D_S}{r}\left[r\frac{\partial^2 S}{\partial r^2}+\frac{\partial S}{\partial r}\right]_{r=rb} = A_3k_l(L_{(Ei-1)} - L_{(Si-1)}) \qquad (4\text{-}26)$$

$$A_3 = 2\pi r_b \Delta z \qquad (4\text{-}27)$$

Where k_l is the liquid mass transfer coefficient, L_E is the concentration at the outer edge of the biofilm and L_S the concentration in the liquid, and V is the volume of the last biofilm cell.

4.7.6 Suspension: The liquid suspension is treated the same as the biofilm, and its analysis again begins with the continuity equation (Bird et al, 1960), shown in Equation (4-28). The same set of equations is used to determine both the toluene and oxygen profiles, with S replaced by O when determining the oxygen profile.

$$\frac{\partial S}{\partial t}+\left[V_r\frac{\partial S}{\partial r}+V_\theta\frac{1}{r}\frac{\partial S}{\partial \theta}+V_z\frac{\partial S}{\partial z}\right]=D_S\left(\frac{1}{r}\frac{\partial}{\partial r}\left(r\frac{\partial S}{\partial r}\right)+\frac{1}{r^2}\frac{\partial^2 S}{\partial \theta^2}+\frac{\partial^2 S}{\partial z^2}\right)+R_S \qquad (4\text{-}28)$$

With V_r, V_θ, $\delta^2 S/\delta\theta^2$, $\delta^2 S/\delta z^2$, and $\delta S/\delta t = 0$ but with movement in the axial direction of the liquid phase, and again the removal term being negative, Equation (4-29) results.

$$D_S\left(\frac{1}{r}\frac{\partial}{\partial r}\left(r\frac{\partial S}{\partial r}\right)\right)-R_S=V_z\frac{\partial S}{\partial z} \qquad (4\text{-}29)$$

Taking the derivative using the product rule again (Stewart, 1995, p. 115) and using relationships as shown previously, Equations (4-30) - (4-34) are created. When flow is equal to zero, so is the velocity on the liquid side and Equation (4-30) reduces to the same Equation as shown for the substrate concentration in the biofilm, Equation (4-22). In

virtually all of the measurements taken on the reactor systems, the liquid-phase substrate concentration was constant from inlet to outlet ($\delta S/\delta z = 0$), further reducing the equation in complexity.

$$\frac{D_s}{r}\left[r\frac{\partial^2 S}{\partial r^2}+\frac{\partial S}{\partial r}\right]-R_s=V_z\frac{\partial S}{\partial z} \tag{4-30}$$

$$R=\frac{\mu'X}{Y}\left(\frac{S}{K_s+S}\right)\left(\frac{O}{K_o+O}\right) \tag{4-31}$$

$$k=\frac{\mu'}{Y} \text{ (Metcalf and Eddy, 1991, p 699)} \tag{4-32}$$

$$R=kX\left(\frac{S}{K_s+S}\right)\left(\frac{O}{K_o+O}\right) \tag{4-33}$$

$$\frac{D_s}{r}\left[r\frac{\partial^2 S}{\partial r^2}+\frac{\partial S}{\partial r}\right]-kX\left(\frac{S}{K_s+S}\right)\left(\frac{O}{K_o+O}\right)=V_z\frac{\partial S}{\partial z} \tag{4-34}$$

4.8 THE NUMERIC APPROXIMATION:

Because of the complexity of the system geometry and the complexity of the dual substrate expression itself, there is no analytical solution to the described system of equations. Therefore, numeric differentiation was applied to determine the substrate concentration within the biofilm. Using numeric differentiation, Equation (4-35) becomes Equation (4-36) as derivatives are replaced by deltas.

$$\frac{D_s}{r}\left[r\frac{\partial^2 S}{\partial r^2}+\frac{\partial S}{\partial r}\right]-kX\left(\frac{S}{K_s+S}\right)\left(\frac{O}{K_o+O}\right)=0 \tag{4-35}$$

$$\frac{D_s}{r}\left[r\frac{\Delta^2 S}{\Delta r^2}+\frac{\Delta S}{\Delta r}\right]-kX\left(\frac{S}{K_s+S}\right)\left(\frac{O}{K_o+O}\right)=0 \tag{4-36}$$

Equations (4-37) - (4-40) simplify Equation (4-36),

$$\left[r\frac{\Delta^2 S}{\Delta r^2}+\frac{\Delta S}{\Delta r}\right]=\frac{r}{D_s}kX\left(\frac{S}{K_s+S}\right)\left(\frac{O}{K_o+O}\right) \tag{4-37}$$

$$\left[\frac{\Delta S}{\Delta r}\right]=\frac{r}{D_s}kX\left(\frac{S}{K_s+S}\right)\left(\frac{O}{K_o+O}\right)-r\frac{\Delta^2 S}{\Delta r^2} \tag{4-38}$$

$$\Delta S=r\Delta r\left(\frac{kX}{D_s}\left(\frac{S}{K_s+S}\right)\left(\frac{O}{K_o+O}\right)-\frac{\Delta^2 S}{\Delta r^2}\right) \tag{4-39}$$

$$S_{j-1}-S_j=r\Delta r\left(\frac{kX}{D_s}\left(\frac{S}{K_s+S}\right)\left(\frac{O}{K_o+O}\right)-\frac{\Delta^2 S}{\Delta r^2}\right) \tag{4-40}$$

and solving for the toluene concentration profile, the equation becomes Equation (4-41).

This applies for each numerical element (cell) of the biofilm, which has a coordinate of i

(axial) and j (radial), as shown in Figure 4-12?

$$S_{j-1}=r\Delta r\left(\frac{kX}{D_s}\left(\frac{S}{K_s+S}\right)\left(\frac{O}{K_o+O}\right)-\frac{\Delta^2 S}{\Delta r^2}\right)+S_j \tag{4-41}$$
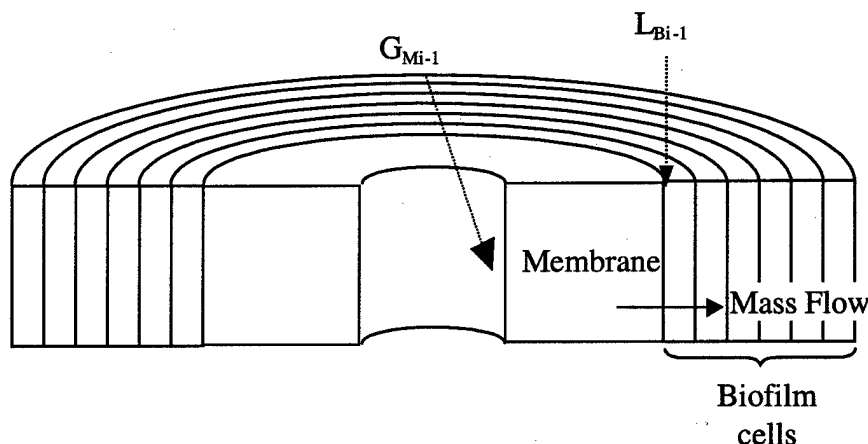
Figure 4-12. Illustration of numerical elements of biofilm solution (Fitch, 2002).

For the oxygen concentration profile, the equation becomes Equation (4-42) where F is the ratio of the mg oxygen consumed for each mg of toluene consumed (Section 4.5)

$$O_{j-1} = r\Delta r \left[\frac{kFX}{D_S} \left(\frac{S}{K_S + S} \right) \left(\frac{O}{K_O + O} \right) - \frac{\Delta^2 O}{\Delta r^2} \right] + O_j \qquad (4\text{-}42)$$

4.9 SECOND DERIVATIVE DETERMINATION:

4.9.1 Shape and Size of the Second Derivative: The model itself presents a problem - estimation of a function from its second derivative. Seven methods were examined for estimating the second derivative, $\delta^2 S / \delta r^2$. An estimation was required since the function is unknown and the second derivative must be used to numerically estimate that function. An eighth method was discussed (Fitch, 2002), that of estimating a substrate concentration profile function, such as Ce^{-r}, however, that too, appeared not to be appropriate.

An *example* of a function with exponential decay was used to understand conceptually what is happening to the function, its first derivative, and its second derivative. Graphs were made of an *assumed* function $(S = Be^{-kr})$ representing the concentration profile across the biofilm, where S represents the concentration in the biofilm at radius location r and B and k are constants. The graphical representation of the

approximated function and its first and second derivatives are shown in Figures (4-13) -

(4-15).
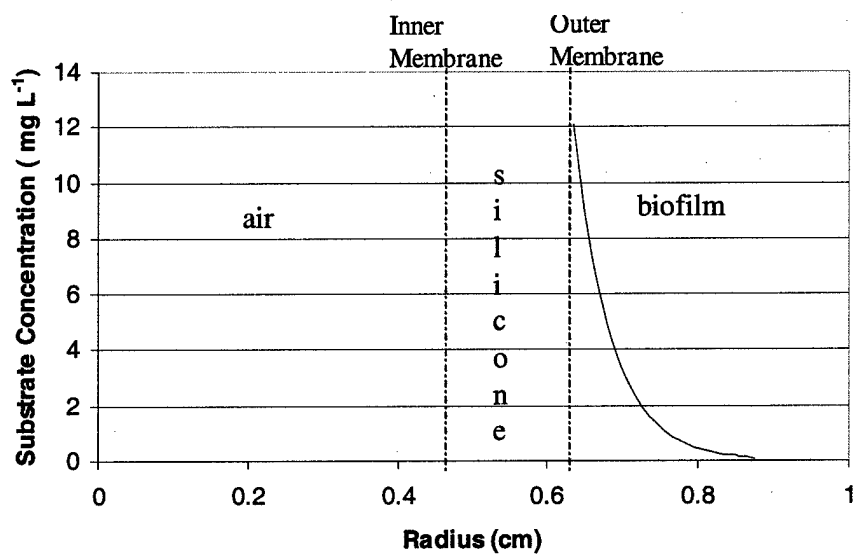
Figure 4-13. Approximated shape of and example substrate concentration profile across the biofilm.
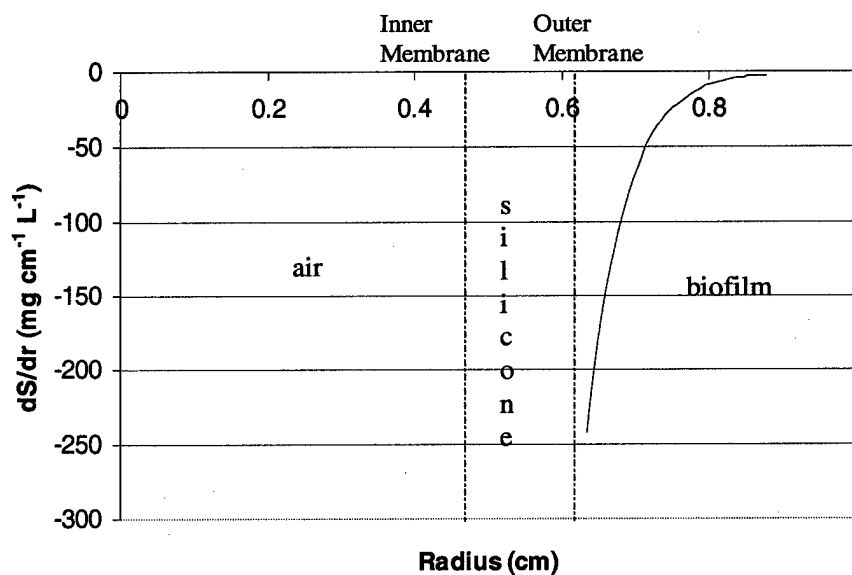

Figure 4-14. Shape of an example first derivative of the approximated function.
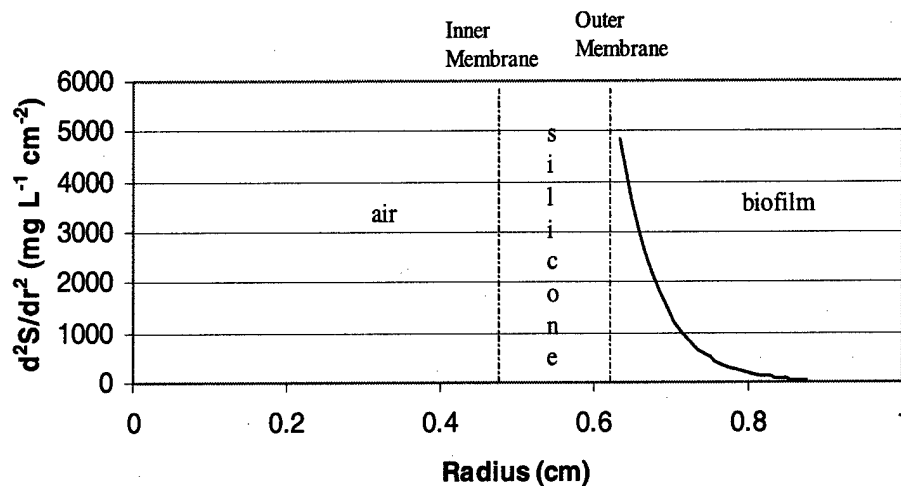
Figure 4-15. Shape of an example second derivative of the approximated function.

4.9.2 Methods for Estimating the Second Derivative:

Method 1. The first method for estimating the second derivative was from Harris and

Hansford (1976) and is shown in Equations (4-43) - (4-45). The second derivative is

estimated to be equal to the rate of removal. However, when this value is placed back

into Equation (4-46), the main equation for determining the substrate concentration

profile across the biofilm, the value within the parentheses becomes zero, indicating no

substrate concentration change across the biofilm. This result is not believed to be

correct.

$$D \frac{\Delta S}{\Delta r} \bigg|_{x=r} - r_{su} = D \frac{\Delta S}{\Delta r} \bigg|_{x=r+\Delta r} \tag{4-43}$$

$$\frac{\Delta^2 S}{\Delta r^2} = \frac{r_{su}}{D} \tag{4-44}$$

$$r_{su} = kX \left(\frac{S}{K_S + S} \right) \tag{4-45}$$

$$S_{j-1} = r\Delta r \left(\frac{kX}{D_S} \left(\frac{S}{K_S + S} \right) - \frac{\Delta^2 S}{\Delta r^2} \right) + S_j \qquad (4\text{-}46)$$

Method 2. The second method examined for estimating the second derivative is shown in Equation (4-47); the second derivative is set equal to zero. Using this second derivative estimate in the substrate concentration profile model yielded a very steep concentration profile within the biofilm, and a gross underestimation of toluene removal by the reactor.

$$\frac{\Delta^2 S}{\Delta r^2} = 0 \qquad (4\text{-}47)$$

Method 3. The third method used to estimate the second derivative is shown in Equations (4-48)-(4-50). This method involved approximating the second derivative by assuming zero order kinetics and linearizing the diffusion equation. When used in the substrate concentration profile model, negative values for the substrate concentration across the biofilm were obtained. The small value of the diffusion coefficient forces r_{su}/D to be a very large number.

$$D \frac{\Delta S}{\Delta r}\bigg|_{x=r} - r_{su} = D \frac{\Delta S}{\Delta r}\bigg|_{x=r+\Delta r} \qquad (4\text{-}48)$$

$$\frac{\Delta^2 S}{\Delta r^2} = \frac{r_{su}}{D} \qquad (4\text{-}49)$$

$$r_{su} = kX \qquad (4\text{-}50)$$

Method 4. The fourth method used to estimate the second derivative is shown in Equations (4-51)-(4-53). This approximated the second derivative by assuming first order kinetics within the biofilm, beginning with the linear approximation of the diffusion equation. When used in the substrate concentration profile model, negative values for the substrate concentration were again generated. The small value of the diffusion coefficient forces r_{su}/D to be a very large number.

$$D \frac{\Delta S}{\Delta r}\bigg|_{x=r} - r_{su} = D \frac{\Delta S}{\Delta r}\bigg|_{x=r+\Delta r} \tag{4-51}$$

$$\frac{\Delta^2 S}{\Delta r^2} = \frac{r_{su}}{D} \tag{4-52}$$

$$r_{su} = \frac{kXS}{K_S} \tag{4-53}$$

Method 5. The fifth method used to estimate the second derivative involved use of the five point Lagrangian approximation as shown in Equation (4-54). This numeric approximation method involves use of first derivatives at previous points to estimate the new second derivative, i.e. to estimate the second derivative at point 6, the first five derivatives and the step size (delta) must be known. The first five values were estimated from the substrate concentration profile generated with $\Delta^2 S / \Delta r^2$. When used in the substrate concentration profile model, extremely large values for the substrate concentration were found, again, indicating this was not a likely candidate for the estimation of the second derivative.

$$\frac{\Delta^2 S}{\Delta r^2}\bigg|_6 = \frac{1}{12\Delta r}\left[3\frac{\Delta S_1}{\Delta r} - 16\frac{\Delta S_2}{\Delta r} + 36\frac{\Delta S_3}{\Delta r} - 48\frac{\Delta S_4}{\Delta r} + 25\frac{\Delta S_5}{\Delta r}\right] \qquad (4\text{-}54)$$

Method 6. An analytical solution to the continuity of mass equation in cylindrical coordinates was attempted by assuming the substrate utilization rate was zero order and the biofilm thickness known. The full algebraic derivation is detailed elsewhere in the author's laboratory notebook but begins with Equation (4-55) and ends with Equation (4-57). When used in the substrate concentration profile model, negative concentration profiles across the biofilm were obtained.

$$D_s\left(\frac{1}{r}\frac{d}{dr}\left(r\frac{dS}{dr}\right)\right) - R_S = kX \qquad (4\text{-}55)$$

$$S = \left(\frac{1}{4}\right)\frac{kXr^2}{D_s} + C_1\ln r + C_2 \qquad (4\text{-}56)$$

$$\frac{d^2 S}{dr^2} = \frac{kX}{2D} - C_1 r^{-2} \qquad (4\text{-}57)$$

Method 7. The seventh method, which was ultimately chosen for estimation of the second derivative, involved subtracting a constant from Equation (4-44), thus giving Equation (4-58). The constant chosen (0.5 mg L^{-1} cm^{-2}) allowed the second derivative to remain close to zero but still to be non-zero. With this equation in the model, reasonable results for removal and biofilm thickness were obtained. Values for the second derivative are generated that fall within the mid-range of values indicated by Method 6. Substrate concentrations generated when Equation (4-58) is used in the substrate concentration profile model are of a reasonable value and are such that biofilm thickness and removals are adequately predicted.

$$\frac{\Delta^2 S}{\Delta r^2} = \frac{r_{su}}{D} - C \qquad\qquad (4\text{-}58)$$

4.10 SINGLE SUBSTRATE LIMITATION:

The previously listed dual substrate limitation equations involve the oxygen concentration throughout the biofilm and the suspension. However, during experimental examination of the bioreactor systems, it was found that the removal in the biofilm and suspension is apparently not related to the oxygen concentration. This lack of oxygen dependence for toluene degradation was evaluated by performing a brief but critical experiment. The experiment was undertaken after review of oxygen readings within the liquid suspension indicated highly variable oxygen levels present at various times, without any apparent increases/decreases of toluene removal.

To determine if oxygen affected the rate of toluene degradation, a batch experiment comparing degradation of toluene within the liquid suspension in the presence of oxygen and in the absence or oxygen was completed. The experimental method is described in Chapter 3.10.13. Degradation of toluene, using GC headspace analysis, was monitored over a period of several hours. Results of both experiments are shown in Figure 4-16. If oxygen was in fact a limiting reactant, there should be no degradation of toluene within the purged (oxygen free) headspace vials.
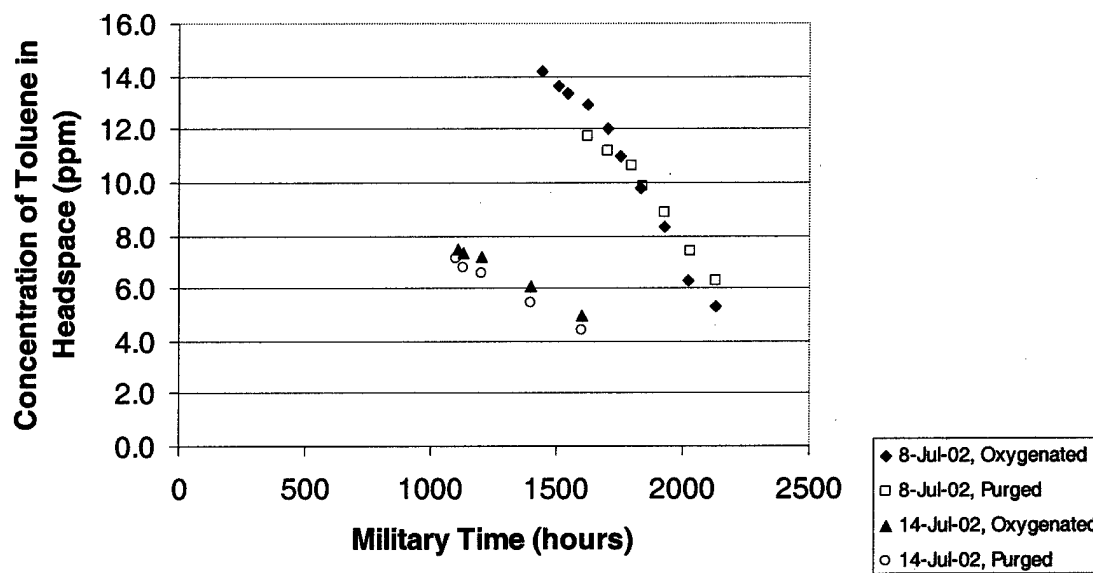
Figure 4-16. Degradation of toluene in purged (anaerobic) and unpurged (aerobic) vials. Degradation rates are similar suggesting oxygen does not influence degradation.

Instead of no degradation, all vials for a given day gave similar rates of removal of toluene. A further experiment (detailed in Chapter 3) examined whether anaerobic organisms were present within the biofilm. Anaerobic growth (15 colonies Plate 1, 6 colonies Plate 2) was detected in two separate experiments, confirming the presence of anaerobic toluene degraders.

The lack of oxygen at the edge of the thick biofilms seen in this study and the presence of anaerobes is not unwarranted. Numerous studies have indicated that in many biofilter systems, oxygen is depleted before the VOC; however, oxygen depletion is generally considered rate-limiting in such cases. In conventional biofilters, effective biofilm thickness will be determined by oxygen rather than VOC availability (Devinny et al, 1999). Baltzis et al (2001) found that oxygen rather than the VOC is depleted first and determined the effective biofilm thickness in the segment of a biotrickling filter closest to the inlet of the contaminated air stream. At the 39th day of their experiment, only one-

third of the biofilm was supplied with oxygen (Debus, 1995). Oxygen was found to be depleted 400 microns into an 810 micron biofilm treating xylene-contaminated water (Debus et al, 1994). In the case of styrene degradation, Cox et al (1997) observed a biofilm thickness around 260 microns but experimental results and model calculations indicated an effective biofilm thickness of about 80 microns. In conventional biofilter biofilms, the active layer is generally an oxic layer, typically 50-200 micrometers in thickness, which corresponds directly to the depth of oxygen penetration into the biofilm (Rishell and Hamer, 2000). The bacteria within these biofilms were speculated to be either obligate aerobes or facultative anaerobes. When steady-state is achieved in a HFMM, biomass immobilized on the outer surface of the hollow fibers would consist of aerobic cells near the membrane surface, and anaerobic cells at the outer periphery of the biofilm (Parvatiyar et al, 1996a).

Because of the apparent lack of importance of oxygen in the biofilters studied in the work reported here, a simpler set of equations (single substrate limitation) was actually used to solve for the toluene concentration through the biofilm. Thus the numerical equation used for the toluene concentration across the biofilm was:

$$S_{j-1} = r\Delta r \left(\frac{kX}{D_s} \left(\frac{S}{K_S + S} \right) - \frac{\Delta^2 S}{\Delta r^2} \right) + S_j \qquad (4\text{-}59)$$

4.11 BOUNDARY CONDITIONS AND NUMERICAL SOLUTION:

The model is designed to predict the effluent toluene concentration in the gas phase (the concentration exiting the each axial cell), and boundary conditions must be applied to provide additional equations to actually solve for the effluent toluene concentration in the gas stream. Also required are additional assumptions to make the

model solvable. The first of those assumptions is complete mixing within the liquid suspension, not just that the liquid side is mixed, but that there is no liquid film resistance, so that the boundary condition shown in Equation (4-60) applies; that is, the toluene concentration at the edge of the biofilm is equal to the concentration in the completely mixed suspension.

$$At\ r = r_b: \quad L_{Ei-1} = L_{Si-1} \quad\quad (4\text{-}60)$$

By applying this boundary condition, the substrate concentration profile within the biofilm may be calculated, moving from the outer edge of the biofilm inwards toward the silicone tube. The suspension concentration must be experimentally measured or assumed; the outermost biofilm element's concentration is thus evaluated and the biofilm profile determined by solving for the next (inward) radial position substrate concentration (S_{j-1}) after the current cell (S_j) has been determined. The substrate concentration profile across the biofilm is thus determined for each radial position and then for each discrete ring along the z axis.

Although the concentration profile has been evaluated, the concentration at the inner edge (boundary condition) is not known. This inner boundary condition and the fundamental premise of the model is that the inner biofilm concentration is such that the flux equals the removal in each axial element, Equation (4-61).

$$\underbrace{Q_{air}(G_{Bi-1} - G_{Bi})}_{\substack{removal\ in\ the\ gas\\ axial\ element}} = \underbrace{K_{combined\ gas\ and\ membrane}A(G_{Bi-1} - L_{Bi-1})}_{mass\ flow;\ L_{Bi-1}\ solved\ u\ u\sin g\ the\ mod\ el} = \underbrace{\sum_{j=1}^{m} v_j r_{su\,j} + r_{su} v_{suspension}}_{deg\,radation\ in\ biofilm\ and\ suspension} \quad (4\text{-}61)$$

The mass flow across the silicone membrane at any "i^{th}" axial element, the middle term in the above equation, must be equal to (or within a certain percentage of) the amount of substrate removed in the biofilm and suspension of that "i^{th}" element, the term on the

right hand side of Equation (4-61). The numerical model, which is solved using a spreadsheet, is designed such that the difference between the mass flow (flux x area) across the membrane, which is the amount of contaminant removed from the gas, and the removal (degradation of substrate in the biofilm and suspension) in each axial element may be examined as a function of possible biofilm thickness. The smallest difference between these determines the numerical solution used for that axial element (i.e. the number of elements m and thus the thickness of the biofilm).

Having determined the thickness of the biofilm and its associated removal, the substrate concentration profile across the biofilm is thus known. The removals are summed across the biofilm for each separate axial element i, as shown in Equation (4-62), where v is the volume of the radial element, $(\pi r_j^2 - \pi r_{j-1}^2)\Delta z$. The substrate removal in the liquid suspension must also be accounted for and is shown in Equation (4-63), where r_{su} is the substrate utilization rate for the suspension, and v is the volume of the suspension $\Delta z(\pi r^2_{module} - \pi r^2_{tubing\ and\ biofilm})$ associated with axial element "i".

$$\text{Removal associated with the biofilm} = \sum_{j=1}^{m} v_j r_{su\,j} \qquad (4\text{-}62)$$

$$\text{Removal associated with the liquid suspension} = r_{su} v_{suspension} \qquad (4\text{-}63)$$

A thicker biofilm (with more radial elements) would result in more degradation, a lower concentration at the membrane-biofilm interface, and thus a greater mass flow across the membrane. This numerical solution process is repeated down the length of the z axis, until the end (i = n) is reached.

4.12 NUMERIC TECHNIQUE USING EXCEL®:

Because there is no analytical solution to Equation 4-59, a numeric solution to that equation was developed as described above. A software technique was required to solve the set of equations describing bioreactor activity numerically. Excel® was chosen based upon the experience of others, and the ability to readily examine the values in each numerical cell (Aziz et al, 1995; Pressman, 1995; Neemann, 1998).

To determine whether the numeric method was rigorous enough for the proposed modeling effort, the effect of changes in the biofilm cell size, Δr, on model results was examined. Specifically, the size of Δr was decreased and the model results compared with respect to toluene removal from the gas phase, the percentage difference in mass flow across the membrane and toluene removal, and the biofilm thickness. The results of that evaluation are shown in Table 4-2. The difference between the value of the mass flow across the membrane (Equation 4-61 center element) and toluene removal ((Equation 4-61 right hand side) was strongly dependent upon the cell size, and there was some variation of both the toluene removal and biofilm thickness with decreasing Δr. The numeric technique solved using Excel® appears to be suitable for the modeling task so long as Δr is 0.02 cm or less.

Table 4-2. Changes in model outcomes with a decrease in Δr.

Δr (cm)	Removal (mg L^{-1})	% Difference Mass Flow/Removal (%)	Biofilm Thickness (cm)
0.2	1.19	15	0.20
0.1	1.20	15	0.20
0.07	1.27	9.3	0.21
0.05	1.20	14	0.20
0.02	1.34	2.2	0.22
0.01	1.38	0.43	0.22
0.009	1.37	0.19	0.22
0.007	1.35	0.13	0.21

4.13 SOLVING THE MODEL:

Several steps are used when running the model. They include the following and are flow charted in Figure 4-17:

1. The parameter values are entered into the model spreadsheet including the number of tubes, air flow, inner and outer tube diameters, kinetic coefficients, diffusion coefficients, air density and air viscosity; appropriate values must be provided for all parameters listed in Table 4-1.

2. The tube length is partitioned into axial elements (Δz) of 1 cm or less.

3. The liquid concentration is entered and is used as the concentration at the edge of the outermost biofilm cell in the first axial element (boundary condition, Eq. 4-60).

4. The removal in the outermost cell is calculated and added to the outer most cell concentration to determine the concentration in the next radial cell (solving Equation 4-59).

5. The process of calculating removal and concentration in adjacent radial cells is repeated, giving 40 possible biofilm thicknesses (between 1 and 40 biofilm cells), each with a differing concentration.

6. The mass flow is calculated for each possible biofilm thickness: the influent gas concentration to the axial element and the innermost radial biofilm cell concentration in that axial element determine the calculated value.

7. The biofilm thickness providing closest agreement (<5% difference) between mass flow and removal is determined manually and is chosen as the biofilm thickness of that axial element.

8. The removal in the biofilm and suspension is subtracted from the axial cell's influent concentration to provide the effluent concentration of that axial cell.

9. Steps 4 – 8 are repeated until the end of the tube is reached. The effluent gas concentration from the last axial element is the model's prediction for the biofilter's effluent gas concentration.
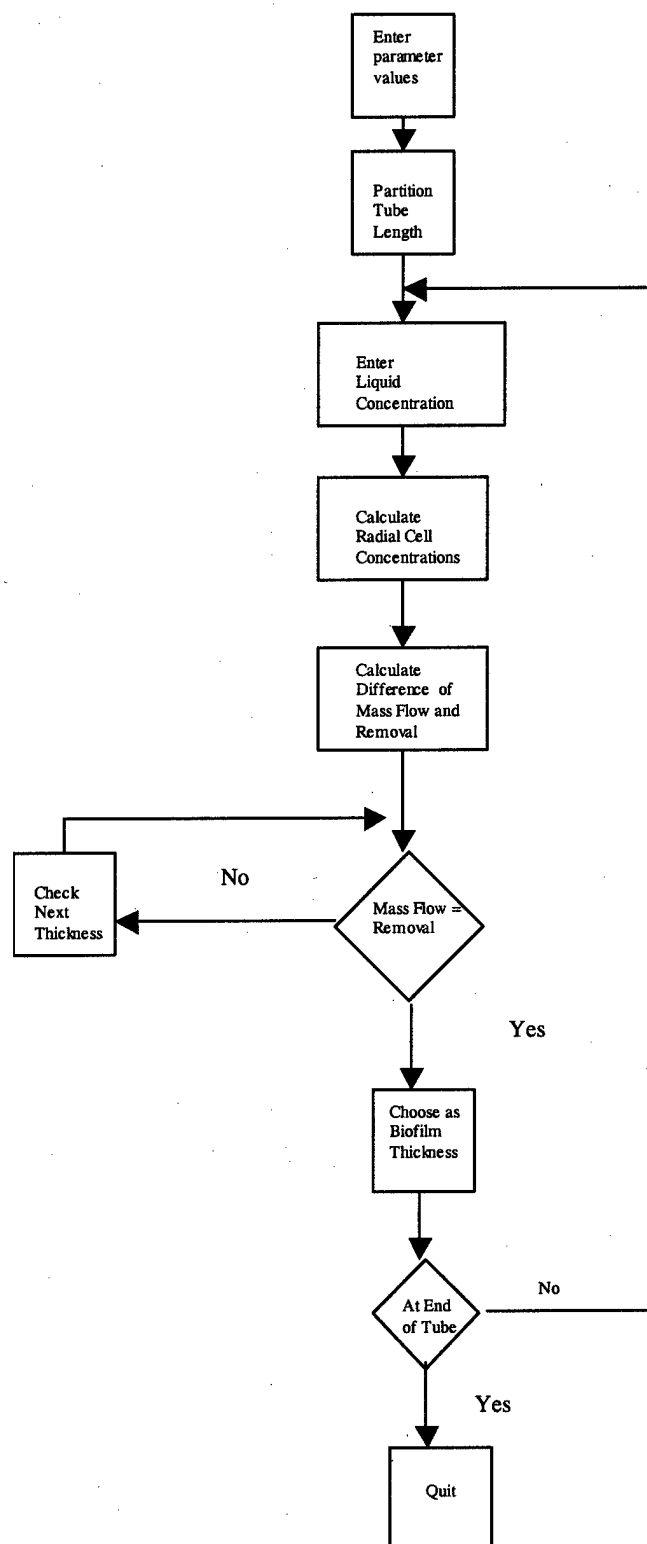
Figure 4-17. Flow chart describing model solution procedures.

4.14 MULTIPLE TUBE MODEL CONSIDERATIONS:

Up until this point, only the single tube model has been considered, however, some of the bioreactors used during this study had several tubes. A multiple tube model was developed by assuming each tube acted as a single tube. To determine the liquid suspension associated with each tube in the case of the multiple tube model, the reactor volume was equally divided amongst the individual tubes, and the individual tube solution was used for the resulting effective diameter, d_e.

The calculations to determine the amount of liquid suspension associated with each silicone tube are shown in Equations (4-47) – (4-49). First the entire cross-sectional area of the reactor was calculated. Then the diameter associated with each individual tube, d_e, was iteratively increased until the sum of the cross sectional areas associated with the individual tubes equaled that of the entire cross sectional area of the reactor module Equation (4-66); values are recorded in Appendix E.

$$\text{Cross sectional Area of Reactor Module} = \frac{\Pi d^2}{4} \qquad (4\text{-}64)$$

$$\text{Cross sectional Area Associated With Each Tube} = \frac{\Pi d_e^{\,2}}{4} \qquad (4\text{-}65)$$

$$\sum \text{Individual tube cross sectional areas} = \text{Cross sectional area of the reactor module} \quad (4\text{-}66)$$

4.15 INPUT PARAMETERS FOR SENSITIVITY ANALYSIS:

4.15.1 General Parameters: The proposed model has a large number of input parameters. Although most parameter values were directly measured for the system, some were taken from the literature. Literature and measured values are presented and

the effect on model results of changing those values was determined (i.e.a sensitivity analysis was performed). Initial input parameters are shown in Table 4-3.

Table 4-3. Input parameters for sensitivity analysis.

Parameter	Value	Source
$K_{S(Biofilm - Toluene)}$	1.0 mg L^{-1}	Measured/Fitted (Section 6.3.3)
$K_{S(Suspension - Toluene)}$	1.0 mg L^{-1}	Measured
$k_{(Biofilm - Toluene)}$	0.198 h^{-1}	Measured/Fitted (Section 6.3.3)
$k_{(Suspension - Toluene)}$	0.1 h^{-1}	Measured
$P_{(Toluene\ in\ Silicone)} = D_m S$	0.003 $cm^2\ s^{-1}$	Adjusted
$D_{(Toluene\ in\ Biofilm)}$	$0.8*D_{Toluene\ in\ Water}$ $cm^2\ s^{-1}$	Characklis (1990, p 117)
$D_{(Toluene\ in\ Water)}$	$9*10^{-6}$ $cm^2\ s^{-1}$	Schwarsenbach (1993) in Holden et al (1997)
$D_{(Toluene\ in\ Air)}$	0.0849 $cm^2\ s^{-1}$	Lugg (1968)
Q_{Air}	0.769 L min^{-1}	Measured
$X_{Biofilm}$	23,800 mg L^{-1}	Measured[1]
$X_{Suspension}$	29 mg L^{-1}	Measured[1]
$H_{(Toluene\ 20^o C)}$	0.275	Sawyer et al (1994)
Δz	0.5 cm	Chosen
Δr	0.01 cm	Chosen
Length	18.5 cm	Measured
r_i	0.47625 cm	Cole Parmer
r_o	0.635 cm	Cole Parmer

[1]Measured using volatile suspended solids analysis

Input parameters for the single tube model runs were selected in the following manner:

- The maximum specific utilization rate (k) and the half saturation constant (K_S) for the suspension were determined based on the batch kinetic experiments detailed in Chapter 6.

- Diffusion coefficients and the Henry's Law coefficient were taken directly from literature values. Diffusion coefficients and Henry's Law coefficients for contaminants are anticipated to be very similar to those in water; the water content of biofilms ranges from 98.1 – 99% (Characklis and Marshall, 1990, p.109).

- The tube radii were supplied by the tubing manufacturer.

- The biofilm density, suspension density, air flow, and reactor length were measured directly in the single tube reactor system.

- The values chosen for Δr and Δz were deemed reasonable choices based upon previous work (Neemann, 1998) and the value of Δr was examined as described previously in Section 6.2.

- The effective permeability was adjusted after numerous model runs using both literature values and directly measured values for silicone effective permeability to toluene showed gross underestimates of removal. The difference in effective permeability values is potentially related to the radius of the tubing. In the reactors studied, tubing was stretched to varying degrees, potentially changing the intrinsic properties of the material or perhaps just changing the radii.

4.15.2 Determination of Effective Permeability of Toluene in Silicone Rubber

(Abiotic Experiments): Because initial model runs using literature values for permeability predicted removals far lower than those observed, the effective permeability of the silicone tubing was examined further. Variation in literature values for permeability in silicone varied by an order of magnitude and also provided justification for further examination of toluene effective permeability in silicone. . The examination began with a repetition of the series resistance model shown in Equation (4-67). This equation assumes no biofilm (abiotic mass transfer).

$$\frac{1}{K_{OV}} = \frac{1}{k_l} + \frac{r_i(\ln(r_o / r_i))}{D_m S} + \frac{r_o / r_i}{k_g H} \qquad (4\text{-}67)$$

For any one airflow, tubing thickness, reactor configuration, and silicone rubber tubing, the equation may be reduced to the form as shown in Equation (4-68), where K_{ov} is the experimentally determined overall mass transfer coefficient for the system, k_l is the liquid phase mass transfer coefficient and C is the constant representing the resistance to mass transfer in the membrane and the air phase.

$$\frac{1}{K_{ov}} = \frac{1}{k_l} + C \qquad (4\text{-}68)$$

The liquid phase mass transfer coefficient is known to be a function of liquid flow rate, with increased liquid flow rates contributing to higher mass transfer rates due to the reduction in the thickness of the liquid thin film boundary layer. That liquid film mass transfer coefficient and the relationship with flow rate (Q) may be represented by Equation (4-69) with A being a constant. The overall mass transfer resistance is thus written as shown in Equation (4-70). Equation (4-70) is, conveniently, the equation of a line in the form y = mx + b. Therefore, by examining a plot of experimentally determined $1/K_{ov}$ versus Q under abiotic operating conditions, the constants A and n may be determined by fitting a line to the data. The constant C may then be determined. C is represented by Equation (4-71) and the effective permeability (P=S*D) may then be determined since all other variables are known or calculated; k_g found in Equation 4-4.

$$k_l = AQ^n \qquad (4\text{-}69)$$

$$\frac{1}{K_{ov}} = \frac{1}{AQ^n} + C \qquad (4\text{-}70)$$

$$C = \frac{r_i \ln\left(r_o/r_i\right)}{P} + \frac{r_o/r_i}{k_g H} \qquad (4\text{-}71)$$

A "best fit" of data obtained from an abiotic experiment using a 50 cm long silicone tube with an inner diameter of 0.9525 cm (3/8 inch) and outer diameter of 1.27 cm (1/2 inch) and an air flow rate of 651 mL min^{-1} of toluene-contaminated air yielded an effective permeability coefficient of 0.0005 cm^2 s^{-1}.

A best fit of data obtained from an abiotic experiment using a 15 cm long latex rubber tube with inner diameter of 0.9525 cm (3/8 inch) and outer diameter of 1.27 cm (1/2 inch) and an air flow rate of 207 mL min^{-1} of benzene-contaminated air yielded an effective permeability coefficient of 0.0004 cm^2 s^{-1}. The data used for this calculation was taken from Neemann (1998). It must be noted that effective permeability data should only be used as an approximation because of differences in the composition of silicone from different manufacturers (Casey et al, 2000). Tabular data is shown in Appendix A.

4.15.3 Determination of Maximum Specific Utilization Rate Within the Biofilm:

The selection of the most reasonable value for k and K_S of the biofilm proved to be the most difficult task for the first run of the model. Kinetic tests completed in the Environmental Research Center showed a wide range of possibilities of k (from 0.02 to 0.42 h^{-1}) under different bioreactor conditions. The kinetic tests were done by measuring the headspace concentration of toluene in batch cultures over time and the data fit with the Monod expression as detailed in Chapter 3 and Chapter 6.

Modeling results were unsatisfactory with a biofilm utilization rate of 0.02 h^{-1} as measured during biofilm culture tests, so a better method for estimating the biofilm

utilization rate was sought. Because the biofilm was taken from the reactor and put directly into a suspension bottle without mixing, the sample was essentially a "blob" of biomass that perhaps presented some diffusional limitation to mass transfer. In other words, the toluene had to diffuse into the interior of the mass before being degraded, yielding an apparent decrease in the maximum specific utilization rate as compared to a completely mixed suspension.

In an attempt to examine the toluene profile through the biofilm sphere, the biomass "blob" was modeled as a spherical particle with radius "i" to determine the true maximum specific utilization rate constant. A numeric method using Excel® was again employed to calculate the substrate concentration profile through the biofilm. Headspace measurements of toluene with time, for each culture bottle, served as the experimental data used in the model. A graphical representation of the sphere is shown in Figure 4-18.
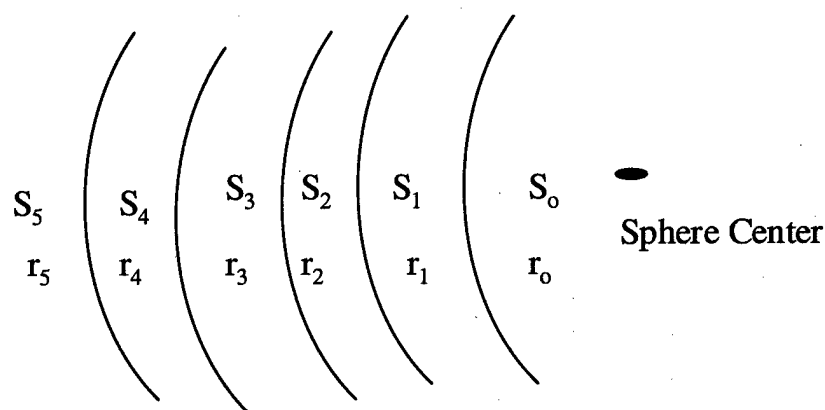
Figure 4-18. Graphical representation of the spherical particle and the associated substrate concentrations and radii used to model the specific substrate utilization rate of toluene in the biofilm.

The spherical biofilm modeling steps included the following:

1. The total volume of the sphere approximation of the biomass blob was determined for each culture bottle by dividing the mass of biofilm (determined from VSS measurement) by the biomass density (determined from the biofilm density measurements).

2. The radius of the imaginary sphere was then determined using the biomass volume.

$$\left(\frac{4}{3}\right)\pi r^3 = \text{Biomass Volume} \qquad (4\text{-}72)$$

3. The surface area of the imaginary sphere was then determined from the radius found in Equation (4-72), using Equation (4-73).

$$4\pi r^2 = \text{Surface Area Sphere} \qquad (4\text{-}73)$$

4. The diffusional flux associated with a change in radius of the sphere was calculated using a numeric approximation of Fick's First Law of Diffusion (Characklis and Marshall, 1990) as shown in Equation (4-74). $\Delta S/\Delta t$ is the observed initial substrate utilization rate as measured for each culture bottle which is represented as R_{obs}, V is the total volume of the sphere, A the surface area of the sphere, D the diffusion coefficient of toluene in biofilm, S the toluene concentration in the liquid, and r the sphere radius. Solving for S_i, the concentration of toluene in the ith biofilm layer, yields Equation (4-77).

$$D\frac{\Delta S}{\Delta r} = \frac{V\Delta S}{A\Delta t} = \frac{V}{A}R_{obs} \tag{4-74}$$

$$\Delta S = \frac{\Delta r}{D}\left(\frac{V}{A}R_{obs}\right) \tag{4-75}$$

$$S_i - S_{i-1} = \frac{\Delta r}{D}\left(\frac{V}{A}R_{obs}\right) \tag{4-76}$$

$$S_{i-1} = S_i - \frac{\Delta r}{D}\left(\frac{V}{A}R_{obs}\right) \tag{4-77}$$

5. The substrate utilization rate is then calculated for the numeric biofilm layer as shown in Equation (4-78), where k is the maximum specific utilization rate, X the biomass density, S the toluene concentration and K_S the half saturation constant.

$$r_{su} = \frac{kXS}{K_S + S} \tag{4-78}$$

6. The removal in the cell is calculated by multiplying the substrate utilization rate by the volume of the cell as shown in Equation (4-79).

$$R = \text{Removal in the cell} = r_{su}\frac{4}{3}\Pi(r_j^3 - r_{j-1}^3) \tag{4-79}$$

7. The next biofilm layer's substrate concentration is determined by linearizing the substrate change as shown in Equation (4-80) and solving for S_{i-1} in Equations (4-81) - (4-84).

$$D\frac{\Delta S}{\Delta r}\bigg|_{x=r} - r_{su} = D\frac{\Delta S}{\Delta r}\bigg|_{x=r-\Delta r} \tag{4-80}$$

$$D\frac{\Delta^2 S}{\Delta r^2} = r_{su} \tag{4-81}$$

$$\frac{\Delta^2 S}{\Delta r^2} = \frac{r_{su}}{D} \tag{4-82}$$

$$S_i - S_{i-1} = \Delta r^2 \frac{r_{su}}{D} \tag{4-83}$$

$$S_{i-1} = S_i - \frac{\left(\Delta r^2 r_{su}\right)}{D} \tag{4-84}$$

8. The removals in each cell of the imaginary sphere are then summed according to Equation (4-85) and the total observed $V\Delta S/\Delta t$ calculated. The difference between the calculated removal, $V\Delta S/\Delta t$, and the observed removal, VR_{obs}, was then squared and Excel® Solver used to minimize the sum of the differences.

$$\sum_{r=0}^{i} v_i r_{su\,i} = V\frac{\Delta S}{\Delta t} \tag{4-85}$$

9. Results using Solver® were unacceptable - multiple minima were observed yielding a variety of possible half saturation constants and maximum specific utilization rates. Therefore, a manual examination of the residual sum of squares (RSS) was accomplished. Results of that examination are shown in Figure 4-19. The multiple minima are shown in the 3-D plot, however, the smallest RSS appears to be located at a maximum utilization rate of 0.198 h^{-1} and half saturation constant of 1 mg L^{-1}. These two values were therefore used in all runs of the model.

RSS Plot
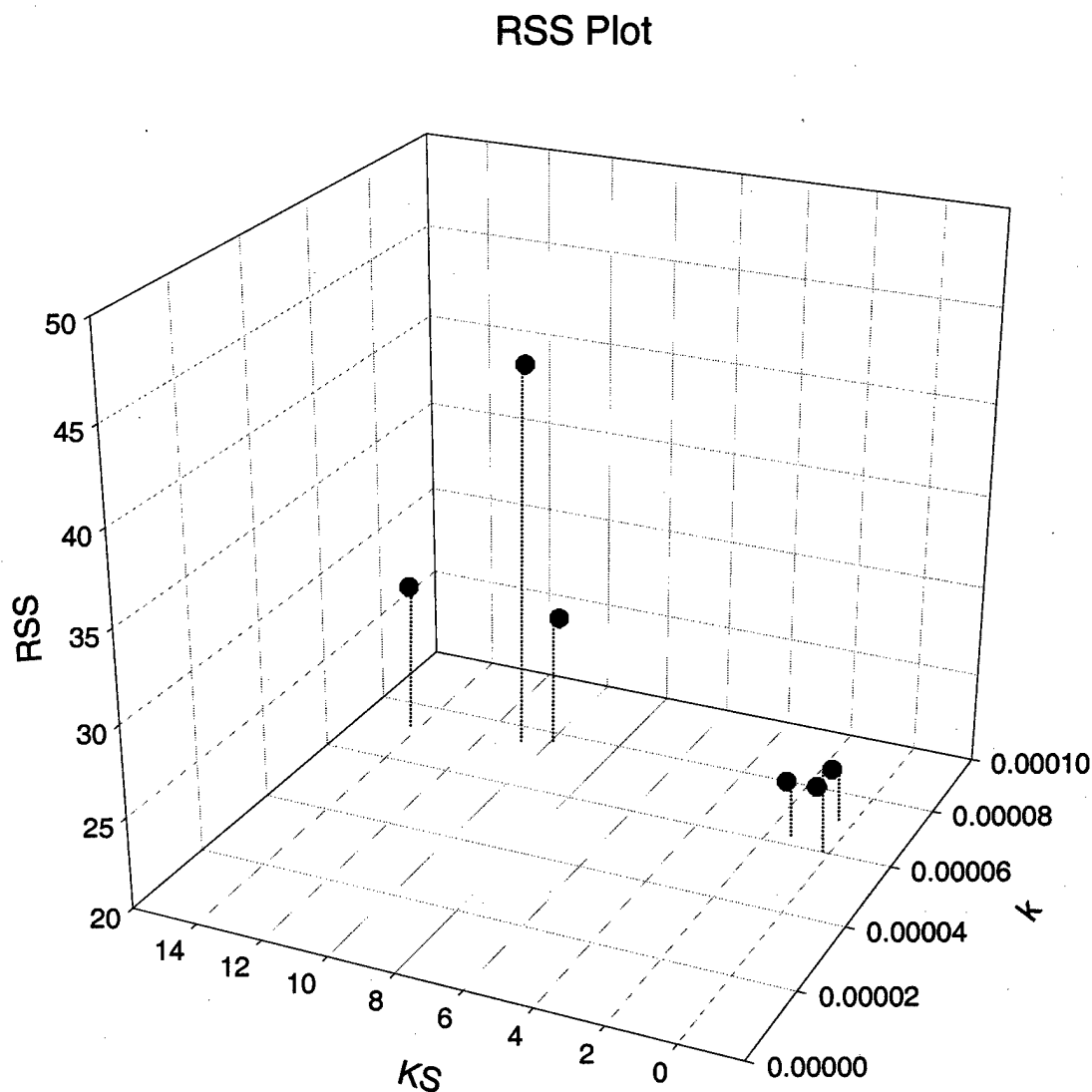
Figure 4-19. Representation of residual sum of squares minima associated with various combinations of K_S and k.

4.16 SENSITIVITY ANALYSIS:

The sensitivity analysis was performed by varying the parameter of interest over

several orders of magnitude while holding all other parameter values constant.

Parameters were varied across a range of values representative of those found in the

literature or determined during experimental measurements. The effect on toluene

removal from the air and the effect on calculated biofilm thickness were both examined during the sensitivity analysis. Changes in removal and biofilm thickness are shown with each of the parameter changes and discussed subsequently.

4.16.1 Toluene Diffusion Coefficient in Air: The effect of manipulating the toluene diffusion coefficient in air was first examined. The diffusion coefficient in air is contained within the formula, Equation 4-86, for the gas phase mass transfer coefficient and therefore is anticipated to affect the mass transfer of toluene across the thin film.

$$Sherwood\ Number = \frac{k_g d}{D_a} = 1.64 \left(\frac{d^2 v}{D_a l} \right)^{0.33} \tag{4-86}$$

Diffusion coefficient values found within the literature for toluene and benzene in air are shown in Table (4-4). Results of sensitivity analysis are shown for the toluene removal from air and the biofilm thickness in Figures 4-20 and 4-21. As the diffusion coefficient in air increases, so does the predicted biofilm thickness and the toluene removal from air. The change in removal was relatively minor: a 100-fold increase in diffusion coefficient results in a modeled increase in absolute removal of no more than 8%.

Table 4-4. Diffusion coefficients in air for toluene and benzene.

Substance	Value (cm^2 s^{-1})	Value (cm^2 s^{-1})
Toluene in air	0.0849/25 °C	(Lugg, 1968)
Toluene in air	0.088/30 °C	(University of Alabama, 2002)
Benzene in air	0.095/25 °C	(University of California, 2002)

127
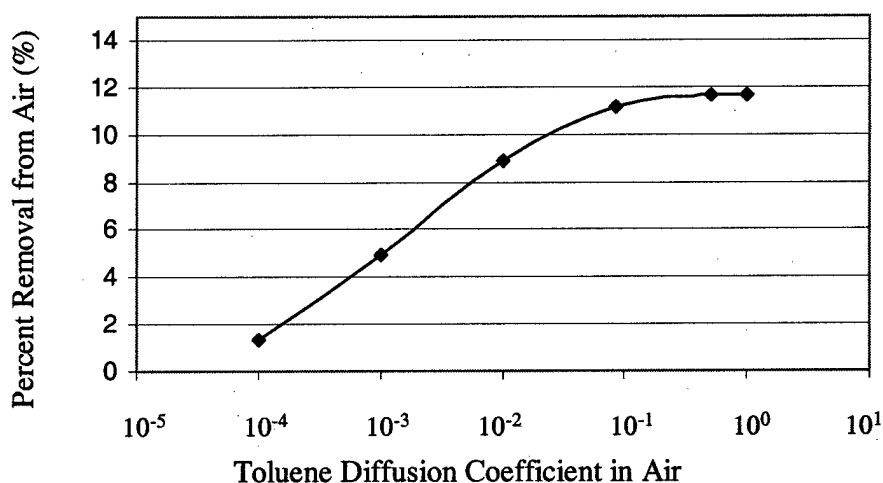
Figure 4-20. The effect of the toluene diffusion coefficient in air on toluene removal. Higher diffusion coefficients resulted in higher predicted removal of toluene from air.

Toluene Diffusion Coefficient in Air (cm² s⁻¹)
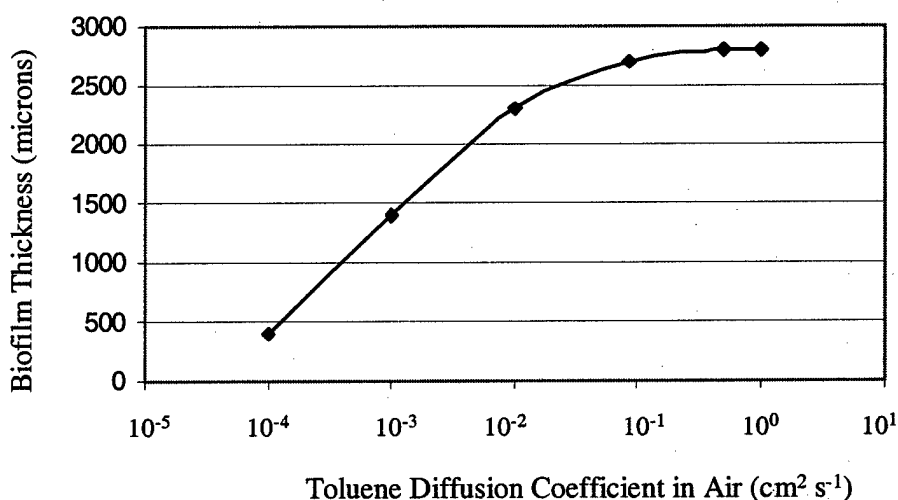
Figure 4-21. The effect of the toluene diffusion coefficient in air on the biofilm thickness. Higher diffusion coefficients resulted in an increase of predicted biofilm thickness.

4.16.2 Toluene Diffusion Coefficient in Water: The effect on removal and biofilm

thickness of the toluene diffusion coefficient in water was examined. Toluene diffusion

coefficients from the literature are shown in Table 4-5. Also shown are the diffusion

coefficients of the structurally similar compound, benzene. Results of the sensitivity

analysis are shown in Figure 4-22. The diffusion coefficient was found to have no effect on the biofilm thickness nor on the toluene removal from the air. No effect was seen due to the method used for estimating the second derivative. As can be seen in Equations (4-87) and (4-89), in the anticipated range of diffusion coefficients, the effect of the diffusion coefficient on the substrate concentration profile (and consequently the removal in a volume of biofilm) canceled out. Effectively the method use to evaluate the second derivative results in the model having a kinetic rate-limited rather than mass transfer-limited biofilm. This result contrasts with Ergas et al (1999) where the sensitivity analysis of the model indicated that the removal was a strong function of the liquid phase biomass density and biofilm diffusion coefficient.

$$S_{j-1} = r\Delta r\left(\frac{kX}{D_S}\left(\frac{S}{K_S+S}\right) - \frac{\Delta^2 S}{\Delta r^2}\right) + S_j \qquad (4\text{-}87)$$

$$\frac{\Delta^2 S}{\Delta r^2} = \frac{kX}{D_S}\left(\frac{S}{K_S+S}\right) - C \qquad (4\text{-}88)$$

$$S_{j-1} = r\Delta r(C) + S_j \qquad (4\text{-}89)$$

Table 4-5. Diffusion Coefficient Values for Toluene and Benzene

Substance	Value (cm^2 s^{-1})	Reference (cm^2 s^{-1})
Toluene in Water	$9.4*10^{-6}$	(State of Iowa, 2002)
Toluene in Water	$8.6*10^{-6}$	(Texas Natural Resources Commission, 2002)
Toluene in Water	$9*10^{-6}$	(Schwarsenbach, 1993) in (Holden et al, 1997)
Benzene in Water	$1.1*10^{-5}$	(UCSB, 2002)
Benzene in Water	$8.91*10^{-6}$	(AWWA, 1990) in (Neemann, 199)
Toluene in Biofilm	$1.3*10^{-7}$	(Holden et al, 1997)
VOCs in Biofilm	$0.8*D_w$	(Characklis and Marshall, 199)
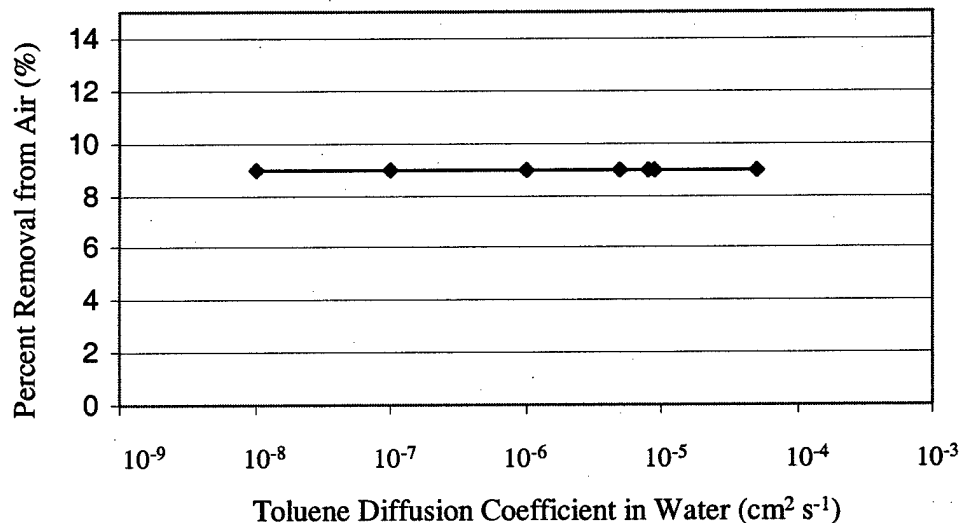
Figure 4-22. Predicted toluene removal from air with changes in the diffusion coefficient. Diffusion coefficients in water had no effect on toluene removal from air.

4.16.3 Silicone Permeability: Results of an extensive literature search for chemical permeabilities and solubilities yielded rather disappointing results. Information from the literature as well as experimentally determined values for the permeability of toluene and benzene are shown in Table 4-6; a large range was found. Some additional diffusivities and solubilities of organics in polymers were also found in Stern and Shiah, (1981); Cao and Henson, (2002); Du Plessis et al, (2001); Barson and Dong, (1990); Favre et al, (1994); Johansson and Leufven, (1997); and Choy et al, (1984). To determine the effect of the range of permeabilites, the changes in toluene removal from air and biofilm thickness were examined with changes in the effective permeability of the silicone rubber tubing. Results of that analysis are shown in Figures 4-23 and 4-24. The effective permeability was found to greatly affect both the predicted removal of toluene from the air as well as biofilm thickness. The model indicates that as biofilm thickness increases, so does the removal within the bioreactor. This increase is, however, not unanticipated.

Mass flow across the membrane being equal to removal within the biofilm and the

suspension is the main premise of the entire model; the effective permeability and the

mass transfer across the membrane determines the biofilm thickness and the associated

removal!

Table 4-6. Permeabilities of selected VOCs in silicone at room temperature.

Substance	Value (cm^2 s^{-1})	Reference
Toluene in silicone	$8.2*10^{-5}$	Nijhuis et al (1991) in (Reij et al, 1998)
Toluene in silicone	$4.7*10^{-4}$	Abiotic Single Tube, Experimental[1]
Toluene in silicone	$4.32*10^{-4}$	(Ji et al, 1994)
Benzene in latex	$3.9*10^{-4}$	Abiotic Single Tube, Experimental (Neemann, 1998)[1]

[1]Information found in Appendix A
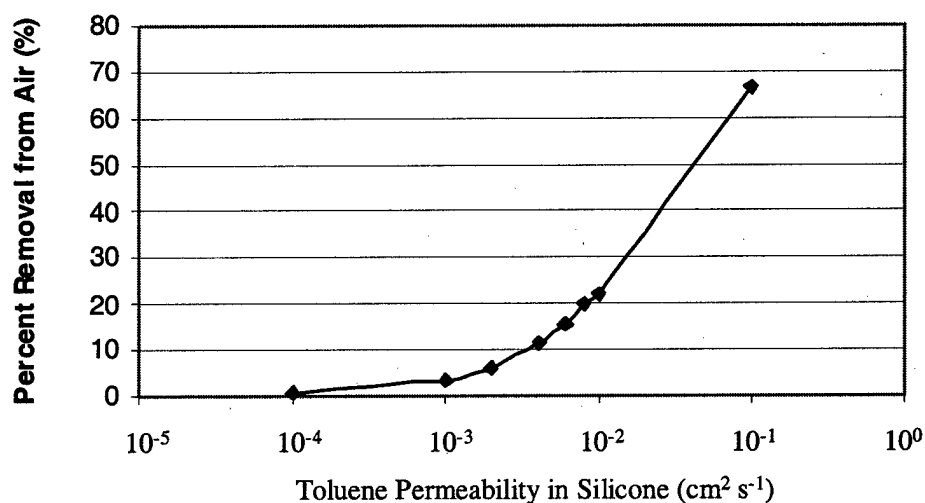
Figure 4-23. Predicted toluene removal from air with changes in silicone effective permeability. Increases in silicone effective permeability to toluene resulted in higher predicted removals of toluene from air.
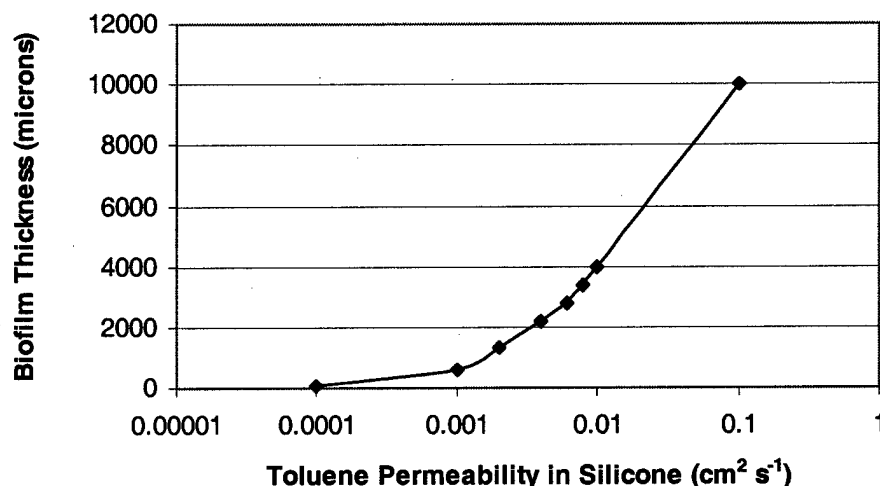
Figure 4-24. Predicted biofilm thickness with changes in silicone effective permeability. Increases in silicone effective permeability to toluene resulted in higher predicted biofilm thicknesses.

4.16.4 Maximum Specific Utilization Rate (k): Maximum specific utilization rates found in the literature are shown in Table 4-7. Rates found in the literature ranged from 0.01 - 0.45 h^{-1}. Experimental values for the maximum specific utilization rate measured during this study ranged from 0.01 - 0.42 h^{-1}, all falling with the reported literature values.

Table 4-7. Tabular comparison of literature values of kinetic coefficients.

Microorganism	Study	K_S (mg L^{-1})	k (h^{-1})
Pseudomonas	Mirpuri et al, (1997)	3.98	--
Mixed Culture	Arcangeli and Arvin, (1994)	0.17 - 1.7	0.05 - 0.08
Pseudomonas	Woo, (1999)	3.0	0.16
Various	Ottengraf and van den Oerver, (1983)	--	0.025
Various	Young-Sook et al, (1994)	--	0.4
Various	Reported in Bekins et al, (1998)	0.044 - 17.4	0.01 - 0.45

The sensitivity analysis results for changes in k are shown in Figures 4-25 and 4-26. Biofilm utilization rates were found to greatly influence the predicted thickness of the biofilm, however, did not significantly change the predicted toluene removal. The small variations in removal shown in Figure 4-25 are the result of step size changes (the

value of Δr and n) necessary when running the model. Again, the result of a thinner

biofilm is not unanticipated because as the maximum specific utilization rate increases,

toluene utilization will also increase, therefore, the same removal will be seen within a

smaller biofilm volume.
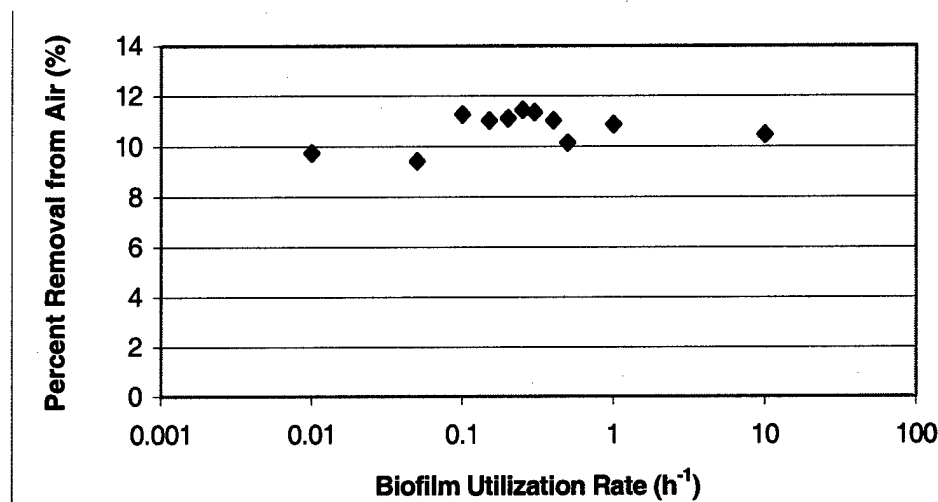
Figure 4-25. Changes in predicted toluene removal with changes in biofilm maximum specific utilization rate (k). Predicted removal was not influenced by maximum specific utilization rate increases.
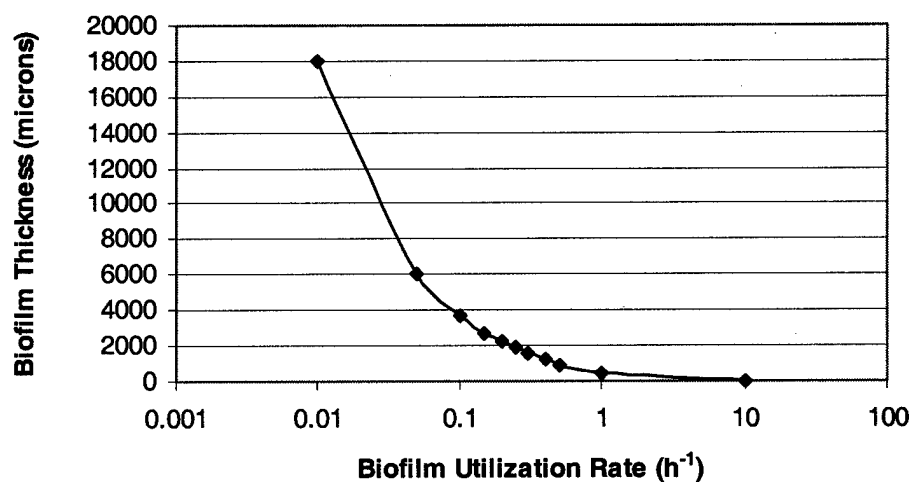
Figure 4-26. Predicted changes in biofilm thickness with biofilm maximum specific utilization rate (k) changes. Predicted biofilm thicknesses decreased as maximum specific biofilm utilization rates increased.

4.16.5 Half Saturation Constant: Half saturation constants found in the literature are shown in Table 4-7 and range from 0.17-17.4 mg L^{-1}. Experimental values for the half saturation constant for toluene measured during this study ranged from 0.14-14.3 mg L^{-1}, most falling within the reported literature values. Figures 4-27 and 4-28 show the effect of changing the value of the half saturation constant. Increases in the half saturation constant decrease the predicted removal rate, therefore, less toluene is removed in the same biofilm volume. Again, small changes in the removal percentage are a result in step size changes in the model at the higher values of the half saturation coefficient.
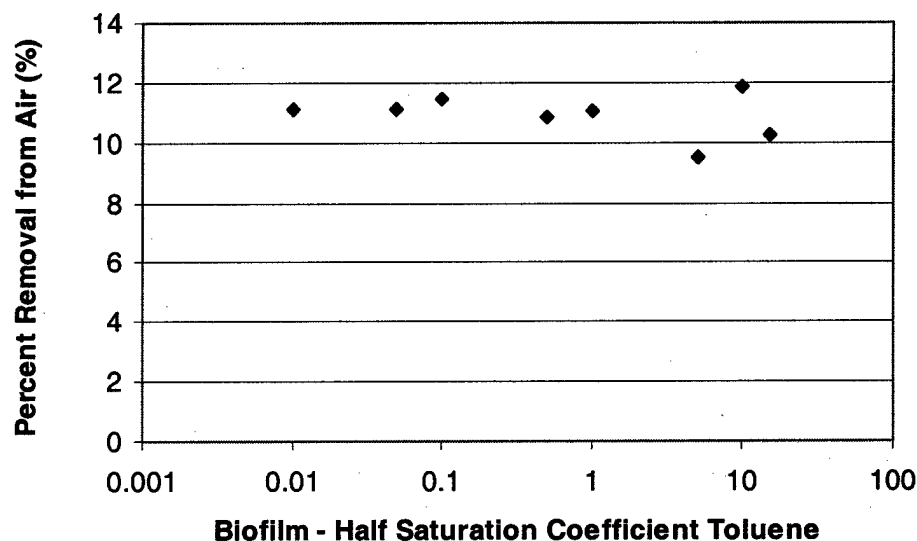
Figure 4-27. Predicted changes in toluene removal from air with changes in K_S. No influence in predicted removal was seen with increases in K_S.
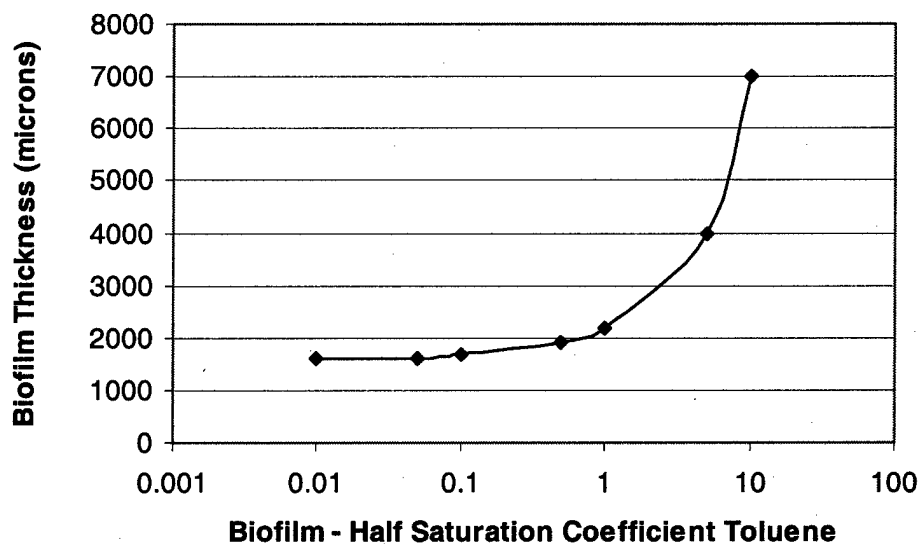
Figure 4-28. Predicted changes in biofilm thickness with changes in K_S. Predicted biofilm thickness were found to increases with increases of K_S.

4.16.6 Biofilm Density and Thickness: Biofilm densities have been shown to range from 10,000 to 105,000 mg L^{-1} (Characklis and Marshall, 1990). The biofilm densities measured during these experiments ranged from 5,350 - 23,800 mg L^{-1}. The densities measured are shown in Table 4-8 and were collected after disassembly of the bioreactor systems. The low biofilm density found in the long, single tube was most likely related to system problems. Throughout parts of the experiment, the biofilm split and sloughed and did not reattach. The reasons for the biofilm splitting remain unexplained.

Of related interest is the biofilm thickness. Biofilm thicknesses may range from 10 microns to 30,000 microns (Characklis and Marshall 1990); the low end representing contaminating biofilms, such as those on medical equipment and high end represents bacterial mats present in fresh and seawater. Biofilm thicknesses measured during this study were near 2000 microns, however, by visual observation alone, the biofilm thickness varied greatly down the length of the silicone tube. Results of the sensitivity analysis are shown in Figures 4-29 and 4-30.

Table 4-8. Measured biofilm densities.

Reactor	Measured Biofilm Density (mg L^{-1})
Long, single tube	5,350
Short, single tube	23,800
Dual tube	22,876
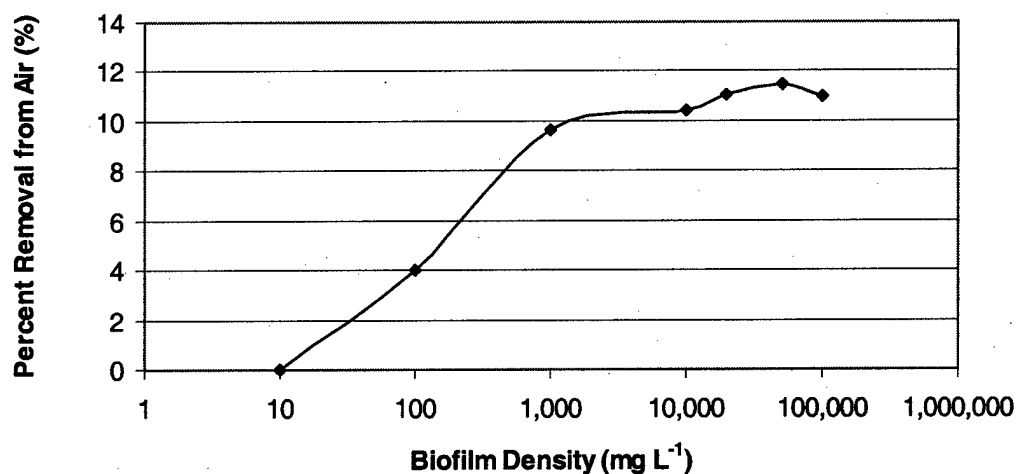
Figure 4-29. Predicted percent removal from air with changes in biofilm density. As biofilm density increased, predicted removal also increased.
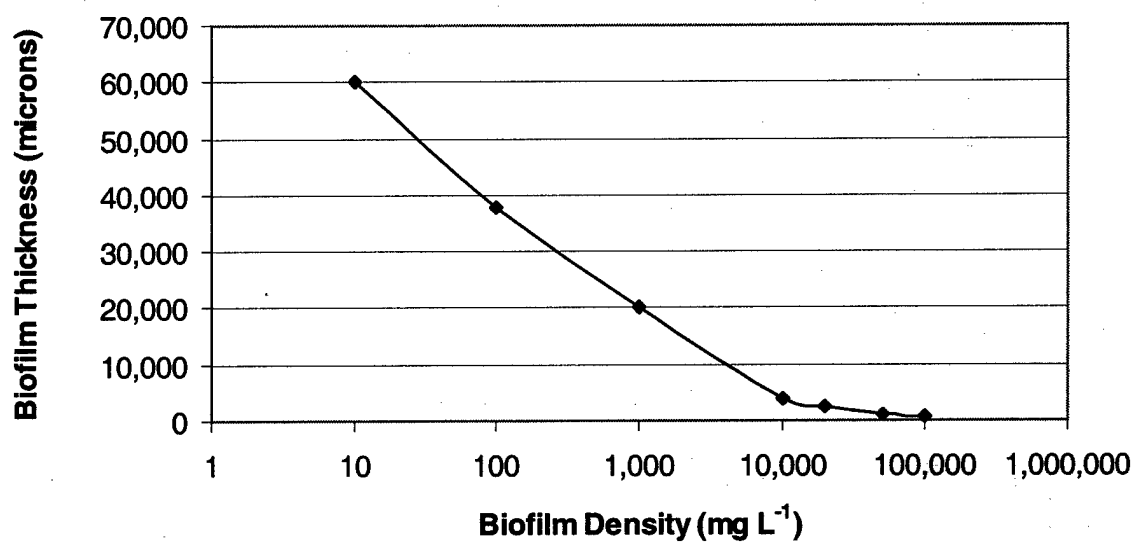
Figure 4-30. Changes in predicted biofilm thickness with changes in biofilm density. As biofilm density increased, predicted biofilm thickness decreased.

4.16.7 Kinetics of the Suspension: Measurement of kinetic parameters are shown in Table 4-9 and is detailed in Chapter 6. Sensitivity analysis indicated that neither the maximum specific utilization rate, liquid cell density, nor the half saturation constant of the suspension showed any significant effect on removal or the predicted biofilm thickness within the range of anticipated values. The lack of effect is actually a significant prediction - previously it was unknown the exact contribution to removal being made from the liquid suspension.

Table 4-9. Measured values of kinetic parameters.

Reactor	Flow Condition	Form	K_S (mg L^{-1})	k (h^{-1})
Single tube	Recirculating	Biofilm	12.0	0.21
Single tube[1]	Recirculating	Suspension	1.5	0.01
Single tube	Stagnant	Biofilm	7.0	0.08
Single tube	Stagnant	Suspension	5.2	0.04
Single tube	Recirculating/Heat	Suspension	1.3	0.07
Single tube	Recirculating/Heat	Biofilm	0.79	0.09
Dual tube	Recirculating	Biofilm	1.6	0.12
Dual tube	Recirculating	Suspension	7.0	0.16
Dual tube	Stagnant	Biofilm	14.3	0.42
Dual tube	Stagnant	Suspension	4.5	0.11
Single tube	Stagnant	Biofilm	5.0	0.11
Single tube	Stagnant	Biofilm	5.6	0.25
Single tube	Stagnant	Biofilm	10.5	0.15
Pilot[1]	Recirculating	Non-Growth	5.0	0.1
Single tube[2]	Recirculating	Non-Growth	0.14	0.02

[1]Estimated from data - no curve fit possible due to minimal data.
[2]Section of biofilm placed in a headspace vial and substrate utilization measured.

4.16.8 Biomass Removal Experiment: To examine whether the predicted effect (or lack of effect) from the suspension was real, the suspension biomass was removed from

the dual tube reactor. After the dual tube reactor liquid suspension concentration and removal from the gas phase were measured, the liquid suspension was drained and replaced with fresh nutrient solution doped to the same concentration of toluene (0.1 mg L^{-1}). Removal of toluene from the gas phase was then again measured. Figure 4-31 shows the removal with and without the presence of biomass within the suspension; no differences in removal were noted. If the liquid suspension was, in fact, responsible for any significant removal of toluene, an immediate decrease in removal of toluene from the air would have been anticipated. This result of lack of contribution from the suspension to removal is similar to results found by Attaway (2001) for a filter treating BTEX in air. In a spirally wound silicone tube reactor, the results of specific activity testing at the system's termination indicated that the unattached organisms recycling through the system had less activity against BTEX than the attached biofilm organisms; the unattached organisms were probably in a starvation or death phase due to lack of substrate (Attaway, 2001)

138
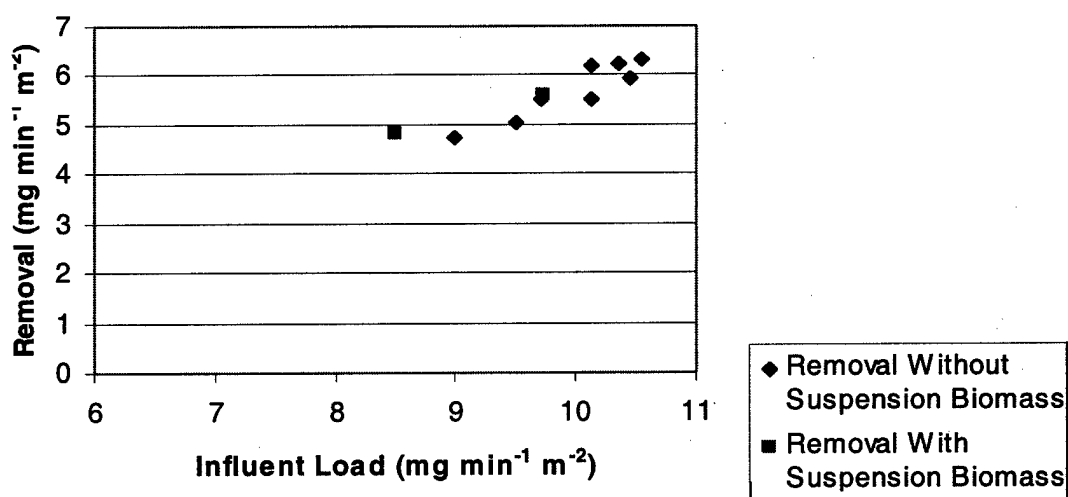
Figure 4-31. Removal of toluene with and without biomass in the liquid suspension. Removal of toluene was similar, suggesting liquid biomass contributes very little to toluene removal in the bioreactor.

4.16.9 Toluene Concentration, Edge of Biofilm: Although the toluene concentration at the edge of the biofilm is a measured parameter and considered non-adjustable in the model, examining the changes in removal and in the biofilm thickness with changes in the liquid concentration is of interest. Figures 4-32 and 4-33 show the predicted changes in toluene removal from air and the change in biofilm thickness with the changes in toluene concentration in the bulk liquid. Both the removal and the biofilm thickness decrease as the toluene concentration increases. This is expected because more toluene is appearing in the liquid, meaning that less is being degraded in the biofilm.
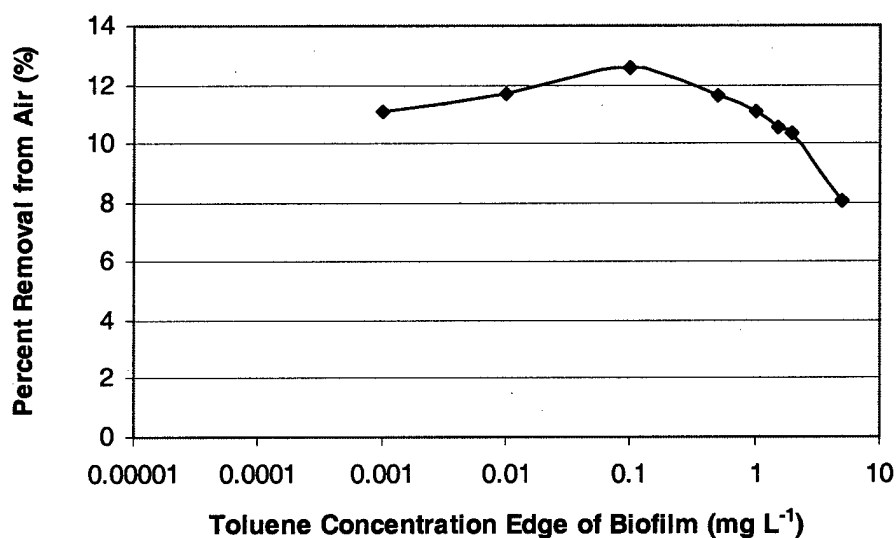
Figure 4-32. Changes in the toluene removal from air with changes in the toluene concentration within the liquid phase.
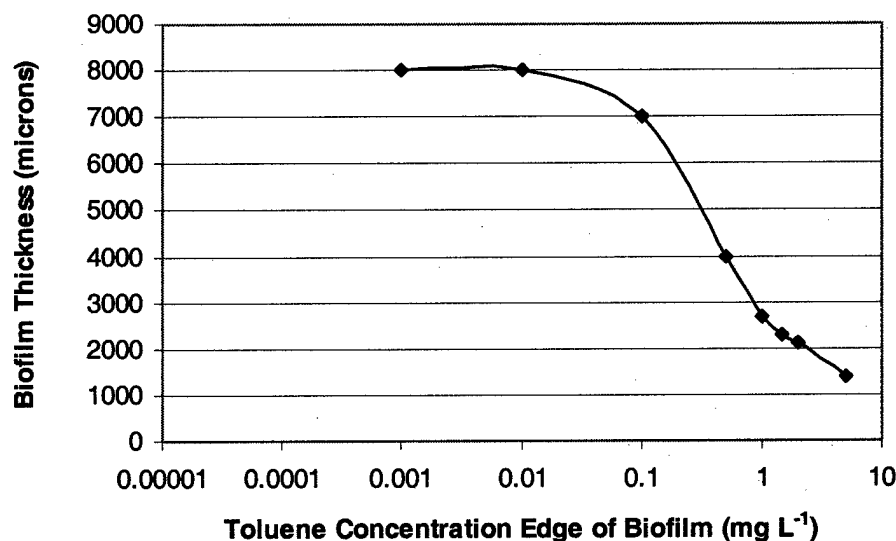
Figure 4-33. Changes in the predicted biofilm thickness with changes in the toluene concentration within the liquid phase.

In summary, the sensitivity analysis of the model indicated that predicted toluene removal from air was influenced the most by changes in the effective permeability values of silicone for toluene. Other parameters had far less influence on predicted removal over their range of most likely values. Again, the major influence of the effective permeability would be anticipated based upon the way the model is designed; the mass flow across the membrane determines the thickness of the biofilm and the associated removal under any one set of conditions. Associated with the sensitivity analysis is the result of related experimentation. The measured concentration of toluene within the liquid suspension also influences the predicted removal, as this sets the boundary condition for the biofilm. Additionally, the suspension biomass was found to have virtually no influence on the removal seen within the bioreactor. Examination of the substrate concentration profile through the biofilm and the lack of complete removal of toluene indicates the system is kinetically limited. The reasons for the kinetic limitation are not clear, however, may be related to the decrease in pH seen within all reactor

systems or may be the result of a build-up of an inhibiting metabolite. Potential

limitations of hollow-fiber reactors include diffusion of toxic metabolites away from the

cells (Beeton et al, 1991).

A separate experiment was performed in an attempt to determine the cause of the

kinetic limitation. Vapor and liquid samples were analyzed using the gas chromatograph

to search for metabolites, based on the idea that an inhibitory metabolite might be

building up in the biofilm or solution. Nutrient solution spiked with toluene served as the

control for the liquid experiment while the headspace vapor of DI water spiked with

toluene served as the control for the vapor samples. Results of the assays were

inconclusive. The very small peaks observed from liquid samples taken from the semi-

pilot-scale reactor were very similar to peaks observed for the control. However,

consistent peaks were not seen in each liquid sample. Peaks observed in the headspace

samples were virtually identical to those seen within the controls, suggesting that if

inhibiting substances were present in the liquid they are of such low concentration or of

such low volatility that they avoided detection.

The low toluene concentrations at the membrane indicate the system (rather than

just the biofilm) is mass transfer limited, suffering from a large mass transfer resistance

associated with the thick silicone membrane. This finding is similar to the findings of

other researchers. The mass transfer resistance of composites and dense membranes is

nearly all in the membrane (De Bo et al, 2000), and for compounds with low values of

solubility the membrane resistance term is dominant (Brookes and Livingston, 1995).

4.16.10 Other Values for the Dual Substrate Model: Although the values for

parameters associated with oxygen were not actually used in the model after it was

determined that there existed only a single substrate limitation, they are presented here for reference purposes in Tables (4-10) - (4-12).

Table 4-10. Oxygen half saturation coefficients.

Value (mg L^{-1})	Reference
0.014, 0.033, 0.073	(Hao et al, 1983)
0.025	(Sinclair and Ryder in Harris and Hansford, 1976)
0.048	(Sun et al, 1998)
4.5	(Munch et al, 1996)

Table 4-11. Oxygen diffusion coefficients in various media.

Parameter	Value (cm^2 s^{-1})	Reference
Air	0.291	(Richard, 2002)
Biofilm	(2.107)(10^{-5}) (1.97-2.09)(10^{-5}) (2.11)(10^{-5})	(Beyenal et al, 1997)
Biofilm	(1.2)(10^{-5})	(Khlebnikov et al, 1998)
Water	(2.26)(10^{-5})	(Casey et al, 2000)
Water	(2.1)(10^{-5})	(University of California, 2002)

Table 4-12. Oxygen permeabilities in silicone.

Value	Reference
(500)(10^{-8}) cm^2 s^{-1} atm^{-1}	(VanAmerongen, 1967)
(7961)(10^{-11}) cm^2 s^{-1} (cm Hg)$^{-1}$	(Cole-Parmer, 2002)
(1.63)(10^{-13})mol m^{-1} s^{-1} Pa^{-1}	(Cote' et al, 1989)[1]

4.17   MODEL CALIBRATION: ACTUAL REMOVAL VS. PREDICTED REMOVAL IN THE SINGLE TUBE SYSTEM:

To determine whether the single silicone tube prediction model can perform under a variety of operating conditions, the model was applied to the dual tube system and the semi-pilot scale system. Using or applying the single tube model to larger systems was accomplished in an attempt to validate the model and extend the model's design application.

Input parameters from the literature and from measurements were used with the single tube model. The only parameter adjusted was the silicone tubing effective permeability to toluene. The adjustment in effective permeability was made only after model runs indicated that measured values and literature values for effective permeability resulted in gross underestimation of toluene removal from air as described in Section 6.3.2. Therefore, the effective permeability parameter was fit to a single datum from the single tube system. The effective permeability was adjusted from 0.0005 cm^2 s^{-1} to 0.003 cm^2 s^{-1}. Realizing that fitting a parameter to data is unacceptable without a proper explanation or reasoning, a search for the difference in effective permeability data was undertaken. Several plausible explanations for the difference in effective permeability of silicone exist. First, the manufacturer of the silicone tubing used in the single tube system is unknown. It is unknown whether the tubing was supplied by Cole Parmer or from Fisher Scientific, or perhaps from another source. Differences in the manufacturing process of tubing (for example, density) are anticipated to cause differences in permeability. Most rubbers contain considerable amounts of fillers which may exert a considerable effect on diffusivity, solubility, and permeability (Van Amerongen, 1967). With a filler concentration above about 50% by volume the permeability increases sharply, corresponding to the appearance of discontinuities in the rubber phase (Van Amerongen, 1967). Additionally, in the single tube reactor as well as the dual and semi-pilot-scale reactor, the tubing was tightly clamped to the air supply tubing and at least slightly stretched between ends of the reactor. This stretching may have resulted in a thinner membrane, showing up as a perceived increase in effective permeability. Further, the stretching itself may have changed the intrinsic properties of

the silicone membrane, affecting the solubility or diffusivity of the toluene within the silicone.

4.17.1 Abiotic Results: To determine whether the model was performing as desired, the semi-pilot-scale model was run abiotically (the maximum specific utilization rate was set to zero in the biofilm and in the suspension). Air flow, liquid phase concentration, and gas phase concentration data were used from semi-pilot-scale abiotic tests. The only modification made to the model to perform this run was to use the overall K_{OV} found during the semi-pilot-scale test. The overall mass transfer coefficient, K_{OV}, must be used to account for the liquid phase resistance, in addition to the gas and membrane resistances that are present. Experimental abiotic testing showed a toluene removal of 1.75 mg L^{-1} (as liquid) while the model predicted a removal of 1.74 mg L^{-1}.

4.17.2 Modeling Results - Actual Versus Predicted: Model results for the single tube system are shown in Figure 4-34. Two experimental runs were predicted well by the model. The third point was not far off the predicted removal line.
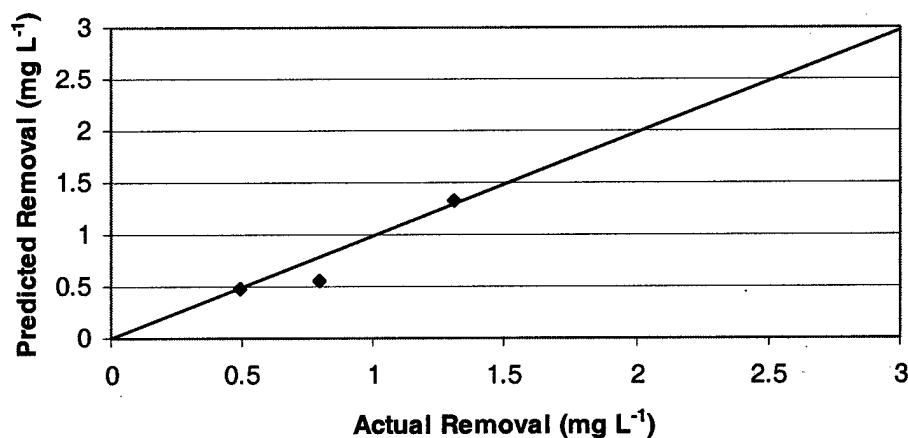
Figure 4-34. Actual vs. predicted removal of the single tube bioreactor. Actual and predicted removals were very close.

4.18 LIMITATIONS:

There are several limitations to the model, especially in terms of its predictive capabilities. Probably the main limitation is the requirement that the concentration of contaminant in the liquid suspension be known to begin prediction of removal or prediction of the biofilm thickness. The model suspension concentration of substrate cannot be assumed to be zero, which will be futher explored in Chapter 5. Therefore, an accurate measurement or appropriate estimate of the liquid suspension concentration of substrate must be obtained. Another limitation of the model is its number of assumptions. Of particular concern is the assumption of concentration independence of the membrane effective permeability. Unlike most gases, the diffusion coefficient of many easily condensable vapors in rubber is concentration dependent (Van Amerongen, 1967). When deriving diffusion coefficients from absorption-time curves it should be borne in mind that time-dependent relaxation processes caused by swelling of the polymer by the penetrant could be very disturbing. It would render D not only concentration dependent but also time-dependent (Van Amerongen, 1967). Another apparent limitation is the microorganisms; for any one system, the organisms or community of organisms may differ slightly, potentially affecting the kinetic parameters used within the model. Finally, the measurement error associated with each parameter will contribute to differences in actual removals seen during experimentation versus toluene removals predicted by the model.

CHAPTER 5
EXPERIMENTAL RESULTS

5.1 OVERVIEW:

Several experiments were undertaken to determine the effect of changes in operation

of bioreactors. The experimental conditions were developed to represent possible

operating conditions of bioreactors in the field. Parameters such as kinetic coefficients

were also measured. The following is an overview of the experimental studies:

5.2 Characterization of kinetic parameters for cultures from various membrane biofilter configurations.

5.3 Determination whether stopping the liquid flow in the reactor affected removal or other parameters.

5.4 Restriction of nutrients to a bioreactor to find if such restriction is detrimental to removal efficiency.

5.5 Operation of various sizes and configurations of membrane biofilters, including

scale-up.

5.6 In-series reactor operation.

5.7 Comparison of reactor systems.

5.8 Heat transfer studies and increased temperature operation.

5.9 Diurnal loading.

5.2 KINETIC EXPERIMENTS:

5.2.1 Kinetic Coefficient Determination: The kinetic studies examined the substrate

utilization rates of the bacteria or, more appropriately, the utilization rates of the

consortia existing in both the biofilm and the suspension of each reactor system.

Accurate substrate utilization rates were necessary as a model parameter input for

prediction of contaminant removal.

Maximum specific substrate utilization rates (k) and the half saturation constants (K_S) were determined for both the butanol and toluene bioreactors used throughout the various phases of this research. Butanol-consuming microorganim kinetics of a continuous flow stirred-tank reactor (CFSTR) culture were determined by Zhang (2000). K_S was estimated as 8.9 mg L^{-1} while k was determined to be 0.18 h^{-1}.

A summary of the toluene-degrading microorganism kinetic coefficients measured during the current toluene studies is shown in Table 5-1. As presented in the Methods and Materials Section, the degradation of toluene in the headspace of batch cultures was monitored over time. Degradation curves were fit with Monod-like kinetics and the values of k and K_S determined. Very generally, K_S of the biofilms grown in cultures were higher than those of the bioreactor suspensions. It is known that the same organisms may have a high K_S in one culture medium and a low K_S in another (Characklis and Marshall, 1990). Maximum utilization rates of suspended cultures grown from biofilm samples were also generally higher than those of suspended cultures derived from the biofilter suspension. For comparison purposes, a summary of some toluene degradation kinetic constants found within the current literature are shown in Table 5-2. All but one value measured during the current study fall within the range of coefficients reported for toluene-degrading microorganisms in the literature.

Table 5-1. Tabular comparison of suspension and biofilm kinetic coefficients.

Reactor	Flow Condition	Form	K_S (mg L^{-1})	k (h^{-1})	k/K_S
Single tube	Recirculating	Biofilm	12.0	0.21	0.0175
Single tube[1]	Recirculating	Suspension	1.5	0.01	0.0067
Single tube	Stagnant	Biofilm	7.0	0.08	0.0114
Single tube	Stagnant	Suspension	5.2	0.04	0.0077

Single tube	Recirculating /Heat	Suspension	1.3	0.07	0.0538
Single tube	Recirculating /Heat	Biofilm	0.79	0.09	0.1139
Dual tube	Recirculating	Biofilm	1.6	0.12	0.075
Dual tube	Recirculating	Suspension	7.0	0.16	0.0229
Dual tube	Stagnant	Biofilm	14.3	0.42	0.0294
Dual tube	Stagnant	Suspension	4.5	0.11	0.0244
Single tube	Stagnant	Biofilm	5.0	0.11	0.0220
Single tube	Stagnant	Biofilm	5.6	0.25	0.0446
Single tube	Stagnant	Biofilm	10.5	0.15	0.0143
Pilot[1]	Recirculating	Non-Growth	5.0	0.1	0.0200
Single tube[2]	Recirculating	Non-Growth	0.14	0.02	0.1429
Overall range	Various	Suspension	1.3 – 7.0	0.01 – 0.16	--
Overall range	Various	Biofilm	0.79 – 14.3	0.08 – 0.42	--

[1]Estimated from data - no curve fit possible due to minimal data.
[2]Section of biofilm placed in a headspace vial and substrate utilization measured.

Table 5-2. Tabular comparison of literature values of kinetic coefficients.

Microorganism	Study	K_S $(mg\ L^{-1})$	k (h^{-1})
Pseudomonas	Mirpuri et al, 1997	3.98	--
Mixed Culture	Arcangeli and Arvin, 1994	0.17 - 1.7	0.05 - 0.08
Pseudomonas	Woo, 1999	3.0	0.16
Various	Reported in Bekins et al, 1998	0.044 - 17.4	0.01 - 0.45
Mixed, Suspension	This report	1.3 – 7.0	0.01 – 0.16
Mixed, Biofilm	This report	0.79 – 14.3	0.08 – 0.42

5.2.2 Comparison of Monod Curve Fits: After several kinetic studies were completed, it was evident the shape of the curves fitted to the data were distinctly different from one another. A comparison of the curves generated are shown in Figures 5-1 and 5-2. Differences in curve shapes may be related to microorganism's physiology due to the variety of biofilm and suspension conditions present. Curve shape (kinetic) differences may also be related to differences between actual communities as they developed within the bioreactors. Although inoculated with bacteria from the same culture, the actual mix

of bacteria present may be different in each bioreactor (or each culture grown), possibly

resulting in the different kinetic coefficients. Of note, the use of a mixed population for

inoculation often proves to be more successful than the use of single strains alone

(Bustard et al, 2001) and inoculation with microbes using the substrate has been found to

assist in more rapid acclimation of the biofilter (Devinny et al, 1999). Inoculation with

pure strains shortened the start-up period for a conventional biofilter, while the results

from short term operation showed that pure cultures and mixed cultures did not vary

greatly (Veiga and Kennes, 2001).

The individual kinetic study results are shown in Appendix B. Shapes of

utilization curves for the various cultures are somewhat different and possibly suggest

differences in the consortia present. Scatter in many of the graphs is high despite the use

of an average of three readings of concentration for each time.
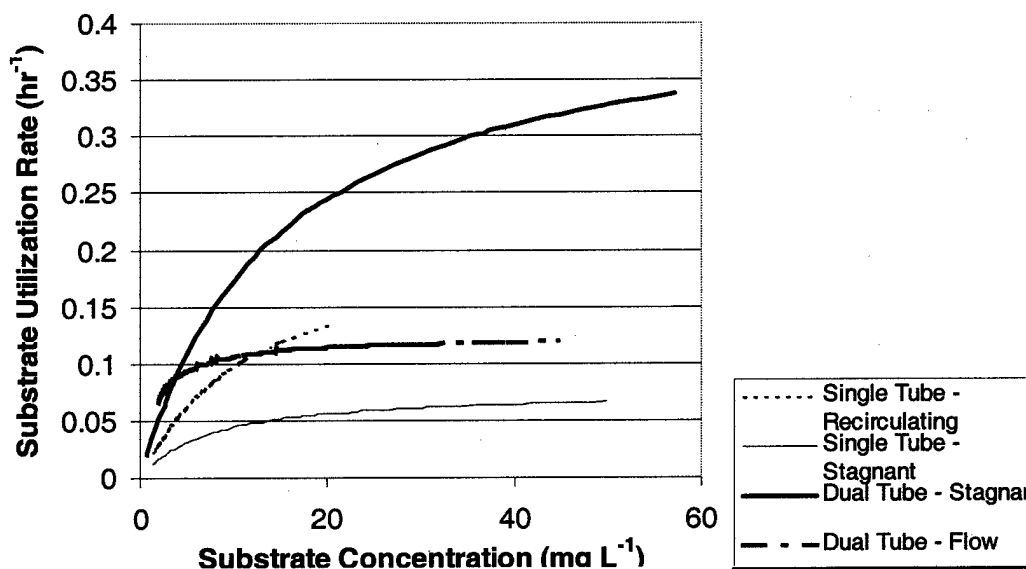
Figure 5-1. Comparison of substrate utilization curves for biofilms. Substrate utilization rates were found to be different in the separate reactors, suggesting the presence of different microorganism communitites with the separate biofilms.
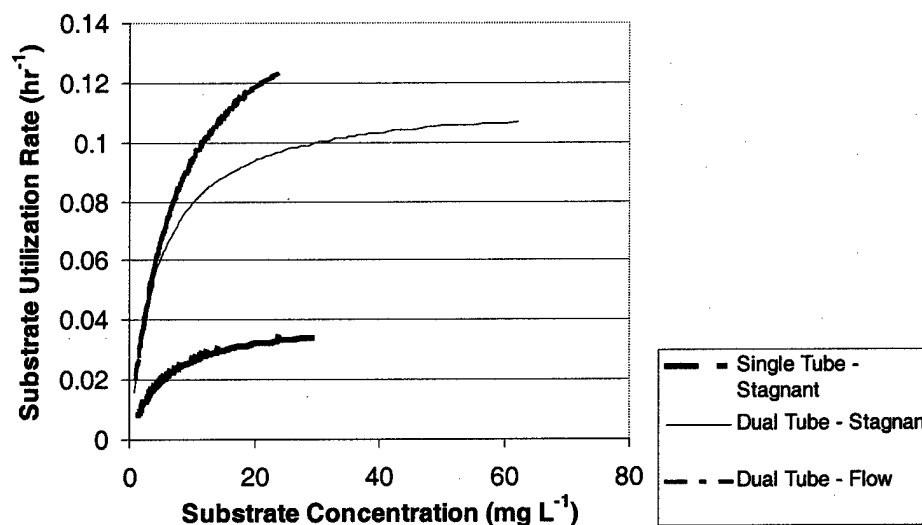
Figure 5-2. Comparison of substrate utilization curves for suspensions. Substrate utilization rates were found to be different in the separate reactors, suggesting the presence of different microorganism communitites with the separate liquid suspensions.

5.2.3 Colony Isolation and Identification:

As discussed in the Methods and Materials Section, the biofilm of the long, single silicone tube bioreactor was cultured and plated (grown on toluene) in an attempt to determine information about the different microorganisms present. Three different colony morphologies were observed. These three isolates were grown in suspensions and their kinetic parameters determined. A comparison of the Monod kinetic behavior for the three different bacteria found on plates and the original biofilm is shown in Figure 5-3. From the graph, which shows the fitted rate for each culture, it is evident that Bacteria 2 had the highest maximum specific utilization rate. Also interesting is the lower maximum utilization rate of the biofilm as a whole. The lower value may illustrate the competition between the three organisms contained with the same culture for the substrate, some other form of competitive or inhibitory interaction or possibly the presence of inactive biomass in the biofilm. When

all three colony types isolated from the stagnant flow single tube bioreactor were gram stained; all three stained positive. Attempts at identifying the organisms using DNA analysis and an Analytical Profile Index (API) were inconclusive.
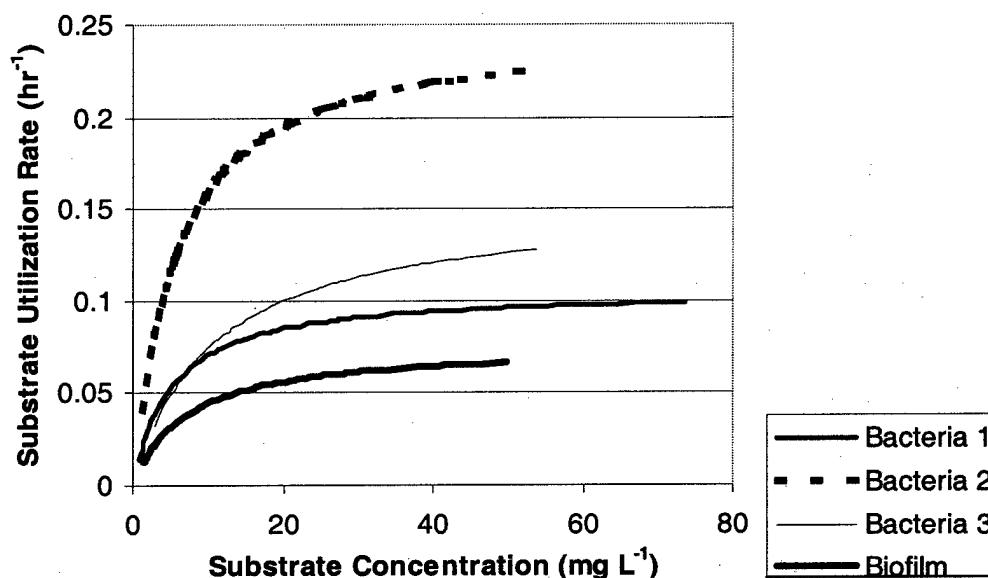
Figure 5-3. Comparison of Monod kinetics for three colonies of bacteria found within the single tube stagnant flow biofilm. Differences in substrate utilization rates, along with colony morphologies, suggest the bacteria were three separate types.

5.2.4 Biofilm "Chunk" Kinetics: The kinetic coefficients determined within batch cultures may or may not represent the actual coefficients of the biofilms and suspension contained within the bioreactors. Microorganisms growing attached to solid supports often exhibit marked differences in physiology from their suspended counterparts (Irvine et al (1997) in Moe and Irvine (2001c)). The character of cell walls often changes, some enzyme systems are modified, and pH, substrate, and oxygen gradients are generated.

In an effort to determine the impact on kinetic coefficients associated with suspended cells within a culture bottle versus those contained within the biofilm, eight

pieces of biofilm were removed from the long, single silicone tube bioreactor. Toluene was added and the concentration within the headspace vials monitored with gentle agitation to prevent the chunks of biofilm from breaking apart, resulting in Figure 5-4. When compared with other coefficients generated during experiments with suspended cells, the maximum specific utilization rate was lower than most others measured. Additionally, the half saturation coefficient was lower than other measured values. There may be a variety of reasons for the lower coefficients, however, the most likely explanation is that only a small portion of the biofilm is actually metabolically active. Zhang and Bishop (1994) found that lower layers of a biofilm might only have 5-11% of cells that are metabolically active while upper layers (i.e. in contact with the substrate) in a biofilm might be 72-86% active cells. In two different biofilm models used to predict substrate utilization within a bioreactor, an inactive as well as an active layer was assumed in the biofilm (Harris and Hansford, 1976; Baltzis et al, 2001). If a large portion of the biofilm chunks were inactive, a lower k, when compared to growing cultures, would indeed be anticipated. The very low K_S value indicates that over virtually the entire range of concentration, zero order kinetics were exhibited. Another explanation may be diffusional limitations experienced by the biofilm chunk. A model of a spherical biofilm particle, to further explore this potential is presented in Chapter 4. Results of that model were a k of 0.198 h^{-1} and a K_S of 1 mg L^{-1}; a large variation from values shown in Figure 5-4.
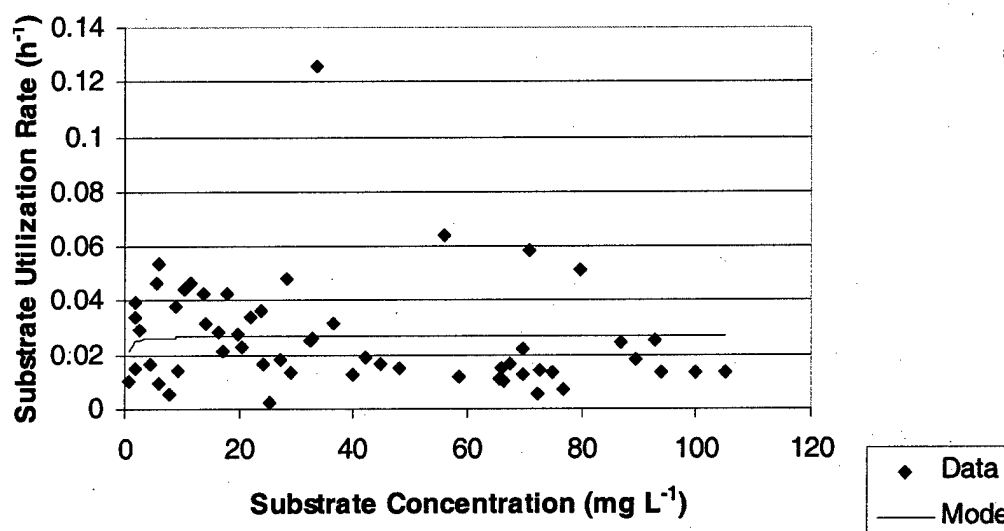
Figure 5-4. Kinetic coefficient determination for a chunk of biofilm removed from the long, single tube bioreactor, K_S = 0.14 mg L^{-1}, k = 0.02 h^{-1}. The maximum utilization rate was determined to be much lower than those determined for free suspensions.

5.2.5 Abiotic Characterization of Mass Transfer: During the course of the research reported here, four silicone tubing and one polysulfone reactors were operated. Each reactor was characterized for abiotic mass transfer before inoculating with microorganisms. Abiotic data was collected by passing contaminated air through the lumen and circulating tap water through the liquid side of the module. Abiotic data is shown in Appendix D. In all cases, abiotic removal was lower than removal observed with a fully developed biofilm present when reactors were operated at the same influent loading.

5.3 STAGNANT LIQUID EXPERIMENTS:

5.3.1 Overview: Membrane bioreactors used for the treatment of contaminated air have usually been operated with a recirculating liquid to enhance mass transfer (Ergas et al, 1999; Pressman et al, 2000); convection is usually associated with improved mass transfer coefficients and improved mass transfer rates from reduction of the thickness of

the thin liquid film. However, there would be at least some benefit to operating a membrane bioreactor with no liquid circulation or under stagnant liquid conditions. If no liquid circulation is required, pumps are not necessary and thus energy costs might be reduced. Therefore, a stagnant liquid condition in two membrane bioreactors was investigated. Both bioreactors, the short, single silicone rubber tube bioreactor and the dual silicone tube reactor, were first operated with recirculating liquid flow. The liquid flow was then stopped, toluene removal monitored over time, and subsequently compared to the removal seen during the liquid recirculation condition.

5.3.2 Single Silicone Tube Bioreactor, Recirculating Liquid Conditions: A single silicone tube bioreactor, previously operated by Scott Cole, was restarted by resuming a constant feed of toluene. The bioreactor was fed toluene for approximately 30 days. Towards the end of the 30-day period, gas inlet and outlet sampling was begun. Six days of sampling gave an average toluene removal of 93 ppm (LCL 77 ppm, UCL 109 ppm). During this sampling period, the bioreactor had an average influent concentration of 986 ppm and an average effluent concentration of 893 ppm. The influent and effluent air sampling data is shown in Figure 5-5. A loading (on membrane area basis) and removal curve is shown in Figure 5-6. As seen in this graph, removal was approximately 32 mg m^{-2} min^{-1} at an influent load of 390 mg m^{-2} h^{-1}. Removal averaged 9% over the operational period. For comparison, Attaway (2000) found the removal was 99% and then dropped to 87% at an influent concentration of 1200 ppm BTEX in a silicone tube membrane reactor removing toluene. The removal rate in Attaway (2000) averaged 5 mg m^{-2} min^{-1}. The disparity in removal percentages between this study and Attaway (2000)

may result from differences in air flows, membrane surface area and/or biofilm

composition.
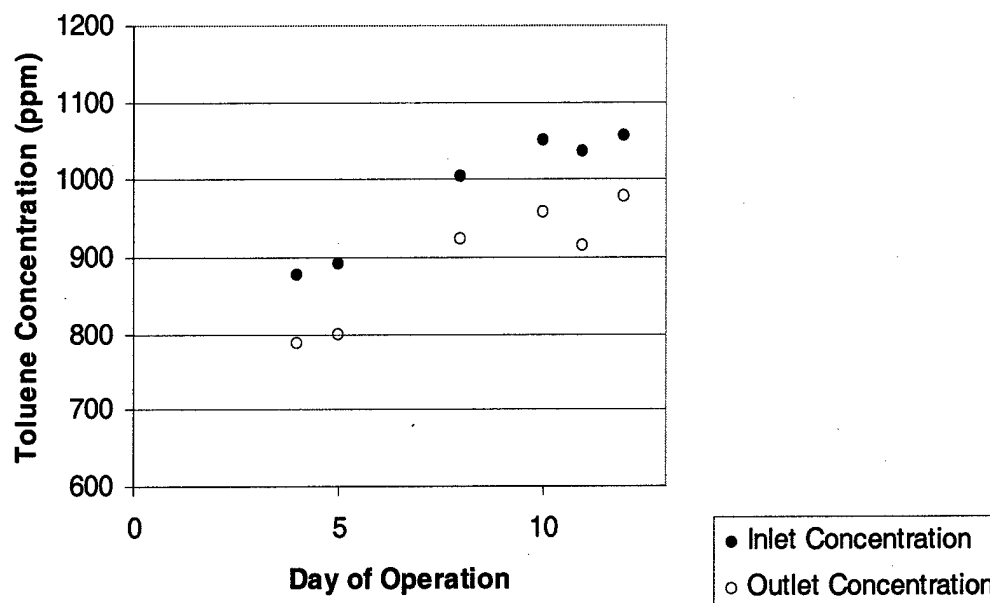
Figure 5-5. Toluene removal in the single silicone tube bioreactor under recirculating liquid conditions. Six days of sampling gave an average toluene removal of 93 ppm (LCL 77 ppm, UCL 109 ppm).
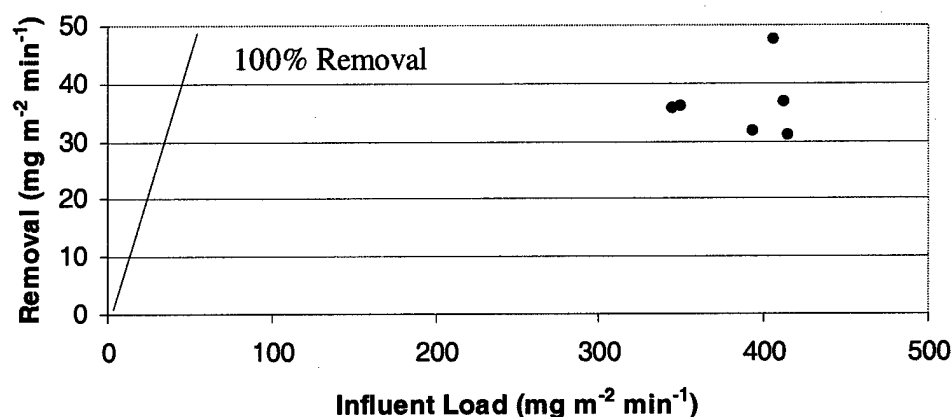
Figure 5-6. Loading and removal in the single silicone tube reactor.

5.3.3 Dual Silicone Tube Bioreactor, Recirculating Liquid Conditions: Toluene

removal in the dual silicone tube bioreactor with recirculating liquid is shown in Figure

5-7. Sampling over days 30 - 70 showed an average removal of 396 ppm (LCL 299

ppm, UCL 493 ppm). The last seven operational days were chosen as their influent concentration was relatively steady, i.e. neither increasing nor declining. The bioreactor had an average toluene influent concentration of 721 ppm and an average effluent concentration of 325 ppm during the sampling period. The loading curve for this reactor is shown in Figure 5-8. Removal was approximately 42 mg m^{-2} h^{-1} at an influent concentration of 80 mg m^{-2} h^{-1}. Removal over the entire operational period of recirculating conditions averaged 42%.

During the study, the liquid recirculation tubing detached from the reactor causing a partial draining of the system. Biofilm slid down the tubing or slumped. Check valves or other backflow prevention devices might have prevented this. Noticeable bacterial regrowth on the tubing began within 48 hours, but also noticed several days later was a black growth, apparently underneath the bacterial biofilm. The black growth was speculated to be a fungus (Mihalcik, 2002). Upon later draining of the system, the biofilm did not slump where the black substance was present, suggesting the fungus may be instrumental in firm attachment of the biofilm to the tubing.

156
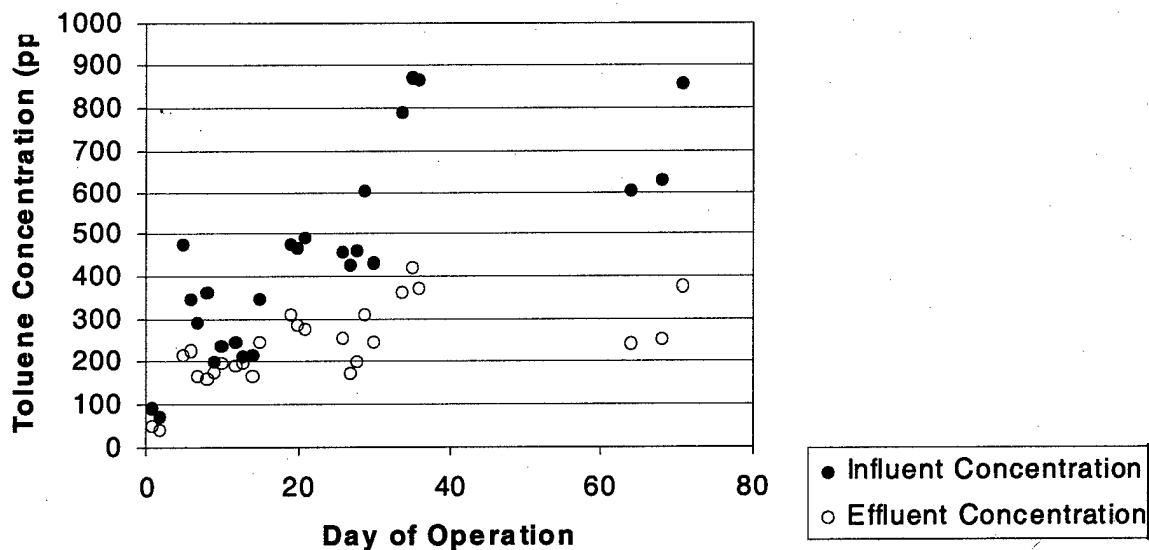
Figure 5-7. Influent and effluent toluene concentrations in the dual tube bioreactor with recirculating liquid. Sampling over days 30 - 70 showed an average removal of 396 ppm (LCL 299 ppm, UCL 493 ppm).
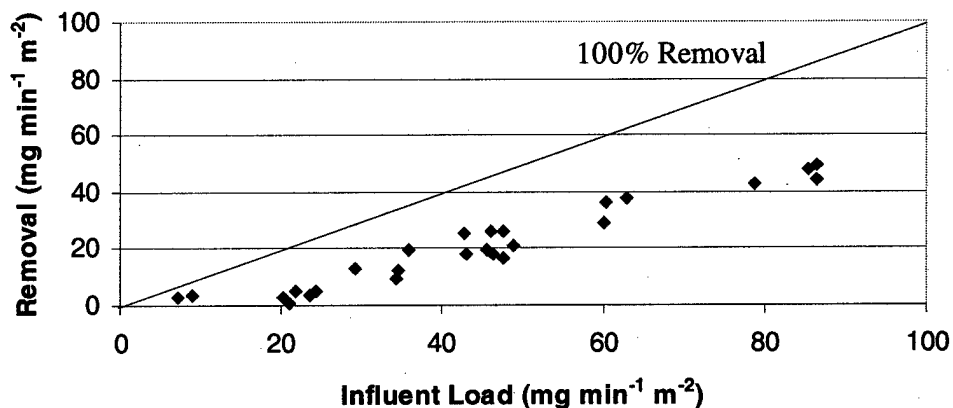
Figure 5-8. Loading curve for the dual silicone rubber bioreactor under recirculating liquid conditions. Two lowest influent load points from initial days of reactor operation.

5.3.4 Single Silicone Tube Bioreactor, Stagnant Liquid Conditions: After operation

with recirculating liquid, as described in Section 5.3.2, the liquid flow of the single

silicone tube bioreactor was turned off and the influent and effluent toluene

concentrations monitored over time. Sampling over the operational period showed an

average removal of 102 ppm (LCL 89 ppm, UCL 114 ppm). The bioreactor had an

average influent concentration of 921 ppm and an average effluent concentration of 820

ppm during the sampling period. The influent and effluent data is shown in Figure 5-9.

The loading curve is shown in Figure 5-10. Removal was approximately 41 mg m^{-2} h^{-1} at

an influent concentration of 400 mg m^{-2} h^{-1}. Removal over the entire operational period

of stagnant liquid conditions averaged 12%.
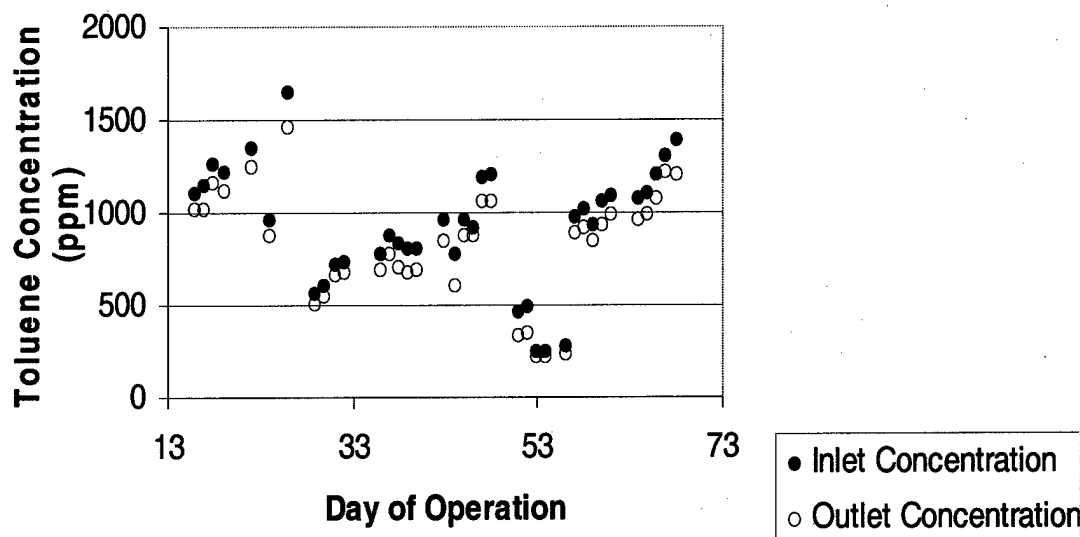
Figure 5-9. Influent and effluent concentrations of the single silicone tube bioreactor under stagnant liquid conditions. Sampling over the operational period showed an average removal of 102 ppm (LCL 89 ppm, UCL 114 ppm).
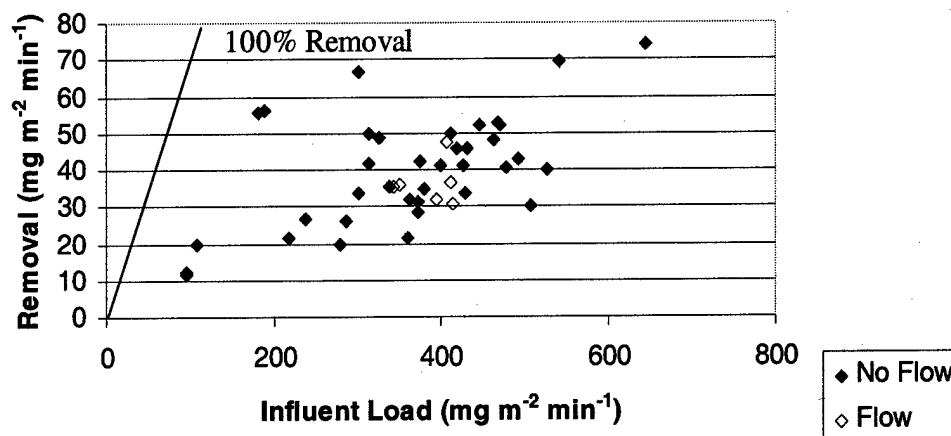
Figure 5-10. Removal and loading of the single silicone tube bioreactor under stagnant liquid conditions. No significant differences were found in removal betwwen the recirculating and the stagnant liquid reactors.

5.3.5 Dual Silicone Tube Bioreactor, Stagnant Liquid Conditions:

In the dual tube bioreactor, sampling over the operational period with stagnant liquid showed an average removal of 319 ppm (LCL 286 ppm, UCL 352 ppm). The bioreactor had an average influent concentration of 665 ppm and an average effluent concentration of 346 ppm during the sampling period. The influent and effluent toluene concentration data is shown in Figure 5-11. The loading curve is shown in Figure 5-12. Removal was approximately 40 mg m^{-2} h^{-1} at an influent concentration of 80 mg m^{-2} h^{-1}. Removal averaged 47% over the entire operational period of stagnant liquid, or non-recirculating conditions.
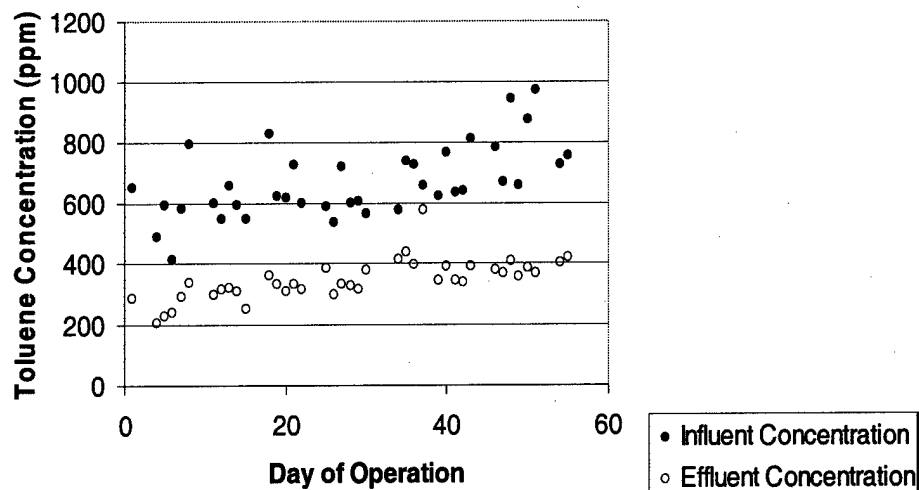
Figure 5-11. Removal of toluene in the dual silicone tube bioreactor under stagnant liquid conditions. Sampling over the operational period with stagnant liquid showed an average removal of 319 ppm (LCL 286 ppm, UCL 352 ppm).
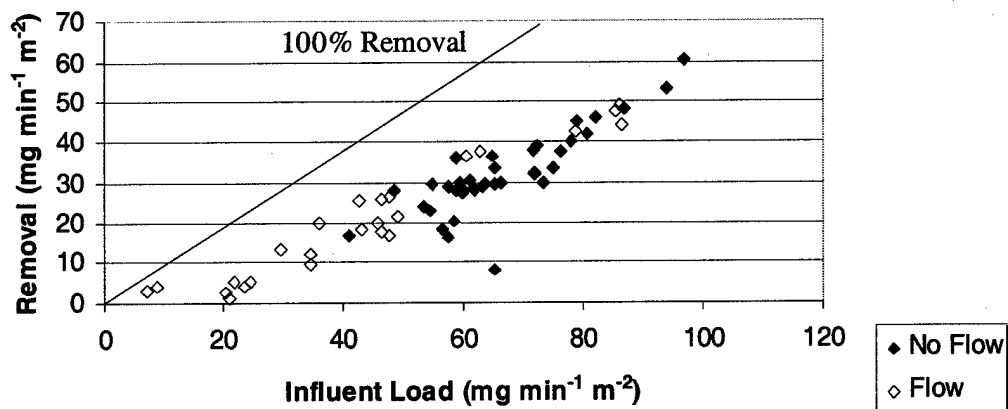
Figure 5-12. Loading curve of the dual silicone tube bioreactor under no liquid flow conditions. No significant differences were found in removal between the recirculating and the stagnant liquid reactors.

5.3.6 Discussion: The single silicone tube bioreactor operated with recirculating liquid flow provided toluene removal of 93 ppm (LCL 77 ppm; UCL 109 ppm) while the same reactor under stagnant flow conditions provided a removal of 102 ppm (LCL 89 ppm; UCL 114 ppm). The dual silicone tube bioreactor with recirculating liquid flow provided a removal of 396 ppm (LCL 299 ppm, UCL 493 ppm) while the dual silicone tube bioreactor with stagnant flow provided a removal of 319 ppm (LCL 286 ppm, UCL 352 ppm). In both the single and dual silicone bioreactors, stopping the liquid flow had no apparent effect on the removal efficiency for toluene; there was no difference at the 95% confidence level.

Liquid flow apparently does not have any substantial impact on the toluene removal in operational bioreactors (at least those with a thick biofilm present) at the liquid flow rates that were studied. If liquid flow improved mass transfer from the biofilm into the suspension (by lowering the liquid mass transfer resistance/shrinking the thickness of the liquid boundary layer), stopping the flow should have resulted in at least a moderate efficiency decline. The results support other findings in this study that indicate the suspension does not contribute substantially to toluene degradation within the bioreactors.

5.4 NUTRIENT LIMITATION STUDIES:

5.4.1 Overview: Microorganisms require essential nutrients in order to function and produce new cells. Most often these nutrients and growth factors are not present in the waste gas and have to be supplied externally to a biofilter (Waweru et al, 2000). Nutrient limitation is considered as a major factor limiting biofilter efficiency with nitrogen being an essential nutrient for microbial growth; other macronutrients needed include

phosphorous, sulfur, potassium, magnesium, calcium, sodium and iron (Lim et al, 2001).
Indeed, excessive biomass accumulation in a trickle bed air filter was found to be
controlled by limiting the amount of inorganic nutrients available for growth (Weber and
Hartmans, 1996). The absence of phosphorous led other researchers to postulate that
nutrient limitation might have contributed to effective biomass control (Sorial et al,
2001).

To explore whether nutrient limitations might have an effect on bioreactor
performance, a single silicone tube and a dual silicone tube bioreactor were operated with
a full nutrient solution complete in N and P as well as other nutrients as listed in ATCC
Culture Medium 1981 M-R2A. After operation with complete nutrient solutions, the
bioreactors were again operated - one devoid of nitrogen and the second devoid of
phosphorous, and their removals compared.

5.4.2 Single Silicone Tube Bioreactor, Full Nutrient Solution: Gaseous influent and
effluent sampling over the days of the operational period with full nutrient solution
showed an average removal of 146 ppm (LCL_{95} 100 ppm, UCL_{95} 191 ppm). The
bioreactor had an average influent concentration of 1483 ppm and an average effluent
concentration of 1337 ppm during the sampling period when influent concentrations were
closest to 1500 ppm (n = 13). The influent concentration of this bioreactor changed
throughout the study, therefore only the 13 data points were used for comparison with the
nutrient limited conditions. The influent and effluent data for the entire operational
period is shown in Figure 5-13.
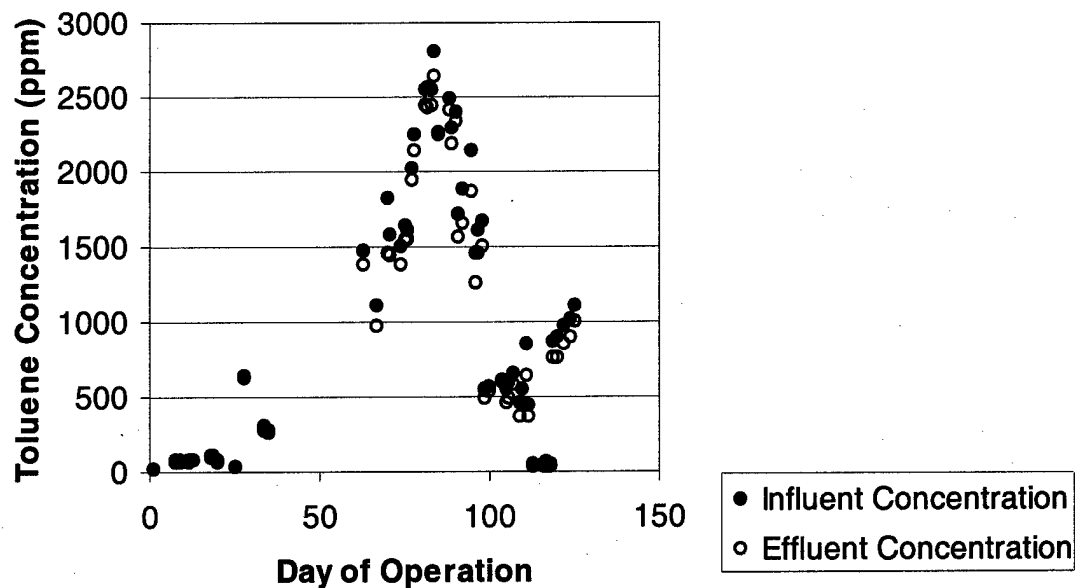
Figure 5-13. Removal in the single silicone tube bioreactor with full nutrient solution. Gaseous influent and effluent sampling over the days of the operational period with full nutrient solution showed an average removal of 146 ppm (LCL$_{95}$ 100 ppm, UCL$_{95}$ 191 ppm).

Removal was approximately 19 mg m^{-2} h^{-1} at an influent load of 200 mg m^{-2} h^{-1} with the loading curve shown in Figure 5-14. Toluene removal averaged 9.8%.
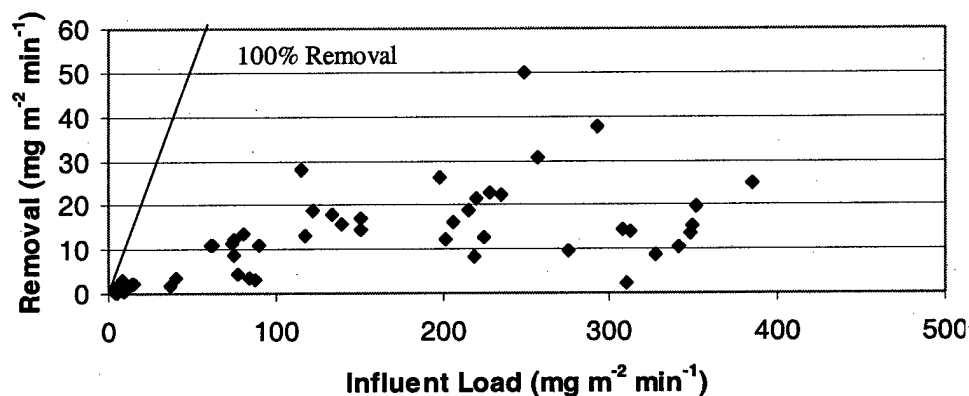
Figure 5-14. Loading curve for the single silicone tube bioreactor with full nutrient solution.

5.4.3 Single Silicone Tube Bioreactor, Devoid of Nitrogen:
Sampling over the operational period with the single silicone tube bioreactor devoid of nitrogen showed an average removal of 124 ppm (LCL 107 ppm, UCL 141 ppm). The bioreactor had an average influent concentration of 1479 ppm and an average effluent concentration of 1355 ppm during the sampling period. The influent and effluent data is shown in Figure 5-15. Removal was approximately 13 mg m^{-2} h^{-1} at an influent concentration of 200 mg m^{-2} h^{-1}. Removal averaged 8.3%. The loading curve comparing full and nitrogen limited conditions is shown in Figure 5-16.
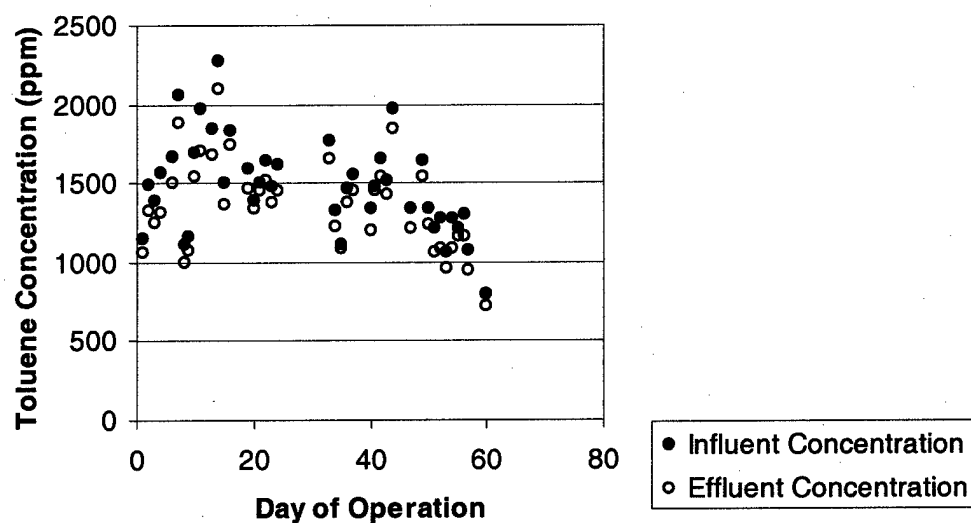
Figure 5-15. Removal in the single tube bioreactor under nitrogen limitation. Sampling over the operational period with the single silicone tube bioreactor devoid of nitrogen showed an average removal of 124 ppm (LCL 107 ppm, UCL 141 ppm).
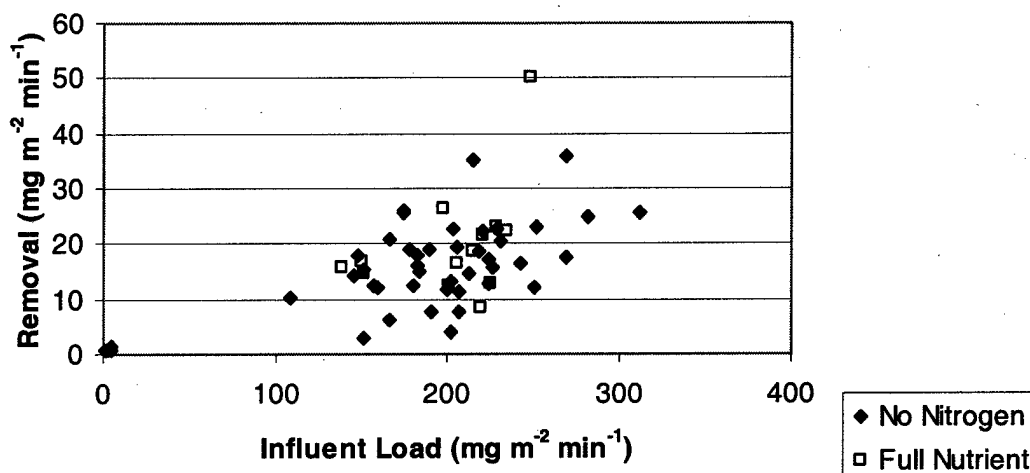
Figure 5-16. Loading curve of the single tube bioreactor under full and nitrogen limited conditions. No significant differences in removal were found between the ful nutrient and limited nutrient reactors.

5.4.4 Dual Silicone Tube Bioreactor, Full Nutrient Solution: The last seven sampling events during full nutrient operation, as shown in Figure 5-17, showed an average removal of 396 ppm (LCL 299 ppm, UCL 493 ppm) in the dual tube bioreactor. Again, the last seven data points were chosen as their influent concentration was relatively steady. The bioreactor had an average influent concentration of 721 ppm and an average effluent concentration of 325 ppm during the sampling period. The influent and effluent data for the dual tube reactor is shown in Figure 5-17. Removal was approximately 42 $mg\ m^{-2}\ h^{-1}$ at an influent concentration of 80 $mg\ m^{-2}\ h^{-1}$. The loading curve is shown in Figure 5-18.
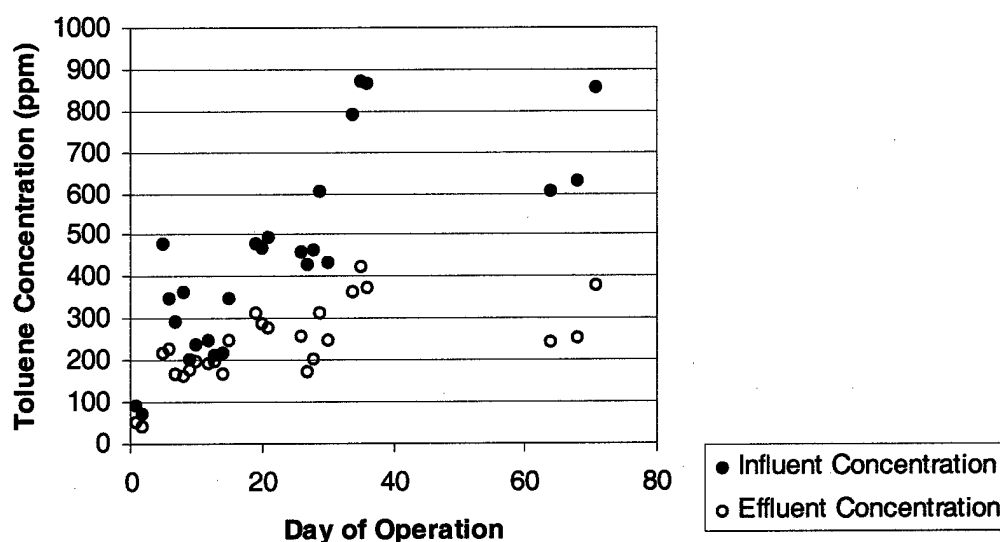
Figure 5-17. Removal in the dual tube bioreactor with full nutrient solution. The last seven sampling events during full nutrient operation showed an average removal of 396 ppm (LCL 299 ppm, UCL 493 ppm) in the dual tube bioreactor.
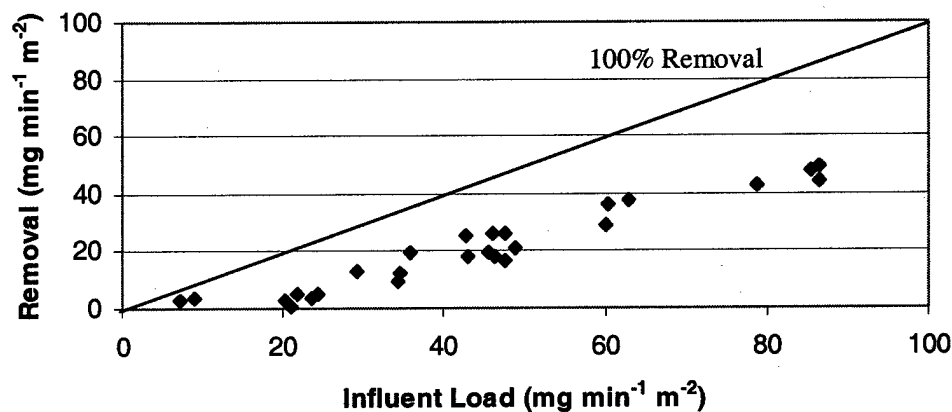
Figure 5-18. Loading curve of the dual tube bioreactor with full nutrient solution.

5.4.5 Dual Silicone Tube Bioreactor, Devoid of Phosphorous: Sampling over the operational period showed an average removal of 342 ppm (LCL 312 ppm, UCL 373 ppm). The bioreactor had an average influent concentration of 692 ppm and an average effluent concentration of 349 ppm during the sampling period. The influent and effluent

data is shown in Figure 5-19. Removal was approximately $20 \text{ mg m}^{-2} \text{h}^{-1}$ at an influent concentration of $40 \text{ mg m}^{-2} \text{h}^{-1}$. A comparison of the loading curves for the full nutrient condition and the no-phosphorous condition is shown in Figure 5-20.
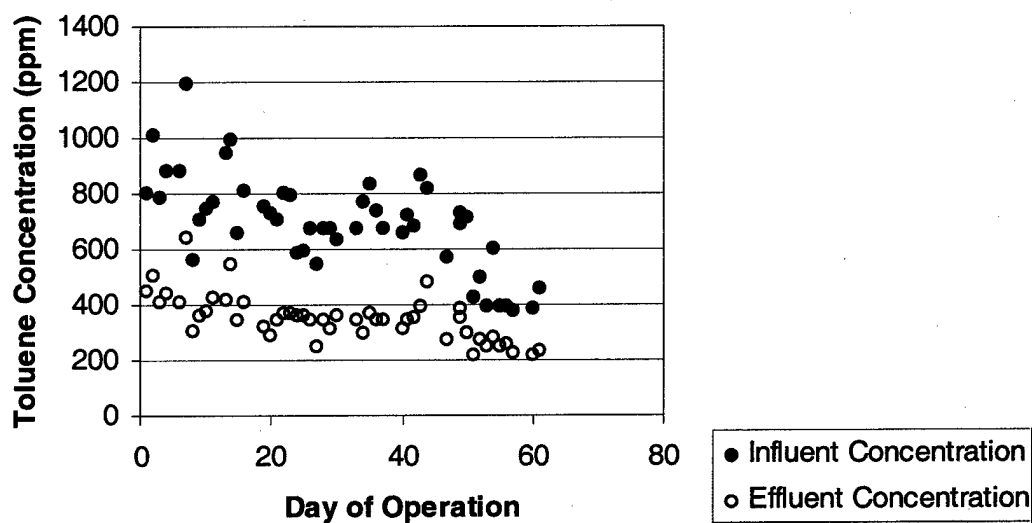
Figure 5-19. Toluene removal in the dual tube reactor under phosphorous limitation. Sampling over the operational period showed an average removal of 342 ppm (LCL 312 ppm, UCL 373 ppm).
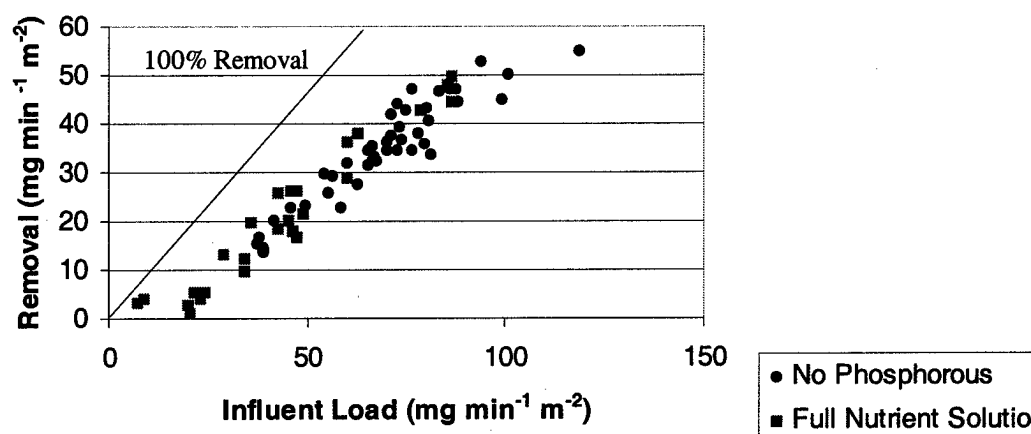
Figure 5-20. Loading curve of the dual tube reactor under phosphorous limitation. No significant differences in removal were found between the ful nutrient and limited nutrient reactors.

5.4.6 Discussion: The single silicone tube bioreactor operated with full nutrient solution provided toluene removal of 146 ppm (LCL 100 ppm; UCL 191 ppm) while the same reactor under nitrogen limited conditions provided a removal of 124 ppm (LCL 107 ppm; UCL 141 ppm). The dual silicone tube bioreactor with full nutrient solution provided a removal of 396 ppm (LCL 299 ppm, UCL 493 ppm) while the dual silicone tube bioreactor with nutrient solution devoid of phosphorous provided a removal of 342 ppm (LCL 312 ppm, UCL 373 ppm). In both the single and dual tube bioreactors, depleting the nutrients N and P had no apparent effect on the removal efficiency for toluene in the operational bioreactors.

Several studies have indicated nutrient deprivation may impact removal or control biomass growth (Kinney et al (1998) (in Moe and Irvine, 2001a); Smet et al, 1999). Although not anticipated from the aforementioned studies, the lack of efficiency decline in the present study fits well with results from at least one other study. Cherry and Thompson (1997) indicated it should not be necessary to add nutrients perpetually to

maintain activity in a bioreactor once the proper population of microorganisms has been obtained. The lack of decline in efficiency suggests that nutrients are potentially cycling within the biofilm through diffusion. There remains the question whether nutrient limitation would be a serious detriment over a long period of operation (Moe and Irvine, 1991), however, this short study suggests that at least for short periods, nutrient deprivation will not greatly impact removal in the silicone tube bioreactor systems.

5.5 REACTOR OPERATION AND SCALE-UP:

5.5.1 Semi-Pilot-Scale Reactor: Because no report of a pilot-scale membrane bioreactor was found in the literature, a semi-pilot-scale unit was built and operated for a 150 day period. A loading curve is shown for that semi-pilot-scale reactor in Figure 5-21. Figure 5-22 shows the removal on the basis of loading per cubic meter of bioreactor volume, the proposed conventional method for reporting biofilter performance (Devinny et al, 1999). Toluene removals from the air ranged from 10-100%, and varied with influent concentration; higher loads gave smaller percentage removals with the lower loads giving 100% removal in some cases. The first days of operation generally gave lower removals, most likely related to lack of complete biofilm formation at that time. As a note, when examining removal data, it appears to the author that using loading curves is most appropriate and least confusing. Loading curves take into account the airflow, influent concentrations, and reactor surface area and volume.
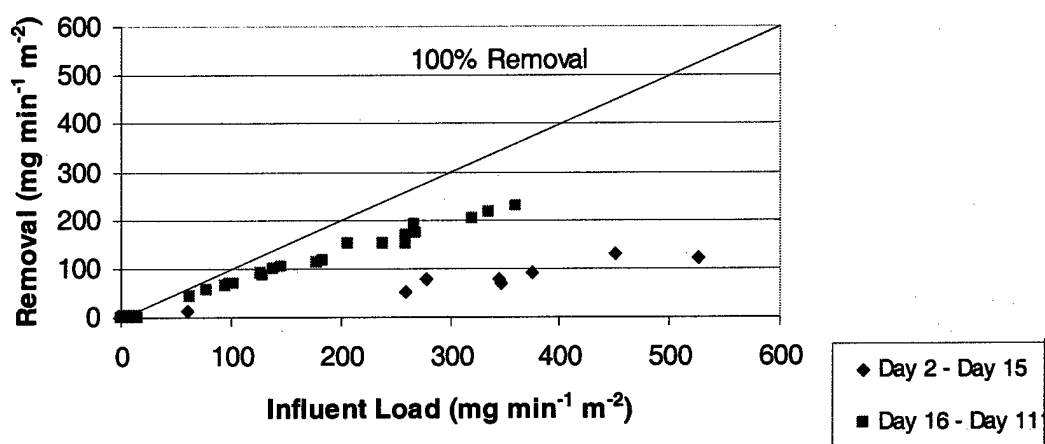
Figure 5-21. Removal per membrane area in the semi-pilot-scale reactor. The first fifteen days showed lower removals because of incomplete biofilm growth.
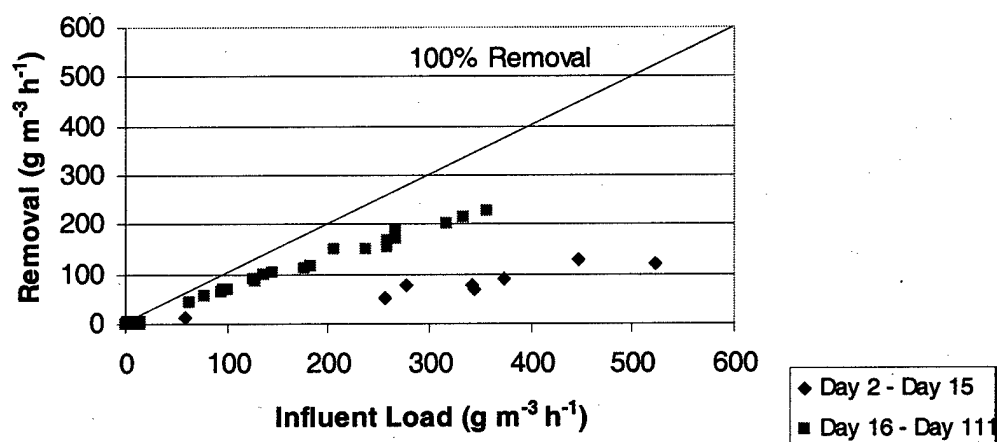
Figure 5-22. Removal per volume in the semi-pilot-scale reactor.

5.5.2 Discussion: As a comparison with conventional biofilters, the semi-pilot scale reactor offers comparable removals in terms of loading. Elimination capacities for BTEX compounds ranged from 8–60 g m^{-3} h^{-1} while removals for VOCs ranged from 5-229 g m^{-3} h^{-1} (Devinny et al, 1999). The semi-pilot scale reactor in the present study showed removals of <1 - 220 g m^{-3} h^{-1}. Increased removal with increased loading is most likely related to a greater concentration gradient across the membrane because of increased air

contaminant concentration (providing a larger driving force) and/or an increase in substrate utilization by the microorganisms associated with the higher concentration. The lack of apparent scaling is most likely related to differences in microorganisms communites present, differences in silicone tubing radii caused by stretching of the tubing or perhaps even differences in the age of the tubing itself.

5.6 IN SERIES REACTOR OPERATION:

5.6.1 Removal in reactors: To determine whether two bioreactors in series would perform adequately, the dual tube bioreactor was placed in series with a newly constructed single tube bioreactor. Results of the in-series operation are shown in Figure 5-23. Removal while operated in series in the dual tube bioreactor was approximately twice that of the single tube bioreactor on a per area basis. Differences in removal of the individual units may be related to how the reactors were constructed. In the dual tube reactor, tubes were stretched while in the new single tube reactor, the tube was not tightly stretched. Also in the new single tube reactor some splitting of the biofilm was noted, so there was not 100% coverage of the tube at all time of operation. However, the single tube did provide further removal of toluene when placed in series with the dual tube reactor; two bioreactors in series provided more removal than one bioreactor alone.

5.6.2 Discussion: Of note is the difference of removal seen in the dual tube bioreactor during its first few months of operation and the removal seen during the in-series experiment. Removal in the dual tube biofilter alone was 20 mg m^{-2} min^{-1} while during the in-series experiment removal was 10 mg m^{-2} min^{-1} (both experiments at a loading rate of 40 mg m^{-2} min^{-1}), a very apparent decrease. At the time the experiment was completed, the dual tube bioreactor biofilm was approximately 7 months old. Aging of

the biofilm or the silicone tube may have contributed to the differences in removal over time for the dual tube reactor. Shifting in biofilm communities may have also contributed to the differences in removal seen at the various times.
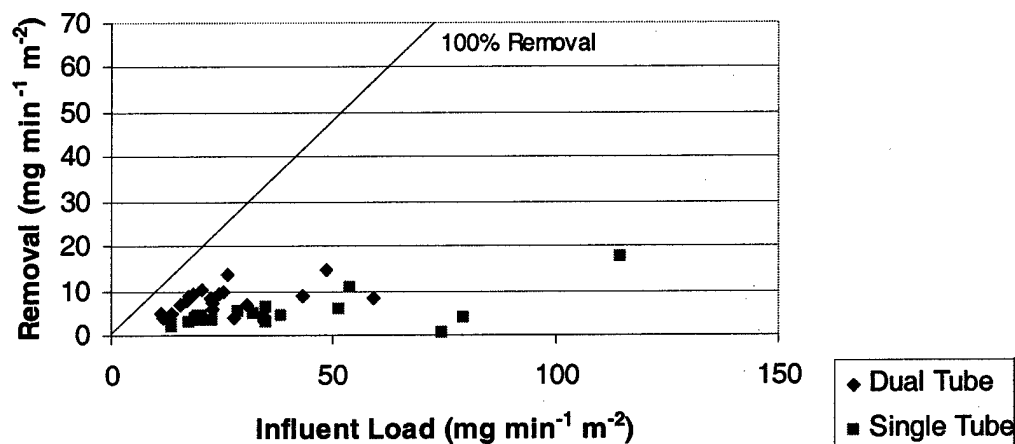
Figure 5-23. Removal in the in-series reactors.

5.7 COMPARISON OF TOLUENE REACTOR SYSTEMS:

An overall comparison of reactor systems examined during the present study is shown in Figure 5-24. There are distinct differences in removals seen between the reactor systems. Exact comparison is difficult as reactors were not operated with exactly the same dimensionless parameters, and the reactors also may not have exactly the same bacteria or bacterial communities present. Additionally, the single bioreactor was an older biofilm (possibly impacting the kinetics) and the manufacturer of the silicone tubing is believed to have been different than the manufacturer of the tubing used in the semi-pilot-scale and the dual tube reactors (possibly impacting the effective permeability of the silicone). The airflow patterns, and the method of introduction of air into each reactor may have also contributed to differences in removal; velocity profiles may or may

not have been fully developed. Each of these factors may contribute to the differences in removal and are more thoroughly discussed in the modeling results section.

The reactors may be further compared by examining parameters periodically measured during the study, with complete data shown in Appendix D. More measurements would have been completed, however, each time measurements were taken, the biofilm and bioreactor system was disturbed causing some sloughing of biofilm. Probably the most notable trends seen in the measurement are the frequently changing dissolved oxygen concentrations within the liquid phase ranging from 0-4.91 mg L^{-1}, the limited pressure drop across the reactors ranging from 0-$^{15}/_{16}$ inches of water, the limited need for nutrient solution replacement, and the distinct drop in pH over the period of operation, i.e. 6.15 dropping to 3.3 in the dual tube reactor. The differences in oxygen readings are most likely attributed to disturbance of the liquid suspension during meaurement and the accidental introduction of air.

pH drop during reactor operation is very large. This drop in pH may be related to bacterial metabolism changes or to accumulation of metabolic wastes within the system (Bleckmann, 2003). The pH recorded during the course of experimentation was measured in the liquid and perhaps does not reflect the pH that actually exists within the biofilm matrix. The bacteria themselves may be at least partially shielded from the low pH due to the presence of large quantities of exopolymeric substances (EPS). Perhaps the biofilm is stratified with the most acid tolerant bacteria positioned towards the liquid with the less tolerant tube side. Unfortunately, the exact reason for the drop in pH cannot be explained without further knowledge and analysis.
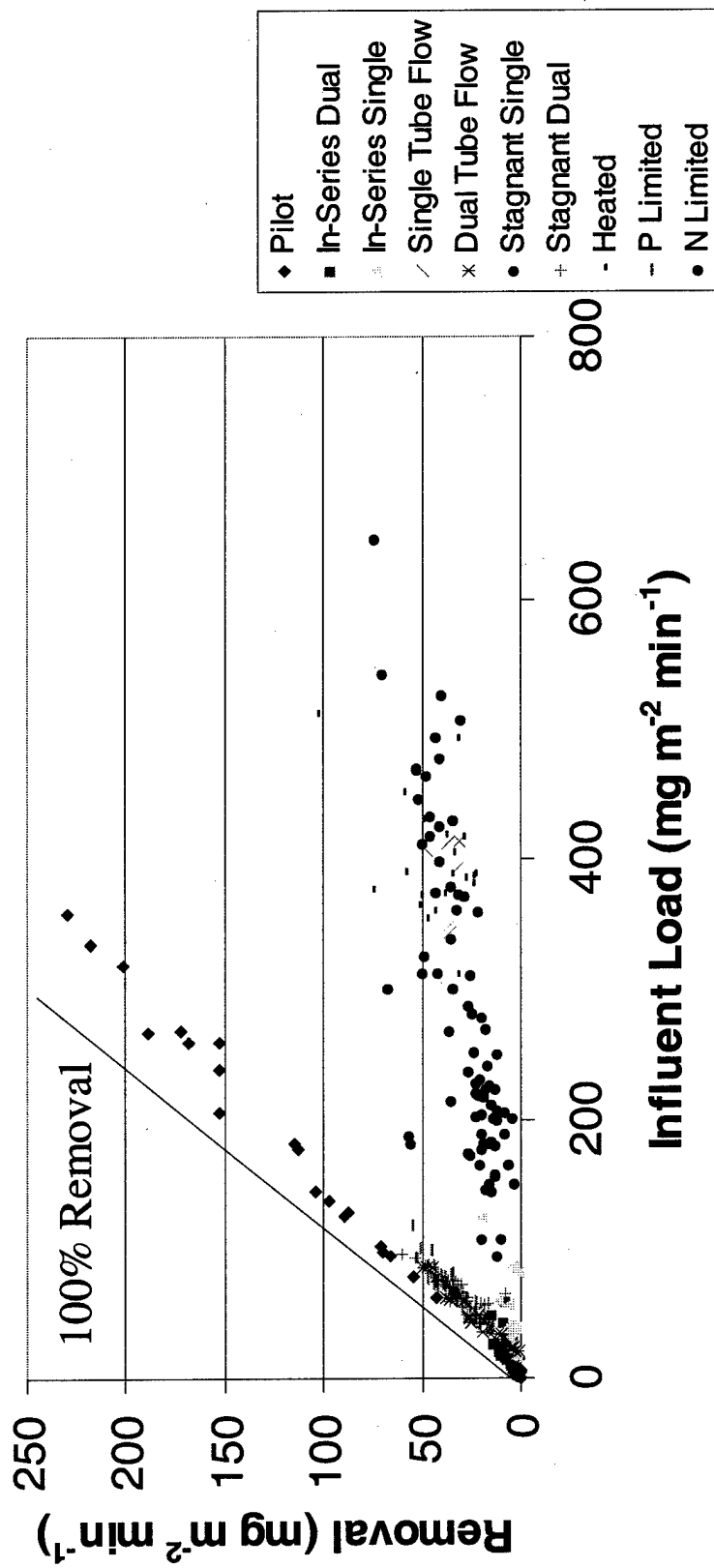
Figure 5-24a. Removal in the reactor systems.

Comparison of Reactor Systems

Legend:
- ◆ Pilot
- ■ In-Series Dual
- ▲ In-Series Single
- ✖ Dual Tube Flow
- + Stagnant Dual
- – P Limited

Y-axis: Removal (mg m^{-2} min^{-1})

X-axis: Influent Load (mg m^{-2} min^{-1})
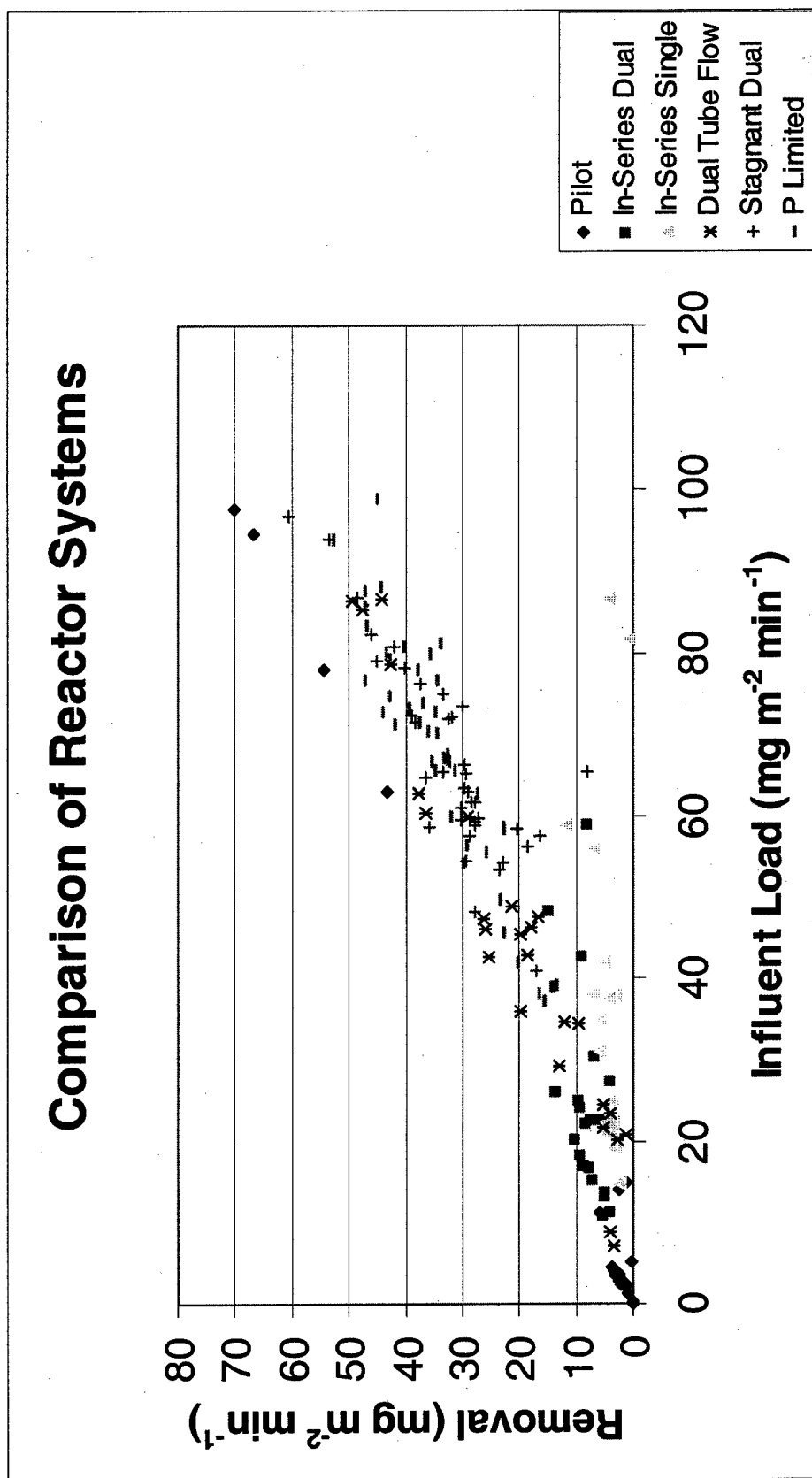
Figure 5-24b. Removal in the reactor systems at lower influent loading. Model permeabilities (p) were 0.03, 0.01, and 0.01 cm^2 s^{-1}, for the single, dual and pilot reactors, respectively.

5.8 HEAT TRANSFER STUDIES AND INCREASED TEMPERATURE OPERATION:

5.8.1 Introduction: Membrane bioreactors may have the potential to effectively treat elevated temperature contaminated gas streams. High temperature contaminated gas streams may exist in virtually any industry where dryers, ovens, or heaters are used or where combustion occurs. More commonly known industries that have high temperature gas stream emissions include wood products manufacturing (NCASI, 1999), the power generation, metal-castings and automobile manufacturing industries.

To determine heat transfer coefficients in membrane modules, several configurations of the temperature measurement apparatus described in the Methods and Materials Section were used. Three membrane materials were examined: silicone, latex, and polysulfone. Heat transfer coefficients were calculated for each membrane module under two air flow rates (high and low) and several liquid flow rates. Each membrane module was examined under insulated and uninsulated conditions. A measurement of the membrane surface temperature was also taken.

5.8.2 Heat Transfer Coefficients: A tabular comparison of the modules used is shown in Table 5-3 while the measurement ranges are shown in Table 5-4. The comparative information is shown graphically in Figure 5-25. The results indicate that the polysulfone module had lower heat transfer coefficients than the silicone and latex modules. The lower values are most likely related to the differences in reactor sizes, membrane surface area, and module configurations. The latex and silicone modules had heat transfer coefficients very similar to one another, again, possibly related to their very similar sizes, reactor configuration and membrane surface areas.

Table 5-3. Membrane units used during heat transfer experiments.

Membrane Unit	Liquid Flow Rates (mL min^{-1})	Air Flow Rates (L min^{-1})	Unit Length (mm)	Fiber O.D. (mm)	Membrane Area (m^2)
Silicone Rubber	5.9 - 83.9	1.18, 3.69	240	12.7	0.009574
Latex Rubber	2.6 - 88.8	1.26, 5.37	240	12.7	0.009574
Polysulfone	8.0 - 89.1	0.98, 2.60	177.8	3.9	0.018517

Table 5-4. Range of heat transfer coefficients (U), reported in W m^{-2} K^{-1} and surface temperature (K) at the exterior membrane surface.

Material	Insulated High Flow[1]	Insulated Low Flow[2]	Uninsulated High Flow[1]	Uninsulated Low Flow[2]	Influent Air/Membrane Surface Temp (K)
Silicone	13.2 - 17.4	8.9 - 12.1	13.8 - 15.2	7.7 - 9.2	365.2/299.5
Latex	13.6 - 14.1	9.6 - 12.9	14.1 - 15.4	9.1 - 11.3	370.0/309.9
Polysulfone	12.6 - 16.7	2.9 - 3.9	10.7 - 11.3	6.7 - 6.8	363.6/294.5

[1]High Air Flow (L min^{-1}) - Silicone 3.7; Latex 5.4; Polysulfone 2.6.
[2]Low Air Flow (L min^{-1}) - Silicone 1.2; Latex 1.3; Polysulfone 1.0.
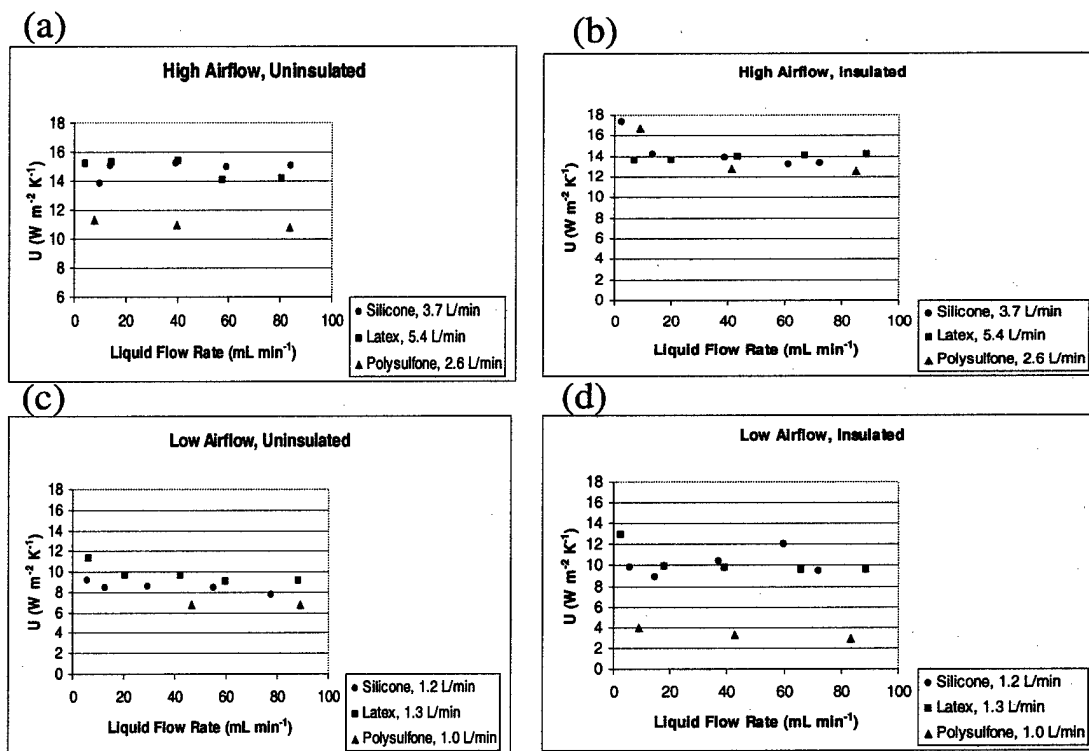
Figure 5-25. Summary comparison of heat transfer coefficients for uninsulated and insulated modules at high and low air flow rates; a. high airflow, uninslated; b. high airflow insulated; c. low airflow, uninsulated; d. low airflow insulated. U represents the heat transfer coefficient. Heat transfer coefficients ranged from 2.9-17.4 $W\ m^{-2}\ K^{-1}$.

Graphs of each measurement/experiment are shown in Appendix C. Error bars are shown on some graphs indicating 95% confidence intervals using the Student's t distribution. Lower airflow rates tended to give lower heat transfer coefficients as predicted by heat transfer theory. Little change in U was seen across the range of liquid flow rates investigated.

In an attempt to characterize the relative contributions of convective heat transfer, a model of heat transfer resistance for the single tube reactor configuration was adapted (Kakac and Liu, 1998, p. 286). The overall heat transfer coefficient for a shell and tube heat exchanger (and thus the reactor module) is shown in Equation 5-10:

$$\frac{1}{U_c} = \frac{1}{h_o} + \frac{d_o}{h_i d_i} + \frac{r_o \ln(r_o / r_i)}{k} \qquad (5\text{-}10)$$

where

U_c = Overall heat transfer coefficient
h_o = Heat transfer coefficient of the liquid side
h_i = Heater transfer coefficient of air side
d_i = Inner diameter of tube
d_o = Outer diameter of tube
r_o = Outer radius of tube
r_i = Inner radius of tube
k = Thermal conductivity of the tube material

There is extensive documentation of convection correlations (e.g. Kakac and Liu, 1998). The only forced convection equation that represents simultaneously developing laminar flow and temperature in smooth ducts is shown in Equation (5-11), however, it is not valid for the diameter and length configuration of the single tube modules, therefore, the Nusselt number of 4.36 was used; representative of fully developed flow in a smooth duct (Kakac and Liu, 1998, p. 77 and 84). Neither equation nor singular value is an ideal assumption.

$$Nu = (0.664)\left(\frac{\operatorname{Re}\operatorname{Pr}d}{L}\right)^{1/2} \operatorname{Pr}^{-1/6} \qquad (5\text{-}11)$$

where:

Nu = Nusselt number (dimmensionless)
Re = Reynolds number (dimensionless)
Pr = Prandtl number = kinematic viscosity/thermal diffusivity (dimensionless)

d = Diameter of tube (m)
L = Length of tube (m)

The convective heat transfer coefficient can be represented by Equation (5-12) (Clark, 1996, p.341).

$$h = \frac{Nu\,k_{air}}{d_i}$$

(5-12)

Using values shown in Table 5-5, and Equation 5-12, convective transfer appears to dominate Equation 5-10. However, to make certain this was the case, more exacting measurements over the air flow regimes actually used would be necessary to develop the exact Nusselt number correlations and subsequently the convective heat transfer coefficient. Additionally, determination of the thermal conductivity of the exact silicone rubber in use might yield more information about relative contributions of to heat transfer resistance.

Table 5-5. Input parameters for Equation 5-10.

Parameter	Unit	Value
U_c	W m^{-2} k^{-1}	15
k	W m^{-1} K^{-1}	0.0257
d_i	m	0.009525
Nu	--	4.36

Several difficulties were experienced during the measurement of heat transfer coefficients. High temperature air was extremely difficult to generate with the equipment available. Low air flow rates were particularly troublesome; although very high temperature air was generated in the heater, temperatures declined very rapidly after exiting the heater. Attempts to insulate influent portions of the apparatus did not yield any better results. The apparatus also was very small, and the short distance between

influent and effluent measurement ports potentially influenced results. At higher airflow rates, the heating device's rheostat was ultra sensitive to movement, making exacting temperature control difficult. Additionally, the apparatus was not enclosed in a temperature controlled box or placed in a very stable temperature room, therefore, there is the possibility that room temperatures may have slightly influenced results, since readings were taken on different days. Because of these difficulties related to the construction of the heat transfer measurement apparatus, only *qualitative* statements are warranted concerning the various membrane materials and module configurations.

Measured values of U in this study (2.9 - 17.4 W m^{-2} K^{-1}) are lower than those found in the literature, but consistent with convective heat transfer. The film heat transfer coefficient for a low-temperature distillation unit employing hydrophobic membranes was 29 W m^{-2} K^{-1} (Aremu, 1990), 5000 W m^{-2} K^{-1} in a microporous membrane distillation process (Schofield, 1989), and 1.75 x 10^7 W m^{-2} K^{-1} for rubber to air (Sae-Oui et al, 1999). The great differences in the values cited, as well as the difference with those measured during this study, are most likely related to the variety of use and measurement conditions of the various membranes. In this case, the air phase seems to dominate the resistance to heat transfer.

5.8.3 Bioreactor Operation: To establish a baseline for comparison with higher temperature operation, the small single silicone tube bioreactor was first operated at ambient temperature (~ 23 °C) for a period of two weeks. During the period of ambient temperature operation influent toluene concentrations averaged 986 ppm, effluent 893 ppm and toluene removal averaged 93 ppm (LCL_{95} 77 ppm; UCL_{95} 109 ppm), with an average mass removal of 17 g m^{-3} h^{-1} (total reactor volume basis). Later, the same

bioreactor was operated with the liquid flow heated. The liquid temperatures in the

center of the reactor liquid volume was 37.5 °C, an increase of approximately 15 °C

above ambient temperature operation. During the 36-day operational period of the heated

bioreactor, influent toluene concentrations averaged 1020 ppm, effluent 909 ppm, and

toluene removal averaged 111 ppm (LCL$_{95}$ 90 ppm; UCL$_{95}$ 133 ppm) with an average

mass removal of 20 g m^{-3} h^{-1} (total external reactor volume basis). A graphical

presentation of the influent and effluent data and the loading curves are shown in Figures

5-26 - 5-28.
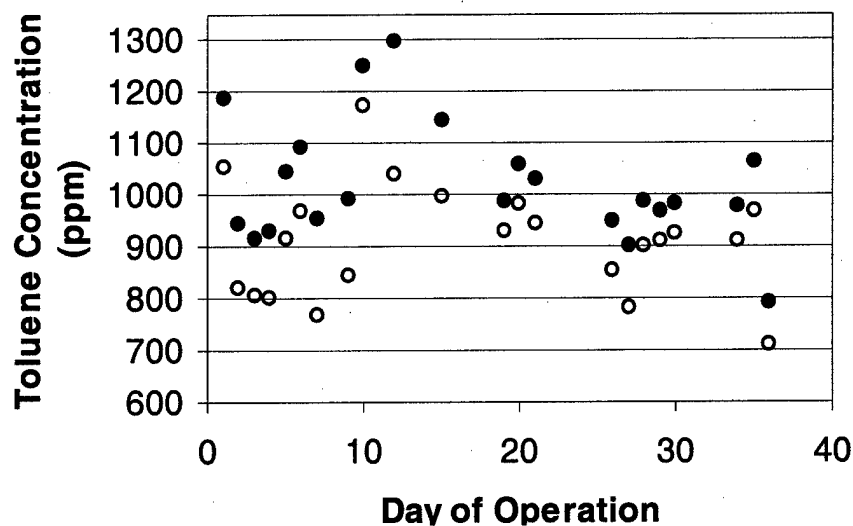
Figure 5-26. Influent and effluent concentrations of the heated bioreactor. Gas inlet (●) and gas outlet concentrations (o) are shown for each respective day. During the 36-day operational period of the heated bioreactor, influent toluene concentrations averaged 1020 ppm, effluent 909 ppm, and toluene removal averaged 111 ppm (LCL$_{95}$ 90 ppm; UCL$_{95}$ 133 ppm).
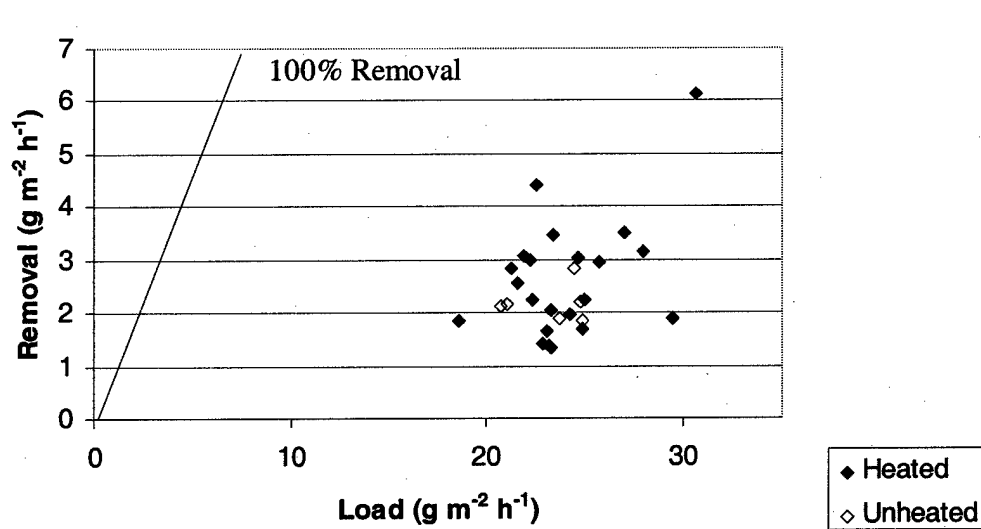
Figure 5-27. Surface loading versus removal in the heated bioreactor.
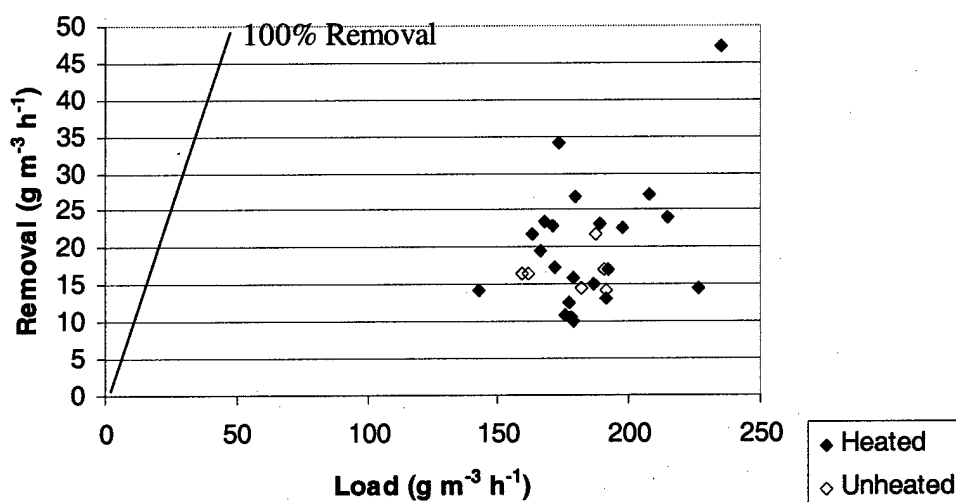
Figure 5-28. Volumetric loading versus removal in the heated bioreactor. No significant differences were found in removal between the ambient temperature and the heated reactor systems.

Operation of the heated bioreactor was generally unremarkable and was indistinguishable from operation of the bioreactor during ambient temperature operation with one exception. At day 19, a definite color change (beige to pink) of the suspension and biofilm was observed. Over the next several days, the biofilm and microorganisms attached to the glass reactor interior also turned pink. The color change was most likely

indicative of a shift in relative numbers of microorganisms. Later, small amounts of

algae were seen growing on the interior of the reactor, again indicating that the

approximately 15°C increase in temperature resulted in a different microbial community.

Kinetic data from both the biofilm and suspension were collected to explain the

anticipated differences in bioreactor performance under ambient and elevated

temperature conditions. Biokinetic parameters are shown in Table 5-6.

Table 5-6. Biokinetic parameters for ambient and elevated temperature operation.

	Ambient Temperature	Elevated Temperature
Suspension K_S (mg L^{-1})	1.5	1.3
Suspension k (h^{-1})	0.01	0.07
Biofilm K_S (mg L^{-1})	12.0	0.8
Biofilm k (h^{-1})	0.2	0.09

Although the measured kinetic values for the ambient and heated bioreactor suspension

were very similar, the biofilm kinetic parameters changed markedly. The change may be

related to the change in population, suggested by the color shift during operation. In a

thermophyllic study of alpha-pinene removal, analysis of the microbial community using

DNA fingerprinting indicated that there were distinct communities present at the different

temperatures of operation (Allen et al, 2000).

Although anticipated to provide higher removal rates at elevated temperatures, the

bioreactor provided only a small apparent improvement in average removal, and that

improvement was not actually statistically significant. An improvement in performance

was expected based on reports that biological reaction rates approximately double when

the temperature rises 10 °C (Devinny et al, 1999). Expectations for improvement were

also warranted based upon other studies; toluene removal in a conventional biofilter

increased 37% after a 10 °C increase in feed temperature, and the same unit had a 10%

increase in removal when ambient temperatures were increased 10 $^{\circ}$C (Ahmed, 1997). In support of the lack of improvement, Cox and Deshusses (2000) found elimination capacities for ethanol were similar for both an ambient temperature biotrickling filter (22 $^{\circ}$C) and one at high temperature (53 $^{\circ}$C) while removals were similar at different temperatures in a bioreactor removing NO_x (Min et al, 2002).

The lack of improvement in removal might be explained by both physical - chemical and biological factors. The slightly higher temperature in the reactor may have created an unfavorable physico-chemical environment. As the Henry's Law coefficient rises with temperature for most gases, less of the compound may be dissolved in the water and sorption may also be reduced (Devinny et al, 1999). The limited increase in removal might also be related to the apparent shift in microorganism populations. Additionally, the experimental design may have influenced the result. Although the interior of the reactor only achieved a temperature of 37.5 $^{\circ}$C, the liquid in the hot plate was at 72 $^{\circ}$C. Thus it is possible that some, if not all, of the mesophilic bacterial suspension passing through the flask was negatively affected.

5.9 DIURNAL LOADING STUDIES:

5.9.1 Significance of Transient Loading Studies: Examination of VOC removal under non-steady state or transient loading conditions is of interest because biofilters operating in industry are generally exposed to a spectrum of changing conditions, particularly when assigned to the treatment of waste air from discontinuous processes. Within the paint coating industry, which may have highly varying emissions over time, effluent streams containing mixtures of ketones, alcohols and xylene with concentration surges of up to 20,000 ppm have been reported (Bustard et al, 2001). Additionally, shift work may be

used and the bioreactor will not have a steady flow of contaminant. For example, a worker may begin the work shift by turning on the paint booth exhaust ventilation system (the contaminated gas supply to the bioreactor), complete an 8-h work shift painting vehicles (VOCs are generated and delivered to the bioreactor), and turn off the ventilation system at the end of the work shift (VOC supply to the bioreactor is halted or reduced). Therefore, a starvation period would occur after a period of relatively steady carbon supply. It seems pertinent to obtain reliable data on the transient behavior of membrane bioreactors under the conditions encountered in field operation, in order to ascertain whether a bioreactor could respond effectively to sudden changes in operating conditions, shutdowns and restarts, and contaminant spike loadings.

The main objective of this study was to examine the removal of a contaminant from a contaminated gas stream, using a polysulfone microporous membrane module, under "shift work" conditions. 1-butanol was selected for study because benzene, the contaminant originally chosen for study (Zhang, 2000), was found to be absorbed by the polysulfone module. Toluene, the contaminant used for other experiments in the present study was anticipated to also absorb into the membrane and was not used. The 1-butanol removal efficiency under the periodic carbon supply conditions was compared to 1-butanol removal under constant contaminant concentration conditions. The study had three separate phases of operation: continuous, steady-state operation of the bioreactor (Zhang, 2000); start-up with immediate placement onto an 8-h "on" and 16-h "off" condition with a weekend "off" condition added later; and start-up into a continuous operation followed by 8-h "on" and 16-h "off" condition.

5.9.2 Phase I - Bioreactor Continuous Loading:

5.9.2.1 Biokinetic Parameters: Monod-like biokinetic parameters were determined for the biofilter cultures degrading 1-butanol by Zhang (2000). Non-linear least squares regression produced a maximum specific utilization rate, k, of 4.3 d^{-1} and a half saturation constant, K_S, of 8.9 mg L^{-1}.

5.9.2.2 Abiotic Mass Transfer: For the various combinations of gas and liquid flow rates examined (Zhang, 2000), mass closure ranged from 93-135% and overall removal of 1-butanol from the gas stream into the liquid stream ranged from 58-96%. As expected from models and similar reactors (Ergas 1999; Aziz 1995) the degree of abiotic removal was dominated by the liquid velocity. Abiotic mass transfer and mass closure served as a control for the experiment.

5.9.2.3 Continuous Loading: The bioreactor was operated under a continuous loading condition for 30 days (Zhang, 2000). Daily removal percentages are shown in Figure 5-29. 1-butanol removal generally improved over time. Influent concentrations were changed until greater than 99% removal at an influent concentration
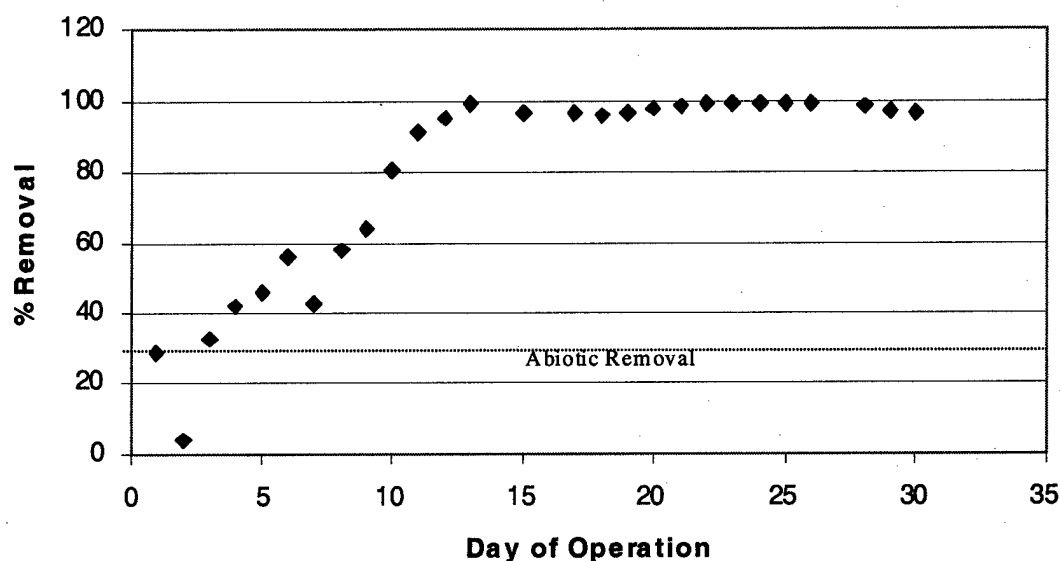
Figure 5-29. Removal of 1-butanol under continuous loading conditions, Phase I; data from Zhang (2000). Gas flow rate of 220 mL min^{-1}, liquid flow 5-40 mL min^{-1} and influent concentration averaging 200 ppm. Removals increased as the biofilm developed.

of 200 ppm (73 g m^{-3} h^{-1}) was achieved. Only three conventional biofilter studies

concerning butanol removal have been described in the literature (Baltzis et al, 1997;

Heinze and Friedrich, 1997; Tang et al, 1995); no study has reported 1-butanol removal

in membrane biofiltration units. Baltzis et al (1997) modeled removal from the gas phase

and emphasized the importance of adequate oxygen for the degradation of butanol while

Heinze and Friedrich (1997) correlated the volumetric respiration rate with the

volumetric degradation rate of n-butanol by the stoichiometry of n-butanol oxidation. A

peat and perlite biofilter removing ethanol and butanol under shock loadings never failed

(Tang et al, 1995).

During this portion of the study, no degradation intermediates were detected

during headspace analysis of the air or liquid phases. Inlet liquid concentrations in this

countercurrent flow apparatus were typically <1 mg L^{-1} while the liquid outlet concentrations were typically at 2 mg L^{-1}, indicating that some degradation was occurring in the liquid suspension in the bubble catcher, in addition to the degradation occurring in the attached membrane biofilm.

5.9.3 Phase II - Bioreactor Diurnal Loading: Beginning in September 2000, the polysulfone membrane module was seeded with a 1-butanol degrading culture, and placed immediately onto a diurnal loading schedule of 8 h "on" and 16 h "off", 7 days a week. At Day 22, the gas flow and contaminant feed to the bioreactor was manually turned off on weekends, in addition to being turned off at night. Figure 5-30 shows end-of-day removal percentages over the course of operation. End-of day percentages were used to analyze the data as they were usually the lowest removal efficiency noted through the 8-h day. Anomalously high removal efficiencies seen on Days 16, 17, 25, and 63 and low readings remain unexplained. However, they are most likely due to mechanical failures in the system; influent concentrations tended to vary due to the type of pumps used and the evaporation rate of 1-butanol. Removal efficiency averaged 29%.
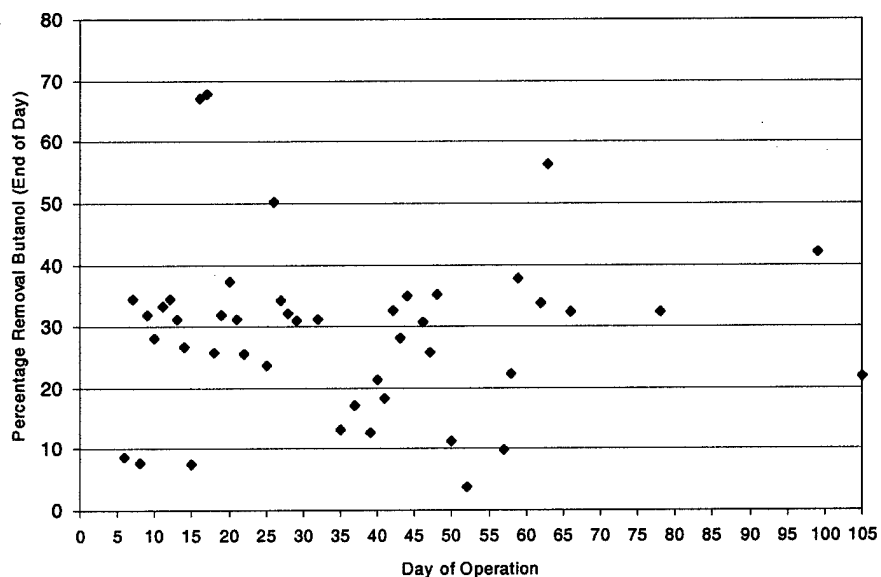
Figure 5-30. End of day 1-butanol removal (% basis), diurnal loading conditions. Removal efficiency averaged 29%.
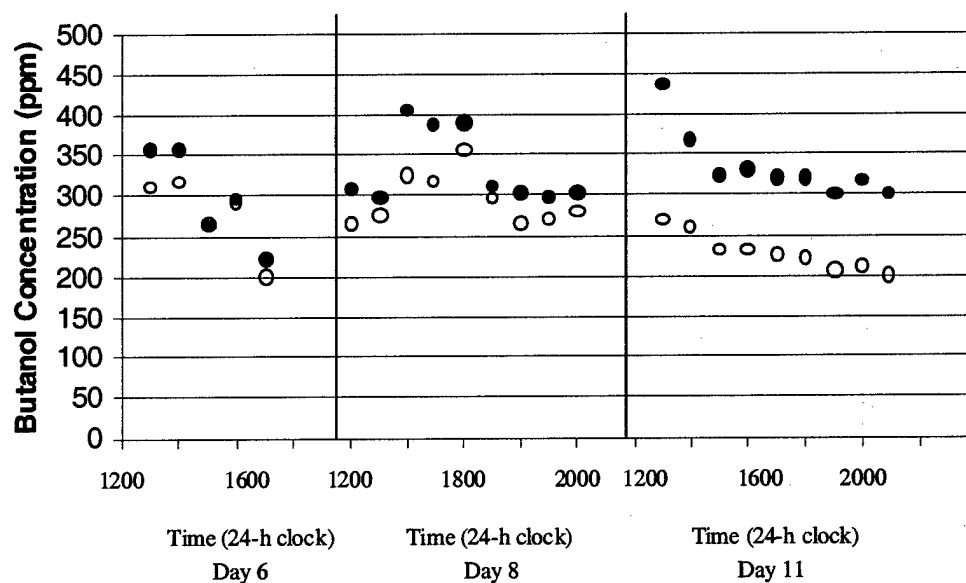
Figure 5-31. Improvement in hourly 1-butanol removal after bioreactor start-up. Gas inlet (•) and gas outlet concentrations (o) are shown for each respective day. Improvements were most likely related to increased biofilm growth.

The improvement in bioreactor operation over the initial start-up period is seen in Figure 5-31. As seen in most bioreactor studies, time is required for the microorganisms to acclimate to influent concentrations and to multiply to a viable population number. After approximately Day 8, hourly removal patterns were fairly stable and resembled the pattern seen on Day 11.

Greater removal efficiencies were seen immediately after bioreactor start-up each day as compared to the end of the day. To further examine what was occurring, influent and effluent measurements were taken approximately every fifteen minutes directly following start-up. Removal percentage stabilized after approximately one hour and the removal over a typical day is shown in Figure 5-32. Higher removal efficiencies after start-up each day might be explained by consumption of 1-butanol in the biofilm and liquid phase while the normal air feed was turned off, thus increasing the concentration gradient at start up, driving diffusion of the 1-butanol into the liquid phase. In a conventional biofilter, the collection efficiency was found to rise for a short period after the feed was resumed after shutdown (Gerrard et al 1997). The higher removal percentage was most probably due to adsorption in the bed. Paca and Koutsky (1994 in Marek et al, 2000) found a brief increase in efficiency for both xylene and toluene after restarting a biofilter after a 2 h and 24 h period of starvation. Additionally, influent concentrations in the current study were slightly higher in the morning, due to the apparatus configuration; with airflow turned off the 1-butanol was able to saturate the air in the container through which the air flow passed at start-up.
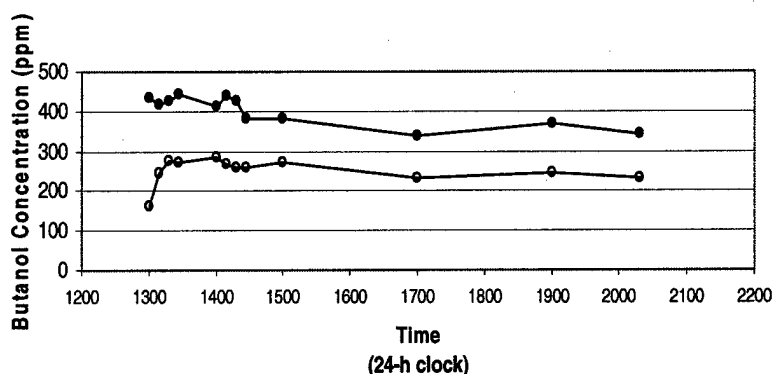
Figure 5-32. A typical 8-h day (Day 13) of 1-butanol under diurnal loading conditions, Phase II. Gas inlet (●) and gas outlet concentrations (o) are shown throughout the day. Removal at start-up was greater than end-of-day removal.

5.9.4 Discussion: The apparent lower removal efficiency during Phase II, 29% (111 ppm) as compared to >99% (200 ppm) removal efficiencies found during continuous operation in Phase I, was first thought to be related to changes in the biofilm or suspension biomass. Several studies have shown that starvation results in metabolic and enzymatic changes of the microorganisms (Cunha, 1994; Papageorgakopoulou and Plakoutsi, 1996; Neubauer et al, 1995; Cunha et al, 1994).

A good explanation of microorganism growth under unsteady-state conditions is provided by Moe and Irvine (2001c). Imposed conditions on bioreactors can cause two types of adaptation in a mixed culture. The first is a change in relative abundance of species present within a mixed microbial community. The second is a shift in physiological state of the microbes. Physiological state refers to organism macromolecular composition. When grown under steady ambient conditions, microbes undergo balanced growth, a condition under which the physiological state remains

constant, i.e. the mass fraction and synthesis rate of macromolecules, such as DNA, RNA, and proteins remains unchanged from one generation to the next.

The physiological state achieved depends on the ambient growth conditions imposed (Moe and Irvine, 2001c). Changes in physiological state occur when microbial consortia are subjected to unsteady-state conditions and growth becomes unbalanced. During unbalanced growth, physiological state is not constant because intracellular macromolecules are changing and continue to change because they are synthesized at different relative rates. Because the protein synthesizing system determines the rate at which catabolic enzymes are synthesized, physiological state impacts the exhibited substrate removal rate. In fact, physiological adaptation can be considered the primary determinant of short-term transient responses because changes in selection and enrichment of the various species within a microbial community generally occur more slowly than changes in physiological state (Moe and Irvine (2001c). Nutrient depletion in the range of a few hours is expected to result in an increase in uptake efficiency and range of substrates utilized rather than a decrease in biofilm activity (Moe and Irvine (2001c)).

After taking into consideration the events that could be occurring in the biofilm and the suspension, the amount removed was compared on a reactor basis which accounts for the airflow through the biofilter, the volume of the reactor, and the influent concentration. When the amount removed was compared on a reactor volume basis, both Phase I and Phase II had essentially the same removal (Phase I, 73 $g\ m^{-3}\ h^{-1}$, Phase II, 74 $g\ m^{-3}\ h^{-1}$)!

5.9.5 Phase III - Bioreactor Diurnal Loading After Steady-State Continuous

Operation: Because it was originally believed (after Phase II) that the microorganisms were experiencing starvation and physiological changes because of immediate placement onto the "on" and "off" feeding schedule, a third part of the study was undertaken. The bioreactor was again seeded with the 1-butanol degrading culture isolated from activated sludge, and was operated continuously for 90 days. At the end of the 90-day period, measurements indicated an apparent steady state had been achieved. The bioreactor was then placed on a 7-day-a-week, 8-h on, 16-h off schedule.

A typical day of operation during Phase III is shown in Figure 5-33. Influent concentrations were near 700 ppm and end-of-day removal averaged 38% (269 ppm, 145 g m^{-3} h^{-1}) over a 30 day period of operation. When compared to Phase II, there was an increase in the amount of 1-butanol removed per hour during Phase III.
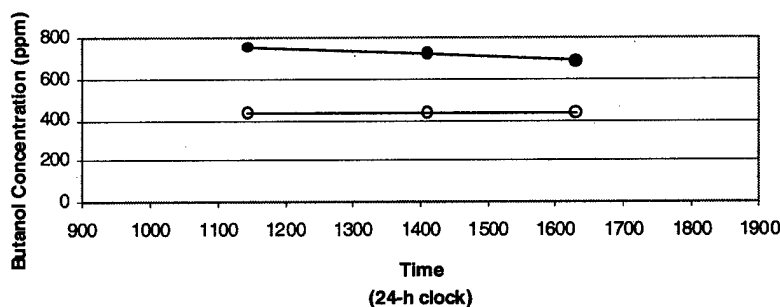
Figure 5-33. A typical day of n-butanol removal, Phase III. Gas inlet (•) and gas outlet concentrations (o) are shown throughout the day. Removal efficiency was constant throughout the day.

The improvement in removal efficiency when first placed under continuous load, allowed to achieve a steady-state condition, and then subsequently moved to a diurnal

schedule might be explained by an overall higher quantity of biomass in the suspension and/or a higher density or thickness of biofilm. Although not specifically measured, visual observation of the liquid in the bubble catcher indicated a higher quantity of biomass present (optical density) when compared to Phase II operation. Also, more biofilm coverage of the membranes was noted. During Phase III, virtually 100% of the membrane surfaces appeared to be coated with biofilm while during Phase II, there was only 75% coverage, at best. Another possible explanation is that the bioreactor was operated at a higher influent concentration during Phase III than during Phase II. The higher influent concentration in the gas phase provided a higher concentration of substrate to the microorganisms in the biofilm for subsequent degradation.

5.9.6 Discussion: This study is the first report of the effect of diurnal variation on biofilter operation. The polysulfone membrane module as part of a countercurrent, continuous flow bioreactor achieved greater than 99% (200 ppm, 73 g m^{-3} h^{-1}) removal of 1-butanol from a contaminated air stream. When the bioreactor was restarted and immediately placed upon a diurnal operating schedule, end-of-day removal of 1-butanol averaged 29% (111 ppm, 74 g m^{-3} h^{-1}). A third restart of the reactor, using continuous stead-state operation, a higher inlet concentration of 1-butanol, and then placement on the diurnal schedule, resulted in an end of day average removal of 38% (269 ppm, 145 g m^{-3} h^{-1}). The results suggest that biofilters operated on a diurnal schedule do not suffer performance declines compared to those operated with continuous feed supply.

5.10 SUMMARY OF OPERATIONAL RESULTS:

During the course of study described in this chapter, a number of membrane biofilters of differing size were operated. Broadly stated, toluene removal was

comparable to BTEX removal seen in conventional biofilters (8-60 g m^{-3} h^{-1}) (Devinny et al, 1999). However, removal did not scale from small to large reactor configurations, most likely related to differences in biological communities present within different reactor systems, tubing radii due to stretching, or tubing effective permeability.

The issues that were examined were:

- Kinetic parameters – the best fits of Monod kinetics to batch data were comparable to literature values with k ranging from 0.01-0.16 h^{-1} and K$_S$ ranging from 0.08-0.42 h^{-1}.

- Stagnant liquid conditions - stopping the circulating liquid flow in the reactors did not adversely affect toluene removal. Reactors might thus be operated with reduced power requirements for pumping.

- Nutrient limitation - Depleting the liquid nutrient solution of phosphorous and nitrogen did not adversely affect the operation of reactors with developed biofilms.

- Reactors operated in series provided more removal than those operated singly. Reactors might thus be operated together to improve removal of contaminants.

- Heat transfer - increased temperature operation did not improve bioreactor performance; removals were the same for unheated and heated reactor systems. Heat transfer coefficients were found to range from 2.9-17.4 W m^{-2} K^{-1}.

- Diurnal loading – no significant differences in 1-butanol removal were found when reactors were operated under diurnal loading conditions. The short periods of starvation did not adversely affect operation.

CHAPTER 6
MODELING RESULTS

6.1 OVERVIEW:

The model equations developed and the actual model demonstration runs performed during this study were completed to determine what is actually occurring within the different areas of the bioreactor system (such as the biofilm) and to assist in the design process of larger membrane bioreactor systems. To accomplish these goals, a specific analysis process was undertaken. Actual vs. predicted removals in several reactor systems were evaluated, and results discussed with regards to what is known about the bioreactor systems and what is not known. The following are the specific areas covered by the modeling results chapter:

6.2 Examination of actual removal compared to predicted removal in several bioreactor systems and under a variety of operating conditions.

6.3 Overall discussion of modeling results with specific emphasis on the initial model assumptions.

6.4 Discussion of experimental results with regard to the model presented.

6.5 Overall model performance.

Certain points concerning the model development are critical to understanding the model outcomes and bear repeating here. The single tube model was developed to predict the removal of a chemical contaminant (in this study toluene) from a waste gas stream. The main premise of the model, as presented in Chapter 4, is to predict the removal in any one axial segment along the length of the reactor by matching the mass flow across the membrane to the removal of that contaminant as a result of microbial

activity in the biofilm and the suspension. By predicting the removal in each axial segment sequentially down the vertical axis, a final effluent gas concentration may be determined. The model involves using a measured liquid concentration of substrate to represent the substrate concentration at the edge of the biofilm, calculation of the biofilm concentration profile from the liquid side inwards towards the membrane with a subsequent calculation of the mass flow across the membrane and then comparison of that mass flow with substrate removal/degradation. Only the single Monod kinetics equation was used, instead of the dual Monod equation, because oxygen was determined not to be a rate limiting substrate for the bioreactor systems used during this study.

6.2 EXAMINATION OF ACTUAL VS. PREDICTED REMOVAL:

After the model had been calibrated and validated, several model runs were completed to show the relative effect of parameter changes related to design. These model runs were similar to those accomplished during the sensitivity analysis (Chapter 4). The word "relative" is used as the liquid concentration value, necessary to perform the predictions, does vary during different model runs. That is, one must *assume* a liquid concentration of substrate in the liquid suspension to start the model run. The parameters changed during these model runs were associated with possible design changes and different configurations. For example, the effect of changes in tubing size, number of tubes, air flow, and changes in the Henry's Law coefficient were examined. The analysis was completed to determine if the model can be applied to different situations and to determine what affect design changes make on the system. The following model runs were made using the dual tube model, rather than the single tube model.

6.2.1 Changes in the Henry's Law Coefficient and Permeability: Changes in the Henry's Law coefficient might be anticipated if new chemical compounds are used in the experimental bioreactor system. A brief listing of Henry's Law coefficients is shown in Table 6-1. Additionally, Henry's Law has a strong temperature dependence; organics are less volatile at lower temperatures (Sawyer et al, 1994). Model predictions with changes in the Henry's Law coefficient are shown in Figures 6-1 and 6-2. Increases in the Henry's Law constants led to decreases in predicted biofilm thicknesses and decreases in contaminant removal from the air; the contaminant is less likely to partition into the liquid phase. Although the graph is not shown, decreases in permeability that might be associated with changes in contaminants supplied to the bioreactor were also shown to decrease predicted removal in the system. Again, decreases in permeability increase the resistance to mass transfer.

Table 6-1. Some selected chemicals and their Henry's Law constants[1].

Chemical	H Constant (Dimensionless)	Temperature (°C)
Vinyl Chloride	100	20
Toluene	0.275	20
Napthalene	0.019	20
Phenol	$(1.9)(10^{-5})$	20

[1]Adapted from Sawyer et al (1994), page 266-268. Henry's Law constants divided by the universal gas constant multiplied by the temperature (RT) at 20 °C to determine the dimensionless values.
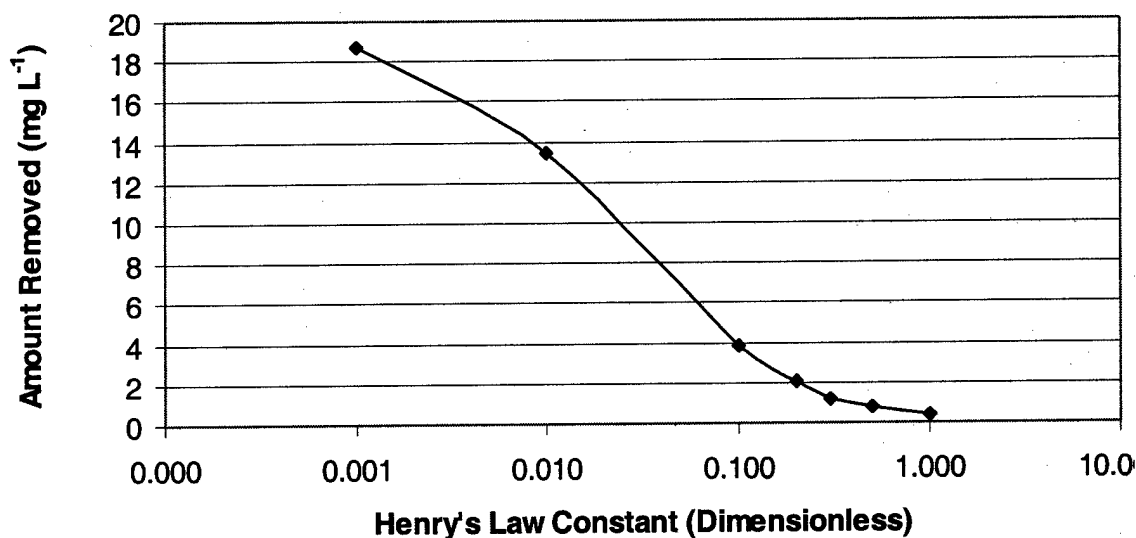
Figure 6-1. Predicted contaminant removal with changes in the Henry's Law coefficient. As Henry's Law Constants increase, removal of toluene from the air decreased.
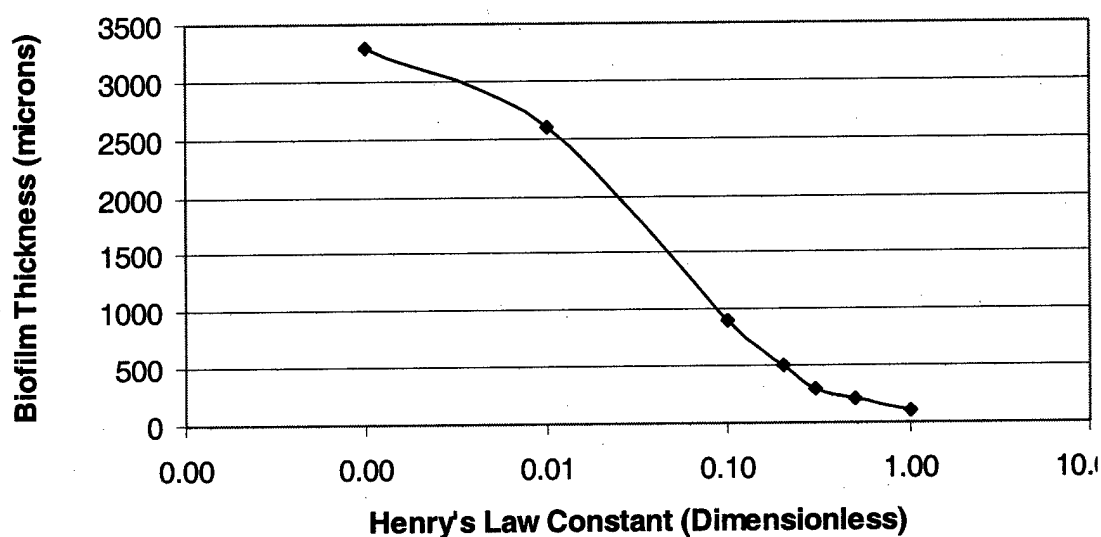
Figure 6-2. Predicted biofilm thicknesses with changes in the Henry's Law constant. As Henry's Law Constants increased, predicted biofilm thicknesses decreased.

6.2.2 Changes in Air Flow: The effect of changes in air flow was also examined for the dual tube system, keeping all other parameters constant. Increases in air flow led to decreases in the predicted removal of toluene from the air, as shown in Figure 6-3. This change could be anticipated when the equation for removal in each cell, Equation (6-1), is

examined. As air flow increases, that value (Q) begins to dominate the equation, leading the value for C_{out} closer to C_{in}. Predicted biofilm thicknesses remained between 300-400 microns for the values of air flow used in the model.

$$C_{out} = \frac{(C_{in} * Q_{air}) - (\sum_{r=r_o}^{r=rb} r_{su} V_{cell} + r_{su} V_{suspension})}{Q_{air}}$$ (6-1)
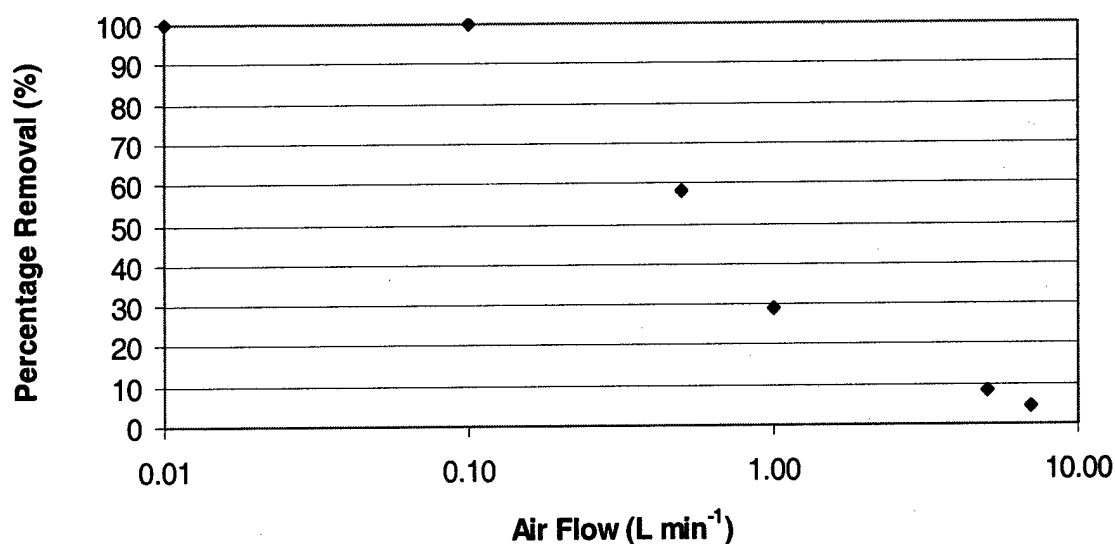
Figure 6-3. Predicted toluene removal from air with changes in air flow. As air flow through the reactor increased, removal of contaminant from air decreased.

6.2.3 Changes in Number of Tubes: To determine whether increasing the number of tubes and, therefore, the surface area available for mass transfer and biofilm growth, would affect the toluene removal or the biofilm thickness, the dual tube model was run and the number of tubes increased from 1-7. To complete this model run, again all constants remained unchanged except for the number of tubes contained within the

module volume. As seen in Figure 6-4, predicted removal increased as the number of

tubes increased.
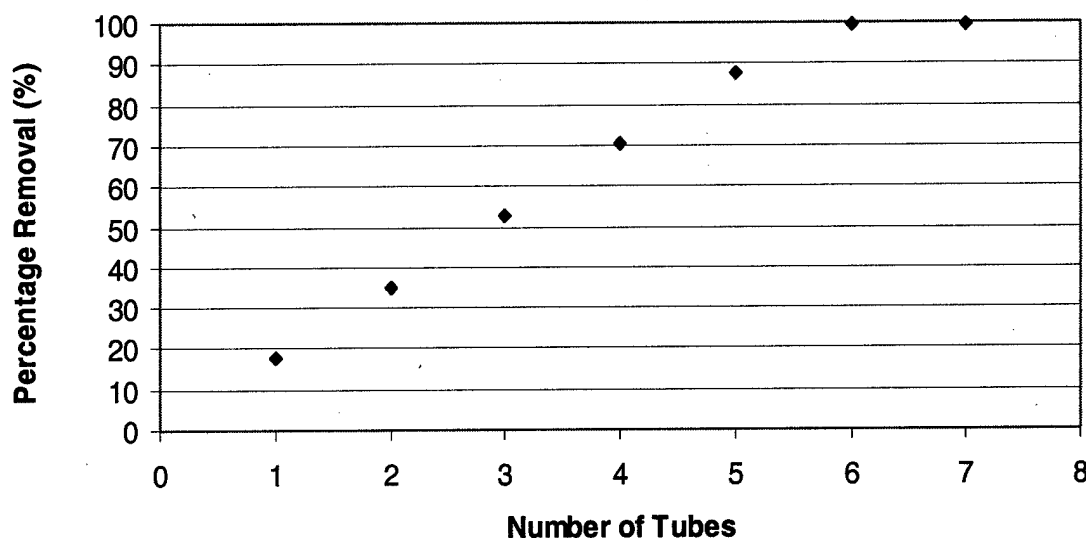
Figure 6-4. Predicted removal from air with changes in the number of tubes within a
particular reactor volume for the same flow rate of air, and same toluene load. Increases
in tube number resulted in increases in removal.

6.2.4 Changes in Tube Diameters and Thickness: The effect of changing the tube

inner and outer diameters was examined. When the outer diameter of the tube was kept

constant, and the thickness of the tube increased by decreasing the inner diameter of the

tubes, removal decreased, which is explained by increases in the mass transfer resistance

caused by the increase in tube thickness. When the outer tube diameter was decreased,

the removal increased as shown in Figure 6-5. The increase in removal was seen due to

the associated decreased mass transfer resistance of the membrane with the decrease in

thickness. Tube thicknesses used were estimates of possible silicone tube thicknesses,

however, it is unknown how thin a silicone tube might be manufactured.

Predicted removal of toluene was increased by decreases in the Henry's Law

Constant, decreases in air flow, and decreases in the tubing thickness. Based upon this

optimization analysis, the silicone tubing membrane bioreactor system appears to be best suited for compounds with lower Henry's Law constants, those with a high permeability in silicone, and those that are easily degraded by microorganisms. Additionally, the removal may be maximized by increasing the number of tubes present, using the thinnest, structurally sound tubes possible, and minimizing the liquid suspension present.
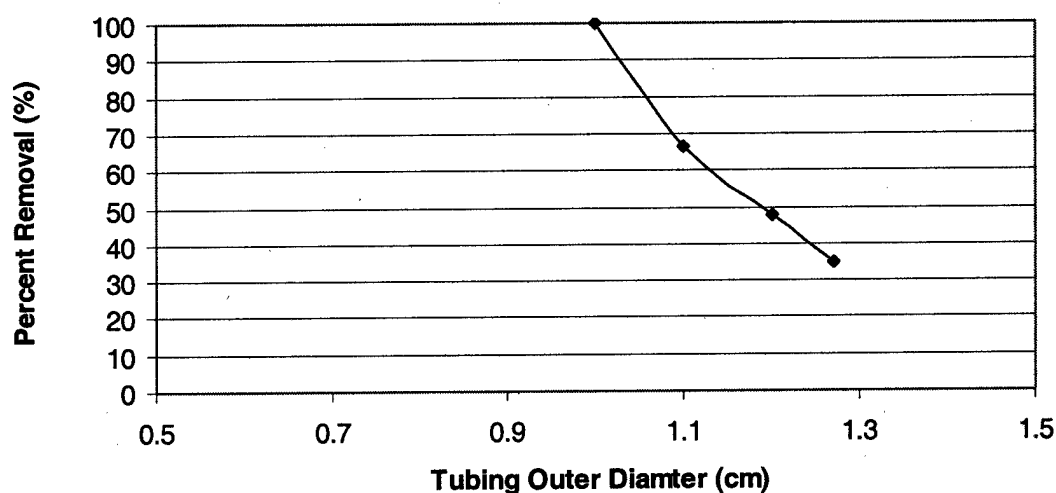
Figure 6-5. Predicted removal with changes in outer diameter of the tubing. As the outer diameter of the tube increased, effectively increasing tube thickness, predicted removal of toluene from air decreased.

6.2.5 Actual vs. Predicted Results During Model Runs: The single tube and dual tube model trials are shown in Figures 6-6 and 6-7 and the semi-pilot-scale reactor experimental runs are shown in Figure 6-8. The effective permeability values used in the modeling exercise appear to be of importance to model predictions and were 0.003 cm^2 s^{-1} for the single tube reactor and 0.002 cm^2 s^{-1} for the dual and semi-pilot scale reactors. In both cases, the model both underpredicted and overpredicted, depending upon the experimental run. Figure 6-9 shows model runs with data from a silicone tubing reactor

removing benzene from air (Neemann, 1998). For this data set, virtually all experimental data points were overpredicted by the model. A summary comparison of all the reactor systems is shown in Figure 6-10. Actual values from the modeling exercises are reported in Appendix E. A representative model run and a pictorial representation of concentrations in the biofilm and the liquid suspension are also shown in Appendix E.
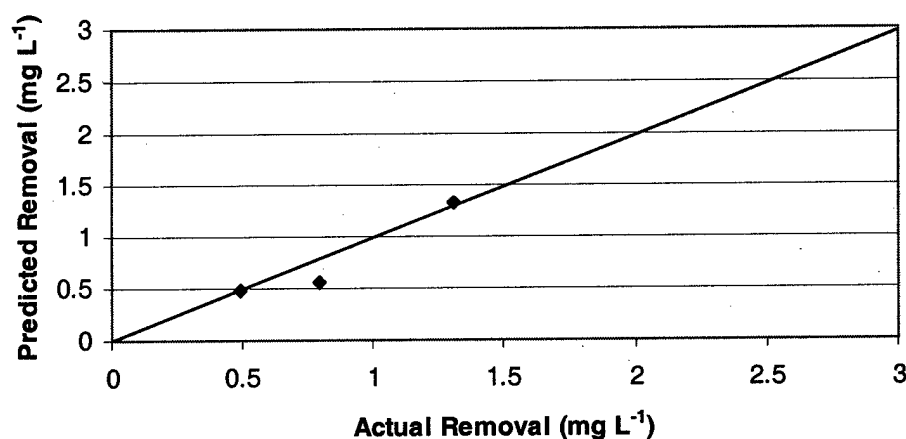
Figure 6-6. Actual vs. predicted removal in the single tube bioreactor. Actual removals matched closely the predicted removals.
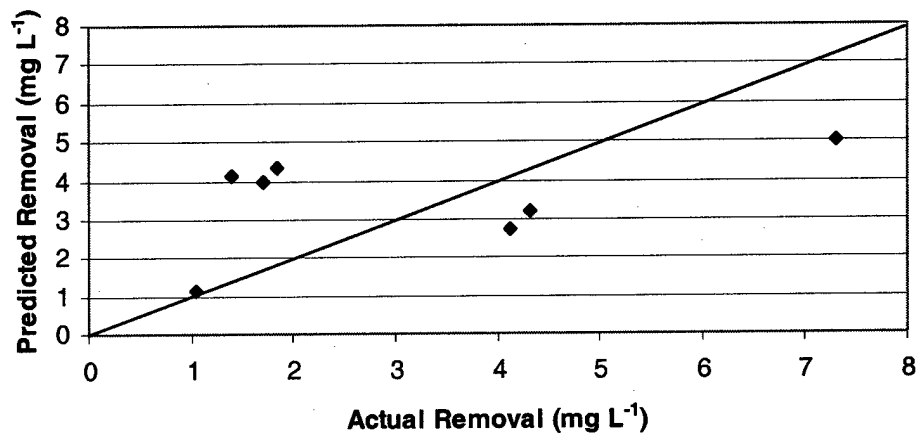
Figure 6-7. Actual vs. predicted removal in the dual tube bioreactor. Removals were both underpredicted and overpredicted in certain instances.

Semi-Pilot-Scale Bioreactor
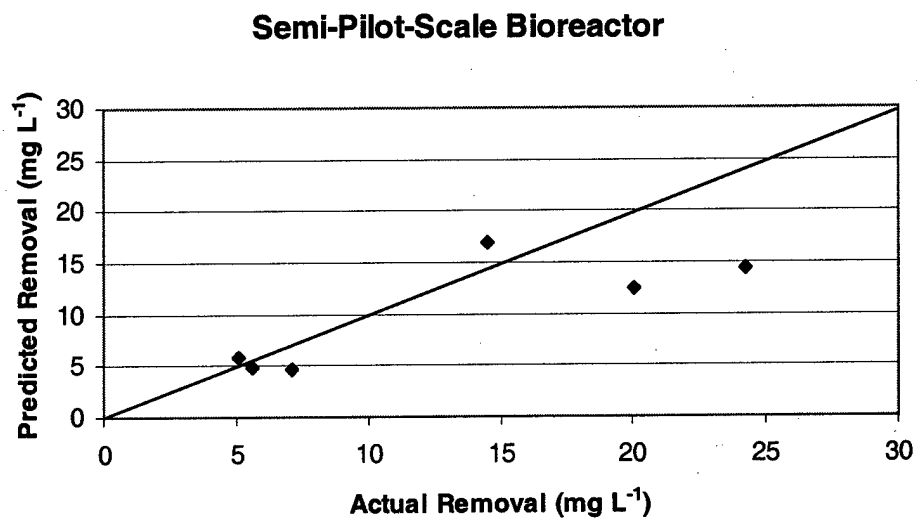
Figure 6-8. Actual vs. predicted removal in the semi-pilot-scale bioreactor. Removals were overpredicted by the model in several cases.
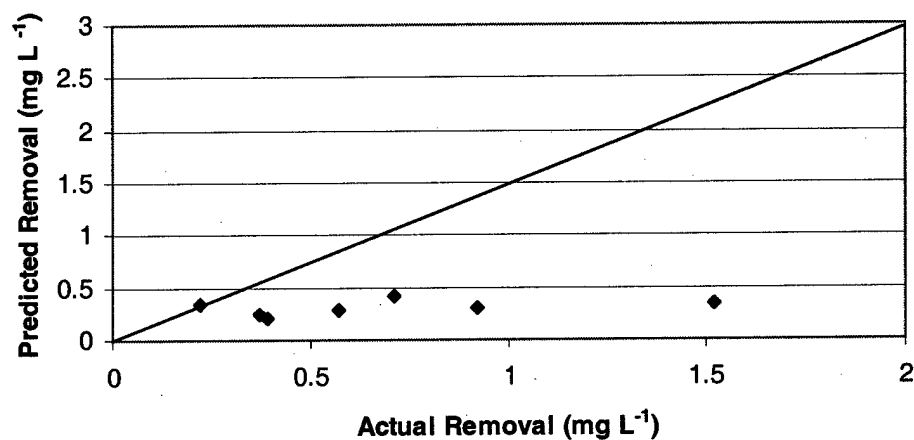
Figure 6-9. Predicted and actual results using Neemann (1999) data from removal of benzene in a silicone tubing bioreactor. Benzene removals were overpredicted by the model.
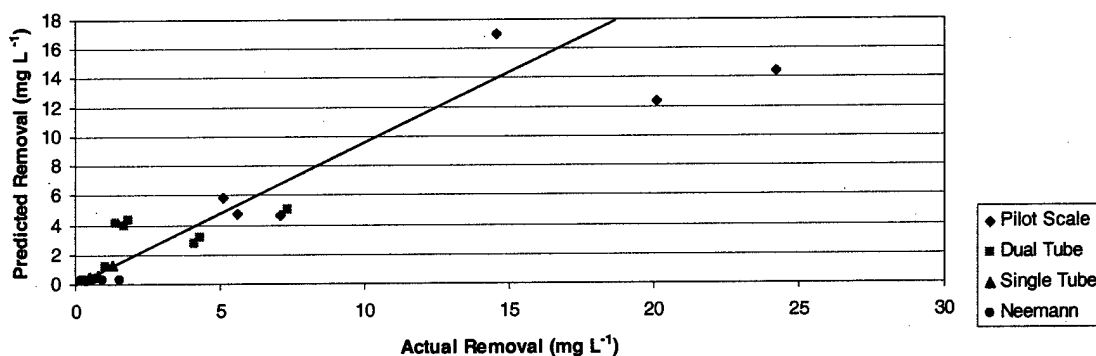
Figure 6-10. Comparison of actual and predicted removals in several biofilm systems.

6.2.6 Substrate Concentration Profile: Model-determined toluene concentration profiles through the biofilm for three reactor systems are shown in Figure 6-11. The figure is representative of the profiles seen during many model runs. The toluene concentration profiles through the biofilm were found to be very flat, increasing only slightly from liquid suspension to the edge of the silicone membrane tube. The flat toluene concentration profile, and in many cases the lack of complete degradation, implies a kinetic limitation within the biofilm. Thus, the reactor is limited by mass transfer across the membrane, and the biofilm is kinetically limited – diffusion is more rapid than the removal.

Figure 6-12 shows a concentration profile along the z axis of the bioreactor. The concentration profile was developed from the dual tube model. Predicted biofilm thickness is larger at the inlet than at the outlet of the reactor. The predicted biofilm thickness might also be interpreted as the active or effective biofilm thickness. The thicker biofilm at the inlet is most likely related to the larger toluene concentration present at the inlet, causing concentrations at the membrane to be higher, the result of

more mass being transferred across the membrane. Concentration profiles across the

entire reactor are shown in Figure 6-13.
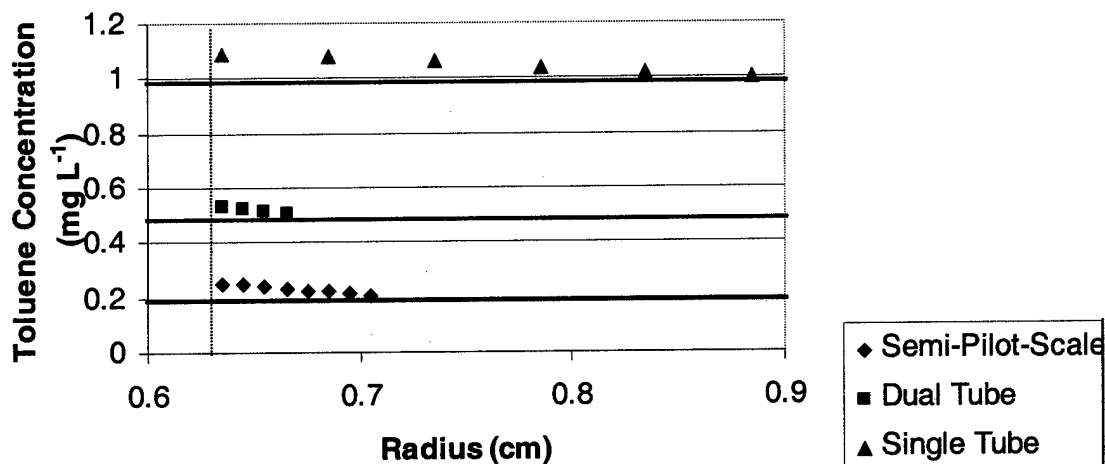
Figure 6-11. Predicted substrate concentration profile across the biofilm Dashed line indicates the tubing edge and bold lines indicate the liquid concentration for each respective bioreactor. Biofilm concentration profiles were flat across the biofilm.
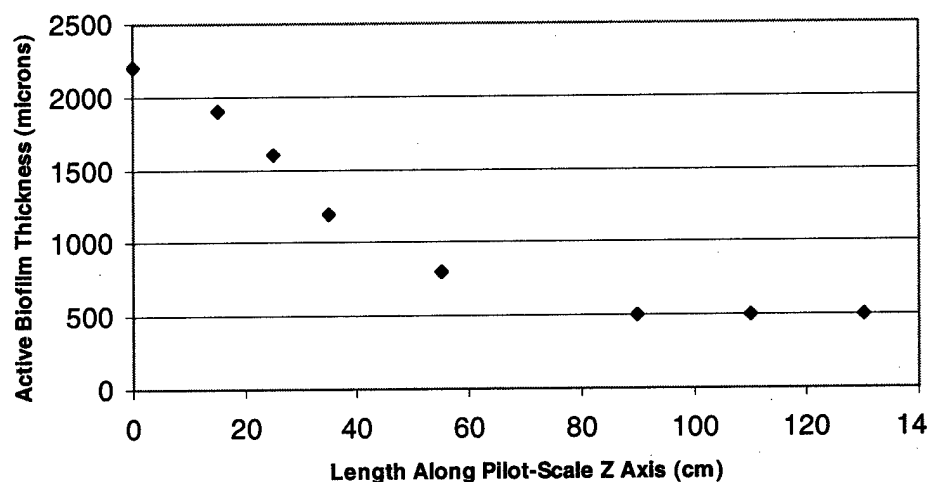
Figure 6-12. Predicted biofilm thickness along the z axis of the semi-pilot-scale biofilter. Predicted biofilm thickness is greatest at the influent end of the reactor and least at the effluent.
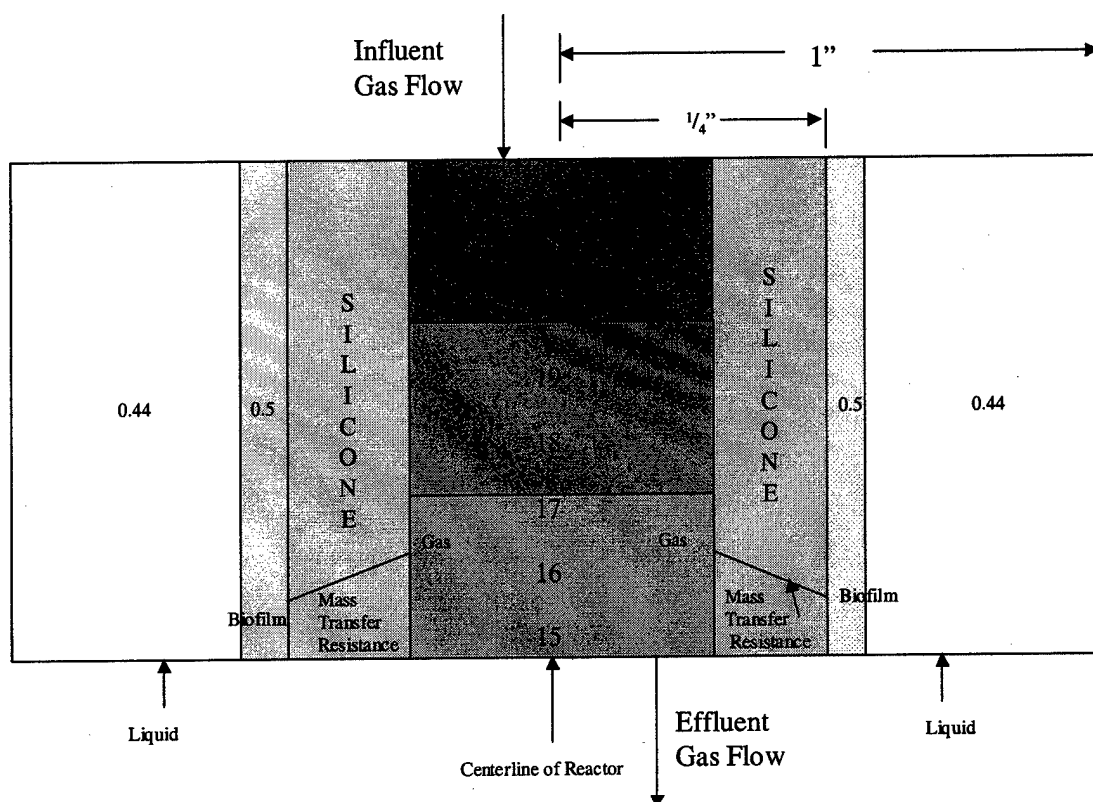
Figure 6-13. Toluene concentration profiles as calculated by the model for the semi-pilot-scale reactor, 5 Aug 02.

6.2.7 Overall Discussion of Actual vs. Predicted Results: The difference between the actual removals and the predicted removals were plotted against the air flow rates, the influent toluene concentrations and the load (Q*C). With the exception of one datum, a possible relationship between the magnitude of the model's underprediction and the influent concentration is suggested as shown in Figure 6-14. As the concentration increased, the magnitude of the difference between actual values observed and those predicted by the model increased. Perhaps the increase in toluene concentration is leading to an increase in the effective permeability of the silicone tube. Similar plots for the dual tube, single tube and Neemann's data (data and plots not shown) do not indicate

any clearer relationship. Additionally, when the dual tube data (Figure 6-7) is examined

on a time basis, the data from 2001 is underpredicted by the model while the data from

2002 is overpredicted. To explore why the model overpredicts in some cases and

underpredicts in others would take further experimentation with better control of influent

concentrations, flow rates, and monitoring toluene removal over time. Ideally one could

measure the influent/effluent gas concentrations and influent/effluent liquid

concentrations over time while changing other parameters such as air flow rates and

influent concentrations very precisely.
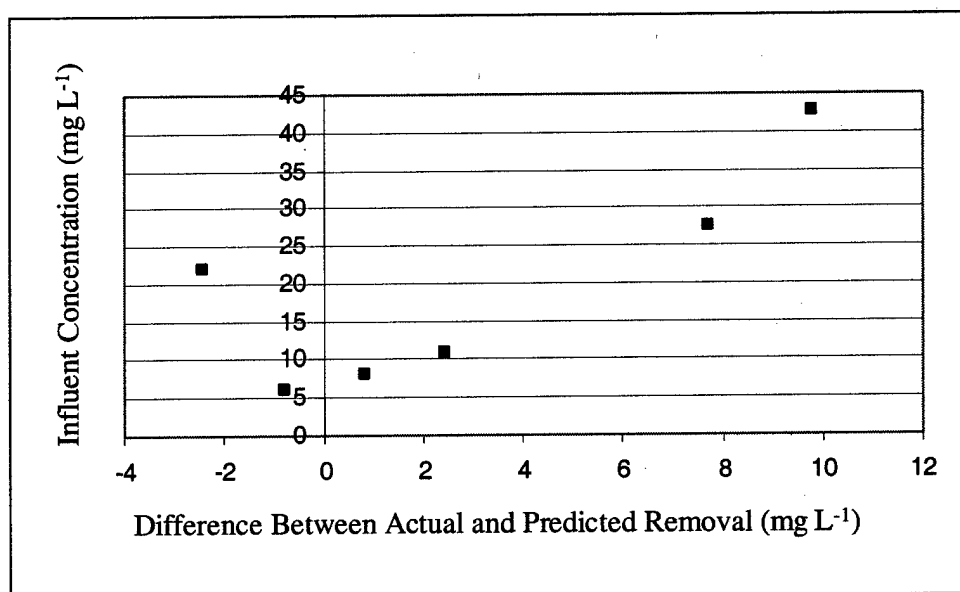
Figure 6-14. The difference between actual and predicted removal from the air phase for the semi-pilot-scale reactor, reported as equivalent liquid concentration, plotted against the influent toluene concentration to the bioreactor. Larger differences actual and predcited removals were seen with higher influent concentrations, with the exception of one data point.

Intuitively, removals in all operational reactors would be the same when

compared on a surface area basis (mg L^{-1} cm^2). However, Figures 5-24a and 5-24b do

not show this constant relationship. To determine what other factor might be contributing

to the differences in removal, numerous concentration versus removal plots were generated for operational reactors and are shown in Appendix G. The removal versus influent concentration graphs indicate removal generally increases with increasing influent concentration. However, removals between reactor systems are not consistent.

Modeling results are shown in Figure 6-15. Figure 6-15 was generated by examining all model runs and plotting influent concentration versus predicted toluene removal (mg L^{-1}) per silicone tubing unit area (cm^2). To develop the figure, at each axial segment, the influent concentration to that segment was recorded as was the removal in that segment (mg L^{-1} air/cm^2 of silicone surface area). Figure 6-15 suggests a relationship between influent concentration and removal for each bioreactor. In fact, predicted removals per unit surface area for each type of reactor are similar – as one would intuitively predict. Overall, more toluene is removed per cm^2 at higher concentrations delivered to an axial segment than at lower concentrations.
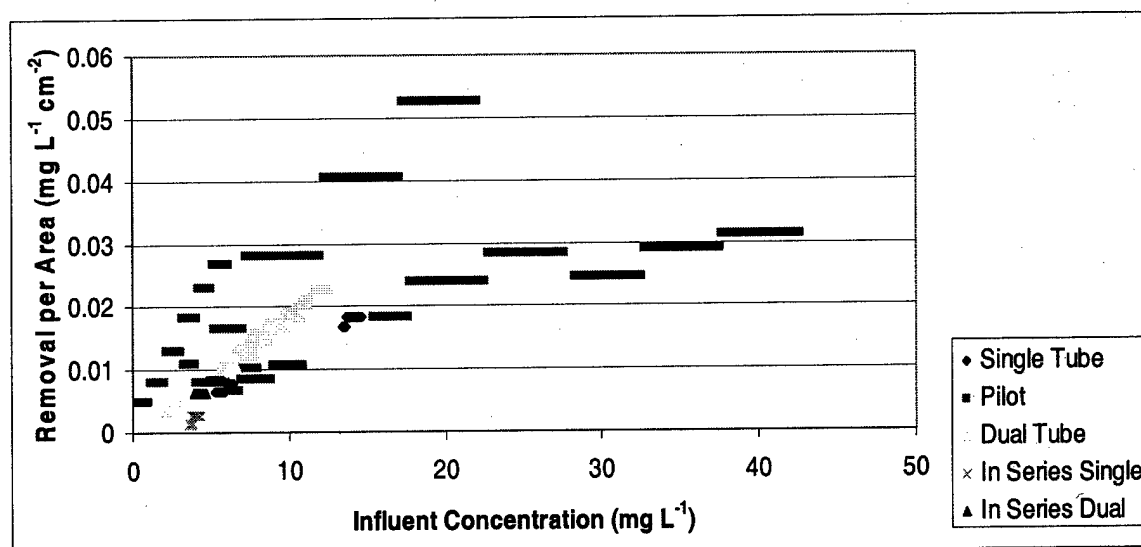
Figure 6-15. Influent concentration versus removal per unit area. Increased concentrations show increased removals.

However for the semi-pilot scale reactor there appears to be a range of values for each influent concentration. Several influent concentrations for the pilot scale reactor were examined and the results shown in Table 6-2 in an attempt to determine the cause. Higher airflows within the pilot scale reactor gave the lower removals.

Table 6-2. Comparison of airflow and removal.

Influent Concentration $(mg\ L^{-1})$	Date	Airflow $(L\ min^{-1})$	Removal $(mg\ L^{-1}\ cm^{-2})$	Length from top of tube (cm)
5	1 Aug 02	4	0.02	10
5	8 Aug02	14	0.007	79
10	5 Aug 02	7.7	0.03	73
10	6 Aug 02	20	0.01	20
20	5 Aug 02	7.7	0.05	10
20	2 Aug 02	18	0.02	71

The difference between predictions in the semi-pilot scale reactor suggests some other factor used in the model may have an influence. In particular, the liquid concentration used as the input parameter to the model may be suspect. Perhaps in some of the cases the pilot scale system had not reached equilibrium when the liquid concentration reading was taken. To determine whether the liquid concentration would make a difference, model results were examined. The original sensitivity analysis completed for the model showed that variations in liquid toluene concentrations over a possible range of $0.1 - 2\ mg\ L^{-1}$ could make a difference of about 25% in removal. This does not explain all of the variability seen in Figure 6-15, however, could explain some of the variation seen in the semi-pilot-scale reactor values.

Based upon the preceding analysis using both model and operational results, influent concentration does appear to influence removal. The greater the influent concentration, the greater the removal per unit surface area of silicon tubing. The most likely explanation for the removal differences seen during reactor operation are variations

in kinetics of each reactor system. Although each reactor system was inoculated with the same bacterial consortia, perhaps actual kinetic coefficients of the biofilm differed between the reactor systems. Actual measurement of kinetic coefficients *in situ* were not accomplished, therefore, the actual variability in kinetic coefficients between reactor systems is unknown. Of great importance, in each case examined, the model provided predictions of removal that matched well with removals actually observed for those reactor systems. The ability to accurately predict removal was the main goal of the modeling accomplished.

A calculation was completed to determine the impact upon toluene removal from inadvertent stretching of the silicone tubes during mounting in the reactor. In the case of the dual tube silicone membrane bioreactor, tubes were stretched approximately 4 inches during mounting. The stretching was discovered only after the bioreactor was disassembled. A representative diagram is shown in Figure 6-16.
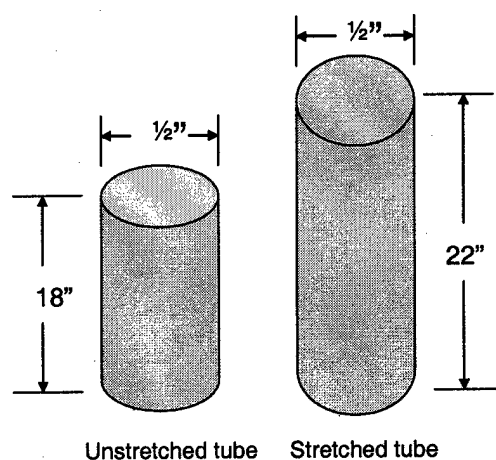
Figure 6-16. Diagram of stretched and unstretched tubes.

When tubes are stretched, the silicone volume remains constant, however, the inner and outer radii of the tubes, and therefore the thickness of the silicone membrane itself will be

changed. The initial conversion of tube length in inches to centimeters is shown in Equation (6-2) while the stretched tube conversion is shown in Equation (6-3).

$$l = (18 \text{ inches})*(2.54 \text{ cm inch}^{-1}) = 45.72 \text{ cm} \qquad (6\text{-}2)$$

$$l = (22 \text{ inches})*(2.54 \text{ cm inch}^{-1}) = 55.88 \text{ cm} \qquad (6\text{-}3)$$

The volume of the unstretched and stretched silicone tube is shown and calculated in Equations (6-4-6-6).

$$V = \pi(r_o^2 - r_i^2)l \qquad (6\text{-}4)$$

Where
V = volume of silicone
r_o = outer radius of tube
r_i = inner radius of tube
l = length of tube

$$V = \pi*(0.635^2 - 0.47625^2)*45.72 = 25.3 \text{ cm}^3 \qquad (6\text{-}5)$$

To actually calculate the outer radius and the thickness after tube stretching, the inner radius is assumed to be constant and Equation (5) solved for the value of the outer radius r_o which is determined to be 0.60922 cm.

$$V = \pi*(r_o^2 - 0.47625^2)*55.88 = 25.3 \text{ cm}^3 \qquad (6\text{-}6)$$

The new values of the outer radius were then used in the dual tube model developed for prediction of toluene removal. The results of model runs using the unstretched and stretched tubes are shown in Table 6-3. Stretching, with the associated reduction in tubing thickness, contributes to a small increase in removal of toluene from the air.

Table 6-3. Model predictions of unstretched and stretched tube removal of toluene.

	Predicted Toluene Removal	Predicted Toluene Removal

	Model Run, 2 Aug 02 (mg L^{-1})	Model Run, 5 Aug 02 (mg L^{-1})
Unstretched	3.97	4.15
Stretched	4.37	4.43
% Difference	10.1	6.71

6.3 OVERALL SUMMARY DISCUSSION OF MODEL RESULTS:

The possible reasons for the model underpredicting or overpredicting removal are numerous. Any one or any combination of the assumptions used for the model may not be valid in all instances or at any one point in time. A number of the assumptions and their potential impact on results will be discussed individually:

6.3.1 Steady State. The first assumption of the model was operation at steady state, in other words, no changes in concentration with time, ($\delta S/\delta t = 0$). In the systems operated during the study, influent concentrations were known to vary considerably without any adjustments to the system. Therefore, at any one sampling point in time, the influent concentration may have been changing or may have shown a higher concentration than moments before. However, liquid concentrations would not necessarily change instantaneously in response to those influent toluene concentrations. Therefore, the liquid concentration input into the model may not have corresponded exactly with the true influent concentration. This incongruity might account for the over prediction of removal in some cases and under prediction in others; the liquid concentration is the model boundary condition that sets the substrate concentration profile within the biofilm.

6.3.2 Permeability is concentration independent. The second assumption, that permeability is independent of concentration, may be false. Differences in permeabilities might be anticipated as the permeability of silicone may change with filler content and

may also change with concentration of the permeating compound. Swelling of rubber can cause an increase in rate of diffusion not only of the swelling agent itself, but also of any other molecule (Van Amerongen, 1967). A contrasting opinion is expressed by Sun and Chen (1994); who suggest that toluene and xylene tend to cluster in polydimethylsiloxane (PDMS) so that the mobility of each toluene or xylene molecule is reduced, and consequently the diffusion coefficient of each solvent in PDMS decreases with vapor activity or sorbed concentration. Support for changes in permeability with time is also found in Van Amerongen (1967). Oxidation of rubber generally has a considerable decreasing effect on diffusivity and permeability, not only for oxygen but for all foreign molecules (Van Amerongen, 1967). An experimental observation in the work reported here indicated that changes in the tubing may, in fact, be occurring. When high concentrations of toluene were passed through the reactor (usually accidentally while trying to adjust influent concentrations) the reactor tubing stretched. Tubing went from taut, straight tubes to loose tubes that actually slumped enough to touch one another. After resuming a more normal concentration of several hundred ppm, the tubing shrunk again to its original size.

For the case of multi-component gas streams, when applying the model to other circumstances, changes in permeability might again have to be considered. Generally, the presence of one component in the membrane will affect the sorption and diffusion properties of the other components in the membrane through interactions such as plasticizing effects on the membrane, clustering of one or more penetrants, hydrogen bonding effects, and mutual interaction between the penetrants and the membrane (Smart et al, 1998).

6.3.3 CSTR behavior. The eighth assumption, that the liquid suspension is completely mixed, is also most likely not true at the flow rates used in these studies. Flow rates for the bench scale reactors were in the range of 10 mL min^{-1}, making velocities in the liquid very low. Diffusion from the biofilm into the liquid likely dominated the reactors, rather than convection. For example, Reynolds numbers for the liquid flows used during the experiments were very low (<100), indicating a laminar flow. Laminar flow would suggest a thick liquid film.. By assuming a completely mixed reactor with a liquid concentration equal to that at the effluent liquid side of the reactors, true concentrations at the biofilm/liquid interface may have been either underestimated or overestimated.

6.3.4 Constant kinetic parameters. The eleventh assumption, that kinetic parameters remain constant for each reactor system and over time, may also be false. Additionally, the wide range of kinetic parameters found during experimental testing suggests the possibility that any of the actual kinetic parameters may be different from the input values actually used.

Several research studies have indicated that cells may be actively growing and reproducing in one area of the biofilm while being either in a maintenance state or completely inactive in other parts of the biofilm. Reij et al (1993) examined protein content of biofilms at day 6 and at day 13 and found cells were less active at day 13 than at day 6, indicating growth at the membrane and cell death at the liquid side had occurred. Zhang and Bishop (1994a) found that at bottom layers of a biofilm only 1/4 to 1/7 of living bacteria were metabolically active; other living biomass could be dormant cells, and about 2/3 of the total biomass was inert while the living bacteria [exposed to oxygen] may essentially all be metabolically active. In another study, active biomass

represented only 8% of total biomass of the biofilm (Auria et al, 2000). Biofilms were found to switch from a highly active log growth phase to a low activity stationary (maintenance) phase as nutrients are depleted (Mysliwiec et al, 2001). Measuring the carbon balance of a silicone membrane system, Freitos dos Santos et al (1995) found evidence of steady-state growth and decay, not simply growth. Under steady state conditions, the biomass is in a "maintenance state"; the microorganisms use the pollutants as an energy source to be able to survive and to grow at a rate which compensates for the death of cells (Dirk-Faitakis and Allen, 2000). With mature biofilms where growth is minimal, the vast majority of component bacteria are in a non-dividing state (stationary phase) where growth, but not activity, has ceased (Rishell and Hamer 2000).

6.3.3 Constant biomass density. Assumption thirteen concerns the biomass density being constant throughout the system. This assumption is, undoubtedly, false. However, it must be made, at least initially to allow modeling of the systems. Zhang and Bishop (1994b) showed direct experimental evidence indicating the stratified structure of biofilms, which conflicts with the a priori assumption of many biofilm models, i.e. a uniform distribution of the particular components (Zhang and Bishop, 1994b). Density may also be dependent on the bacterial species present ; it has been suggested that biofilm density could increase with C/N ratio (Freitas dos Santos and Livingston, 1995a). Surface-averaged biomass density has been shown to depended on liquid flow velocity at which the biofilms were grown (Beyenal et al, 1998). Higher velocities gave denser biofilms.

6.3.3 Biofilm activity. Assumption eighteen is that all or a significant part of the biofilm are active. Perhaps there is only a small, very dense, fraction of the biofilm removing the

toluene. To appropriately determine what is happening within each small area of the biofilm, extensive probing, sectioning, and monitoring of the biofilm would be necessary. An experimental observation supports the possibility of biofilm density changes and variation. After major sloughing events - such as when liquid drained from the reactor, the biofilm did not reattach to the tubing as readily. It also was visually very much less dense than the originally formed biofilm.

6.3.3 Even air flow. Assumption sixteen also may not be true in all cases. For each of the different systems modeled, the airflow entered the reactor in a different manner. In the single tube reactors, air flow entered directly into the tube, in the dual tube reactor, airflow was split and then entered directly into each tube and in the semi-pilot-scale reactor, air essentially entered a plenum before entering the tubes. Perhaps the airflow was turbulent in some of these cases or perhaps the airflow did not even enter certain tubes equally.

6.4 DISCUSSION OF EXPERIMENTAL RESULTS AS RELATED TO THE MODEL:

To link experimental results as described in Chapter 6 to the modeling results the following discussion is included.

6.4.1 High Temperature Operation: Experimental results indicated that there was no improvement in toluene removal when the reactor liquid was heated. Prior to the experiment, it was hypothesized that there would be an improvement in removal, as the reaction rate of microorganisms doubles for each 10 $^\circ$C increase in temperature (Characklis and Marshall, 1990). Additionally, depending on the type of rubber and gas, the diffusion coefficient increases by a factor of 1.2 to about 3 for every 10 $^\circ$C

temperature rise in the region between about 10 - 60 °C (Van Amerongen, 1967). The apparent difference between what was observed and what was hypothesized before the experiment might be due to the decrease in solubility of most gases in rubber associated with increasing temperature. As the solubility of many gases decreases on increase of temperature, it often occurs that this effect predominates over the increase in diffusivity with increasing temperature so that the permeability decreases as temperature increases (Van Amerongen, 1967). Increases in the Henry's Law coefficient with increased temperature may also have contributed to the lack of effect.

6.4.2 Nutrient Limitation: As will be presented later, lack of nutrients apparently had no effect on the removal of toluene within operational membrane bioreactors. Had nutrient limitation affected the operation of the bioreactors, the proposed model would not explicitly account for such effect, but those changes could be modeled by the inclusion of changes in the biofilm and suspension kinetic parameters. Since there was no change in removal with nutrient limitation, kinetics of the system may not have changed substantially, suggesting that nutrients are cycling within the biofilm or are otherwise available for use by the microorganisms.

6.4.3 Stagnant Liquid Conditions: As will be shown subsequently, stopping the flow to the membrane bioreactors had no effect on toluene removal efficiency. Stagnant flow conditions could be modeled by applying the continuity of mass equation in cylindrical coordinates, Equation (6-7), to the suspension, in addition to the biofilm.

$$\frac{\partial S}{\partial t} + \left[V_r \frac{\partial S}{\partial r} + V_\theta \frac{1}{r}\frac{\partial S}{\partial \theta} + V_z \frac{\partial S}{\partial z} \right] = D_s \left(\frac{1}{r}\frac{\partial}{\partial r}\left(r\frac{\partial S}{\partial r} \right) + \frac{1}{r^2}\frac{\partial^2 S}{\partial \theta^2} + \frac{\partial^2 S}{\partial z^2} \right) + R_s \qquad (6\text{-}7)$$

For one model run, such a stagnant profile was included, yielding the results shown in Figure 6-17. The results of this steady-state model run show that, as in the biofilm, the substrate concentration profile is fairly flat. The results of the profile may only be used as an estimate of the concentration profile, as no experimental liquid concentration measurement was actually taken at the very edge of the reactor module. Therefore, the liquid concentration value from the outlet was used as the concentration at the edge of the biofilm, and the removal associated with the liquid volume was set equal to that seen during one flow experiment. The profile was then generated.
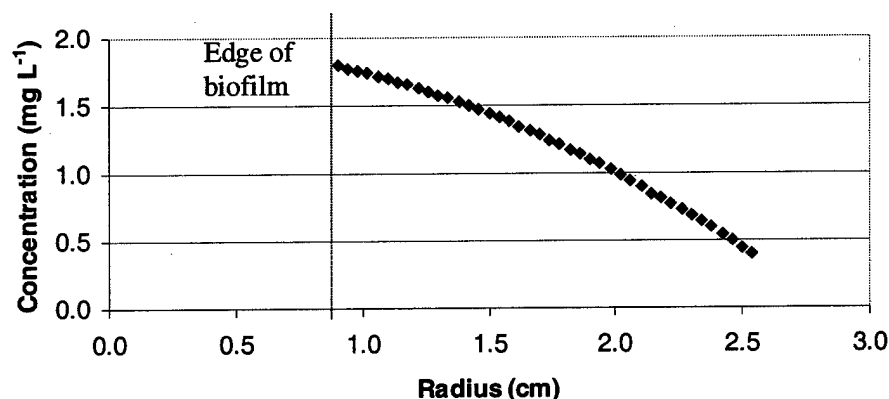
Figure 6-17. Predcited concentration gradient within the liquid suspension. Liquid concentrations are highest near the biofilm and lowest at the reactor module edge.

6.4.4 In Series Operation: As will be seen in a subsequent chapter, reactors placed "in-series" with one another are able to remove additional toluene than a single reactor. To determine how closely the model could predict removal for the in-series system, two model runs were accomplished. The results of the model runs versus the actual removal seen within the bioreactors are shown in Figure 6-18. Actual and predicted removals were very close.

Figure 6-19. Predicted oxygen and toluene concentration profile across the biofilm. In this example, oxygen is shown to be depleted before toluene.

6.5 OVERALL MODEL PERFORMANCE:

The model performs reasonably well at predicting effluent toluene concentrations in single and multiple tube membrane bioreactors. Over-prediction in design is a more serious issue for environmental releases than underprediction and the model tends to underpredict more often then overpredict. The underpredictions and overpredictions may be related to the ability to input precise and accurate parameter values into the model, or may be related to the model assumptions. With the plethora of input parameters, error, and the propagation of that error, must be considered as a possible cause of the discrepancy between predicted and actual removals.

However, it would appear that model performance is probably related to changes in the permeability of the membrane material with concentration. Instead of supplying only a constant value for a chemical's permeability in the membrane material, a set of

differential equations relating the change in permeability with concentration might be used and result in improved prediction.

CHAPTER 7
CONCLUSIONS

7.1 CONCLUSIONS:

The purpose of this research was to study the operation of membrane bioreactors (most using silicone rubber tubing) used to treat toluene-contaminated air under a variety of operating conditions. The experiments described in the previous chapters focused on scale-up of the bioreactor systems, stagnant flow conditions, nutrient limitation, and diurnal loading. A polyporous membrane system was used to remove butanol from the air and heat transfer coefficients were calculated for three membrane system configurations. A computer model was developed to compare with the experimental data, to explain what is happening within the system, to predict future performance of the system and optimize design. Studies were completed by running systems abiotically to measure mass transfer coefficients and then inoculated with a culture of toluene-degrading bacteria. Readings were taken every weekday to measure inlet and outlet concentrations of toluene.

To properly conclude the study, a restatement of the objectives and a determination of whether they were met is also in order. The objectives of the research included the following:

(1) Investigate the scale-up of silicone membrane bioreactors from single, through dual and to multiple tubes by monitoring air contaminant removal and developing loading curves for each type of reactor system.

(2) Manufacture a semi-pilot-scale multiple tube reactor system for air treatment.

(3) Construct, calibrate, and validate a computer model to predict removal in single and multiple tube silicone membrane bioreactors.

(4) Use the model to optimize design of silicone tubing membrane bioreactors and apply the model to other similar systems, i.e. benzene removal using silicone tubing bioreactors.

(5) Examine the operation of single and multiple silicone tube bioreactors under a variety of operating conditions that reflect potential operating or desired operating conditions including:

    (a) Stagnant liquid conditions in the module.

    (b) Nutrient limitation in the liquid suspension.

    (c) Heated liquid conditions.

    (d) In-series operation of membrane bioreactors.

    (e) Diurnal operation.

(6) Measure overall heat transfer coefficients for three membrane module configurations.

Each objective was obtained and the major conclusions for those experiments and future recommendations are summarized below.

Lab-scale and semi-pilot scale multiple tube bioreactors were successfully built and operated, however, the same removal for identical loads was not observed, indicating that removal does not scale within the reactor systems as shown in Section 6.7. The differences in toluene removal between reactors at similar toluene loadings may be related to differences in permeability of the silicone tubing or differences in the thickness of tubing, from differences in reactor construction. Differences in removal may also be related to differences in microorganisms or in microorganism communities contained within the various reactors.

The model developed to describe performance and predict future performance of membrane bioreactors under a variety of conditions was calibrated and validated for the conditions studied. In many instances the model tended to underestimate the removal of air contaminants. Underestimation was apparently related to changes in permeability of the silicone tubing with contaminant concentration, or possibly due to lack of a steady-state condition of the influent toluene concentration. If the assumption of the entire biofilm being active is correct, the presence or absence of oxygen appears to have no effect on the removal of toluene, and the presence of anaerobic toluene-degrading bacteria was verified. Therefore, the single substrate model applies, rather than the dual substrate model originally constructed for this work.

Based on the model runs and the experimental results, removal in the reactor is limited by mass transfer through the membrane; the way to maximize membrane reactor performance is to increase the number of tubes present, using the thinnest, structurally sound tubes possible, minimize the liquid suspension present, and mounting the tubes so they may be uniformly coated with a biofilm. For example, tubes might be mounted straight and taut, as in the semi-pilot-scale reactor, so biofilm may grow on the tube but not attached to the biofilm on an adjacent tube.

The liquid suspension appears to be of very little importance to the removal of toluene from the air phase. The circulation of the liquid suspension also appears to have no effect on the system's removal of toluene. Non-recirculating liquid systems showed the same removal as the recirculating systems. The vast majority of toluene degradation appears to take place within the biofilm.

Nutrient limitation of nitrogen and phosphorous in the liquid nutrient suspension appears to have no effect on toluene removal from air for operational membrane bioreactors over the relatively short operational periods monitored. This result implies that sufficient nutrients are contained within and are being recycled or reused within the biofilm once it is developed.

A reactor with a heated liquid suspension did not show improved removal for toluene. Heat transfer coefficients measured for three reactor configurations ranged from 2.9 to 17.4 $W \, m^{-2} \, K^{-1}$. The polysulfone module had overall lower heat transfer coefficients than the latex and silicone tubing reactor modules, most likely due to its increased membrane surface area. On the other hand, reactors operated in-series provided more removal than one reactor alone. This indicates more surface area may not only be obtained by placing more tubes in one reactor volume, but may be obtained by using more reactors linked together in series.

Diurnal loading of a polyporous membrane module removing butanol from the air had no overall detrimental effect on performance of the system. Removal of butanol from the air was slightly greater after periods of shut down, most likely related to depletion of n-butanol in the biofilm and liquid suspension by microorganism activity.

7.2 RECOMMENDATIONS FOR FUTURE RESEARCH:

Numerous questions remain unanswered and new questions were raised both during the research and as a result of the research. The questions emanate from two areas; the science of membrane bioreactors and the technology development of membrane bioreactors. For the systems studied here, at least these questions remain:

(1) Why does the biofilm appear to stop increasing in size and what portions of the biofilm are actually active - either growing or carrying out maintenance metabolism?

(2) What are the true densities and kinetic rate constants throughout the biofilm? Associated with the kinetic question, is there a section of the biofilm where the dual substrate model applies and where it does not?

(3) Why is the biofilm apparently kinetically limited and how can that kinetic limitation be overcome? Is there an inhibiting substance present that is causing the limitation or would buffering of the liquid suspension or periodic replacement of the liquid suspension improve the removal in the biofilm and the suspension?

(4) What are the true substrate and oxygen concentration profiles in the biofilm?

(5) What are the true mass transfer correlations for each reactor system design over the full range of possible liquid and gas flow rates?

(6) Would a change to co-current, instead of counter-current flow improve the performance?

(7) Could on-line measurement of both the influent and effluent gas streams of the reactor more effectively show the immediate response of the bioreactor to changes in influent concentrations?

With respect to technology development and optimization of the bioreactor systems the following questions need to be answered:

(1) What is the long term performance of these membrane bioreactor systems? Most current data shows only information from relatively short studies (days and weeks) rather than long studies of months or years. Over years of operation, biofilm changes, such as shifting populations, as well as tubing permeability changes might be anticipated, perhaps decreasing removal.

(2) How do large-scale systems perform under "real world" conditions where multiple VOCs may be present and influent contaminant concentrations fluctuate?

(3) How thin can a silicone tube be manufactured to have structural integrity while reducing the mass transfer resistance to a minimum? Could composite membranes improve removal?

(4) What is the smallest diameter of tubing that can be placed in a reactor module, so as to fill the module without causing significant pressure drop across the reactor?

(5) Would innoculation with a selected organism improve performance?

Each of these questions provide ample opportunity for future research.

7.3 OPERATIONAL RECOMMENDATIONS:

(1) PVC demonstrated its utility as a bioreactor module casing and is more rugged than glass. Clear PVC was also shown to be useful as it allowed the viewing of biofilm growth, however, it was unavailable in very large diameters and was moderately expensive in comparison to regular opaque PVC piping at the time of study.

(2) External standards prepared in bottles and headspace analysis vials used during degradation analyses should be allowed to equilibrate for one to two hours to avoid improper headspace and liquid readings.

(3) Because of the more appropriate use of the Student's t distribution and the highly variable influent air concentrations, six to ten readings are recommended for GC analysis during each sampling event.

(4) Toluene standards should be made daily (and the GC should be calibrated daily) - headspace bottles may leak overnight, even when inverted.

(5) A fungus (or dark-colored bacteria) appears to be of importance in the more permanent attachment of the biofilm to the silicone membrane.

(6) Check valves should be installed on future membrane bioreactor modules to prevent backflow and dumping of the system.

(7) Toluene concentrations varied in the influent most likely due to minute variations in the pumping rate and differences in the evaporation rate of toluene. In an attempt to control changes in influent concentrations, a serious source or error and frustration, mass flow controllers should be used. Alternatively, bench air should be used - the slight pressure associated with bench air yields more consistent airflow and concentrations in the small diameter tubing.

Appendix A
Permeability Experiments

Data for the abiotic permeability experiments using a long single silicone tube module to remove toluene is shown in Table A-1 and Figure A-1. Data for abiotic experiments using a short single latex tube module to remove benzene (Neemann, 1998) is shown in Table A-2 and Figure A-2. Formulae used for calculation of values are found in Equations (3-2) and (5-3) – (5-5). Mass closures were good, ranging from 79 – 99% for the toluene data and 85 – 96% for the benzene reactor.

Table A-1. Liquid flow data for abiotic toluene permeability experiment.

	A	8.85197		
	C2	311.4625		
	n	15.04775		
Q $mL\ min^{-1}$	Q $cm^3\ s^{-1}$	$1/K_{OV}$ $s\ cm^{-1}$	Calculated $s\ cm^{-1}$	Difference Squared
32.77	0.546167	1.32E+03	1.32E+03	2.51E-05
421.35	7.0225	5.46E+02	3.11E+02	54805.76
597.609	9.96015	7.74E+01	3.11E+02	54807.13
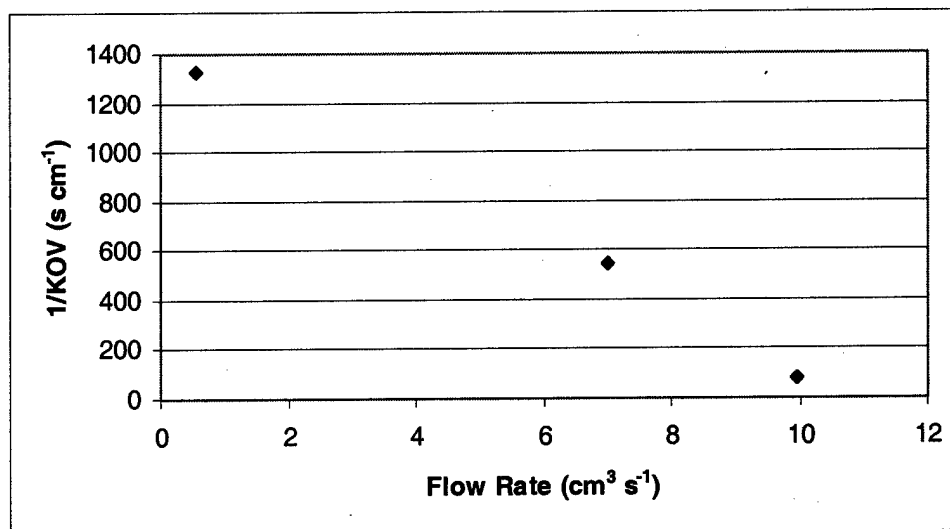
Figure A-1. Liquid flow data for abiotic toluene permeability experiment. As liquid flow rates increased, overall resistance to mass transfer decreased.

Table A-2. Liquid flow data for abiotic benzene experiments.

	A	700		
	C2	368.4583		
	n	0.453811		
Q	Q	$1/K_{OV}$ s cm^{-1}	Calculated s cm^{-1}	Difference Squared
mL min^{-1}	cm^3 s-1			
4.6	0.076667	4.57E+02	3.68E+02	7772.542
20.8	0.346667	2.77E+02	3.68E+02	8363.161
9.5	0.158333	3.72E+02	3.68E+02	10.81376
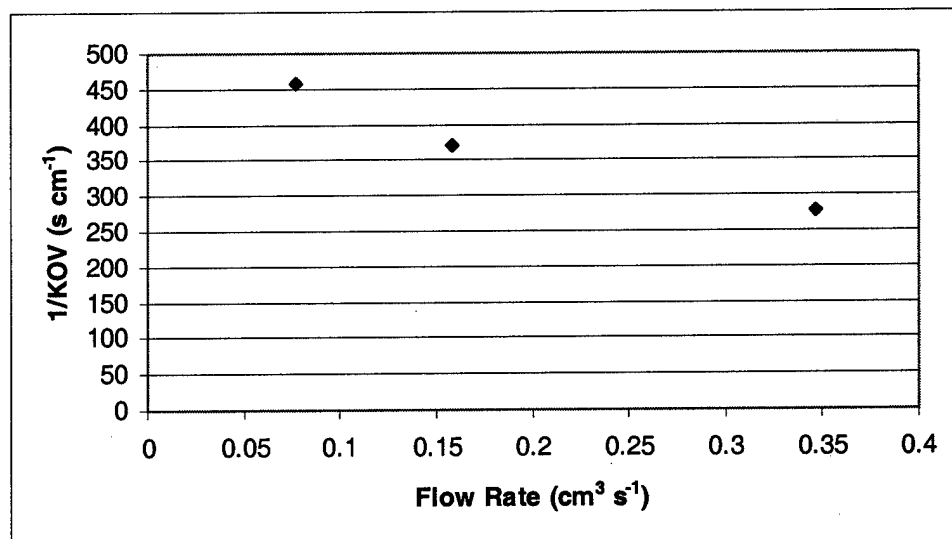
Figure A-2. Flow data for abiotic benzene experiments. As liquid flow rates increased, overall resistance to mass transfer decreased.

Appendix B
Kinetic Study Charts

The following figures show individual batch analyses of toluene degraders. The data was fit as described in Chapter 3. The data and fits are available in a file format recorded on a CD-ROM that is on deposit with Dr. Mark Fitch.
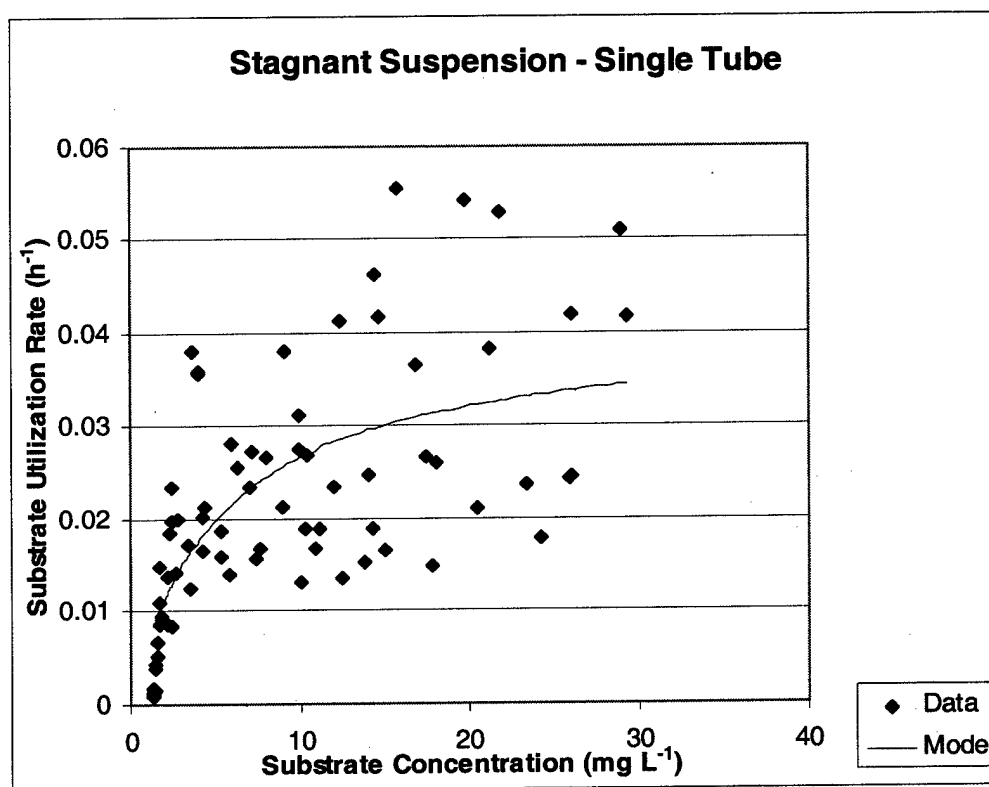
Figure B-1. Kinetic coefficients for single tube stagnant suspension, $K_S = 5.2$ mg L^{-1}, $k = 0.04$ h^{-1}.
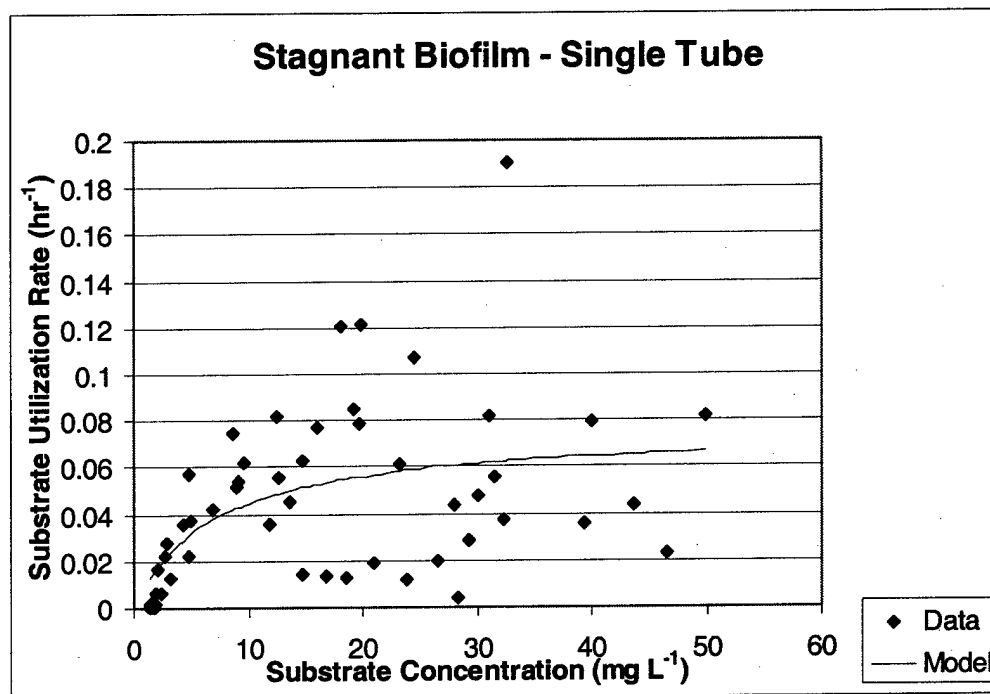
Figure B-2. Kinetic coefficients for single tube stagnant suspension, $K_S = 7.0$ mg L^{-1}, $k = 0.08$ h^{-1}.
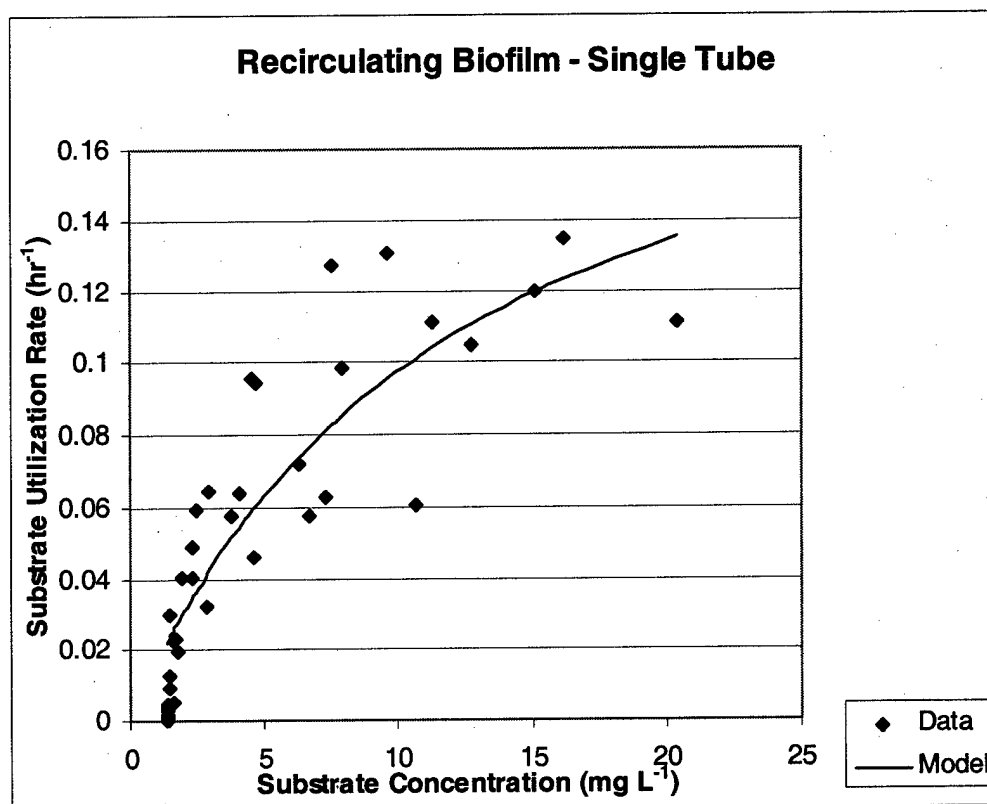
Figure B-3. Kinetic coefficients for single tube recirculating biofilm, K_S = 12.0 mg L^{-1}, k = 0.21 h^{-1}.
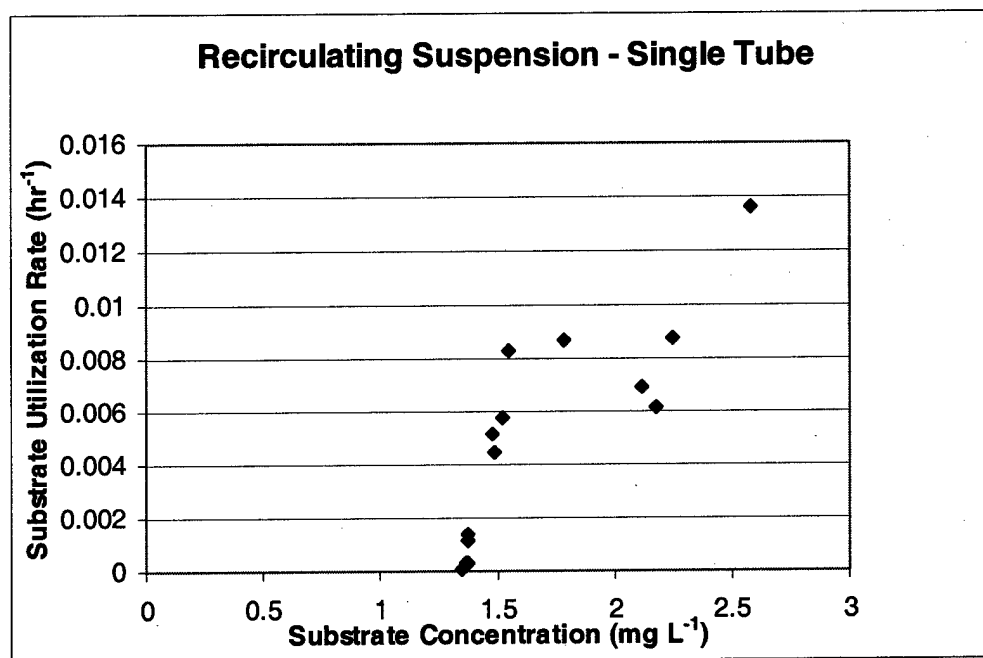
Figure B-4. Kinetic coefficients for single tube recirculating suspension, K_S = 1.5 mg L^{-1}, k = 0.01 h^{-1}.
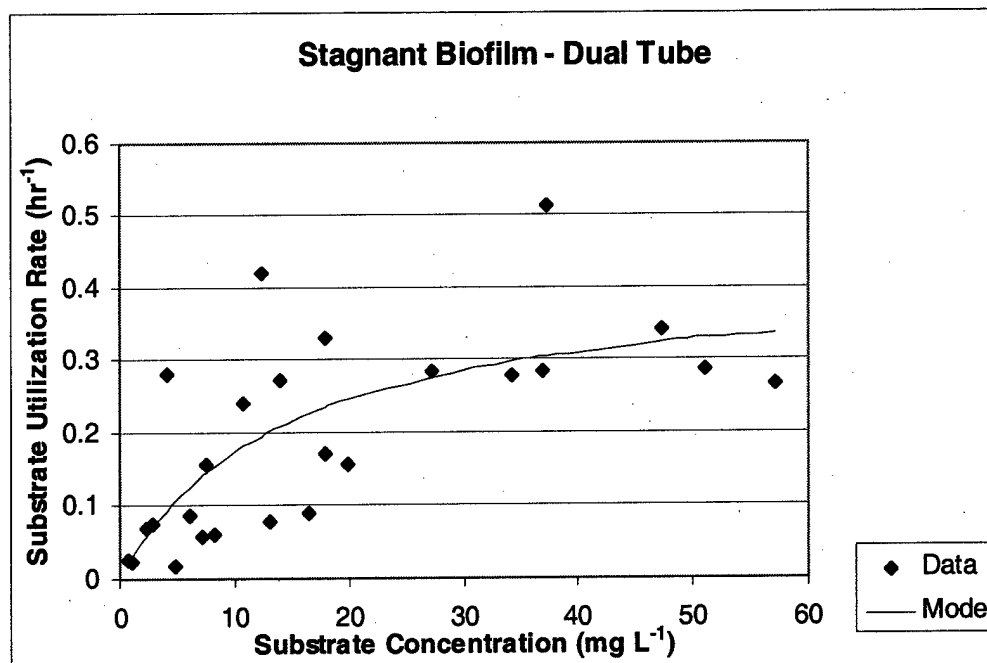
Figure B-5. Kinetic coefficients for the dual tube stagnant biofilm, $K_S = 14.3$ mg L^{-1}, k= 0.42 h^{-1}.
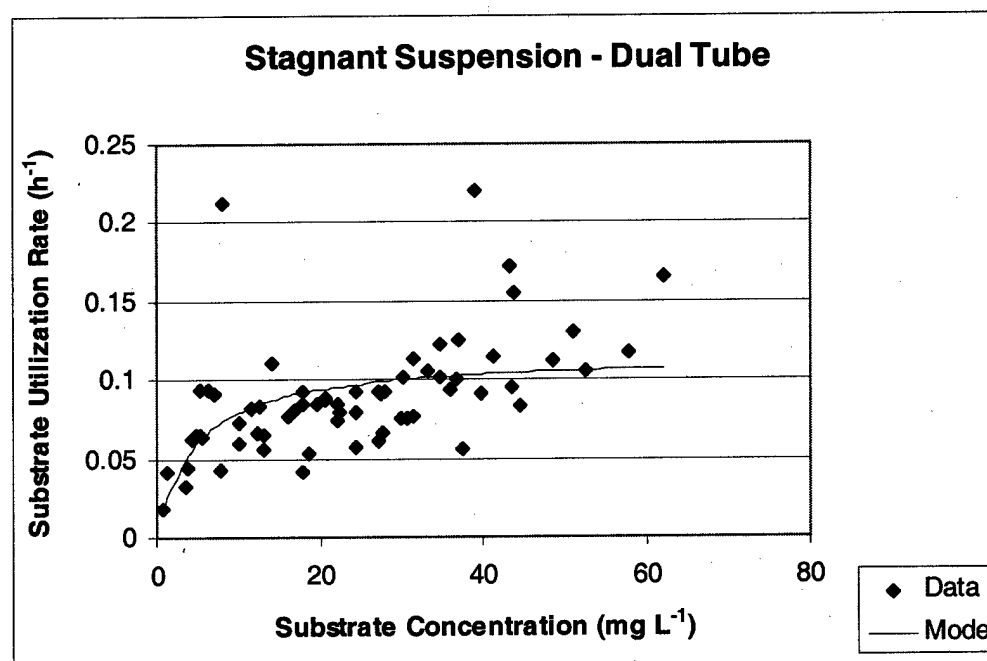
Figure B-6. Kinetic coefficients for the dual tube stagnant suspension, $K_S = 4.5$ mg L^{-1}, k = 0.11 h^{-1}.
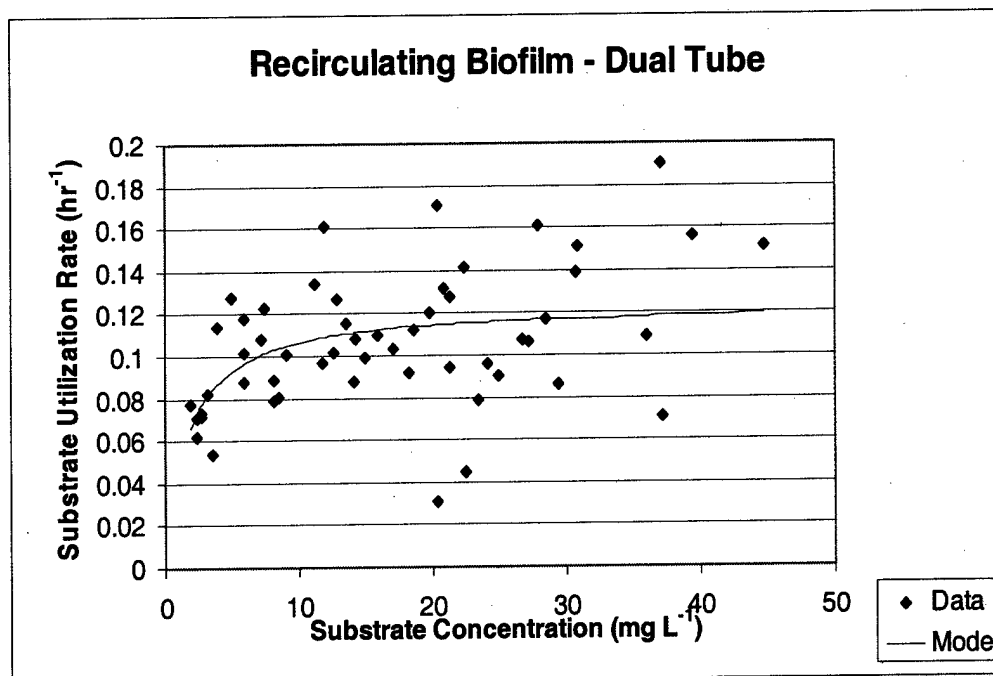
Figure B-7. Kinetic coefficients for the dual tube recirculating biofilm, $K_S = 1.6$ mg L^{-1}, $k = 0.12$ h^{-1}.
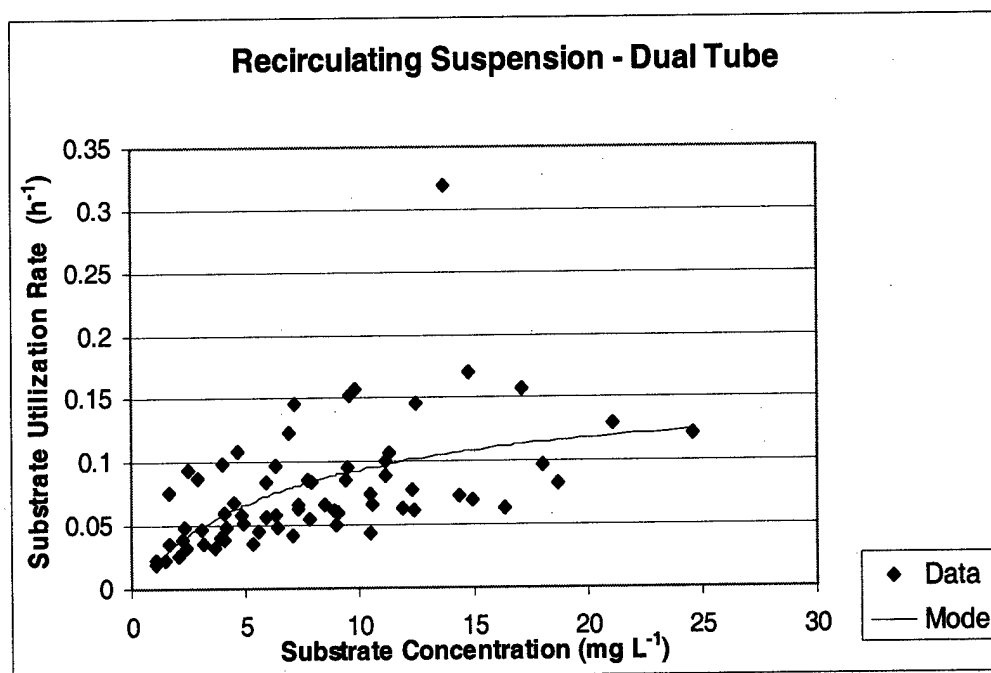
Figure B-8. Kinetic coefficients for the dual tube recirculating suspension, $K_S = 7.0$ mg

L^{-1}, k = 0.16 h^{-1}.
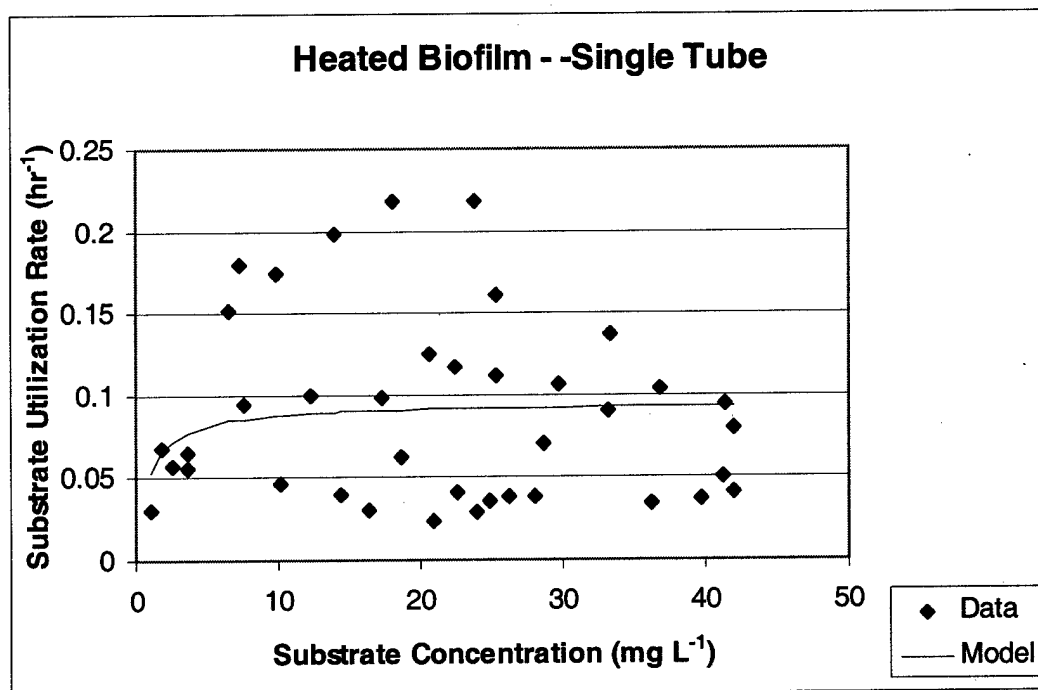
Figure B-9. Kinetic coefficients for the single tube heated biofilm, K_S = 0.79 mg L^{-1}, k = 0.09 h^{-1}.
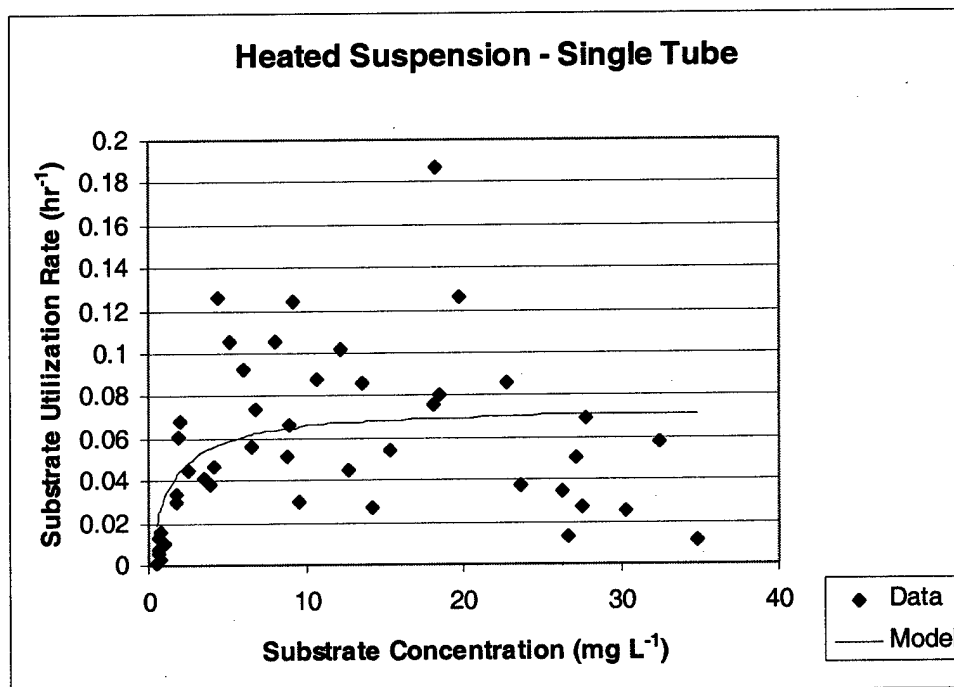
Figure B-10. Kinetic coefficients for the single tube heated suspension, K_S = 1.3 mg L^{-1}, k = 0.07 h^{-1}.

Appendix C
Heat Transfer Charts

The data was measured as described in Chapter 3 and results summarized in Chapter 6. All raw and processed data is available in a file format recorded on a CD-ROM that is on deposit with Dr. Mark Fitch. In each chart, the error bars are 95% confidence intervals.
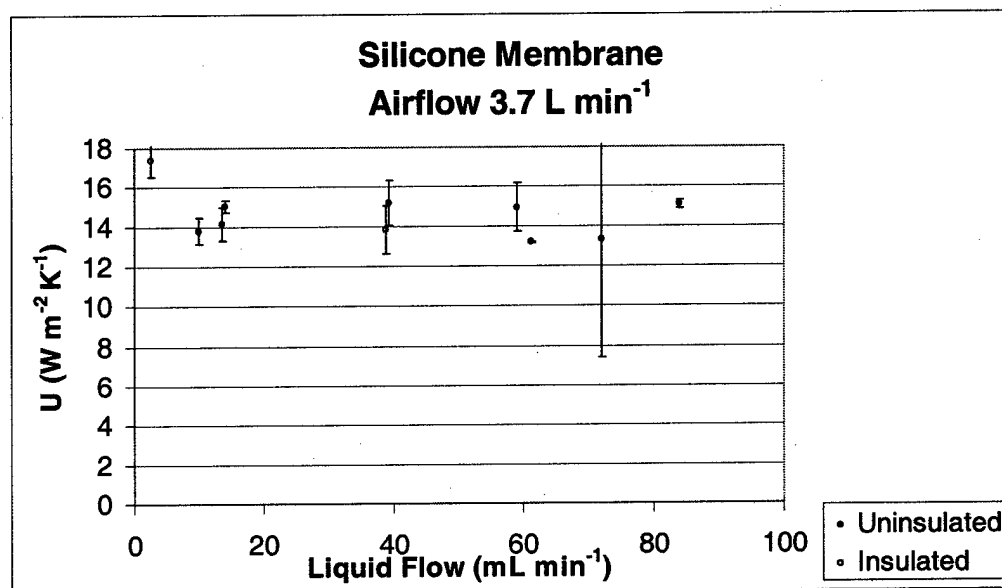
Figure C-1. Heat transfer coefficient measurement, silicone membrane higher airflow rate.
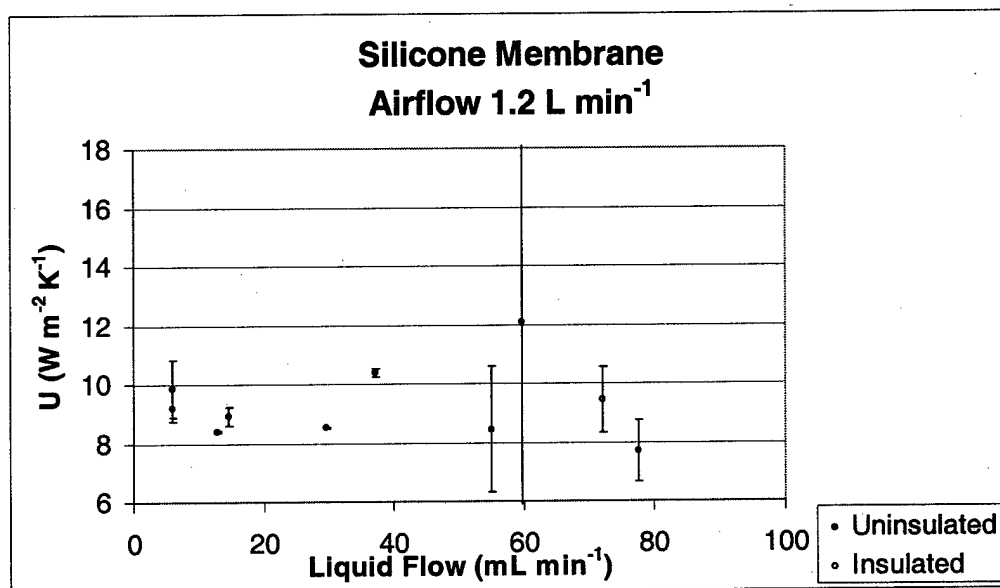
Figure C-2. Heat transfer coefficient measurement, silicone membrane lower airflow rate.
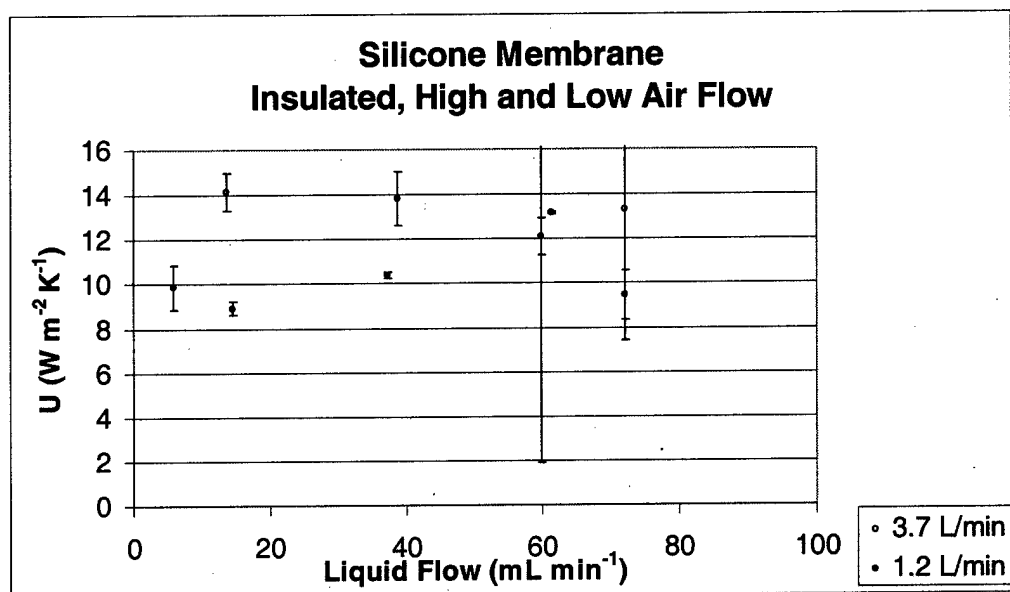
Figure C-3. Heat transfer coefficient measurement, insulated silicone membrane.
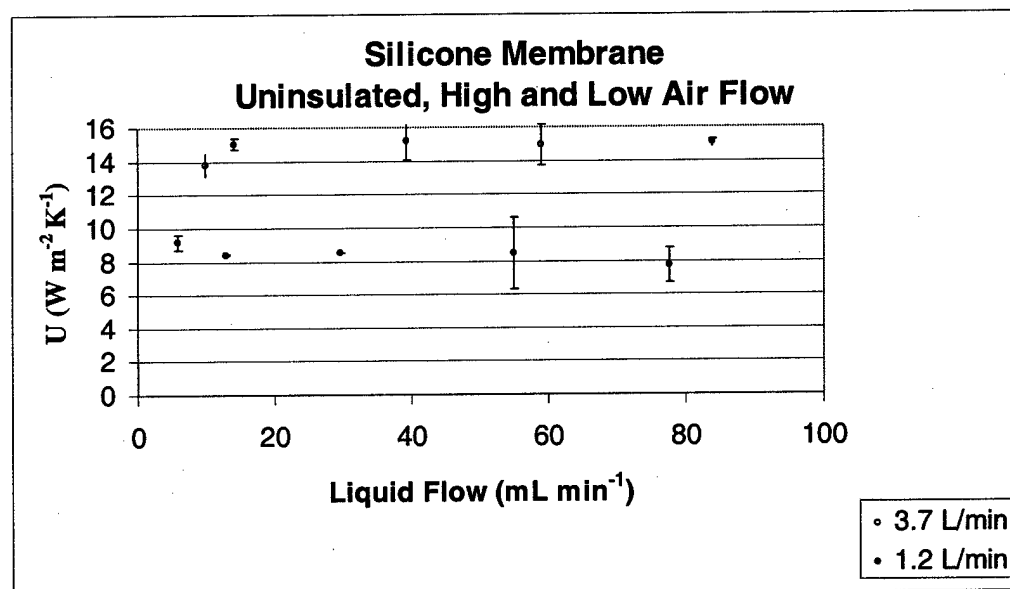
Figure C-4. Heat transfer coefficient measurement, uninsulated silicone membrane.
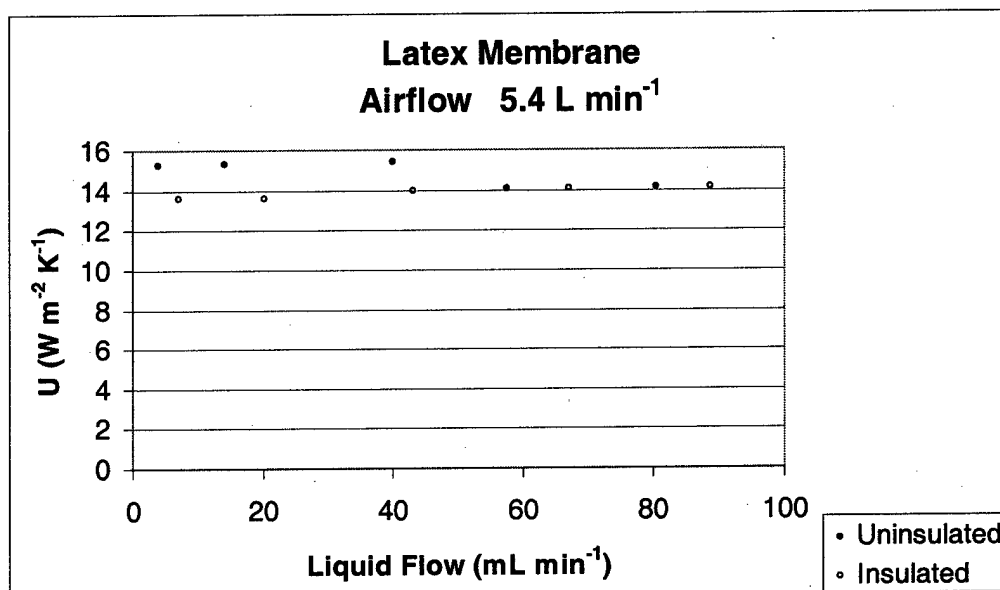
Figure C-5 . Heat transfer coefficient measurement, latex membrane higher airflow rate.
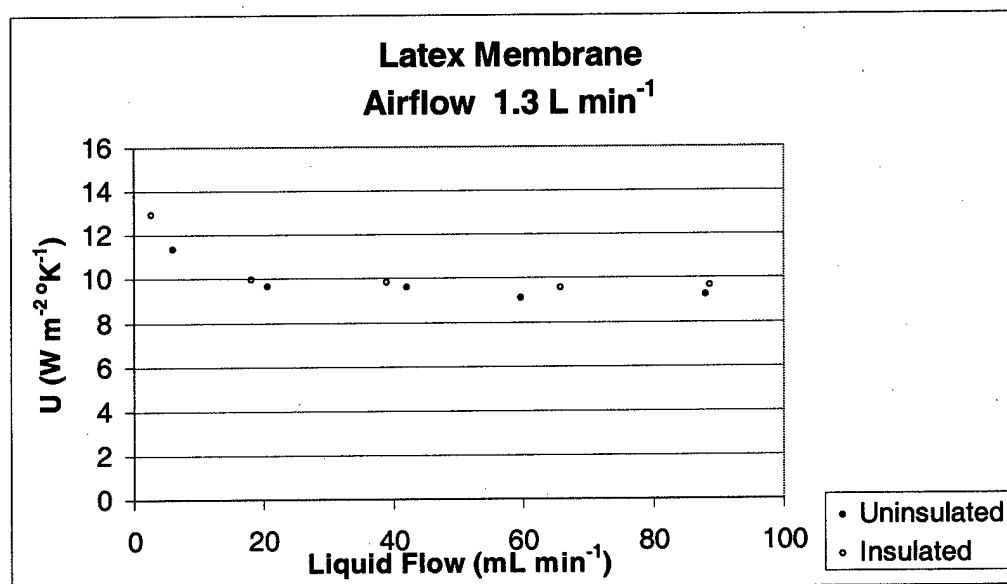
Figure C-6. Heat transfer coefficient measurement, latex membrane lower airflow rate.
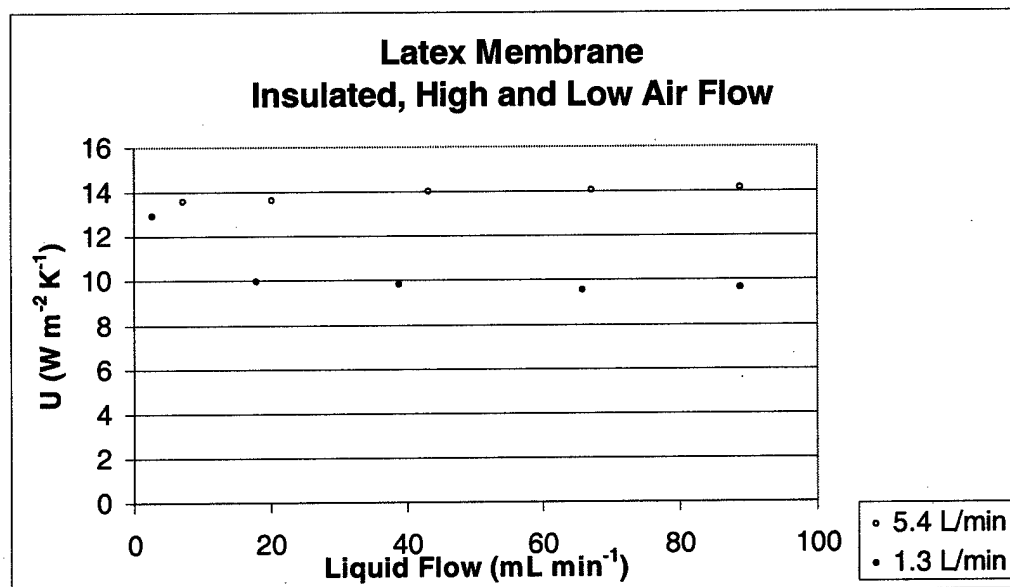
Figure C-7. Heat transfer coefficient measurement, insulated latex membrane.
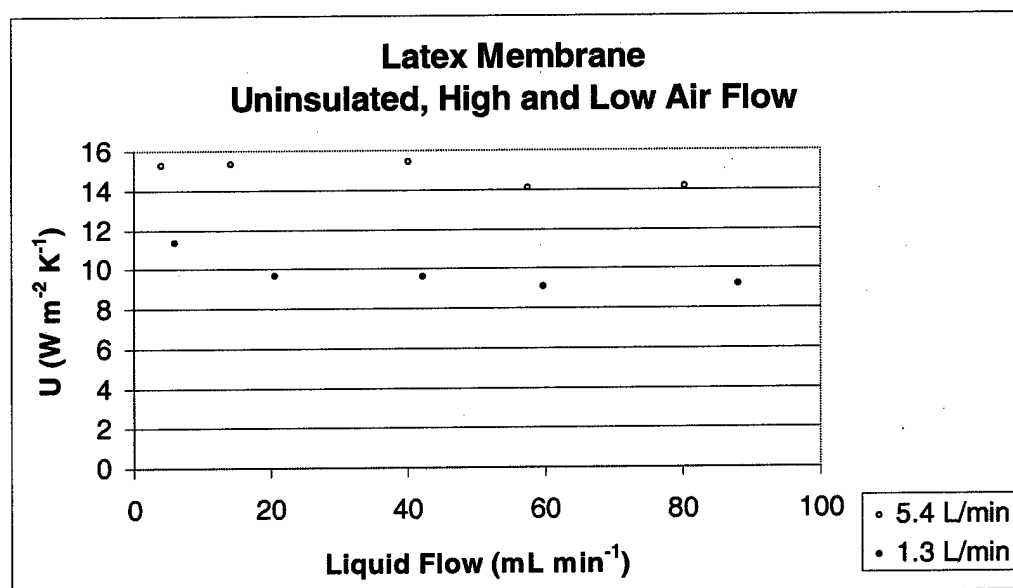
Figure C-8. Heat transfer coefficient measurement uninsulated latex membrane.
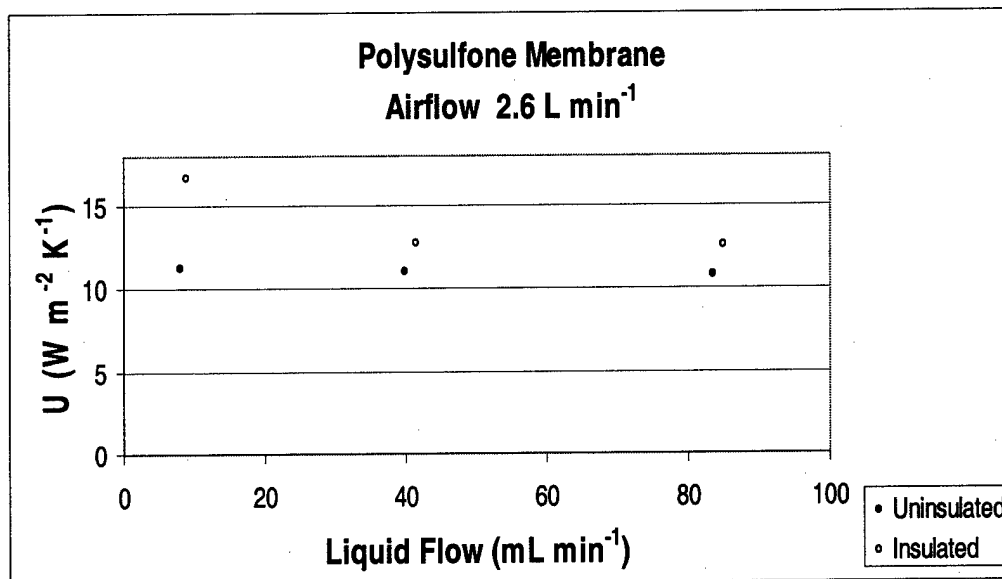
Figure C-9. Heat transfer coefficient measurement, polysulfone membrane higher airflow rate.
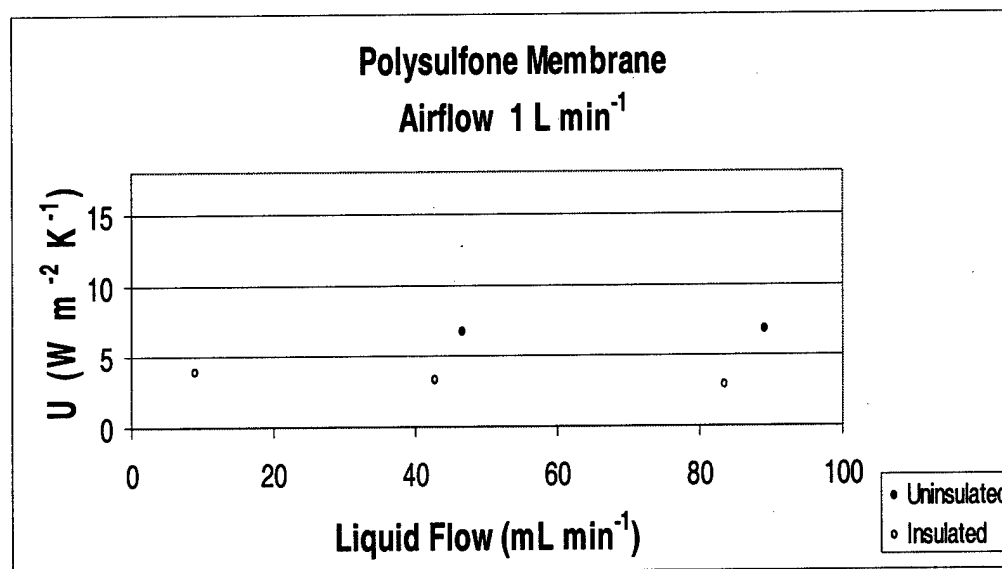
Figure C-10. Heat transfer coefficient measurement, polysulfone membrane lower airflow rate.
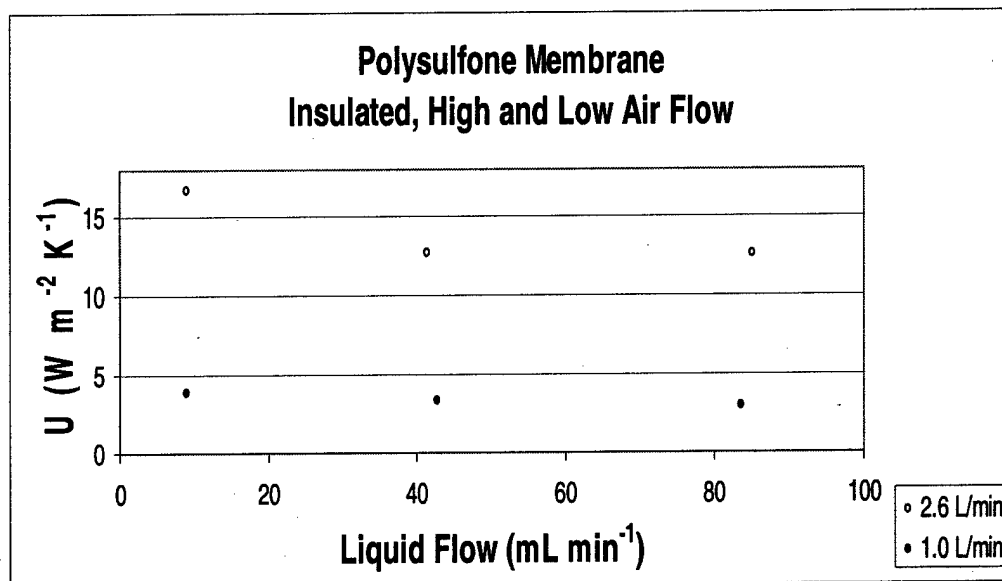
Figure C-11. Heat transfer coefficient measurement insulated polysulfone membrane.
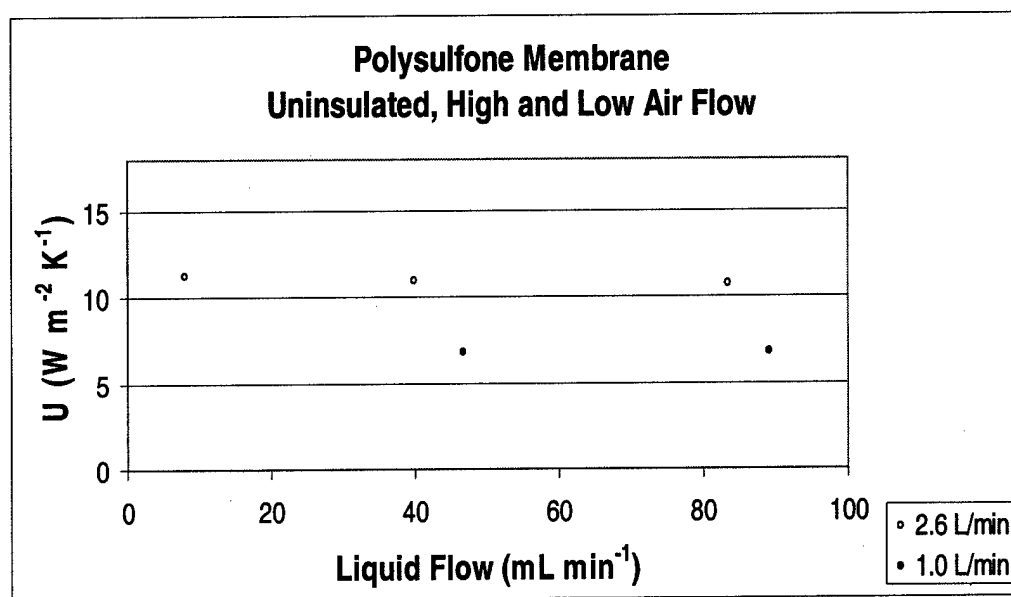
Figure C-12. Heat transfer coefficient measurement, uninsulated polysulfone membrane.

Appendix D
Periodic Monitoring Data

Table D-1. Periodically measured parameters for the separate reactors

Date	Reactor	DO (mg L^{-1})	pH	Water Added (mL)	OD	Pressure Drop (Inches)
5 Aug 02	Pilot-Scale	0	5.7	1400	0.137	0
24 Apr 02	Pilot-Scale	0	6.9	1000	0.128	0
3 Apr 02	Pilot-Scale	1.11	6.7	0	0.203	0
28 Feb 02	Dual Tube	0.55	3.3	10	0.328	7/8
29 Jan 02	Dual Tube	0.6	6.2	5	0.245	3/4
7 Jan 02	Dual Tube	0.71	6.6	15	0.215	3/8
6 Dec 01	Dual Tube	1.41	5.4	11	0.216	11/4
21 Nov 01	Dual Tube	1.95	5.8	3	0.184	11/4
9 Nov 01	Dual Tube	2.58	6.30	0	0.210	11/4
25 Oct 01	Dual Tube	0.17	6.15	5	0.154	1/2
24 Apr 02	Long Single Tube Nutrient Limited	1.28	6.6	62	0.082	1/4
3 Apr 02	Long Single Tube Nutrient LImited	0	6.5	82	0.153	1/2
24 Apr 02	Dual Tube/Nutrient Limited	0.28	4.2	43	0.227	9/16
3 Apr 02	Dual Tube/Nutrient Limited	0	4.6	50	0.393	15/16
28 Feb 02	Long Single Tube	1.77	5.2	30	0.224	1/2
29 Jan 02	Long Single Tube	2.49	7.3	50	0.317	1/2
6 Dec 01	Long Single Tube	3.11	4.2	0	0.080	11/16
9 Nov 01	Long Single Tube	4.91	7.53	0	0.060	1/4
6 Dec 01	Heated Single Tube	1.95	6.2	21	0.199	5/8
21 Nov 01	Heated Single Tube	1.65	6.2	2	0.153	3/4
9 Nov 01	Heated Single Tube	1.85	6.56	0	0.088	5/16
18 Oct 01	Small/Stagnant	0.21	5.63	0	0.130	1/2
11 Oct 01	Small/Stagnant	0.13	5.83	0	0.167	1/2
5 Oct 01	Small/Stagnant	0.27	4.97	0	0.221	1/16
27 Sep 01	Small/Stagnant	0.1	5.39	0	0.147	1/2
20 Sep 01	Small/Stagnant	0	5.32	0	0.245	1/2
14 Sep 01	Small/Stagnant	0	5.46	0	0.238	1/2
6 Sep 01	Small/Stagnant	2.0	5.94	5	0.284	1/2
30 Aug 01	Small/Flow	1.43	5.32	0	0.192	7/16

Table D-2. Abiotic operating data.

Reactor	Abiotic Removal (%)
Short single silicone tube	12[a]
Long single silicone tube	3
Dual silicone tube	38
Semi-pilot-scale silicone tube	10
Polysulfone	30

[a](Cole, 2001)

Appendix E
Modeling Run Results

Table E-1. Summary of model run results.

Model Run	Axial Size (cm)	Radial Size (cm)	Axial Gas Phase Concentration Range (mg L^{-1})	Removal Range (mg s^{-1})	Biofilm Thickness Range (cm)
Single Tube 21 Aug 01	0.5	0.01	5.85-6.41	$(1.64-1.96)*10^{-4}$	0.11-0.13
Single Tube 22 Aug 01	0.5	0.01	5.19-5.67	$(1.48-1.64)*10^{-4}$	0.10-0.11
Single Tube 4 Sep 01	0.5	0.02	13.32-14.63	$(4.21-4.60)*10^{-4}$	0.26-0.28
Dual Tube 1 Aug 02	1	0.01	6.91-11.26	$(0.34-0.55)*10^{-4}$	0.07-0.11
Dual Tube 2 Aug 02	1	0.01	6.86-10.83	$(0.34-0.56)*10^{-4}$	0.07-0.11
Dual Tube 5 Aug 02	1	0.01	6.34-10.49	$(0.32-0.52)*10^{-4}$	0.07-0.11
Dual Tube 10 Nov 01	1	0.01	2.12-3.28	$(0.86-1.28)*10^{-4}$	0.02-0.03
Dual Tube 26 Nov 01	1	0.01	4.93-7.67	$(2.38-3.37)*10^{-4}$	0.05-0.07
Dual Tube 29 Nov 01	1	0.01	5.36-8.57	$(2.47-4.02)*10^{-4}$	0.05-0.08
Dual Tube 6 Dec 01	1	0.01	7.52-12.54	$(4.41-6.26)*10^{-4}$	0.11-0.15
Pilot 1 Aug 02	1	0.01	0.19-6.07	$(0.51-2.84)*10^{-4}$	0.05-0.21
Pilot 2 Aug 02	1	0.02	15.25-27.63	$(8.94-13.77)*10^{-4}$	0.38-0.48
Pilot 5 Aug 02	1	0.01	5.09-22.08	$(3.38-10.79)*10^{-4}$	0.17-0.38
Pilot 6 Aug 02	1	0.01	6.23-10.86	$(3.51-5.59)*10^{-4}$	0.31-0.39
Pilot 7 Aug 02	1	0.02	28.18-42.63	$(16.57-21.12)*10^{-4}$	0.40-0.46
Pilot 8 Aug 02	1	0.01	3.19-7.99	$(3.90-4.14)*10^{-4}$	0.33-0.34
In-Series Dual 11 Jun 02	1	0.01	3.90-5.81	$(1.55-2.06)*10^{-4}$	0.03-0.04
In-Series Dual 14 Jun 02	1	0.01	3.88-5.79	$(1.55-2.06)*10^{-4}$	0.03-0.04
In-Series Single 11 Jun 02	1	0.01	3.74-4.31	$(0.67-1.02)*10^{-4}$	0.02-0.03
In-Series Single 14 Jun 02	1	0.01	3.57-3.91	$(0.67-1.02)*10^{-4}$	0.02-0.03
Neemann Single 30 Dec 97	0.5	0.02	0.40-2.17	$(1.35-1.54)*10^{-4}$	0.30-0.32
Neemann Single 2 Jan 98	0.5	0.01	0.34-1.83	$(1.04-1.34)*10^{-4}$	0.25-0.28
Neemann Single 10 Jan 98	0.5	0.01	1.12-1.37	$(0.83-0.91)*10^{-4}$	0.21-0.22

Neemann Single 21 Jan 98	0.5	0.01	1.30-1.59	$(0.93-1.09)*10^{-4}$	0.18-0.20
Neemann Single 25 Jan 98	0.5	0.01	1.34-1.64	$(0.96-1.15)*10^{-4}$	0.21-0.23
Neemann Single 28 Jan 98	0.5	0.01	0.91-1.12	$(0.68-0.75)*10^{-4}$	0.19-0.20
Neemann Single 5 Feb 98	0.5	0.02	1.45-1.83	$(1.17-1.35)*10^{-4}$	0.28-0.30

Table E-2. Calculated radius and diameter for dual tube reactor.

	Units	Value
Outer Module Diameter	cm	5.08
Outer Diameter of Each Tube	cm	1.27
Total Module Cross Sec Area	cm^2	20.27
Diameter for Each tube	cm	3.592
Calculated Cross Sec Area	cm^2	20.27
R associated with each tube	cm	1.796

Table E-3. Calculated radius and diameter for pilot scale reactor.

	Units	Value
Outer Module Diameter	cm	25.4
Outer Diameter of Each Tube	cm	1.27
Total Module Cross Sec Area	cm^2	506.7
Diameter for Each tube	cm	5.08
Calculated Cross Sec Area	cm^2	506.7
R associated with each tube	cm	2.54

Axial Position cm	Air Phase Concentration (mg L^{-1} as Liquid)	0.635	0.655	0.675	0.695	0.715	0.735	0.755	0.775	0.785	Liquid Suspension		
0	22.078199					0.49216	0.4775	0.46295	0.44775	0.44	0.44	0.44	0.44
2	21.955507					0.49215	0.4775	0.46295	0.44775	0.44	0.44	0.44	0.44
3	21.894100					0.49215	0.4775	0.46295	0.44775	0.44	0.44	0.44	0.44
5	21.771468					0.49215	0.4775	0.46295	0.44775	0.44	0.44	0.44	0.44
7	21.648776					0.49215	0.4775	0.46295	0.44775	0.44	0.44	0.44	0.44
9	21.526083					0.49215	0.4775	0.46295	0.44775	0.44	0.44	0.44	0.44
11	21.403391					0.49215	0.4775	0.46295	0.44775	0.44	0.44	0.44	0.44
13	21.280698					0.49215	0.4775	0.46295	0.44775	0.44	0.44	0.44	0.44
15	21.158006					0.49215	0.4775	0.46295	0.44775	0.44	0.44	0.44	0.44
17	21.035314					0.49215	0.4775	0.46295	0.44775	0.44	0.44	0.44	0.44
19	20.912621					0.49215	0.4775	0.46295	0.44775	0.44	0.44	0.44	0.44
21	20.789929					0.49215	0.4775	0.46295	0.44775	0.44	0.44	0.44	0.44
23	20.667237					0.49215	0.4775	0.46295	0.44775	0.44	0.44	0.44	0.44
25	20.544544					0.49215	0.4775	0.46295	0.44775	0.44	0.44	0.44	0.44
27	20.421852					0.49215	0.4775	0.46295	0.44775	0.44	0.44	0.44	0.44
29	20.299159					0.49215	0.4775	0.46295	0.44775	0.44	0.44	0.44	0.44
33	20.053775					0.49215	0.4775	0.46295	0.44775	0.44	0.44	0.44	0.44
35	19.931082					0.49215	0.4775	0.46295	0.44775	0.44	0.44	0.44	0.44
37	19.808390					0.49215	0.4775	0.46295	0.44775	0.44	0.44	0.44	0.44
39	19.685697					0.49215	0.4775	0.46295	0.44775	0.44	0.44	0.44	0.44
41	19.563005					0.49215	0.4775	0.46295	0.44775	0.44	0.44	0.44	0.44
43	19.440313					0.49215	0.4775	0.46295	0.44775	0.44	0.44	0.44	0.44
45	19.317620					0.49215	0.4775	0.46295	0.44775	0.44	0.44	0.44	0.44
47	19.194928					0.49215	0.4775	0.46295	0.44775	0.44	0.44	0.44	0.44
49	19.072236					0.49215	0.4775	0.46295	0.44775	0.44	0.44	0.44	0.44
51	18.949643				0.49075	0.47675	0.46235	0.44755	0.44	0.44	0.44	0.44	0.44
53	18.826951				0.49075	0.47675	0.46235	0.44755	0.44	0.44	0.44	0.44	0.44
55	18.704158				0.49075	0.47675	0.46235	0.44755	0.44	0.44	0.44	0.44	0.44
57	18.581466				0.49075	0.47675	0.46235	0.44755	0.44	0.44	0.44	0.44	0.44
59	18.458773				0.49075	0.47675	0.46235	0.44755	0.44	0.44	0.44	0.44	0.44
65	18.090696				0.49075	0.47675	0.46235	0.44755	0.44	0.44	0.44	0.44	0.44
67	17.968004				0.49075	0.47675	0.46235	0.44755	0.44	0.44	0.44	0.44	0.44
71	17.722619				0.49075	0.47675	0.46235	0.44755	0.44	0.44	0.44	0.44	0.44
73	17.599927				0.49075	0.47675	0.46235	0.44755	0.44	0.44	0.44	0.44	0.44
75	17.477234				0.49075	0.47675	0.46235	0.44755	0.44	0.44	0.44	0.44	0.44
77	17.354542				0.49075	0.47675	0.46235	0.44755	0.44	0.44	0.44	0.44	0.44
79	17.231849				0.49075	0.47675	0.46235	0.44755	0.44	0.44	0.44	0.44	0.44
81	17.109152				0.49075	0.47675	0.46235	0.44755	0.44	0.44	0.44	0.44	0.44
85				0.4968	0.4832	0.4692	0.4548	0.44	0.44	0.44	0.44	0.44	0.44
87				0.4968	0.4832	0.4692	0.4548	0.44	0.44	0.44	0.44	0.44	0.44
89				0.4968	0.4832	0.4692	0.4548	0.44	0.44	0.44	0.44	0.44	0.44
91				0.4968	0.4832	0.4692	0.4548	0.44	0.44	0.44	0.44	0.44	0.44
93				0.4968	0.4832	0.4692	0.4548	0.44	0.44	0.44	0.44	0.44	0.44
95				0.4968	0.4832	0.4692	0.4548	0.44	0.44	0.44	0.44	0.44	0.44
97				0.4968	0.4832	0.4692	0.4548	0.44	0.44	0.44	0.44	0.44	0.44
99				0.4968	0.4832	0.4692	0.4548	0.44	0.44	0.44	0.44	0.44	0.44
101				0.4968	0.4832	0.4692	0.4548	0.44	0.44	0.44	0.44	0.44	0.44
103				0.4968	0.4832	0.4692	0.4548	0.44	0.44	0.44	0.44	0.44	0.44
105				0.4968	0.4832	0.4692	0.4548	0.44	0.44	0.44	0.44	0.44	0.44
107				0.4968	0.4832	0.4692	0.4548	0.44	0.44	0.44	0.44	0.44	0.44
109				0.4968	0.4832	0.4692	0.4548	0.44	0.44	0.44	0.44	0.44	0.44
111				0.4968	0.4832	0.4692	0.4548	0.44	0.44	0.44	0.44	0.44	0.44
113				0.4968	0.4832	0.4692	0.4548	0.44	0.44	0.44	0.44	0.44	0.44
115				0.4968	0.4832	0.4692	0.4548	0.44	0.44	0.44	0.44	0.44	0.44
117				0.4968	0.4832	0.4692	0.4548	0.44	0.44	0.44	0.44	0.44	0.44
123				0.4968	0.4832	0.4692	0.4548	0.44	0.44	0.44	0.44	0.44	0.44
127				0.4968	0.4832	0.4692	0.4548	0.44	0.44	0.44	0.44	0.44	0.44
129				0.4968	0.4832	0.4692	0.4548	0.44	0.44	0.44	0.44	0.44	0.44

Figure E-1. Toluene concentration profile across the reactor.

Appendix G
Concentration Plots

Removal vs. Concentration at a Given Q. The following graphs indicate removal increases with increasing influent concentration. Removals observed in different reactor systems are reported and did not show a consistent trend.
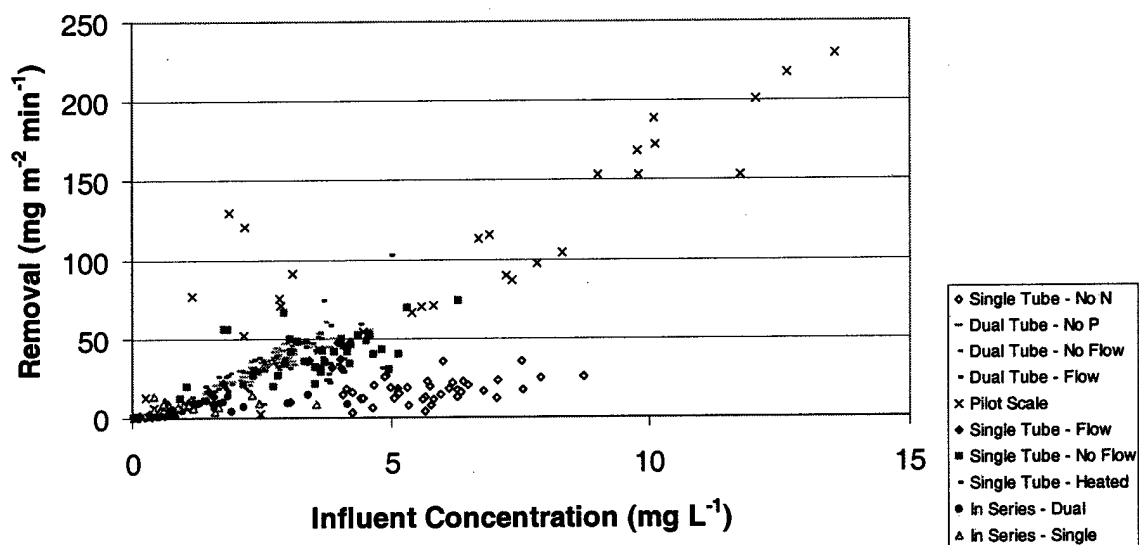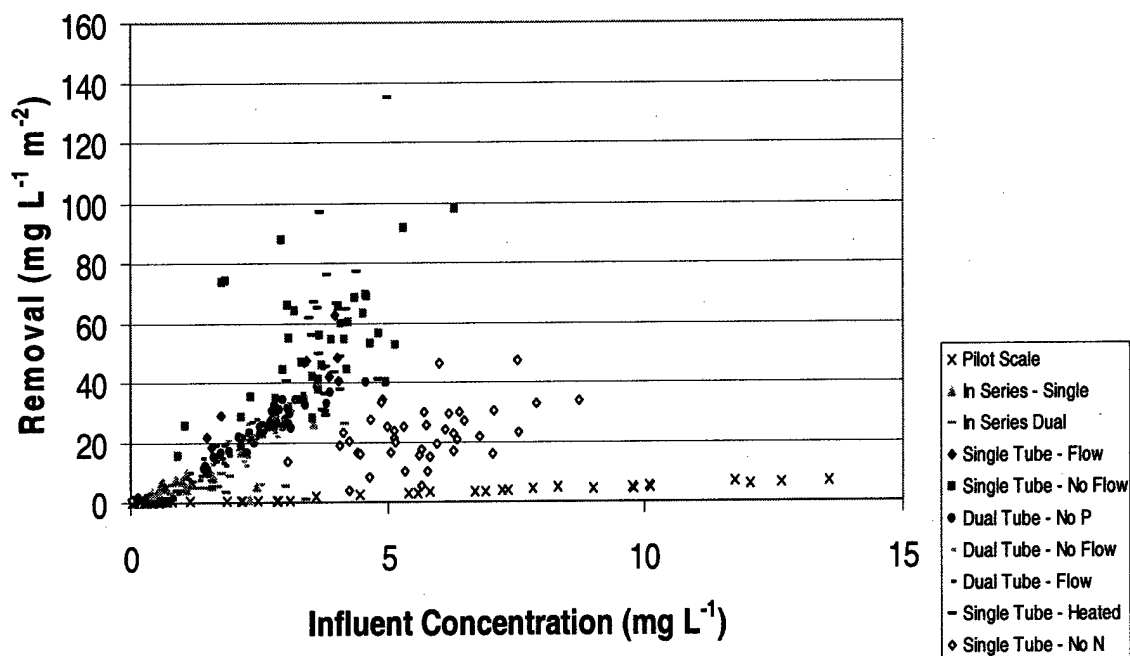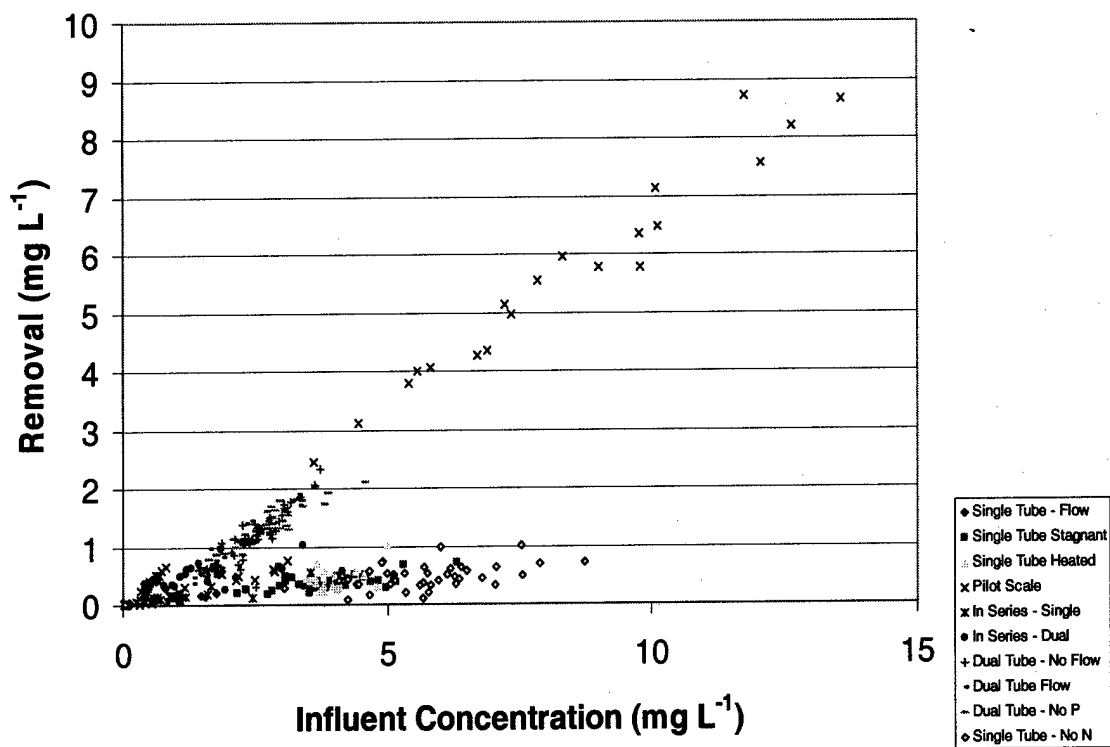
BIBLIOGRAPHY

Ahmed, A. 1997. Masters Thesis. King Fahd University of Petroleum and Minerals, Saudi Arabia.

Air Science Technologies. 2001. Biofiltration of gaseous effluents, www.enviroaccess.ca/fiches_2/F2-04-96ba.html. Accessed 15 Sep 01.

Aizpuru, A., L. Malhautier, and J. Fanlo. 2000. Biofiltration of a complex VOC mixture. Presented at the USC-TRG Conference on Biofiltration (An Air Pollution Control Technology).

Alexandrino, M., C. Knief, and A. Lipski. 2001. Stable-isotope based labeling of styrene degrading micro-organisms in biofilters. Applied and Environmental Microbiology. 67(10):4796-4804.

Allcock, H. R., and F. W. Lampe. 1981. Contemporary Polymer Chemistry. Prentice-Hall, New Jersey.

Allen, E. 1996. Biofiltration control of VOC and air toxic emissions: n-butane and benzene. Presented at the Emerging Solutions VOC Air Toxics Control Conference. 351-362.

Allen, D., Z. Kong, R. Fulthorpe, and L. Farhana. 2000. Thermophilic biofiltration of volatile organic compounds. Proceedings of the Air and Waste Management Association Annual Conference and Exhibition. 2318-2337.

American Conference of Governmental Industrial Hygienists. 2000. 2000 Threshold limit Values and Biological Exposure Indices. ACGIH, Cincinnati, OH.

American Public Health Association, American Water Works Association and Water Environment Federation. 1995. Standard Methods for the Examination of Water and Wastewater. American Public Health Association, Washington, D.C.

Andersson, A. 2000. Evaluation of rockwool biofilter media for the treatment of restaurant emissions. Presented at the USC-TRG Conference on Biofiltration (An Air Pollution Control Technology). 239-246.

Anit, S., and R. Artuz. 2000. Biofiltration of air. 2001. Rensselaer Institute. www.rensselaer.edu/dept/chem-eng/Biotech-Environ/MIS/biofilt/biofiltration.htm.

Arcangeli, J., and E. Arvin. 1992. Toluene biodegradation and biofilm growth in an aerobic fixed-film reactor. Applied Microbiology and Biotechnology. 37(4):510-517.

Attaway, H., C. Gooding, and M. Schmidt. 2001. Biodegradation of BTEX vapors in a silicone membrane bioreactor system. Journal of Industrial Microbiology and

Biotechnology. 26:316-325.

Aziz, C. E., M. W. Fitch, L. K. Linquist, J. G. Pressman, G. Georgiou, and G. E. Speitel. 1995. Methanotrophic biodegradation of trichloroethylene in a hollow fiber membrane bioreactor. Environmental Science and Technology. 29(10):2574-2538.

Bae, W., and B. Rittmann. 1996. A structured model of dual-limitation kinetics. Biotechnology and Bioengineering. 49:683-689.

Bakke, R., R. Kommedal, and S. Kalvenes. 2001. Quantification of biofilm accumulation by an optical approach. Journal of Microbiological Methods. 44(1):13-26.

Baltzis, B. C., S. M. Wojdyla, and S. M. Zarook. 1997. Modeling biofiltration of VOC mixtures under steady-state conditions. Journal of Environmental Engineering. 123(6):599-605.

Baltzis, B., J. Mpanias, and S. Bhattacharya. 2001. Modeling the removal of VOC mixtures in biotrickling filters. Biotechnology and Bioengineering. 72(4):389-401.

Barson, C., and Y. Dong. 1990. Diffusion and swelling studies of ethanol and ethyl laurate with dry polypropylene and polyethylene terephthalate films using a radiotracer technique. European Polymer Journal. 26(4):449-451.

Beeton, S., H. R. Millward, B. J. Bellhouse, A. M. Nicholson, N. Jenkins, and C. J. Knowles. 1991. Gas transfer characteristics of a novel membrane bioreactor. Biotechnology & Bioengineering. 38:1233-1238.

Beeton, S., B. Bellhouse, C. Knowles, H. Millward, A. Nicholson, and J. Wyatt. 1994. A novel membrane bioreactor for microbial growth. Applied Microbiology and Biotechnology. 40:812-817.

Beyenal, H., S. Seker, A. Tanyolac, and B. Salih. 1997. Diffusion coefficients of phenol and oxygen in a biofilm of *Pseudomonas putida*. AIChE Journal. 43(1):243-250.

Beyenal, H., A. Tanyolac, and Z. Lewandowski. 1998. Measurement of local effective diffusivity in heterogeneous biofilms. Water Science and Technology. 38(8-9):171-178.

Bhattacharya, S., and B. Baltzis. 2000. Removal of ortho-dichlorobenzene in a biotrickling filter in the presence of ethanol. Presented at the USC-TRG Conference on Biofiltration (An Air Pollution Control Technology). 91-98.

Bibeau, L., K. Kiared, A. Lerous, R. Brzezinski, G. Viel, and M. Heitz. 1997. Biological purification of exhaust air containing toluene vapor in a filter-bed reactor. Canadian Journal of Chemical Engineering 75(5):921-929.

Bird, R., W. Stewart, and E. Lightfoot. 1960. Transport Phenomenon. John Wiley and

Sons, New York, NY.

Blume, I., P. Schwering, M. Mulder, and C. Smolders. 1989. Sorption and permeation properties of poly(dimethylsiloxane) film. Proceedings of the Fourth International Conference on Pervaporation Processes in the Chemical Industry. 115-126.

Brookes, P., and A. Livingston. 1995. Aqueous-aqueous extraction of organic pollutants through tubular silicone membranes. Journal of Membrane Science. 104:119 - 137.

Burgess, J. E., S. A. Parsons, and R. M. Stuetz. 2001. Developments in odour control and waste gas treatment biotechnology: a review. Biotechnology Advances. 19(1):35-63.

Bustard, M., V. Meeyoo, and P. Wright. 2001. Biodegradation of high concentration isopropanol vapour in a biofilter inoculated with a solvent-tolerant microbial consortium. Transactions of the Institute of Chemical Engineers. 79(C):129-135.

Cao, B., and M. Henson. 2002. Modeling of spiral wound pervaporation modules with application to the separation of styrene/ethylbenzene mixtures. Journal of Membrane Science. 197:117-146.

Caravanos, J. 1991. Quantitative Industrial Hygiene. American Conference of Governmental Industrial Hygienists, Cincinnati, OH.

Casey, E., B. Glennon, and G. Hamer. 2000. Biofilm development in a membrane-aerated biofilm reactor: effect of intra-membrane oxygen pressure on performance. Bioprocess Engineering. 23:457-465.

Chang, A., D. Choi, and J. Devinny. 2000. Low-pH biofiltration of hydrogen sulfide and volatile organic compounds. Presented at the USC-TRG Conference on Biofiltration (An Air Pollution Control Technology). 281-288.

Chang, K., C. Lu, and M. Lin. 2001. Treatment of volatile organic compounds from polyurethane and epoxy manufacture by a trickle-bed air biofilter. Journal of Bioscience and Bioengineering. 92(2):126-130.

Characklis, W. G., and K. C. Marshall. 1990. Biofilms. John Wiley and Sons, New York.

Cherry, R., and D. Thompson. 1997. Shift from growth to nutrient-limited maintenance kinetics during biofilter acclimation. Biotechnology and Bioengineering. 56(3):330-339.

Cho, K., M. Hirai, and M. Shoda. 1992. Enhanced removal efficiency of malodorous gases in a pilot-scale peat biofilter inoculated with *Thiobacillus thioparus* DW44. Journal of Hazardous Materials. 53(1-3):19-33.

Choy, C., W. Leung, and T. Ma. 1984. Sorption and diffusion of toluene in highly oriented polypropylene. Journal of Polymer Science. 22:707-719.

Chung, Y., C. Huang, and C. Tseng. 2001. Biological elimination of H_2S and NH_3 from waste gases by a biofilter packed with immobilized heterotrophic bacteria. Chemosphere. 43:1043-1050.

Clapp, L., R. Hartono, J. Newman, and J. Park. 1996. Trichloroethylene degradation in a novel membrane bioreactor. Presented at the WEFTEC '96 Annual Conference and Exposition. 379-390.

Clark, M. Transport Modeling for Environmental Engineers and Scientists. 1996. John Wiley and Sons, 1996.

Cole, S. 2001. Membrane biofiltration treatment of contaminated airstreams. Undergraduate Research Experience Report. University of Missouri - Rolla, Rolla, MO.

Cole-Parmer Instruments. 2002. Personal Communication. Technical Support.

Cooper, C., V. Godlewski, R. Hanson, M. Koletzke, and N. Webster. 2001. Odor investigation and control at a WWTP in Orange County, Florida. Environmental Progress. 20(3):133-143.

Cox, H., and M. Deshusses. 2000. Thermophilic biotrickling filtration of ethanol vapors. Presented at the USC-TRG Conference on Biofiltration (An Air Pollution Control Technology). 159-166.

Crank, J., and G. S. Park. 1968. Diffusion in Polymers. Academic Press, London, England.

Cunha, L., H. Bungay, and R. Mormino. 1994. Continuous culture models for low nutrient concentrations. Binary-Computing in Microbiology. 6(5):167-172.

Current, R., E. Kozliak, and A. Borgerding. 2001. Monitoring biodegradation of VOCs using high speed gas chromatography with a dual-point sampling system. Environmental Science and Technology. 35:1452-1457.

Daubert, I., C. Lafforgue, C. Fonade, and C. Maranges. 1999. Feasibility study of a new VOC treatment process. Presented at the Societe Francaise de Genie des European Congress. 455-462.

Davis, W. 2000. Air Pollution Engineering Manual. Air and Waste Management Association. John Wiley and Sons, New York, NY.

Davison, B., J. Barton, K. Klasson, and A. Francisco. 2000. Effect of biomass on the measured solubility of sparingly soluble organics in aqueous bioremediation systems. Presented at the USC-TRG Conference on Biofiltration (An Air Pollution Control Technology). 182-190.

De Bo, I., H. Van Langenhove, P. Pruuost, and I. Van De Steene. 2000. Oxygen supply and adhesion of monocultures in a membrane bioreactor. Toegepast Biol. Wet. 65(3a):63-69.

Debus, O., H. Baumgartl, and I. Sekoulov. 1994. Influence of fluid velocities on the degradation of volatile aromatic compounds in membrane bound biofilms. Water Science and Technology. 29(10-11):253-262.

Debus, O. 1995. Transport and reaction of aromatics, O_2 and CO_2 within a membrane bound biofilm in competition with suspended biomass. Water Science and Technology. 31(1):129-141.

Deront, M., F. Samb, N. Adler, and P. Peringer. 1998. Biomass growth monitoring using pressure drop in a cocurrent biofilter. Biotechnology and Bioengineering. 60(1):97 - 104.

Deshusses, M., G. Hamer, and I. Dunn. 1995. Behavior of biofilters for waste air biotreatment. 1. Dynamic model development. Environmental Science and Technology. 29(4):1048-58.

Deshusses, M., G. Hamer, and I. Dunn. 1996. Transient-state behavior of a biofilter removing mixtures of MEK and MIBJ from air. Biotechnology and Bioengineering. 49(5):587-598.

Devinny, J., M. Deshusses, and T. Webster. 1999. Biofiltration for Air Pollution Control. Lewis Publishers, Washington, D.C.

Dewulf, J., H. Langenhove, and J. Dirckx. 2001. Exergy analysis in the assessment of the sustainability of waste gas treatment systems. The Science of the Total Environment. 273:41-52.

Dhamwichukorn, S., G. Kleinheinz, and S. Bagley. 2001. Thermophilic biofiltration of methanol and alpha-pinene. Journal of Industrial Microbiology and Biotechnology. 26(3):127-133.

Diks, R., S. Ottengraf, and S. Vrijland. 1994. The existence of a biological equilibrium in a trickling biofilter for waste gas purification. Biotechnology and Bioengineering. 44:1279-1287.

Dirk-Faitakis, C., and D. Allen. 2000. Biofiltration of cyclic air emissions: experiments and modeling. Presented at the USC-TRG Conference on Biofiltration (An Air Pollution Control Technology). 221-228.

Dolasa, A. R., and S. J. Ergas. 2000. Membrane bioreactor for cometabolism of trichloroethene air emissions. Journal of Environmental Engineering ASCE. 126(10):969-973.

Du Plessis, C., and J. Strauss. 2001. BTEX catabolism interactions in a toluene-acclimatized biofilter. Applied Microbiology and Biotechnology. 55:122-128.

Du Plessis, J., W. Pugh, A. Judefeind, and J. Hadgraft. 2001. The effect of hydrogen bonding on diffusion across model membranes: consideration of the number of H-bonding groups. European Journal of Pharmaceutical Sciences. 13:135-141.

Dupasquier, D., S. Revah, and R. Auria. 2002. Biofiltration of methyl tert-butyl ether vapors and cometabolism with pentane: modeling and experimental approach. Environmental Science and Technology. 36:247-253.

Elkay Silicones. 2002. Functional Silicones for Superior Textile Finishing. www.elkaysiliconesindia.com/abresbottom.htm. Accessed on 15 Sep 2001.

Elmrini, H., H. Jorio, L. Bibeau, and M. Heitz. 2000. Biofiltration of air polluted with xylene: an experimental study. Presented at the USC-TRG Conference on Biofiltration (An Air Pollution Control Technology). 99-106.

Enviro-Access. 2001. Biofiltration of gaseous effluents. www.enviroaccess.ca/fiches_2/F2-04-96-aa.html. Accessed on 15 Sep 2001.

Environmental Protection Agency. 1994. Chemicals in the Environment: Toluene. EPA 749-F-94-021. Office of Pollution Prevention and Toxics.

Environmental Protection Agency. 1994a. Chemicals in the Environment: 1-Butanol. EPA 749-F-94-007. Office of Pollution Prevention and Toxics.

Environmental Protection Agency. 1998. National Air Quality and Emissions Trends Report. www.epa.gov/oar.

Environmental Protection Agency. 2002. Toxic Release Inventory Program. www.epa.gov/tri. Accessed on 21 January 2002.

Ergas, C. 2002. Associate Professor, University of Massachusetts, Amherst, MA Personal Correspondence.

Ergas, S. J., and M. S. McGrath. 1997. Membrane bioreactor for control of volatile organic compound emissions. Journal of Environmental Engineering. 123:593-598.

Ergas, S. J., L. Shumway, M. W. Fitch, and J. J. Neemann. 1999. Membrane process for biological treatment of contaminated gas streams. Biotechnology & Bioengineering. 63:431-441.

Eszenyiova, A., V. Bilska, and H. Rajnohova. 2001. Removal of VOC from waste gases by biofiltration technology. Petroleum and Coal. 43(1):22-26.

Favre, E., Q. Nguyen, P. Schaetzel, R. Clement, and J. Neel. 1993. Sorption of organic solvents into dense silicone membranes. Journal of the Chemical Society, Faraday Transactions. 89(24):4339-4346.

Favre, E., P. Schaetzel, Q. Nguygen, R. Clement, and J. Neel. 1994. Sorption, diffusion and vapor permeation of various penetrants through dense polydimethylsiloxane membranes: a transport analysis. Journal of Membrane Science. 92:169-184.

Fitch, M. PhD Dissertation. University of Texas, Austin, Austin, TX.

Fitch, M. 2001. Associate Professor, University of Missouri-Rolla, Rolla MO. Personal Correspondence.

Fitch, M. 2002. Associate Professor, University of Missouri-Rolla, Rolla MO. Personal Correspondence.

Fitch, M., S. Sauer, and B. Zhang. 2000. Membrane biofilters: material choices and diurnal loading effects. Presented at the USC-TRG Conference on Biofiltration (An Air Pollution Control Technology). 83-90.

Freitas dos Santos, L., U. Hommerich, and A. Livingston. 1995d. Dichloroethane removal from gas streams by an extractive membrane bioreactor. Biotechnology Progress. 11:194-201.

Freitas dos Santos, L. M., and A. G. Livingston. 1993. Novel bioreactors for destruction of volatile organic compounds. Chemical Engineering Research and Design: Transactions of the Institution of Chemical Engineers. 71(A3):324-326.

Freitas dos Santos, L. M., and A. G. Livingston. 1995a. Membrane-attached biofilms for VOC wastewater treatment I: Novel in situ biofilm thickness measurement technique. Biotechnology and Bioengineering. 47:82-89.

Freitas dos Santos, L. M., and A. G. Livingston. 1995b. Membrane-attached biofilms for VOC wastewater treatment II: Effect of biofilm thickness on performance. Biotechnology and Bioengineering. 47:90-95.

Garcia-Payo, M., M. Izquierdo-Gil, and C. Fernandez-Pineda. 2000. Air gap membrane distillation of aqueous alcohol solutions. Journal of Membrane Science. 169(1):61-80.

Geankoplis, C. J. 1993. Transport Processes and Unit Operations. Prentice-Hall, New Jersey.

Gerrard, A., J. Paca, J. Marek, and P. Weigner. 1997. Dynamic behavior of starved biofilters. ICHEME Symposium Series. 143:131-137.

Golriz, M. 1996. Suspension-to-wall heat transfer in a 12-MW circulating fluidized-bed combustor. International Journal of Energy Research. 20(7):569-579.

Gryta, M., M. Tomaszewska, and A. Morawski. 1997. Membrane distillation with laminar flow. Separation and Purification Technology. 11(2):93-101.

Haferkamp, H., and M. Goede. 2000. Waste gas treatment of particular and volatile emissions from laser material processing of polymers - comparison of multifunctional filtration concepts. Presented at the USC-TRG Conference on Biofiltration (An Air Pollution Control Technology). 115-122.

Hao, O., M. Richard, D. Jenkins, and H. Blanch. 1983. The half saturation coefficient for dissolved oxygen a dynamic method for its determination and its effect on dual species competition. Biotechnology and Bioengineering. 25(2):403-416.

Harris, D. 1999. Quantitative Chemical Analysis. W. H. Freeman and Company. New York, NY.

Harris, N., and G. Hansford. 1976. A study of substrate removal in a microbial film reactor. Water Research. 10:935-943.

Hartmans, S., J. Tramper, and J. de Bont. 1990. Biological waste gas treatment. Presented at the European Congress on Biotechnology. 659-662.

Hartmans, S., E. Leenen, and G. Voskuilen. 1992a. Membrane bioreactor with porous hydrophobic membranes for waste-gas treatment. Biotechniques for Air Pollution Abatement and Odour Control Policies 4:103-106.

Hartmans, S. 1992b. Biological waste gas treatment. Presented at the Gas, Oil and Environmental Biotechnology IV Conference. 409-417.

Hesketh, H. 1996. Air pollution Control Traditional and Hazardous Pollutants. Technomic Publishing Company. Lancaster, PA.

Heide, C. 1999. Silicone rubber for medical device applications. Medical Device Link. www.devicelink.com/mddi/archive/99/11/003.html. Accessed on 22 June 2002.

Heinze, U., and C. Friedrich. 1997. Respiratory activity of biofilms: measurement and its significance for the elimination of n-butanol from waste gas. Applied Microbiology and Biotechnology 48(3):411-416.

Hirai, M., M. Kamamoto, M. Yani, and M. Shoda. 2001a. Comparison of the biological NH_3 removal characteristics among four inorganic packing materials. Journal of Bioscience and Bioengineering. 91(4):428-430.

Hirai, M., M. Kamamoto, M. Yani, and M. Shoda. 2001b. Comparison of the biological

H$_2$S removal characteristics among four inorganic packing materials. Journal of Bioscience and Bioengineering. 91(4):396-402.

Hodges, D. 2001a. Full-Scale Biofilter: A case study. TRG Biofilter. www.trgbiofilter.com/biofilterfullscale.htm. Accessed on 7 July 2002.

Hodges, D. 2001b. Biofilter pilot unit: A case study. TRG Biofilter. www.trgbiofilter.com/biofilterpilot.com. Accessed on 7 July 2002.

Hodges, D. 2001c. Modeling removal of air contaminants by biofiltration. TRG Biofilter. www.trgbiofilter.com/modeling.htm. Accessed on 7 July 2002

Holden, P., J. Hunt, and M. Firestone. 1997. Toluene diffusion and reaction in unsaturated *Pseudomonas putida* biofilms. Biotechnology and Bioengineering. 56(6):656-670.

Hounsell, G. 1995. Case studies: selection of high efficiency VOC removal technologies for process air streams. Proceedings of the Annual Meeting - Air and Waste Management Association. 415-422.

Hsu, T., and C. Chiang. 1997. Activated sludge treatment of dispersed dye factory wastewater. Journal of Environmental Science and Health, Part A: Environmental Science and Engineering and Toxic and Hazardous Substance Control. 32(7):1921-1932.

Hsu, S., S. Lin, and K. Shen. 2000. Odor control of acrylic resin manufacturing facility by using a biofilter. Presented at the USC-TRG Conference on Biofiltration (An Air Pollution Control Technology). 3-9.

Hwang, J., S. Jang, Y. Kang, and S. Park. 2000. Evaluation of compost as a biofilter packing material during the treatment of gaseous p-xylene. Presented at the USC-TRG Conference on Biofiltration (An Air Pollution Control Technology). 59-65.

Illinois Corn Growers Association. 2001. Butanol Research - A Multi-Use Product Made From Corn. Illinois Corn Growers Association. www.ilcorn.org/Pages/butanol.htm. Accessed on 22 September 2002.

Janni, K., and R. Nicolai. 2000. Designing biofilters for livestock facilities. Presented at the USC-TRG Conference on Biofiltration (An Air Pollution Control Technology). 11-20.

Ji, W., S. Sikday, and S. Hwang. 1994. Modeling of multi-component pervaporation for removal of volatile organic compounds from water. Journal of Membrane Science. 93:1-19.

Johansson, F., and A. Leufven. 1997. Concentration and interactive effects on the sorption of aroma liquids and vapors into polypropylene. Journal of Food Science.

62(2):355-358.

Jorge, R., and A. Livingston. 2000. Biological treatment of an alternating source of organic compounds in a single tube extractive membrane reactor. Journal of Chemical Technology and Biotechnology. 75:1174-1182.

Jorio, H., K. Kiared, R. Brzezinski, A. Leous, G. Viel, and M. Hetiz. 1998. Treatment of air polluted with high concentrations of toluene and xylene in a pilot-scale biofilter. Journal of Chemical Technology and Biotechnology. 73(3):183-196.

Kaempfer, H. 2001. PhD Defense Proposal. University of Missouri - Rolla, Rolla, MO.

Kakac, S., and H. Liu. 1998. Heat Exchangers Selection, Rating, and Thermal Design. CRC Press, Boca Raton, FL.

Kang, W., R. Shukla, G. Frank, and K. Sirkar. 1988. Evaluation of O_2 and CO_2 transfer coefficients in a locally integrated tubular hollow fiber bioreactor. Applied Biochemistry and Biotechnology. 18:35-51.

Karamanev, D., Y. Matteau, and B. Ramsay. 1999. Experimental study and mathematical modeling of gaseous toluene biofiltration by thermophilic active compost. Canadian Journal of Chemical Engineering. 77(5):1037-1043.

Keskiner, Y., and S. Ergas. 2000. Hollow fiber membrane bioreactor for aqueous and gas phase ammonia removal by nitrification. Hazardous and Industrial Wastes. 32:867-876.

Khlebnikov, A., F. Samb, and P. Peringer. 1998. A transient mathematical model for maximum respiration activity and oxygen diffusion coefficient estimation in non-steady-state biofilms. Journal of Chemical Technology and Biotechnology. 73(3):274-280.

Kim, B., E. Kalis, T. DeWulf, and K. Andrews. 2000. Henry's law constants for paint solvents and their implications on volatile organic compound emissions from automotive painting. Water Environment Research. 72(1):65-74.

Kim, B., J. Adams, P. Klaver, E. Kalis, M. Contrera, M. Griffin, J. Davidson, and T. Pastick. 2000. Biological removal of gaseous VOCs from automotive painting operations. Journal of Environmental Engineering. August:745-753.

Klasson, K., and B. Davison. 2001. Effect of temperature on biofiltration of nitric oxide. Applied Biochemistry and Biotechnology. 91-93:205-211.

Kong, Z., L. Farhana, R. Fulthorpe, and D. Allen. 2001. Treatment of volatile organic compounds in a biotrickling filter under thermophilic conditions. Environmental Science and Technology. 35:4347-4352.

Kozliak, E., and K. Riley. 2000. Efficient removal of the airborne ethyl acetate and toluene by lab-scale fiber-based bioreactors with low amount of biomass. Presented at the USC-TRG Conference on Biofiltration (An Air Pollution Control Technology). 39-46.

Kreulin, H., C. Smolders, G. Versteeg, and W. van Swaaij. 1993. Microporous hollow fibre membrane modules as gas-liquid contactors. Part I. Physical mass transfer processes. Journal of Membrane Science. 78:197-216.

Krishna, M., L. Philip, and C. Venkobachar. 2000. Performance evaluation of a *thiobacillus* denitrifiers immobilized biofilter for the removal of oxides of nitrogen. Presented at the USC-TRG Conference on Biofiltration (An Air Pollution Control Technology). 191-199.

Laurenzis, A., H. Heits, S. M. Wubker, U. Heinze, C. Friedrich, and U. Werner. 1998. Continuous biological waste gas treatment in stirred trickle-bed reactor with discontinuous removal of biomass. Biotechnology & Bioengineering. 57(4):497-503.

Le Cloirec, P., P. Humeau, and E. Ramirez-Lopez. 2001. Biotreatments of odours: control and performances of a biofilter and bioscrubber. Water Science and Technology. 44(9):219-226.

Lee, B., W. Flanagan, J. Barnes, K. Barrett, B. Zaccardi, and W. Apel. 2000. Comparison of three bed packings for the biological removal of nitric oxide from gas streams. Presented at the USC-TRG Conference on Biofiltration (An Air Pollution Control Technology). 211-219.

Lee, B., W. Apel, and W. Smith. 2001. Oxygen effects on thermophilic microbial populations in biofilters treating nitric oxide containing gas streams. Environmental Progress. 20(3):157-166.

Lee, D., A. Lau, and K. Pinder. 2001. Development and performance of an alternative biofilter system. Journal of the Air and Waste Management Society. 51:78-85.

Leonard, D., M. Mercier-Bonin, N. Lindley, and C. Lafforgue. 1998. Novel membrane bioreactor with gas/liquid two-phase flow for high performance degradation of phenol. Biotechnology Progress. 14:680-688.

Lim, J., S. Park, J. Koo, and H. Park. 2001. Evaluation of porous ceramic as microbial carrier of biofilter to remove toluene vapor. Environmental Technology 22(1):47-56.

Lu, C., W. Chu, and M. Lin. 2000. Removal of BTEX vapor from waste gases by a trickle bed biofilter. Journal of the Air and Waste Management Association. 50(3):411-417.

Lu, C., M.-R. Lin, and J. Lin. 2001a. Treatment of n,n-dimethylacetamide waste gas by a trickle-bed air biofilter. Chemosphere. 44:173-180.

Lu, C., M. Lin, and J. Lin. 2001b. Removal of styrene vapor from waste gases by a trickle-bed air biofilter. Journal of Hazardous Materials. B82:233-245.

Lu, C., M. Lin, J. Lin, and K. Chang. 2001c. Removal of ethylacetate vapor from waste gases by a trickle-bed air biofilter. Biotechnology. 87:123-130.

Lugg, G. 1968. Diffusion coefficients of some organic and other vapors in air. Analytical Chemistry. 40:1072-1077.

Luo, J., and S. Lindsey. 2000. Biofilters for controlling rendering odour emissions. Presented at the USC-TRG Conference on Biofiltration. 247-253.

Luo, J. 2001. A pilot-scale study on biofilters for controlling animal rendering process odours. Water Science and Technology. 44(9):277-285.

Malhautier, L., A. Aizpuru, and J. Fanlo. 2000. Quantitative structure activity relationships for predicting VOC elimination in biofilters. Presented at the USC-TRG Conference on Biofiltration (An Air Pollution Control Technology). 133-140.

Malhautier, L., J. Roux, and J. Fanlo. 2001. Biofiltration of a mixture of volatile organic emissions. Journal of the Air and Waste Management Association. 51(12):1662-1670.

Mallany, J., A. Darlington, and M. Dixon. 2000. The biofiltration of indoor air II: microbial loading of the indoor space. Presented at the USC-TRG Conference on Biofiltration (An Air Pollution Control Technology). 263-268.

Marek, J., J. Paca, and A. Gerrard. 2000. Dynamic responses of biofilters to changes in the operating conditions in the process of removing toluene and xylene from air. Acta Biotechnologica. 20(1):17-29.

Marek, J., J. Paca, M. Halecky, B. Koutsky, M. Sobotka, and T. Keshavarz. 2001. Effect of pH and loading manner on the start-up period of peat biofilter degrading xylene and toluene mixture. Folia Microbiologia. 46(3):205-209.

Martens, W., M. Martinec, R. Zapirain, M. Stark, E. Hartung, and U. Palmgren. 2001. Reduction potential of microbial, odour and ammonia emissions from a pig facility by biofilters. International Journal of Hygiene and Environmental Health. 203:335-345.

Martinez, F., W. Moe, and K. Kinney. 2000. Treatment of paint spray booth off-gases in biofilters containing polyurethane foam media. Presented at the USC-TRG Conference on Biofiltration (An Air Pollution Control Technology). 107-114.

Martinez - Diez, L., and M. Vazquez - Gonzalez. 2000. A method to evaluate coefficients affecting flux in membrane distillation. Journal of Membrane Science. 173(2):225-234.

Matrix Environmental Technolgies, I. 2001. Biofiltration. www.matrixbiotech.com/html/biofilter.html. Accessed on 16 October 2001.

Matrix Environmental Technologies, I. 2001. Open bed biofilter for the control of odors and VOCs at a former petroleum bulk storage terminal. www.matrixbiotech.com/html/biofiltercase.html. Accessed on 16 October 2001.

Matteau, Y., and B. Ramsay. 1997. Active compost biofiltration of toluene. Biodegradation. 8(3):135-141.

Matteau, Y., and B. Ramsay. 1999. Thermophilic toluene biofiltration. Journal of the Air and Waste Management Association. 49(3):350-354.

Metcalf and Eddy, I. 1991. Wastewater Engineering Treatment, Disposal, and Reuse, 3rd ed. McGraw-Hill, Boston, MA.

Metris, A., A. Gerrard, R. Cumming, P. Weigner, and J. Paca. 2001. Modeling shock loadings and starvation in the biofiltration of toluene and xylene. Journal of Chemical Technology and Biotechnology. 76:565-572.

Mihalcik, P. 2002. Graduate Student. Personal Correspondence.

Min, K., S. Ergas, and J. Harrison. 2002. Hollow fiber membrane bioreactor for nitric oxide removal. Presented at the Air and Waste Management Association Conference. 5-12.

Moe, W., and R. Irvine. 2001a. Effect of nitrogen limitation on performance of toluene degrading biofilters. Water Resources. 35(5):1407-1414.

Moe, W., and R. Irvine. 2001b. Polyurethane foam based biofilter media for toluene removal. Water Science and Technology. 43(11):35-42.

Moe, W., and R. Irvine. 2001c. Intracellular dynamics of ribonucleic acid (RNA) and protein in microorganisms from periodically operated biofilters. Water Science and Technology. 43(3):241-248.

Mohseni, M., and D. Allen. 1997. Influence of transient conditions on the biofiltration of alpha-pinene using wood-chip/activated carbon biofilters. Presented at the Proceedings of the Air & Waste Management Association's Annual Meeting & Exhibition 1997. 1-10.

Moore, D., and G. McCabe. 1993. Introduction to the Practice of Statistics. W. H. Freeman and Company, New York, NY.

Morales, M., S. Revah, and R. Auria. 1998. Start-up and the effect of gaseous ammonia additions on a biofilter for the elimination of toluene vapors. Biotechnology and Bioengineering. 60(4):483-491.

Morgan-Sagastume, F., B. Sleep, and D. Allen. 2001. Effects of biomass growth on gas pressure drop in biofilters. Journal of Environmental Engineering. 127(5):388-396.

Mormile, M. Assistant Professor or Biological Sciences, University of Missouri-Rolla, Rolla, MO, Personnal Correspondence.

Munch, E., P. Lant, and J. Keller. 1996. Simultaneous nitrification and denitrification in bench-scale sequencing batch reactors. Water Research. 30(2):277-284.

Mysliwiec, M., J. VanderGheynst, M. Rashid, and E. Schroeder. 2001. Dynamic volume-averaged model of heat and mass transport within a compost biofilter: I. Model development. Biotechnology and Bioengineering. 73(4):282-294.

National Council for Air and Stream Improvement. 1999. Volatile organic compound emissions from wood products manufacturing facilities 768. NCASI, Technical Bulletin.

National Institute for Occupational Safety and Health. 1997. NIOSH Pocket Guide to Chemical Hazards. Government Printing Office, Pittsburgh, PA.

Neemann, J. J. 1998. Thesis. University of Missouri, Rolla, Rolla, MO.

Nicolai, R., and K. Janni. 2001. Biofilter media mixture ratio of wood chips and compost treating swine odors. Water Science and Technology. 44(9):261-267.

Nijhaus, H., M. Mulder, and C. Smolders. 1991. Removal of trace organics from aqueous solutions. Effect of membrane thickness. Journal of Membrane Science 15:99-111.

Occupational Safety and Health Administration. 1970. 29 CFR 1910.1000 Table Z-2. Occupational Safety and Health Administration. www.osha.gov. Accessed on 20 December 2001.

Paca, J., and B. Koutsky. 2000. Effect of the packing materials on styrene removal in the biofilter. Presented at the USC-TRG Conference on Biofiltration (An Air Pollution Control Technology). 21-29.

Papageorgakopoulou, N., and F. Plakoutsi. 1996. Study of the gelatinolytic activities of Escherichia coli cells before and after starvation in seawater by substrate gel electrophoresis. Microbiological Research. 151(3):329-335.

Park, S., S. Nam, and E. Choi. 2001. Removal of odor emitted from composting facilities using a porous ceramic biofilter. Water Science and Technology. 44(9):301-308.

Parvatiyar, M. G., R. Govind, and D. F. Bishop. 1996a. Treatment of trichloroethylene (TCE) in a membrane biofilter. Biotechnology and Bioengineering. 50(1):57-64.

Parvatiyar, M. G., R. Govind, and D. F. Bishop. 1996b. Biodegradation of toluene in a membrane biofilter. Journal of Membrane Science. 119:17-24.

Patkar, A., and J. Reinhold. 1993. Novel and hybrid control systems for control of air toxic emissions. Proceedings of the Annual Meeting of the Air and Waste Management Association. 1-13.

Patria, L., M. Cathelain, P. Laurens, and J. Barbere. 2001. Odour removal with a trickling filter at a small WWTP strongly influenced by the tourism season. Water Science and Technology. 44:243-249.

Paul, J., A. Friedl, and K. Mairitsch. 2000. Biological was gas treatment of ethylacetate in a pilot-scale biofilter with different filter material. Presented at the USC-TRG Conference on Biofiltration (An Air Pollution Control Technology). 67-74.

Pavasant, P., L. Freitas dos Santos, E. Pistikopoulos, and A. Livingston. 1996. Prediction of optimal biofilm thickness for membrane-attached biofilms growing in an extractive membrane bioreactor. Biotechnology and Bioengineering. 52:373-386.

Pellegrino, J., and S. Sikdar. 1998. Membrane Technology Fundamentals for Bioremediation . Technomic Publishing Company, Lancaster PA.

Pineda, J., R. Auria, F. Perez-Guevara, and S. Revah. 2000. Biofiltration of toluene vapors using a model support. Bioprocess Engineering. 23:479-486.

Popov, V., A. Bezborodov, A. Murphy, P. Cross, and W. Jackson. 2000. Industrial trickling bed biofilters for abatement of VOCs from air emissions. Presented at the USC-TRG Conference on Biofiltration (An Air Pollution Control Technology). 75-82.

Prenafeta-Boldu, F., A. Kuhn, D. Luykx, H. Anke, van Groenestijn, and J. de Bont. 2001. Isolation and characterization of fungi growing on volatile aromatic hydrocarbons as their sole carbon and energy source. Mycological Research. 105(4):477-484.

Pressman, J. 1995. Mass transfer of chlorinated solvents and biofouling in hollow fiber membrane modules. Masters Thesis. University of Texas at Austin, Austin, TX.

Pressman, J., G. Georgiou, and G. Speital. 1999. Demonstration of efficient trichloroethylene biodegradation in a hollow fiber membrane bioreactor. Biotechnology and Bioengineering. 62(6):681-692.

Pressman, J. G., G. Georgiou, and G. E. Speitel. 2000. A hollow-fiber membrane bioreactor for the removal of trichloroethylene from the vapor phase. Biotechnology & Bioengineering. 68(5):548-556.

Reij, M., G. Voskuilen, and S. Hartmans. 1993. Biofilms in membrane bioreactors for

waste gas treatment. NATO ASI Series. Series E, Applied Sciences. 223:455-460.

Reij, M., and S. Hartmans. 1994a. Membrane bioreactor for waste gas treatment: removal of pollutants with a low solubility in water. Presented in the Proceedings of the 6th European Congress on Biotechnology. 1203-1206.

Reij, M., and S. Hartmans. 1994b. Membrane bioreactor for waste gas treatment. Biologische Abgasreinigung. 15:517-519.

Reij, M. W., D. De Gooijer Kees, A. M. De Bont Jan, and S. Hartmans. 1995. Membrane bioreactor with a porous hydrophobic membrane as a gas-liquid contactor for waste gas treatment. Biotechnology & Bioengineering. 45(2):107-115.

Reij, M. W., and S. Hartmans. 1996. Propene removal from synthetic waste gas using a hollow-fibre membrane bioreactor. Applied Microbiology and Biotechnology. 45:730-736.

Reij, M. W., E. K. Hamann, and S. Hartmans. 1997. Biofiltration of air containing low concentrations of propene using a membrane bioreactor. Biotechnology Progress. 13:380-386.

Reij, M. W., T. F. Keurentjes Jos, and S. Hartmans. 1998. Membrane bioreactors for waste gas treatment. Journal of Biotechnology. 59(3):155-167.

Reynolds, F., and W. Grafton. 1999. Biofiltration: An old technology comes of age. Environmental Technology. July/August:51-52.

Rho, D., M. Talbot, M. Levesque, J. Ribes, and O. Tresse. 2000. Treatment of organic vapors in lab-scale biotrickling filters: microbial population dynamics as evaluated by competitive polymerase chain reaction, denaturing gradient gel electrophoresis and on-line respirometry. Presented at the USC-TRG Conference on Biofiltration (An Air Pollution Control Technology). 201-210.

Richard, T. 2001. Odor Treatment - Biofiltration. Cornell University Composting - Science and Engineering. www.cfe.cornell.edu/compost/odors/odortreat.html. Accessed on 13 January 2002.

Richard, T. 2002. Calculating the oxygen diffusion coefficient in air. Cornell University. www.cfe.cornell.edu/compost/oxygen/oxygen.diff.air.html. Accessed on 13 January 2002.

Riefler, G., D. Ahlfeld, and B. Smets. 1998. Respirometric assay for biofilm kinetics estimation: Parameter identifiability and retrievability. Biotechnology and Bioengineering. 57(1):35-45.

Rishell, S., and G. Hamer. 2000. Air pollutant elimination by methanotrophs in membrane biofilms reactors. Presented at the USC-TRG Conference on Biofiltration (An Air Pollution Control Technology). 229-237.

Roberge, F., M. Gravel, L. Deschenes, C. Guy, and R. Samson. 2001. Biofiltration of dichorobenzenes. Water Science and Technology. 44(9):287-293.

Rogers, J., and K. Reardon. 2000. Modeling substrate interactions during the biodegradation of mixtures of toluene and phenol by *Burkholderia Species* JS150. Biotechnology and Bioengineering. 70(4):428-435.

Rouhana, N., N. Handagama, and R. Bienkowski Paul. 1997. Development of a membrane-based vapor-phase bioreactor. Applied Biochemistry & Biotechnology. 65(0):809-821.

Ruokojarvi, A., J. Ruuskanen, and P. Martikainen. 2001. Oxidation of gas mixtures containing dimethyl sulfide, hydrogen sulfide, and methanethiol using a two-stage biotrickling filter. Journal of the Air and Waste Management Association. 51:11-16.

Sae-oui, P., P. Freakley, and P. Oubridge. 1999. Determination of heat transfer coefficient of rubber to air. Plastics, Rubber and Composites. 28(2):65-68.

Sawyer, C., P. McCarty, and G. Parkin. 1994. Chemistry for Environmental Engineering. McGraw-Hill, New York, NY.

Schofield, R., A. Fane, and C. Fell. 1990. Gas and vapour transport through microporous membranes. II. Membrane distillation. Journal of Membrane Science. 53(1-2):173-185.

Schosengerdt, R., B. Hunter, and R. Hanson. 1999. Incremental hydrogen sulfide loading and diurnal fluctuation of three operating biofilters. Presented at the WEFTEC 1999, New Orleans LA. 1-6.

Schwarz, B., T. Nukunya, J. Devinny, and T. Tsotsis. 2000. A pore network model of biofilter clogging. Presented at the USC-TRG Conference on Biofiltration (An Air Pollution Control Technology). 167-182.

Schwarzenbach, R., P. Gschwend, and D. Imboden. 1993. Environmental Organic Chemistry. Wiley, New York, NY.

Schwedt, G. 1997. The Essential Guide to Analytical Chemistry. John Wiley and Sons, New York, NY.

Shareefdon, Z., and C. Cantwell. 2000. Evaluation of commercial biofilter media biomix and biosorbens for removal of volatile organic compound (VOC) emissions. Presented at the USC-TRG Conference on Biofiltration (An Air Pollution Control Technology). 289-296.

Sinclair, C., and D. Ryder. 1975. Models for the continuous culture of microorganisms under both oxygen and carbon limiting conditions. Biotechnology and Bioengineering. XVII:375-398.

Skladany, G., G. Leso, and D. Hodge. 1995. Biological air pollution control in North America. TRG Biofilter. www.trgbiofilter.com/biofilterconf95.htm. Accessed on 15 September 2001.

Smart, J., V. Starov, R. Schucker, and D. Lloyd. 1998. Pervaporative extraction of volatile organic compounds from aqueous systems with use of a tubular transverse flow module. Part II. Experimental results. Journal of Membrane Science. 143:159-179.

Smet, E., H. Van Langenhove, and G. Philips. 1999. Dolomite limits acidification of a biofilter degrading dimethyl sulphide. Biodegradation. 10(6):399-404.

Song, J., and K. Kinney. 2001. Effect of directional switching frequency on toluene degradation in a vapor phase bioreactor. Applied Microbiology and Biotechnology. 56:108-113.

Sorial, G., F. Smith, and M. Suidan. 1997. Performance of a peat biofilter: Impact of the empty bed residence time, temperature, and toluene loading. Journal of Hazardous Materials. 53(1-3):19-33.

Sorial, G., F. Smith, M. Suidan, and R. Brenner. 2001. Removal of ammonia from contaminated air by trickle bed air biofilters. Journal of the Air and Waste Management Association. 51:756-765.

State of Iowa. 2002. Department of Natural Resources Report. www.state.ia.us/dnr/organiza/wmad/lqbureau/ust/t2app-a.pdf. Accessed on 22 September 2001.

Stern, S., and S. Shiah. 1981. Solubility of inhalation anesthetics in various media: A new correlation. Molecular Phamacology. 19:56-61.

Stewart, J. 1995. Calculus, 3rd ed. Brooks/Cole Publishing Company, Albany, NY.

Sun, Y., and J. Chen. 1994. Sorption/desorption properties of ethanol, toluene, and xylene in poly(dimethylsiloxane) membranes. Journal of Applied Polymer Science. 51:1797-1804.

Sun, A., J. Hong, and T. Wood. 1998. Modeling of trichloroethylene degradation by a recombinant *Pseudomonad* expressing toluene ortho-monooxygenase in a fixed film bioreactor. Biotechnology and Bioengineering. 59(1):40-51.

Tang, H., S. Hwang, and S.-C. Hwang. 1995. Dynamics of toluene degradation in

biofilters. Hazardous Waste and Hazardous Materials 12(3):207-219.

Tawil, A., and G. Hamer. 2000. Removal of alcohol and ketone vapours from air streams: can liquid phase biooxidation data help prediction of gaseous phase biofilter performance. Presented at the USC-TRG Conference on Biofiltration (An Air Pollution Control Technology). 141-149.

Texas Natural Resources Commission. 2002. Department of Natural Resources Report. www.tnrcc.state.tx.us/permitting/remed/rpr/constgw.pdf. Accessed on 22 September 2002.

Thalasso, F., E. Razo-Flores, R. Ancia, H. Naveau, and E. Nyns. 2001. Pressure drops control strategy in a fixed-bed reactor. Journal of Hazardous Materials. B81:115-122.

Tia, S., S. Suwanayuen, C. Tangsatitkulchai, C. Phromvichit, and W. Nimipal. 1996. Heat transfer characteristics in a small-scale fluidized bed boiler. International Journal of Energy Research. 20(6):521-530.

TRG Biofilter, I. 2001. Biofiltration system (or biofilter) to remove toxic and odorous gases from wastewater treatment. TRG Biofilter. www.trgbiofilter.com/ojaiprop.htm.

Triat and G, I. 2001. Normal Butanol Fact Sheet. Triat and G, Inc. www.triat.com/8nba.htm. Accessed on 30 July 2001.

United States Congress. 1970. The Clean Air Act, USC Title 42, Chapter 85, Section 7401.

University of Alabama. 2002. Diffusion coefficient of toluene in air. http://chemenguah.edu/courses/che443f99/che443_hwl.html. Accessed on 27 August 2002.

University of California, Santa Barbara. 2002. Class notes. www.esm.ucsb.edu/fac_staff/fac/keller/courses/esm222/esm222_hw3.pdf. Accessed on 27 August 2002.

University of California, Santa Barbara. 2002. Diffusion coefficient of benzene in air. www.esm.ucsb.edu/fac_staff/fac/keller/courses/esm222/em222_hw3.pdf. Accessed on 27 August 2002.

University of Chicago. 2002. Cylindrical coordinate system. http://sosnick.uchicago.edu/spherical_cylindrical_rectangular.html. Accessed on 27 August 2002.

University of Idaho. 2002. Boltzmann kinetic energy distribution. www.chem.uidaho.edu/~honors/boltz.html. Accessed on 27 August 2002.

University of Minnesota. 2002. The University of Minnesota Biodegradation and Biocatalysis Database. www.umbbd.ahc.umn.edu/index.html.

Van Amerongen, G. J. 1967. Diffusion in Elastomers. Rubber Chemistry and Technology. 1065-1152.

van Groenestijn, J., and P. Hesselink. 1994. Biotechniques for air pollution control. Biodegradation. 4(4):283-301.

van Groenestijn, J., W. van Heiningen, and N. Kraakman. 2001. Biofilters based on the action of fungi. Water Science and Technology. 44(9):227-232.

van Heiningen, W., N. Kraakman, S. Gerbens, and J. van Groenestijn. 2000. The development of a biofilter system using fungi on inert carrier material in combination with mites. Presented at the USC-TRG Conference on Biofiltration (An Air Pollution Control Technology). 277-279.

Veiga, M., and C. Kennes. 2001. Parameters affecting performance and modeling of biofilters treating alkylbenzene-polluted air. Applied Microbiology and Biotechnology. 55(2):254-258.

Wani, A., R. Branion, and A. Lau. 1998. Effects of periods of starvation and fluctuating hydrogen sulfide concentration on biofilter dynamics and performance. Journal of Hazardous Materials. 60(3):287-303.

Wani, A., R. Branion, and A. Lau. 2001. Biofiltration using compost and hog fuel as a means of removing reduced sulphur gases from air emissions. Pulp and Paper Canada. 102(5):27-32.

Wark, K., C. Warner, and W. Davis. 1998. Air Pollution - Its Origin and Control, 3rd ed. Addison Wesley Longman, Menlo Park, CA.

Waweru, M., V. Herrygers, H. Van Langenhove, and W. Verstraete. 2000. Process engineering of waste gas purification. In J. Klein and J. Winter (ed.), Biotechnology, 2nd ed. Wiley-VCH Verlag GmbH, Weinheim, Germany.

Weast, R. C., and S. M. Samuel. 1997. Handbook of Chemistry and Physics. Cincinnati, Ohio.

Weber, F., and S. Hartmans. 1996. Prevention of clogging in a biological trickle-bed reactor removing toluene from contaminated air. Biotechnology and Bioengineering. 50:91-97.

Webster, T., A. Togna, W. Guarini, C. Albritton, C. Carlisle, C. Cha, and J. Wander. 2000. Prevention of clogging in a biological trickle-bed reactor removing toluene from

contaminated air. Presented at the USC-TRG Conference on Biofiltration (An Air Pollution Control Technology). 31-38.

Weigner, P., J. Paca, P. Loskot, B. Koutsky, and M. Sobotka. 2001. The start-up period of styrene degrading biofilters. Folia Microbiologica. 46(3):211-216.

Westenberg, D. 2002. Associate Professor, Biology. Personal Correspondence.

Whitten, K., and K. Gailey. 1981. General Chemistry. Saunders College Publishing, Philadelphia, PA.

Wickramasinghe, S. R., and M. J. Semmens. 1992. Mass transfer in various hollow fiber geometries. Journal of Membrane Science. 69:235-250.

Wilderer, P., F. Kolb, and M. Kriebusch. 1998. Membrane biofilm reactors in Biological Treatment of Hazardous Wastes. John Wiley and Sons, New York, NY.

Woertz, J., and K. Kinney. 2000. Use of the fungus *Exophiala lecanii-corni* to degrade a mixture of VOCs. Presented at the USC-TRG Conference on Biofiltration (An Air Pollution Control Technology). 151-158.

Woertz, J., K. Kinney, and P. Szaniszlo. 2001. A fungal vapor-phase bioreactor for the removal of nitric oxide from waste gas streams. Journal of the Air and Waste Management Association. 51:895-902.

Wright, P., M. Bustard, and V. Meeyoo. 2000. Environmental pollution abatement technologies for the new millennium: novel vapor phase biofiltration of VOCs and other waste gases. Proceedings of the Air and Waste Management Association Conference and Exhibition. 2157-2168.

Wu, L., Y. Loo, and L. Koe. 2001. A pilot study of a biotrickling filter for the treatment of odorous sewage air. Water Science and Technology. 44(9):295-299.

Yang, M., and E. L. Cussler. 1986. Designing hollow-fiber contactors. AIChE Journal. 32(11):1910-1916.

Yeom, S., and A. Daugulis. 2000. Development of a novel bioreactor system for treatment of gaseous benzene. Biotechnology and Bioengineering. 72(2):156-165.

Zahodiakin, P. 1995. Puzzling out the new clean air act. Chemical Engineering. 97(12):24-27.

Zhang, Q., and E. Cussler. 1985. Microporous hollow fibers for gas absorption II. Mass transfer across the membrane. Journal of Membrane Science. 23:333-345.

Zhang, T., and P. Bishop. 1994a. Structure, activity and composition of biofilms. Water

Science Technology. 29(7):335-344.

Zhang, T., and P. Bishop. 1994b. Density, porosity and pore structure of biofilms. Water Research. 28(11):2267-2277.

Zhu, X., M. Suidan, C. Alonso, T. Yu, B. J. Kim, and B. R. Kim. 2001. Biofilm structure and mass transfer in a gas phase trickle-bed biofilter. Water Science and Technology. 43(1):285-293.

Zilli, M., E. Palazzi, L. Sene, A. Converti, and M. Borghi. 2001. Toluene and styrene removal from air in biofilters. Process Biochemistry. 37:423-429.

VITAE

Ellen Claire England was born in Cedar Rapids, Iowa on ██████████ the daughter of ██████████ and ██████████ After an idyllic childhood terminating with graduation from John F. Kennedy High School, Cedar Rapids, Iowa, in 1981, she attended the University of Iowa, in Iowa City, Iowa. During her tenure at the University of Iowa, Ellen joined the Air Force Reserve Officer Training Corps (AFROTC). Subsequent to graduation with a B.S. in Industrial Engineering (1986), she was stationed at Grand Forks AFB, Grand Forks, ND in 1986 as a Bioenvironmental Engineer. Subsequent assignments included Malmstrom AFB, Great Falls, MT, University of Minnesota, Minneapolis, MN, Brooks AFB, San Antonio, TX and the University of Missouri-Rolla, Rolla, MO. An M.S. in General Administration from Central Michigan University was awarded in 1991 and an M.S. in Environmental Health was awarded in 1996 from the University of Minnesota. She is a Certified Industrial Hygienist and Certified Safety Professional. Ellen married ██████████ on October 9, 1999 at Big Portage Lake in Backus Minnesota, where she intends to reside after enduring her career with the Air Force.